Stem cell bandages – an investigation into the therapeutic effect of adipose-derived mesenchymal stem cells in corneal wound healing

Olla M. H. Al-Jaibaji

Doctor of Philosophy (Ph.D.)

Biosciences Institute, Faculty of Medical Sciences, Newcastle University

October 2019

Declaration of work

I declare that this thesis is based on my own work and has not been submitted in any form for another degree at any university or any other tertiary education. Information derived from published and unpublished work of others have been acknowledged in the text and in the list of references given in the bibliography.

Abstract

Human corneal regenerative capacity is not enough to heal deep injuries that causes scars, such abrasions result in the formation of the irregular extracellular matrix that leads to scar and often results in corneal transparency and vision reduction. Because of the limited number of corneal donors for transplantation, there has been an increased interest in cell therapy. Adipose-derived stem cells (ASCs) showed a promising choice for they are environmentally responsive in wound repair. ASCs can secrete paracrine factors and extracellular molecules that have immunomodulatory, angiogenic, trophic, anti-fibrotic, and antimicrobial activity. This thesis explores the formation of bandages; such bandages are formed of sodium alginate. Alginates are present in nature and extracted from brown seaweed. Generally, this material is safe, cost-effective, and wildly used in biomedical applications due to its biocompatibility and ease of handling. Hypothermic temperatures are also explored in here for bandage storage. Hence, this project hypothesized the formation of hypothermically stored ASCs bandages and their beneficial effect on corneal injuries. ASCs bandages were found to improve *in vitro* corneal scratch wounds, while storage at 15°C presented a favorable condition to store the bandages to vastly enhance their therapeutic potential. This storage is suggested to be a hypoxia-induced environment that augments cells ability to produce paracrine factors. Thus, hypoxia-induced ASCs bandages showed a promising therapeutic ability in healing corneal injures. Gene assessment and protein array revealed the production of several paracrine factors including HGF, TSG-6, IL-8, MCP1, TSP-1 that aid in wound healing. *In vivo*, hypoxia-induced ASCs bandages were transferred to adult male mice corneas following a chemical burn, where reduction of immune cell infiltration was observed. Thus, supporting this thesis hypothesis.

Acknowledgment

Alhamdulillah, all praises to Allah for His blessings and kindness that I finally reach the day where I can write this note of appreciation as the finishing touch on my thesis. This Ph.D. has been a long and winding journey – but never once Allah makes me feel left alone nor He leaves my prayers unheard.

I present my heartiest gratitude to my parents, who supported me economically and morally, without them, I would not be who I am today, they have been my pillar of support throughout my life. My sister Dr. Rana Al-Jaibaji for her continues to support and advise. and to my siblings for believing in me and encouraging me. I would like to express my gratitude to all who have helped and supported me throughout my Ph.D. at Newcastle. Importantly, my deepest gratitude goes to my supervisor, Prof Che J Connon for his encouragement, supervision, and support, and my co-supervisor Dr. Annette Meeson for her continuous guidance, motivation, and support. Prof Francisco Figueiredo for his continued supplementation of corneal tissues. I would also like to thank my colleagues for the wonderful times we had in the lab, the support, advice, discussion, and technical assistance. These include Dr. Stephen Swioklo, for his mentoring and encouragement which have been especially valuable. Dr. Ricardo Gouveia for his contribution and directions. Dr. Martina Miotto for her genuine kindness and support. Mr. Thomas Volatier who has been a very good friend to me and I value those conversations that we had while doing our experiments. Not forgetting Dr. Andrei Constantinescu for his guidance in my early research days. I would also like to extend my thanks to Miss Tam Jeewon for her help in doing validation experiments, and Dr. Alex Shortt for performing the animal experiments. My deepest gratitude to my best friend Dr. Sumaya Alkanderi for her continuous encouragement, keen advice, and for opening her home to me throughout my Ph.D. And finally, to Newcastle University Karate Club, my instructor Mr. Steve Potts for his guidance in helping me learn martial arts for the first time and to all the club members for they made me enjoy my time in Newcastle.

Table of Contents

List of Figures

List of Diagrams

List of Tables

Chapter 1. Introduction

1.1 The cornea

The cornea is a small tissue located at the outermost part of the eye. It is the barrier between the eye and the external environment. Due to collagen amount, thickness varies, 551 - 565 μm centrally and 612 – 640 μm peripherally (Fares et al., 2012, Feizi et al., 2014). Cornea is the most sensitive part of the body (due to the high density of nerves contained within the eye), avascular (thus immune-privileged), and transparent acting as the primary lens of the visual system responsible for refracting light onto the retina (Figure 1.1) (Jager et al., 1995, Meek et al., 2003).

Corneal healing following wounding remains a challenge, with millions of people suffering from injuries, trauma, and diseases that could lead to unbearable pain (Fea et al., 2008). The wound healing process is largely dependent on the cells contained within the cornea; their migration, proliferation, and ability to produce growth factors to influence other cells is key in restoring tissue integrity. Whilst there are various methods used for correcting/protecting the eyesight such as spectacles, contact lenses, LASIK (laser-assisted in-situ keratomileusis), LASEK (laser epithelial keratomileusis), PRK (photorefractive keratectomy), and Wavefront-guided LASIK, damage to the cornea remains a global concern. One method employed to treat irreversible damage to the cornea is corneal transplantation (keratoplasty). This method, however, which has been undertaken for over a century, has significant limitations, including reliance on donor availability and compatibility, thus, it does not currently meet the worldwide demand for treatment. It is suggested that 12.7 million people are on the waiting lists for transplantation, with only 1 in 70 individuals receiving transplants due to the shortage of donor tissue (Gain et al., 2016). They further report that 53% of the world's inhabitants did not have access to corneal transplantation. Even in countries where transplantation routinely performed, it is becoming increasingly difficult for eye banks worldwide to meet the growing demand for transplantable tissue, which is in part due to population aging. Thus, cell-based therapies can be used to prevent further damage and to initiate healing.

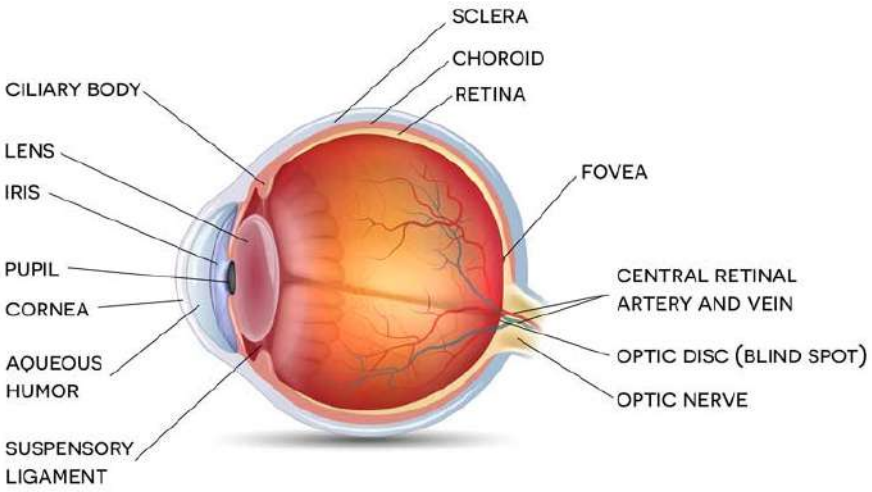

Figure 1.1 – The eye. Represents the major ocular structure; there are three layers of the eye; the fibrous tunic that comprises of sclera and cornea. The vascular tunic that comprises of the choroid, ciliary body, and iris. And the nervous tunic that comprises of the retina. The cornea is the window from which we observe the world. It is the transparent outermost layer of the optical system that is responsible for refracting the light into the retina and separates the eye from the surrounding environment. https://www.lasikrapidcity.com/cornea-rapid-city/.

1.2 Corneal significance and structure

The corneal structure consists of two main areas; the limbus that is the niche for corneal epithelial (Cotsarelis et al., 1989) and stromal stem cells (Funderburgh et al., 2016) (Figure 1.1A), and the central part that consists of uniquely distinctive cellular layers (Figure 1.1B). From the outer surface they are epithelium layer, Bowman's membrane, Stromal layer, Dua's layer, Descemet's membrane, and the endothelial monolayer. Each of these layers has a specific role essential in maintaining corneal function for normal vision and intraocular protection of its contents (Lu et al., 2016).

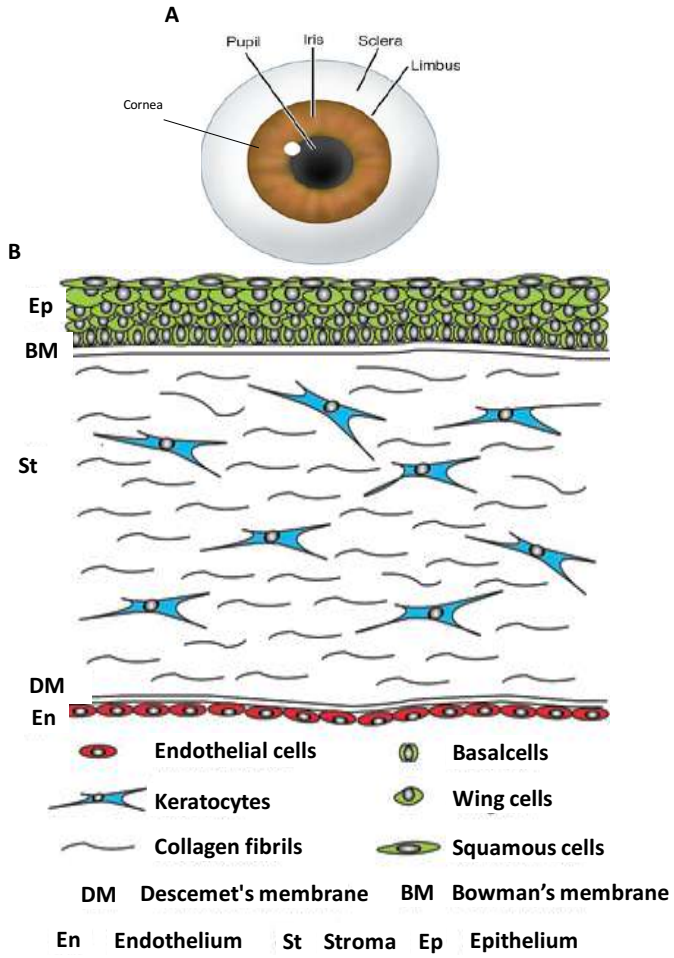

Figure 1.2 – Corneal structure. (A) The limbus is the niche that contains corneal stem cells, located between the cornea and the sclera. (B) A schematic diagram representing the corneal layers in a cross-section. The outer surface contains the epithelial layer based on the basement membrane atop Bowman's membrane. In the middle, there is stroma that is occupied by keratocytes, collagen fibrils, and proteoglycans. Followed by Descemet's membrane and endothelial monolayer (Secker and Daniels, 2009).
(http://lookfordiagnosis.com/mesh_info.php?term=limbus+corneae&lang=1)

1.3 The epithelium

The Epithelium contains 5-7 multi-cellular sheets that cover the front of the cornea and is considered the first line of defense. It contains three layers of non-keratinized cells connected by strong tight junctions (DelMonte and Kim, 2011). These layers are the superficial squamous, suprabasal, and basal layers. The epithelial cells are in a constant healing state, where the squamous cells routinely shed into the tear film. These cells immediately replaced by cells migrating anteriorly from the basal layer and centrally from the limbus (Figure 1.3). The outer superficial layer cells contain microplicae and microvilli that allow tight junction interaction with the tear film and metabolites transport to protect the eye from harm (Klyce, 1972). The superbasal layer contains wing-shaped cells that migrate and differentiate superficially into squamous cells. The single layer basal cells are responsible for generating superbasal cells and mediate cell migration upon injury (Pajoohesh-Ganji and Stepp, 2005). The superficial epithelial cells are in constant renewal that is mediated by the limbal cells, in the limbus area located between the cornea and sclera tight junction. Limbal epithelial stem cells (LESCs) have similar characteristics to somatic stem cells, in terms of size (Romano et al.,2003) and nuclear-cytoplasm ratio (Barrandon and Green, 1987). LESCs lack cytokeratins 3 and CK12 markers, which are expressed by differentiated epithelial cells (Aranguren et al., 2011, Lauweryns et al., 1993). Limbal cells are slow cycling cells and produce transient amplifying cells (TAC) that differentiate following cell division to epithelial cells (Auran et al., 1995, Lehrer et al., 1998). This ability allows them to reduce DNA replication-errors, while upon injury they become extremely proliferative (Lavker and Sun, 2003). TAC would then differentiate to post mitotic cells (PMC) and then terminal differentiated cells (TDC) upon reaching corneal epithelial superficial layer (Li et al., 2007). One method used to detect LESCs is by labeling them with a DNA precursor, such as bromodeoxyuridine (BrdU) or thymidine, followed by a chase phase to detect the label in the slow cycling TAC (Bickenbach and Chism, 1998, Cotsarelis et al., 1989). This allows for the detection of LESCs in the limbus (Watt, 1998). LESCs divide asymmetrically, where one daughter cell remains in the stem cell niche to maintain their number and another daughter cell become TAC, which will go into differentiation. Recently Gouveia (Gouveia et al., 2019) described the

presence of low elastic modulus within the limbal zone that directs cells to retain an undifferentiated state via mechanotransduction processes. In contrast to LESCs, epithelial cells are not considered slow-cycling cells, they have a low proliferative ability; express CK3 and are extremely prone to involuntary debridement with pigment protection (Lehrer et al., 1998). Gouveia et al. suggest this phenotype is a consequence of the limbal epithelial cells migrating centripetally to a stiffer central environment.

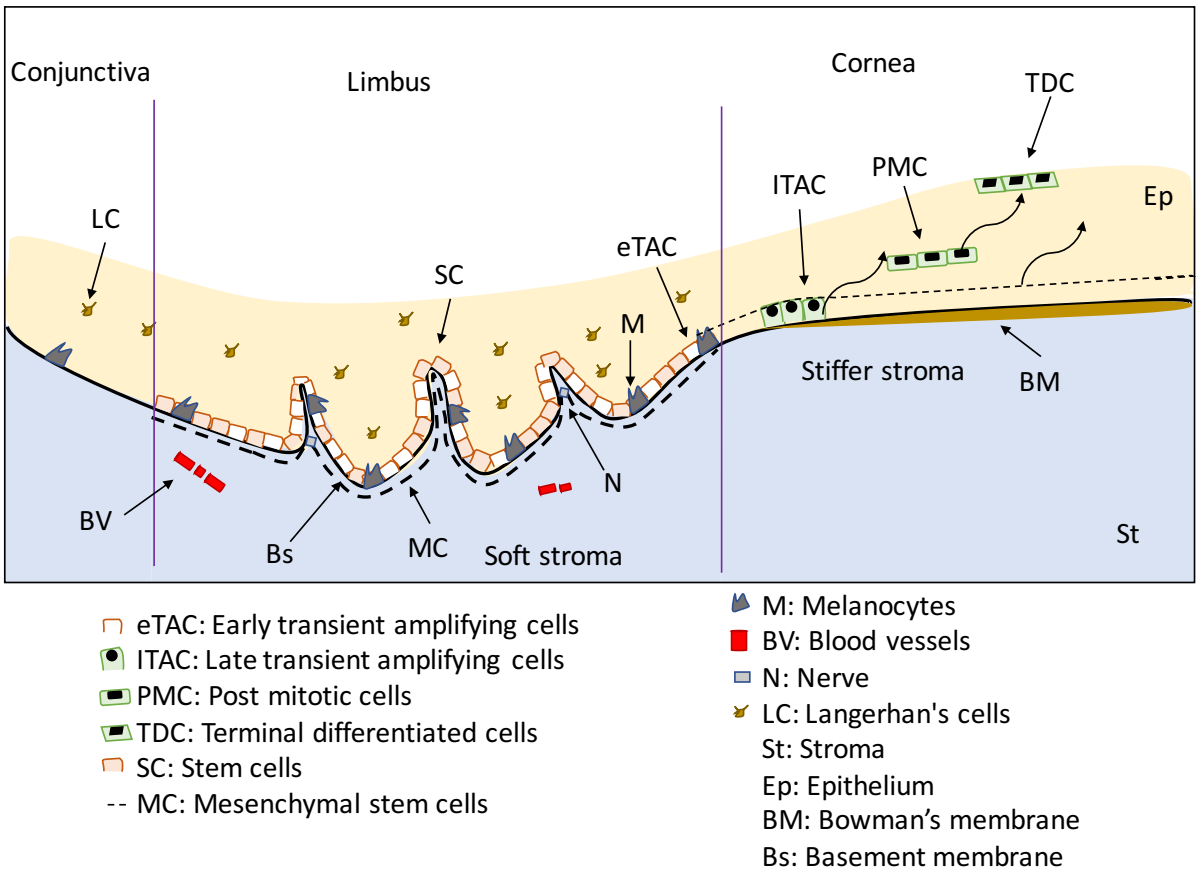

Figure 1.3 – A schematic of the limbal stem cell niche. Limbal stem cells (SC) located at the basal layer. In the basal layer, early transit amplifying cells (eTAC) differentiate into later TAC (ITAC), upon migrating into the suprabasal layer they differentiate into post-mitotic cells (PMC) and then into terminally differentiated cells (TDC) upon reaching the corneal superficial layer. The limbal stroma contains unique softer tissue with mesenchymal cells (MC), upon cells differentiation and migration they transit to the stiffer central stroma.

1.3.1 Bowman's membrane

The Bowman's membrane (BM) is an acellular, smooth, non-regenerating layer located between the epithelial and the stromal layer. This membrane is approximately 8 to 14μm in thickness and is composed of collagen fibrils randomly arranged within the extracellular matrix (ECM) (Last et al., 2012). These collagen fibrils are connecting to the stroma posteriorly and the basement membrane of the epithelial layer anteriorly (Gordon et al., 1994). It is suggested that the limbus compliance state is due to that fact that it lacks BM, which then effects mechanotransduction as the epithelial cells are mainly driven from the limbus by the elasticity gradient across the cornea (Foster et al., 2014, Gouveia et al., 2019). The exact role of the BM is still unknown; however, it is suggested to be superfluous to the corneal function, considering the absence of this layer in patents who underwent PRK surgery. BM may act as a biological barrier to pathological infection and defensive barrier to subepithelial nerve plexus (Wilson and Hong, 2000). Since BM is an acellular layer and viruses need cells for transmitting and spreading, it is highly acceptable that BM likely to function as a biological barrier. BM may also provide resistance to trauma, however, it cannot be regenerated once damaged, thus forms a scar (Lagali et al., 2009, DelMonte and Kim, 2011).

1.3.2 The stroma

The stromal layer is a mesenchymal tissue that comprises 90% of corneal volume where it remains transparent by maintaining the corneal thickness and structure. The stroma consists of keratocytes, collagen fibrils, and proteoglycans that maintains structure. Collagen fibrils consist predominately of collagen molecules type I, type V and type VI arranged in a pack known as lamellae (Fini and Stramer, 2005). Proteoglycans along with collagen arrangement allow the transmission of light (Chakravarti et al., 1998, Connon et al., 2003, Liu et al., 2003). Keratocytes are dormant cells of neural crest origin distributed thinly between the collagen lamellae (Muller et al., 1995). Their key function is to maintain the corneal transparency through the secretion of alpha crystalline proteins that can increase cellular tolerance to stress and prevent denatured proteins precipitation (Jester et al., 1999a, Augusteyn, 2004). Keratocytes also restore the stroma upon injury by differentiation into a fibroblastic phenotype that can migrate and proliferate at the injury site. The

replication of keratocytes leads them to lose their morphological characteristics and become differentiated fibroblasts both *in vivo* and *in vitro*. Fibroblasts were found to secret non-transparent extracellular matrix (ECM) proteins (Funderburgh, 2005). They also produce matrix metalloproteases (MMPs) that are responsible for stromal remodeling throughout wound healing. Authors stated that these fibroblasts cultured *in vitro* could exhibit similar properties to primary keratocytes when cultured with low-mitogen or serum-free media (Gouveia and Connon, 2013). The ECM contains collagen types I and V, MMPs, and glycosaminoglycans (GAGs), where keratin sulfate is the predominant GAG. Dermatan sulfate is the predominant GAG anteriorly, whereas keratin sulfate found posteriorly and is much more hydrophilic (Muller et al., 2001).

1.3.3 Dua's layer

According to a study by Harminder Singh Dua's group, a sixth layer found in the cornea located between the stroma and Descemet's membrane (Dua et al., 2013). Dua's layer is strongly impermeable to air and 15μm in thickness. Many researchers believed that this layer is part of the stroma (McKee et al., 2014). A recent clinical study found this layer in a 74-year-old patient with persistent corneal edema (Dua and Said, 2016). The authors suggested that Dua's layer is formed of collagen I and VI. Its exact function, however, is still unknown.

1.3.4 Descemet's membrane

Descemet's membrane is in constant regeneration via the endothelium cells to form a thick basement membrane between the endothelium layer and the stromal layer (Gipson and Joyce, 2000). Descemet's membrane is composed of collagen IV and VII (Gandhi and Jain, 2015). This membrane is softly attached to the stroma, thus can be easily removed (Anwar and Teichmann, 2002). The main function of Descemet's membrane is its ability to exchange fluids and nutrients between the cornea and the rest of the eye.

1.3.5 The endothelium layer

The endothelium is composed of a single layer of squamous epithelial cells. This layer is essential for the corneal hydration via controlling water content in the stroma. This ability directed by the ion transport system (endothelium pump), that is vital for transparency (Waring et al., 1982). Endothelial cells are not able to regenerate, thus a reduction or damage to this layer leads the remaining endothelial cells to stretch to maintain their function. This stretching, however, leads to a loss in morphology, thus affecting their deturgescence ability (Stiemke et al., 1991).

1.4 Corneal wound healing

1.4.1 Corneal epithelium wound healing

Many wounds can affect the cornea, such as chemical burns, laceration, or abrasion. These injuries can either be simple to heal where no scar may form i.e. surface abrasions that cause blur in vision or deep abrasion and lacerations that could form scar tissue and lead to blindness. Once an injury occurs it activates the extracellular matrix (ECM) proteins and growth factors (GFs) that would induce the healthy cells to migrate, proliferate, and adhere (Figure 1.4). The healing procedure includes (i) an increase in the metabolic activity and actin filament polymerisation and reorganisation of the basal layer (Anderson, 1977). The cells at the wound edges start separating and thickening while the wound site is cleared from damaged and dead cells (Brewitt, 2009, Kuwabara et al., 1976, Crosson et al., 1986, Ljubimov and Saghizadeh, 2015). Polymorphonuclear (PMN) leukocytes a type of white blood cell that travels through the tear film to the wound, to form a temporary monolayer, that will disappear upon epithelial cell migration (Kuo, 2004, Robb and Kuwabara, 1962, Pfister, 1975); (ii) Cells begin flattening, spreading and migrating as a sheet from the wound edges, enveloping the exposed surface until it is closed (Kuwabara et al., 1976). Energy is essential for the cells to start migrating; therefore, there is an increase in the glycogen metabolism and production of proteins and glycoproteins, to serve as an energy source (Gipson and Kiorpes, 1982). A key player in the migration process is the actin filaments rearrangement and the appearance of lamellipodia and filopodia (Buck, 1985, Dua and Forrester, 1987, Dua et al., 1993); (iii) The basal epithelial cells at the limbus start proliferating, migrating, and dividing to produce TAC to become differentiated cell while moving towards the wound site, to restore

the structure and intercellular junction of the epithelium (Cotsarelis et al., 1989); (iv) cell adhesion, where newly regenerated epithelial cells restore the layer to its original state and form anchoring and cells-to-cell contact.

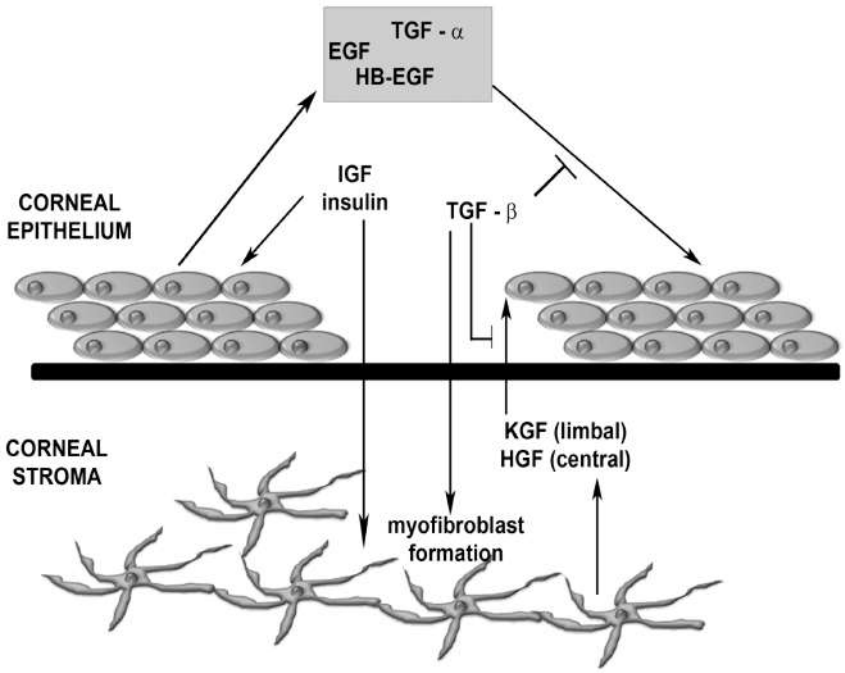

Figure 1.4 – Corneal epithelial wound healing. Upon injury, various cytokines and growth factors released to mediate wound healing. Stromal keratocytes produce hepatocytes growth factor (HGF) and keratinocytes growth factor (KGF). Epithelial cells secret Interleukin-1 (IL1) and platelet-derived growth factor (PDGF) to start stromal injury response. Transforming growth factor β (TGFβ) and epidermal growth factor (EGF) takes part in epithelial and stromal wound repair (Wright et al., 2012).

1.4.2 Corneal stromal wound healing

Deep injuries that affect the stroma initiate healing responses of both epithelial and stromal cells (Figure 1.5). The injury repair starts with Interleukin-1 alpha (IL-1α) secretion by the wounded epithelium (Wilson et al., 2003). This triggers some of the surrounding keratocytes to undergo apoptosis (Wilson et al., 2003), while others activate to proliferate and secrete matrix metalloproteinases (MMPs). The epithelial cells secrete transforming GFs (TGFβ2) into the stroma, to direct keratocyte subpopulations to transform into myofibroblasts that secrets ECM (Jester et al., 1999a). The quiescent keratocytes switch to fibroblastic phenotype, which is

capable of fibrous production and tissue remodeling (Fini and Stramer, 2005). This phenotypic change is hypothesised to be due to the high level of glucose entering the stroma, which in normal cases is prevented by epithelial cells (Foster et al., 2015). Keratocytes only activate when there is a change in the surrounding environment. This ability credited to their production source, the cranial neural crest cells. The cells at the wound site undergo apoptosis and the neighboring cells become active fibroblasts 6 hours post wounding (Wilson et al., 1996), which signals the rest of the cells to start migrating to the injury site and release MMPs (Malecaze et al., 1997). TGFβ2 inhibited when the basement membrane closes, and the number of activated myofibroblasts diminishes. The fibroblasts continue to remodel the ECM by secreting IL-1α until the stromal layer is back to functioning normally.

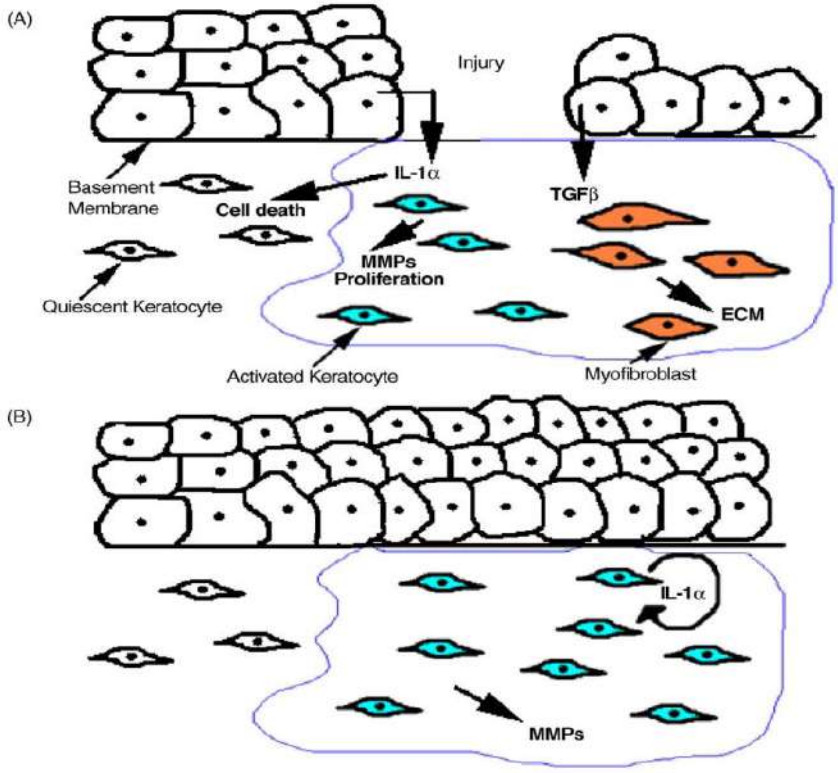

Figure 1.5 – Represents the stromal layer wound healing. (A) Upon injury, epithelial cells release IL-1α to the stroma that induces the keratocytes at the injury site to undergo cell death, whilst adjacent keratocytes undergo proliferation to secrete MMPs and become active. Since the basement membrane is open, the epithelial cells secret TGFβ2 to induce keratocytes subpopulation to become myofibroblasts and secret ECM. (B) The wound healing and the re-formation of the basement membrane stop TGFβ2 release and absence of myofibroblasts phenotype.

Meanwhile, the active keratocytes keep secreting autocrine IL-1α and ECM remodeling (West-Mays and Dwivedi, 2006).

1.5 Corneal injuries and disorders

1.5.1 Corneal abrasions

Corneal abrasions are the induction of a scratch on the transparent cornea, which causes discomfort, teary eye, and susceptibility to infection. Abrasions can be caused by much day-to-day activity, such as paper, debris, sports equipment, etc. The treatment is dependent on the severity of the scratch and the cause (Saghizadeh et al., 2017). Minor scratches can be treated with eye drops that keep the eye moist to allow for the cornea to naturally heal. Other injuries may require antibiotics, steroids, and painkillers. Severe injuries can leave a scar that affects vision. If errors arise in the cells' natural healing process, scars can occur. The best method used until now with a 90% success rate for corneal healing is a corneal transplant. The limitation affecting this therapy is the donor supply, and in some cases, rejection may occur.

1.5.2 Chemical burns

Chemical burns are one of the most common causes of corneal injuries. The severity of the burn can vary from minor burns that affect the corneal surface to more severe burns that penetrate deep into the corneal layers causing inflammation, haze, vascularization, and epithelial damage (Singh et al., 2013, Vaidyanathan et al., 2019). Treatment depends on the severity, where alkali burns are the most dangerous compared to acidic burns (Bizrah et al., 2019b, Bizrah et al., 2019a). Current research is employing different methods of cell and gene therapies. Stem cells hold great promise in the fact they are naturally occurring undifferentiated cells. These cells reside in many types of tissues in the quiescent form. Stem cells activate when there is an external signal produced by the injured cells. Natural scaffolds can be used to maintain the cells, which allow for the cells to be immobilized and functional. The combination of stem cells and scaffold holds great promise in corneal healing.

1.5.3 Keratoconus

Keratoconus (KC) is a bilateral and asymmetrical corneal disorder characterized by thinning of the corneal stroma, which results in corneal protrusion that leads to myopic shift and astigmatism (Romero-Jimenez et al., 2010, Zadnik et al., 1996, Zadnik et al., 2002). It is considered a multifactorial disorder caused by environmental and genetic factors (Bawazeer et al., 2000, Wachtmeister et al., 2009, Fabre et al., 2009). Although KC considered a non-inflammatory disease, inflammatory factors including IL and MMPs have a role in its development (Balasubramanian et al., 2012, Lema et al., 2009, Kaiserman and Sella, 2019). KC treatment depends on the severity of the disease, ranging from spectacles and contact lenses to keratoplasty in severe cases.

1.5.4 Limbal stem cell diseases

Limbal stem cell deficiency (LSCD) alters the function of stem cells at the limbus, which leads to failure in the limbal barrier, causing a malfunction in corneal epithelial healing and reduction in corneal transparency (Ahmad et al., 2010). To address this problem, several investigations were made, including the transfer of healthy LSCs, either limbal autograft or limbal allograft (Pellegrini et al., 1997, Koizumi et al., 2002). However, there is a risk in both these methods where the healthy eye may develop pathogenesis LSCD caused by medical treatment or examination due to the size of the insert that must be taken and inserted (Liang et al., 2009). To overcome this problem, LESCs have been isolated and used to reconstruct the damaged cornea (Figueiredo et al., 2004, Fernandez-Buenaga et al., 2018). Although novel therapies are emerging such as Holoclar® (Pellegrini et al., 2018), conjunctival limbal autograft (CLAU) (Kheirkhah et al., 2008), cultivated limbal epithelial transplantation (CLET) (Sacchetti et al., 2018), simple limbal epithelial transplant (SLET) (Sangwan et al., 2012), and amnion-assisted conjunctival epithelial redirection (ACER) (Dua et al., 2017), they have limitations (Dong et al., 2018, Shanbhag et al., 2019).

1.6 Mesenchymal stem cells and their therapeutic potential

Adult mesenchymal stem cells (MSCs) can be extracted from various tissues, including brain (Gonzalez-Perez, 2012, Siebzehnrubl et al., 2011), lung (Summer et al., 2007), spleen (Hoogduijn et al., 2007), heart (Messina et al., 2004), bone marrow (Peister et al., 2004) and adipose tissue (Bunnell et al., 2008). MSCs are multipotent stromal stem cells with the ability to differentiate into adipocytes, osteocytes, myocytes, and chondrocytes *in vitro* (Prockop, 1997, Yang et al., 2018). MSCs are spindle-shaped fibroblast-like cells, that can be used as a therapeutic agent or a delivery vehicle for therapeutic genes. Their ability to repair the damaged tissues has been shown in many diseases including cartilage repair(Satue et al., 2019), bone tissue engineering (Lin et al., 2017), diabetes (Pileggi, 2012), liver diseases (Tsuchiya et al., 2019), and ischemic heart disease (Klopsch et al., 2018). The International Society of Cellular Therapy stated the minimal criteria for defining MSCs *in vitro* are their adherence to plastic substrates, their ability to expand and differentiate and the surface markers they express (Table 1.1) (Dominici et al., 2006). A rich source of MSCs is the adipose tissue, via liposuction, where each year countless liposuction surgeries performed that yield a large range of lipoaspirate tissue (Alstrup et al., 2019, Schneider et al., 2017). Compared with MSCs, 1g of fat contains 500 times more stem cells compared to 1g of bone marrow MSCs. Hence, ASCs hold great experimental potential.

Positive markers	Negative markers
CD9, CD10, CD13, CD29, CD44, CD49a, CD49b, CD49c, CD51, CD54, CD58, CD61, CD71, CD73, CD90, CD102, CD104, CD105, CD106, CD119, CD120a, CD120b, CD121, CD123, CD124, CD126, CD127, CD140a, CD166, CCR1, CCR4, CCR7, CXCR5, CCR10, VCAM-1, AL-CAM, ICAM-1, STRO-1 (CD140b), HER-2/erbB2 (CD340), Frizzled-9 (CD349), W8B2, W3D5, W4A5, W5C4, W5C5, W7C6, 9A3, 58B1, F9-3C2F1, HEK-3D6	CD11a, CD14, CD15, CD18, CD19, CD25, CD34, CD31, CD40, CD49d, CD50, CD80, CD86, CD62E, CD62P, CD117

Table 1.1 – Markers used to characterize and isolate MSCs in culture as positive or negative expression. These markers depend on the source of MSCs (Data compiled from (Pittenger et al., 1999, Buhring et al., 2007, da Silva Meirelles et al., 2006)).

MSCs characteristics that make them a suitable therapeutic agent are their ease of isolation, in culture expansion, plasticity to plastic, paracrine production, regulation of inflammatory and immune responses, immunosuppressive, migration/reaction to site of injury, ethical concerns and usage in allogeneic transplantation (Chu et al., 2019, Si et al., 2019). Several factors work together to initiate wound healing, i.e., GFs and ECM proteins. A growing body of literature has shown the importance of MSCs in wound healing and their involvement in all phases of wound response (Figure 1.6). In the inflammation phase, MSCs decrease interferon-y (IFN-y) and pro-inflammatory cytokines (TNF-a), whilst increasing anti-inflammatory cytokines IL-4 and IL-10 (Aggarwal and Pittenger, 2005, Newman et al., 2009, Singer and Caplan, 2011). They have an anti-microbial ability where they secret IL-37 and immune factors that control phagocytosis and bacterial removal (Krasnodembskaya et al., 2010, Mei et al., 2010). The improvement and healing of tissue are regulated with MSCs paracrine factors production and differentiation (Saeedi et al., 2019). Research showed the main mechanism responsible for wound healing by MSCs is their paracrine signaling, and the differentiation is only secondary to that (Gnecchi et al., 2008, Duran et al., 2013, Regmi et al., 2019).

These GFs productions were proven by examination of MSC-conditioned medium (MSC-CM), which showed MSCs to release cytokines, GFs and chemokines, i.e. bFGF, VEGF, EGF, PGDF, TGF-B and KGF for tissue repair (Chen et al., 2014, Chen et al., 2008, Jun et al., 2014, Sagaradze et al., 2019). *In vitro*, MSC-CM showed to behave as chemo-attractant for epidermal keratinocytes, macrophages, endothelial cells, and fibroblasts (Gurtner et al., 2008, Hocking and Gibran, 2010, Hwang et al., 2018). It has been shown that MSCs or their CM could enhance wound healing by enhancing the dermal fibroblasts and secreting mitogens to stimulate keratinocytes, endothelial cells, and fibroblasts proliferation i*n vitro* (Smith et al., 2010, Rodriguez-Menocal et al., 2012). From the presented data, MSCs are shown to release GFs that stimulate cell migration and proliferation in response to wounds via HGF and VEGF secretion, whilst maintaining a balanced level of TGF-β3 and TGF-β1 (Colwell et al., 2005, Cha and Falanga, 2007, Lau et al., 2009).

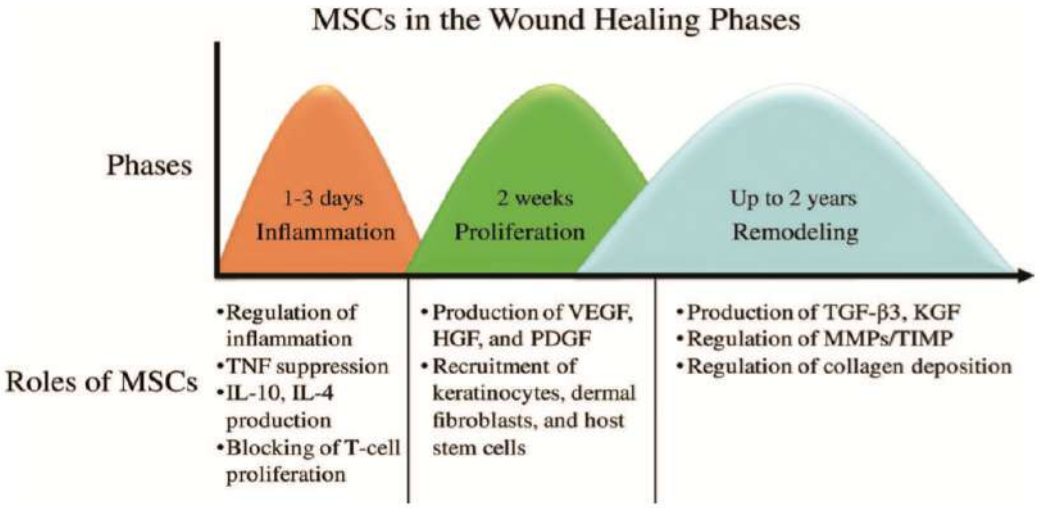

Figure 1.6 – The role of mesenchymal stem cells in wound healing phases. Abbreviations: interleukin, IL; hepatocyte growth factor, HGF; matrix metalloproteinase MMP; keratinocyte growth factor, KGF; platelet-derived growth factor, tissue inhibitor of metalloproteinase, TIMP; PDGF; transforming growth factor, TGF; vascular endothelial growth factor, VEGF; tumor necrosis factor, TNF (Maxson et al., 2012).

1.6.1 Mesenchymal stem cells in corneal treatment

The systemic administration and migration of MSCs are directed by the presence of intracellular signals, proteases, chemokines, adhesion molecules, and chemokines receptors (Chavakis et al., 2008, Wu and Zhao, 2012, Fernandes-Cunha et al., 2019, Tao et al., 2019). *In vivo* studies demonstrated the benefits of using MSCs in treating corneal wounds. The ability MSCs have on local engraftment was proven by the use of alkali burn on rabbit corneas, where it promoted cells proliferating, differentiation, and speed of healing (Ye et al., 2006). Systemically directed MSCs without engraftment were also found to reduce the corneal inflammatory injury via secreting TNF-a (Roddy et al., 2011). Subconjunctival or IV administration of MSCs following corneal injury was found to reduce aSMA, IL-1ß, and TNF-a expression whilst reducing corneal opacity, thus showing the superior efficacy of MSCs (Shukla et al., 2019). One study on a rabbit model investigated the alkali-induced oxidative wounding of the cornea using MSCs derived from rabbit bone marrow (Cejkova et al., 2013). By either seeding MSCs on a nanofiber scaffolds or applying MSCs directly to the cornea and suturing the eyelid for two

days. The results showed the superiority of MSCs seeded on nanofibers by decreasing MMPs and TNF-a production that lead to increasing of corneal thickness. A similar study showed the nanofiber to be effective in the treatment of alkali-induced wounds (Cejka et al., 2016, Treacy et al., 2014).

A great amount of research is being conducted into the use of MSCs in KC treatment (Mansoor et al., 2019). MSCs ability to release growth factors in response to the environment is one of the key therapeutic features of these cells. It has been shown that MSCs release HGF, TGF-ß1, PDGF, etc. These factors although not fully understood, were found to promote cell migration, proliferation, and extracellular matrix protein production (Jiang et al., 2017). ASCs were tested in a pilot clinical trial of advanced KC patients, which resulted in vision improvement, production of collagen which improved corneal thickness (Alio Del Barrio et al., 2017). In another clinical trial, KC patients showed improved corneal transparency when using MSCs in treatment (Alio et al., 2019). These studies however need further validation and longer follow up.

1.6.2 Multipotent adult stem cells in therapy

Multipotent adult progenitor cells (MAPCs) were discovered in 2001 at the University of Minnesota by Catherine Verfaillie (Verfaillie, 2005). Verfaillie described MAPCs as progenitor cells isolated from the bone marrow of adult patients. The cells were biologically and antigenically different from MSCs (Jiang et al., 2002, Khan and Newsome, 2019). Unlike MSCs, MAPCs are primitive cell population, able to expand and double in culture whilst retaining their differentiation potential up-to 80 passages to adipogenic, chondrogenic, osteogenic, hepatic, hematopoietic, myogenic, neuronal, epithelial and endothelial lineages. MAPCs were also shown to present favorable characteristics that are perceived in embryonic stem cells (ESC), however, unlike ESC, MAPCs have no ethical concerns since they are isolated from adult patients with their consent. Therefore, MAPCs present an encouraging source for cell-based therapy, which have been tested in many diseases in vivo, such as acute myocardial infarction (Penn et al., 2012), bone repair and myelodysplasia (Martens et al., 2017, Roobrouck et al., 2017, Plessers et al., 2016), ischemic stroke (Hess et al., 2017), and graft vs host disease (Maziarz et al., 2015). It has been shown that MAPCs have immunomodulatory effects and are able to release a cocktail of growth

factors in response to the wound (Ravanidis et al., 2015, Reading et al., 2013, Carty et al., 2018). These, however, have not been tested on the ocular surface or the cornea, hence, it is expected MAPCs to have a positive effect on corneal recovery. This effect is postulated to be driven by MSC's ability to produce growth factors, including tumor necrosis factor-inducible gene 6 (TSG-6), HGF, and TGF-ß1, among other factors.

1.7 Biomaterials for the production of stem cell bandages

Biomaterials can either be synthetic-based or natural-based materials (Figure 1.7). Naturally derived materials have frequently been used to substitute lost tissues, i.e., prosthetics. In comparison, synthetic-based polymers, metal alloys, and ceramics have presented improved performance and reproducible properties (Ratner and Bryant, 2004, Huebsch and Mooney, 2009). Biomaterials are defined as induced materials to border biological organisms to replace, increase, or treat whichever tissue, function, or organ in the body (Williams, 2009). Naturally derived biomaterials are gaining much attention recently for their unique inherent biocompatibility.

Cell encapsulation within the 3D environment is one of the approaches for the development of stem cell therapy. It is essential that the encapsulation environment is biocompatible with the cells. Ideally, the environment would be similar to the cells *in vivo* original tissue, for the cells to present the same behaviour *in vitro* and when transferred to a patient (Nicodemus and Bryant, 2008, Kachouie et al., 2010). Therefore, for the stem cell bandages approach, choosing the right biomaterial is a key to cell encapsulation and transplantation. A biomaterial should (i) maintain cell survival from days to weeks, (ii) prevents cells aggregation, (iii) aid integration into the host, (vi) control differentiation, whilst (v) allowing nutrients to reach the cells, and (vi) facilitating cell release of paracrine factors (Chai et al., 2017, Yang et al., 2017).

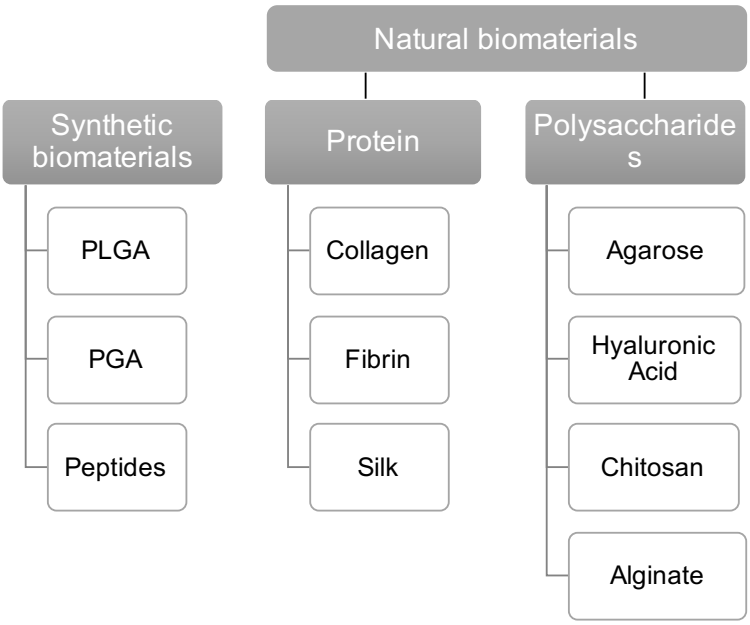

Figure 1.7 – Types of synthetic and natural-based biomaterials

1.7.1 Sodium alginate properties

Sodium alginate is a natural non-toxic water-soluble biopolymer, extracted from brown seaweed with a molecular formula of $C_6H_7NaO_6$ and molecular weight of 216.12g/mol. Alginate is considered one of the safest biomaterials that have been used, it is inexpensive and is available in large quantities. Alginate is considered to be a mucoadhesive biocompatible substance that can help maintain and support the vitality and growth of tissues *in vitro* (Gombotz, 1998). Simple cross-linking with cations can make alginate solidify. Their structure is similar to ECM of living cells; this allows them to be used widely for clinical applications as delivery vehicles (Ashimova et al., 2019). Alginate hydrogels are linear anionic polysaccharide that consists of repeated units of β-D-mannuronic acid (M) and α-L-guluronic acid (G) positioned in a homo-polymeric block (Figure 1.8). Alginate properties are dependent on the G and M residues sequence composition, which is highly dependent on the algae source, and in turn, the G/M ratio of the alginate determines the quality of the microcapsules (Tonnesen and Karlsen, 2002). Alginate hydrogels are mostly prepared as a result of the chemical and physical polymer chains crosslinking. The physicochemical characteristics of the hydrogels depend on the monomers crosslinking contents, distribution, density, molecular weight, as well as the presence of citrate and phosphate (LeRoux et al., 1999). Alginate maintains a hydrated

microenvironment, prevents bacterial infection, and enables wound regeneration (Hay et al., 2013, Bochenek et al., 2018). It can be used for a controlled release of drug molecules ranging from small chemicals to large proteins depending on the cross-linking method and type (Kong et al., 2004b). Moreover, the administration of alginate into the body can either be orally or by injection. Therefore, the use of alginate in cell transfer and transplantation to deliver cells to the injury site is a promising tool for biomedicine (Lee and Mooney, 2012).

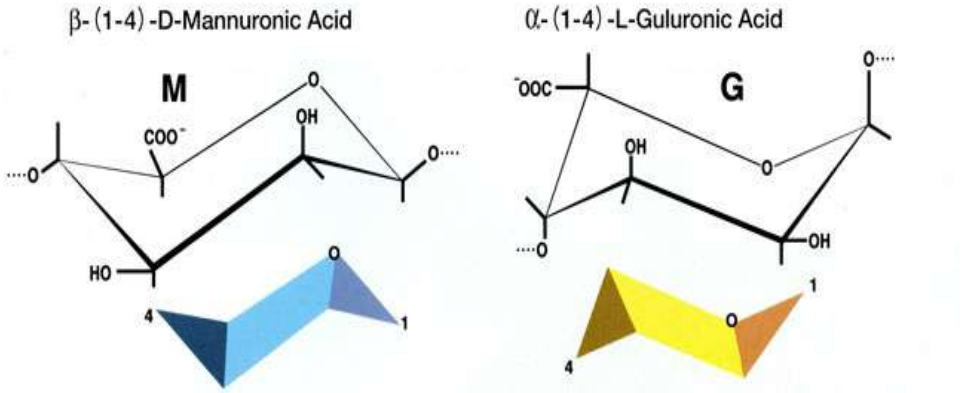

Figure 1.8 – Alginate hydrogels structure. It is composed of two Uronic acids, the Mannuronic acid (M), and the Guluronic acid (G). Three types of polymer segments formed, the M only blocks, the G only blocks and the M&G blocks. The difference in the M/G ratio and the block configuration results in different alginate functionality and properties in gelling and strength. This is dependent on the seaweeds species, location, season, and part. (http://www.kimica-alginate.com/alginate/chemical_structure.html).

The gelation of alginate hydrogels occurs upon the ionic cross-linking with the cations, the interaction of the sodium ions originates from the G blocks with the divalent ions such as calcium and magnesium ions (Ca^{2+}, Mg^{2+}) to produce an “egg-box” structure (Grant et al., 1973, Zimmermann et al., 1992). The gel three-dimensional network can form upon the interaction of every chain with various other chains; these types of gels can contain water up to 95% and can be treated with heat without melting (Kong et al., 2004a). Alginate gels that contain a large number of G residues are strong, stable, and more porous than the ones with M blocks. It has

been stated in previous researches that the higher the G content of the alginate the stronger the prevention of solute transport, and in reverse, the higher the M content in the gel the weaker and more elastic it becomes (Zhao et al., 2010).

1.7.2 Alginate encapsulation in therapy

Transplanting cells is an attractive method to promote healing of the ocular surface, especially when the host cells can respond to the released signals. In a study, MSCs have been encapsulated in alginate-PLL for extended periods where it showed stable cell proliferation and viability; spread cells, with stem cells properties (Goren et al., 2010). This study showed the alginate-encapsulated cells did not affect MSCs properties. Another investigation on the storage of alginate encapsulated MSCs in hypothermic conditions, where it resulted in no change in cell function following 3 days of storage (Swioklo et al., 2016). Therefore, encapsulating MSCs in alginate hydrogels show a promising method of cell therapy, which can improve the biocompatibility and long-term transportation of stem cells bandages.

Alginate has been investigated as a biomaterial for biological use due to its proven biocompatibility, low cost, speed of gelation when crosslinked with calcium ions, and low toxicity (Sun and Tan, 2013, Augst et al., 2006). Alginate as bandages was found to prevent wound dehydration, reduce infection, and initiate wound recovery (Aderibigbe and Buyana, 2018). Alginate therapy tested for the treatment of gastroesophageal reflux disease where it showed improvements in the symptoms (Leiman et al., 2017, Bor et al., 2019). Alginate can be administered orally or injected into the body without causing side effects, thus, it is important in many pharmaceutical applications (Bidarra et al., 2014). Cell therapy is looking into delivering functional cells into the injury site to replace or induce the production of paracrine factors (Kim, 2013). Alginate as a wound dressing material maintains a moist environment, reduce bacterial infection, and induce wound healing. Alginate has also been tested in tumor therapy, where authors loaded arsenic trioxide to alginate that resulted in toxicity reduction (Lian et al., 2019). Depending on the cross-linker used, alginates can be controlled in releasing drug dosage inside the wound, which makes them appealing for pharmaceutical applications (Lee and Mooney, 2012). For this, alginate hydrogels can be used to deliver cells into the injury site to induce the resident cells in regenerating the tissue. (Grøndahl et al.,

2020) Alginate hydrogels have been used in cultivating corneal endothelial and limbal stem cells, where it suggested that alginate can aid in corneal regeneration (Wright et al., 2012, Liang et al., 2011). It has also been found that alginate maintains ASCs viability and functional ability during short-term hypothermic storage (Swioklo and Connon, 2016, Swioklo et al., 2016). This ability of alginate is a key feature in the formation of stem cells bandages (Varaprasad et al., 2020). As such, alginate showed prominence in wound dressing.

1.8 Hypothermic storage effect on viable cell recovery

To develop stem cell therapy the final product must be tested and approved by the regulatory authorities. The absence of contamination is a key step in the formation of the final product (Galvez et al., 2014, Coopman and Medcalf, 2014). Sterility testing is another aspect that must be tested when storage is involved (Use, 2017). Transporting therapeutic cells from the laboratory to the patient is an important consideration for successful therapy (Petrenko et al., 2019). Hydrogels able to maintain cells hydrated state resist physiological damage while preventing cell release into the wound bed. Transporting the bioactive material require storage at a specific temperature. An important aspect is that the storage must not harm the cell, i.e. reduce cells function and viability. Thus, it is vital to test different storage temperatures to find a suitable storage condition.

1.9 Cell therapy delivery and limitations

An important aspect of cell therapy is the delivery of therapeutic cells to the injury site without losing their viability and functionality. Current delivery systems, such as systemic and intradermal injections have limitations of cell loss (Li et al., 2015, Lukomska et al., 2019). During cell migration to the injury site most cells will be trapped in the spleen, kidneys, and lungs while injecting a large number of cells could solve this issue, it could result in low engraftment efficacy due to fast diffusion. Another method is to transfer cells directly to the injury site; however, this method can cause differentiation to the transferred cells which leads to loss of function. Therefore, trapping cells within a functional material presents a solution, where the cells maintain their phenotype, viability, and most importantly, are able to release

therapeutic factors from within the scaffold. It has been found that sodium alginate, a material used in wound dressing (Wang et al., 2016), protein, and cell immobilization (Schmitt et al., 2015) are able to trap MSCs while maintaining their viability. Cell storage is also one of the important aspects to consider in transferring therapeutic cells to the clinic, which should maintain cell viability and function during storage and transfer to induce wound recovery. Previous studies from Prof. Connon's lab has found that entrapping MSCs within sodium alginate maintains their viability and functional recovery following hypothermic storage for a period ranging from days to weeks (Chen et al., 2013, Swioklo et al., 2016). They also show that MSCs in suspension had the highest recovery rate following storage at 15°C compared to cells stored in the same condition without alginate. Therefore, alginate presents a safe, low-cost method of preserving cells for up-to several weeks without losing their viability or function, which gives enough time to transport the cells from the manufacturing site to the clinic.

1.10 Research aim and hypothesis

We are interested in the formation of bioactive, biocompatible, and cost-effective stem cell-based bandages capable of stimulating the wound repair process. Hence, the main aim of this project is the formation of stem cells bandages. These bandages formed using sodium alginate to encapsulate adipose-derived stem cells (ASCs) to speed the migration/healing of human corneal wounds. To address this, we chose ASCs as the main therapeutic cells. ASCs can be extracted in large numbers, hold no ethical concerns, and showed to produced paracrine factors that aid in wound healing (Si et al., 2019, Yang et al., 2010). we also chose sodium alginate as the main carrier material. Alginates are present in nature and extracted from brown seaweed, calcium alginates are used in enzyme immobilizing, food/cosmetic manufacture and in wound dressing. Generally, this material is safe, cost-effective and widely used in biomedical due to its biocompatibility, and ease of handling (Lee and Mooney, 2012). Within the thesis, we used a standard scratch assay to assess the effect of stem cell bandages in a co-culture. The therapeutic effects of ASCs bandages formed in sodium alginate investigated on corneal stromal cells and corneal keratoconus. Their effect was tested following hypothermic storage. Moreover, we evaluated the conditioned media produced from the bandages in scratch healing. Following which, conditioned media tested for soluble protein concentration using Bradford assay, ASCs production of paracrine factors were tested using qPCR and an XL cytokine array kit (such as HGF, TGF, and VEGF) and corneal cells tested for collagen production using Sirius red staining. On the other hand, MAPC bandages were used and compared to ASCs in wound healing. Lastly, an animal study using corneal chemical burn was performed as a proof of concept of ASCs bandages. ASCs bandages improved corneal stromal and keratoconus cells scratch wound healing via the production of paracrine factors. ASCs' ability to influence a secondary population was shown whilst within the bandage. ASCs were found to produce paracrine factors (i.e HGF, EGF, TGF-ß) following hypothermic storage. ASCs bandages also improved *in vivo* corneal chemical wound healing whilst reducing immune cell infiltration. Thus, shown the importance of using ASCs bandages in corneal healing.

Chapter 2. Materials and methods

2.1 Cell culture and isolation

2.1.1 Isolation of human corneal stromal cells

The corneal ring is referred to as the transparent cornea with the conjunctiva cut in a ring shape from the eye for research. Human Corneal rings were collected from healthy cadaver donors as grafting procedures by-products, kindly provided by Prof. Francisco Figueiredo (Royal Victoria Infirmary, Newcastle Upon Tyne, UK). The rings obtained following an informed approval according to Newcastle University and Newcastle Upon Tyne Hospital Trust Research Ethics Committees guidelines. The rings were collected and delivered to the lab within 30 days post mortem, (male/female, with age range +/- 70 years old). The corneas were stored and maintained in a medium with nutrients to keep the cornea fresh in glass flasks. Upon receipt, the corneal ring flasks were maintained at room temperature until further use.

Corneal explants were minced using sterile blade and forceps in a DMEM: F12 digestion medium. Dulbecco's Modified Eagle Medium: Nutrient Mixture F-12 (DMEM: F12) (ThermoFisher Scientific, Cramlington, UK) is a high glucose medium contains GlutaMax™ -1 with phenol red. The basal media is supplemented with 5% Fetal Bovine Serum (FBS) (ThermoFisher Scientific, UK) and 1% penicillin-streptomycin (ThermoFisher Scientific, UK). This media composition is the basic corneal stromal cell extraction and expansion media termed '5% media' in all of the subsequent experiments.

For the extraction of corneal stromal cells (i.e. corneal fibroblasts) (CSF) (Diagram 2.2), the minced explants were incubated with digestion media containing 2mg/mL (450units/mL) collagenase type I (ThermoFisher Scientific, UK) powder dissolved in 10mL of the 5% media and sterilised via filtering in a sterile Sartorius™ Minisart™ syringe filters, with 0.2µm pore size and 26mm diameter (Sigma-Aldrich, St. Louis, Missouri, UK). The explants were transferred into a 15mL centrifuge conical tube (Sigma-Aldrich, UK) along with the digestion media, and placed inside the incubator set at 37°C and under constant rotation for 5 hours.

Collagenase type I is a key enzyme in digesting corneal tissues to allow for CSF extraction. Whilst the rotation of the tissues in the falcon-tube prevents the explants from settling at the bottom of the tube, which otherwise may block the enzyme infiltration and in turn stops CSF extraction. 5 hours following incubation, the medium that now contains CSF along with the enzyme-digested explant were filtered via sterile EASYstrainer^{TM} cell strainer with 40µm pore size (Sigma-Aldrich, UK) into a 50mL centrifuge conical tube (Sigma-Aldrich, UK). Cell strainer only allows for cells to pass throw the filter and so separate cells suspension from the minced corneal explant. The cell suspension was diluted with 0.25% trypsin-EDTA solution (Sigma-Aldrich, UK) in a 1:1 ratio that was also passed through the strainer, to increase the retrieval of cells that did not pass through the strainer. Trypsin functions to cleave C-terminal peptides of lysine and arginine residues while EDTA acts as a chelating agent to prevent any blockage of the trypsin activation via chelation of magnesium and calcium ions. Therefore, this enzyme will dissociate cells aggregation in the medium and prevent their clumping. A cell pellet was obtained after 5 minutes centrifugation at 1500xg and resuspended with 1mL 5% media. Cells in suspension were then transferred into a vented cell culture flask with a surface area of 75cm^2 (Sigma-Aldrich, UK), assigned passage number 0, and incubated at 37°C. in CSF basal media. The media was changed 3 times a week to remove dead cells and cell waste and add fresh nutrients. Upon confluency (typically at 70%), the cells were further passaged (as described in section 2.2.2) and used for subsequent experiments.

2.1.2 Human keratoconus fibroblasts culture

Human keratoconus cell (KC) cultures were received from Dr. Dimitrios Karamichos (University of Oklahoma Health Sciences Centre, Oklahoma City, USA). These primary cell cultures were previously isolated from patients (n = 4) with Keratoconus disorders with Dr. Karamichos' lab as previously described (Karamichos et al., 2012). Cells were received in cryovials containing 1 x 10^6 cells/mL at which point they were defrosted and subsequently expanded in DMEM: F12 medium supplemented with 10% FBS and 1% penicillin-streptomycin. The primary culture of KC cell lines was used up to passage 5 in the subsequent experiments.

2.1.3 Human adipose-derived stem cells culture

StemPro™ human adipose-derived stem cells (ASCs) (Invitrogen, ThermoFisher, UK) were commercially purchased. The cells were isolated from lipoaspirate tissues of healthy donors. The primary cell cultures were expanded for one passage and cryopreserved in 20% DMSO and MesenPRO medium. MesenPRO RS™ Medium (ThermoFisher, UK) is a specific medium for human mesenchymal stem cell growth. The basal medium is formulated with a reduced serum of 2% and supplemented with MesenPRO RS™ growth supplement (ThermoFisher, UK) manufacturer defined, 2% antibiotic-antimycotic (100X) (ThermoFisher, UK) and 1% GlutaMAX (100X) (ThermoFisher, UK). The antibiotic-antimycotic solution prevents bacterial and fungal formation and so prevents cell culture contamination. GlutaMAX improves cell growth and viability and reduces toxic ammonia accumulation. The supplied ASCs were tested for viability, sterility, mycoplasma contamination, human pathogen contamination, and purity by the supplier. In the lab, the cells were tested for their differentiation potential *in vitro* to adipocytes, osteoblasts, and chondrocytes.

The primary cell line of ASCs used in the following experiments originates from lipoaspirate surgery of a 43 years old female, the abdomen of a 45 years old female, and the abdomen of a 63 years old male donors. Each of the donor's cells was provided with a certificate of analysis (including viability, sterility, mycoplasma, a human pathogen, and purity tests) and confirmed to be ASCs, and they meet the requirements for research. The cells were shipped in cryovials in a sealed container, each vial contained 1 x 10^6 cells in 1mL MesenPRO medium. Upon receiving the vials, the cells were expanded to produce a working stock cell, then split and frozen in separate vials, where each vial contains 1 x 10^6 cells/mL and stored in liquid nitrogen until needed.

2.1.4 Human dermal fibroblast culture

Human dermal fibroblasts (hDF) were purchased from Gibco (Invitrogen, UK). Cells were received in cryovials containing 1 x 10^6 cells/mL at which point they were defrosted and subsequently expanded in DMEM: F12 medium supplemented with

10% FBS and 1% penicillin-streptomycin. The cell cultures of hDF cell lines were used up to passage 5 in the subsequent experiments.

2.1.5 Human multipotent adult progenitor cells culture

Human multipotent adult progenitor cells (MAPCs) are a primitive cell population isolated from adult patients, they can expand up-to 80 passages without losing their phenotype. They were found to present favourable characteristics that are shown in embryonic stem cells, with no ethical concern, which makes them favourable in cell therapy. MAPCs were received in association with ReGenesys (Heverlee, Belgium). The cells were stored in cryovials containing 10 x 10^6 cells/mL with Xeno-free media. Xeno-free media (XFM) (XF MAPC medium, GeGenesys, Belgium) is animal free-origin medium supplemented specifically for MAPCs survival and growth in culture by the collaborator. The primary cell line received were labelled as passage 1 and expanded in CellBIND tissue culture plastic (Sigma-Aldrich, UK) as recommended by the supplier. MAPCs cultures were used up to passage 2 in the subsequent experiments.

2.2 Cell cultures detachment

Cell dissociations were performed as follows; media that was original with the cells were removed, and cells washed with sterile phosphate-buffered saline (PBS) (ThermoFisher, UK). PBS is a balanced salt formulated without magnesium, calcium, or phenol red, therefore, it is effective in removing chelators from cell cultures. PBS is mainly used for washing cells prior to detachment, they are supplied as tablets and each tablet is dissolved in 500mL ultrapure distilled water followed by autoclaving. Following PBS wash and removal, TrypLETM Express Enzyme (1X) (ThermoFisher, UK) was added to cover the cells layer and incubated for a maximum of 10 minutes at 37°C at which point the individual cells rounded up and started floating. TrypLETM Express is a recombinant enzyme, animal-origin free, highly purified, with EDTA as a chelating agent that mainly cleaves C-terminal peptide bonds of lysine and arginine. 5% of media was then added to wash the remaining cells with gentle pipetting until all cells were in suspensions. The cell suspension was then transferred into a 15mL conical tube and centrifuged for 5 minutes at 1500xg. The supernatant was then

discarded and the cell pellet was resuspended in 1mL media and cultured in a vented cell culture flask and assigned an increased passage number (i.e. p1, p2) to prepare for further studies.

2.3 Cell counting and viability assessment

Countess II FL Automated Cell Counter (ThermoFisher, UK) was used to give accurate and quick results of cells number. Cell Counting Chamber Slides Kit (ThermoFisher, UK) was used to count the cells. The kit contains 2mL Trypan Blue solution 0.4%, which usually used to determine cell viability employing the dye exclusion test. This test centered on the concept that lives cells do not allow the dye to penetrate inside and only dead cells will be dyed. The kit also contains counting chamber slides, which designed specially to work with the Countessâ. To count cell number 10µL of cells resuspension was mixed with 10µL of trypan blue dye and transferred inside the slide chamber for counting. The Countessâ gives results of the total number of cells, viable cells, dead cells, and their percentages. For the expansion and growth of cell cultures in culture flasks, corneal CSF and KC were seeded in a density of 6 x 103 cells/cm2 and ASCs seeded in a density of 8 x 103 cells/cm2, while MAPCs seeded in a density of 2 x 103 cells/ cm2, all of which were suggested by previous work.

2.4 Corneal cells plating in serum-free media in preparation for subsequent experiments

Corneal cells plating took place after reaching 80 - 90% confluency, during passages 1 - 4. CSF and KC cultures were plated in a Multidish Nunclon 6-well plate 132 x 88mm (ThermoFisher, UK). CSF and KC were seeded in a density of 2.5 x 10^5 cells/well and cultured in 5% media for 24 hours, followed by 72-hour incubation with standard media (serum-free DMEM: F12 supplemented with 1 x 10^{-3} M L-Ascorbic acid (Sigma-Aldrich, UK), 1:100 Insulin-Transferrin-Selenium (ITS-G) (Invitrogen, UK) and 1% penicillin/streptomycin). Serum-free media (SFM) induce CSF to their inactive format, termed ‘CSC’.

2.5 ASCs plating in a transwell

To measure ASCs' effect on a secondary population, ASCs were plated on a transwell and cultured with CSC in a 6 well plate. Two different methods were used to handle ASCs, (i) 5x 105 cells were plated directly on a transwell and incubated for two hours at 37°C and 5% CO2 to allow cell attachment. (ii) 1 x 106 cells were stored in suspension at 4°C and 15°C for 72 hours in cryovials with 1 mL SFM. Following recovery from storage, the cells were resuspended, counted, and incubated on a transwell membrane at 37°C for 2 hours to allow cell attachment. Following this, membranes were washed gently and used for a scratch assay experiments.

2.6 Preparation of stem cells bandages

Stem cell bandage formation took place after reaching >90% confluency, utilising cell culture passages 3 – 5. Cells were detached using TrypLE enzyme and counted using Live/Dead® Viability/Cytotoxicity Assay (ThermoFisher, UK). Live/Dead assay is a mixture of two types of fluorescence dyes, calcein AM stains live cells green while ethidium homodimer (EthD-1) stains dead cells red. These probes recognise cell membrane integrity and intracellular esterase activity, and so, calcein AM can be retained inside live cells whereas EthD-1 is retained inside dead cells. Live/dead stain is mixed with the cells in suspension at a 1:1 ratio and incubated for 15 minutes at 37°C humidified incubator. The mixture is then counted using Countess II FL Automated cell counter to determine the number of cells required to be encapsulated. A 2.4% (w/v) calcium alginate (NovaMatrix, FMC, Norway) working solution was used to encapsulate cells.

A cell suspension containing 1 x 10^6 cells in SFM was suspended in a 1:1 ratio with calcium alginate solution in a total volume of 0.5mL. The mixture, containing calcium alginate ± cells were cast within filter paper moulds (defined below) to form the initial encapsulation (Diagram 2.1 A). The alginate ± cells mixture was crosslinked with 102mM calcium chloride (Sigma-Aldrich, UK) to form and stabilise the bandages. The filter paper moulds (1mm thickness, 24mm diameter) were stacked in a doughnut shape and soaked with 0.5mL $CaCl_2$ for two minutes. Following initial gelling, the bandage was then transferred to 4ml $CaCl_2$ for a further

6 minutes incubation followed by a brief wash with sterile PBS, which resulted in the formation of stable alginate bandage ± cells that were transferred for subsequent experimental use.

Following bandage formation, the stabilised bandages were transferred into a transparent 6-well insert 0.4μm pore diameter (Greiner Bio-One LTD) and placed inside a 6-well plate (Diagram 2.1 B). The plate was then sealed with parafilm (Sigma-Aldrich, UK) and placed into a non-ventilated incubator or fridge that precisely controlled the external temperature facilitating the storage of cells at a fixed temperature of 4°C or 15°C, for three days. The bandages were submerged in a 3.5mL SFM medium to prevent dryness and allow the diffusion of growth factors from the bandage into the surrounding medium.

The bandages + cells were released via incubation with 3mL of 100mM trisodium citrate (Sigma-Aldrich, UK) at room temperature to rapidly dissolve the gel (Diagram 2.1 C). PBS was added to the mixture to make-up a final volume of 10mL before centrifuging at 1500xg for 5 minutes. Cells pellet was then resuspended with 0.2mL medium before counting with live/dead stain.

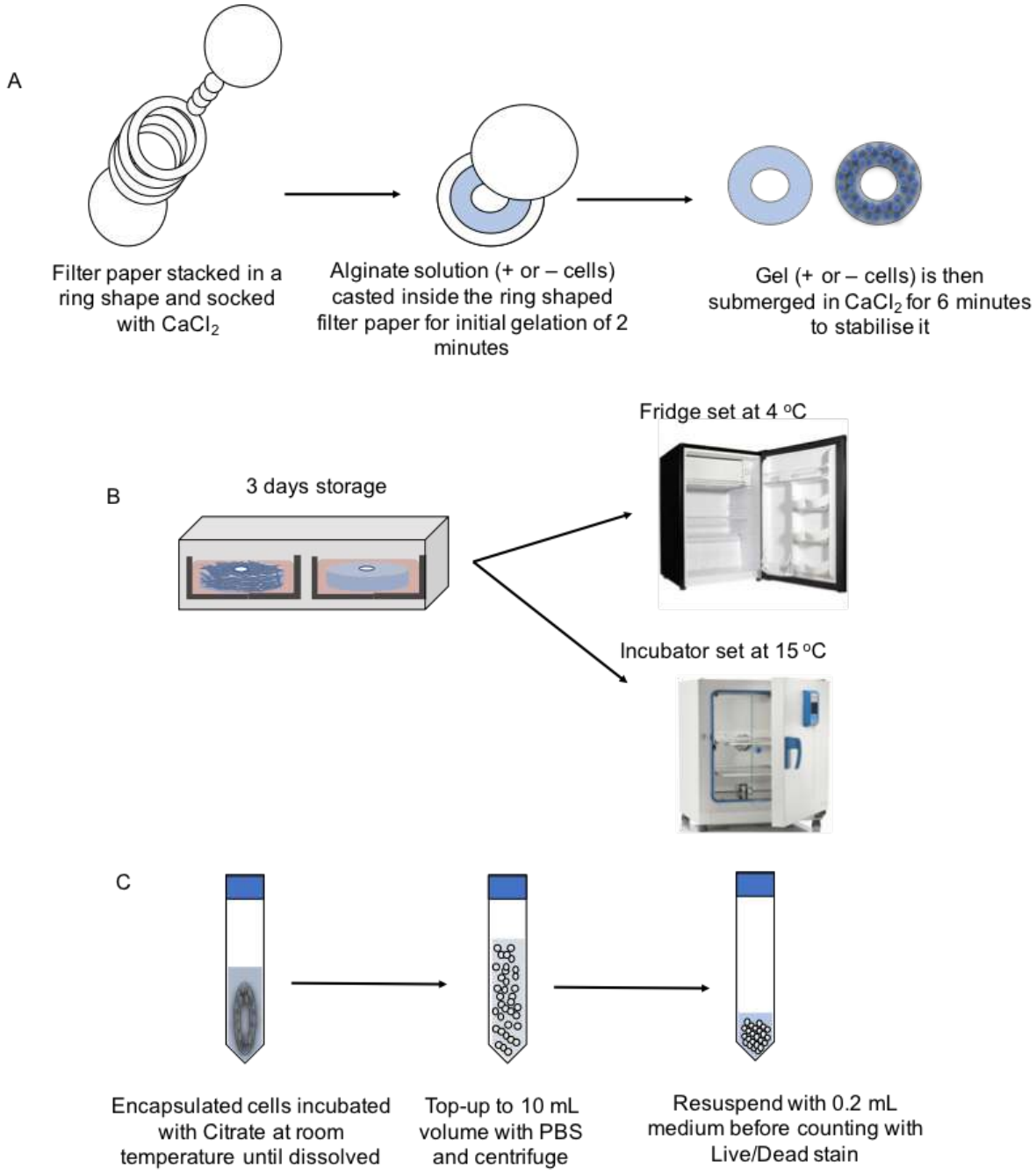

Diagram 2.1 – Formation of stem cell bandages. Cells encapsulation, storage, and release procedure. (A) Filter paper moulds were stacked in a ring-like shape and socked with $CaCl_2$ to cast the already prepared mixture of alginate ± cells for 2 minutes initial gelation before transferring to a 4mL $CaCl_2$ to stabilise the bandage. (B) The stabilised bandage is placed inside a transparent 6-well insert, 0.4µm pore diameter and placed inside a 6-well plate and sealed before placing the plate in temperature controlling container, to prevent a hasty temperature drop that would otherwise kill the cells, the container is then placed in a fridge set at 4°C or incubator set at 15°C for 72 hours. (C) The bandages + cells were incubated with citrate at

room temperature until dissolved before diluting the mixture with PBS and centrifuging for 5 minutes at 1500xg to pellet the cells, cells pellet is then resuspended with 0.2mL media before counting with live/dead stain.

2.7 Light microscopy imaging

Following ASCs release, cells were counted and plated in a 24 wells plate (Greiner Bio-One, Austria) at a density of 5000 cells/cm^2 with MesenPRO medium for 24 hours. Cell morphology assessed using a light microscope (Leica Microsystems, Wetzlar, Germany) imaging system at 10x objective magnification. Cells phenotype was assessed after storage and release from encapsulation and compared to the normal cell culture morphology.

2.8 Flow cytometry

ASCs were assessed for their immune-surface markers before and after cell culture experiments, using positive and negative markers of mesenchymal stem cells. Positive surface markers included CD90, CD73, HLA ABC, and negative markers include CD45, CD14, and HLA DR (BD Biosciences, Becton Dickinson, Franklin Lakes, New Jersey, USA) (Table 2.1).

Flow cytometry (Diagram 2.2), employs cell sorting procedure, all cells that pass through the nozzle get sorted in a single line in the beam. Cells that pass through the beam scatter the light forward (FSC) and a side (SSC) scatter light that is detected by the detectors. While cells labeled with fluorescent antibodies emit fluorescence light to be detected by the detectors. The detectors detect and analyze the cells as they go through the beam. The forward scatter relates to the cell size, while the side scatter relates to the cell density i.e. membrane size and cytoplasmic granules number. Therefore, when using this technique, cells can be sorted and diluted in enough media to be in a single cell and not clumped or aggregated.

Sample preparation for direct immunofluorescence staining was as follows; cells were harvested and counted for a total of 120,000 cells in 0.1mL PBS in a microcentrifuge tube. Cells were incubated with 10µL markers mix of CD90 FITC & CD72 PE, CD45 FITC & CD14 PE, HLA-ABC & HLA-DR, IgG2a PE, IgG1 FITC & IgG1 PE in the dark at room temperature for 20 minutes. The microcentrifuge tubes

were centrifuged at 1500xg for 5 minutes, discarded supernatant leaving 10-20μL and resuspended with 0.1mL PBS, followed by filtration using 30μM cell filters into a FACS tube (Flow Cytometry Core Facility, Newcastle University, UK) to remove cell aggregation or clumps. Lastly, 0.2mL of PBS was added through the filter to increase the volume of cells suspension and to ascertain total cell collection - no cells left in the filter - for the following cell reading.

Flow cytometry BD LSRFortessa™ (BD Biosciences, Wokingham, Berkshire, UK) was used to detect cell markers and results were plotted and processed using BD FACSDIVA software. In the software, the worksheet was adjusted as follows, 'Folder', 'Experiment', 'Specement', and 'Tube' files were made to save the results. In the global worksheet, 2 windows of 'Dot plot' Histograms were made to assess the forward and side scatters before reading the samples. The Histograms were adjusted to read the FITC filter (2-488/530/30-A) and PE filter (2-488/585/42-A). Polygon Gates were placed on the FSC-SSC dot plot. Contour Plot was also chosen to show cell density, and a Dot Plot for florescent reading was used with a quadrant gate. 'Acquire' was chosen after placing the sample tube, and the reading was saved after 15 seconds for all samples. The following parameters were used for the sample readings; voltage FSC 250 and SSC 250, high flow rate 120μL/minute, 10,000 events to record and 100,000 events to display, and negative isotype controls were used to assess the antibody signal, where values of 1.4% were considered optimal.

Antibody	Marker type	Isotype control
CD 90 FITC	Positive	**IgG1 FITC+IgG1 PE**
CD 73 PE	Positive	**IgG1 FITC+IgG1 PE**
CD 45 FITC	Negative	**IgG1 FITC+IgG1 PE**
CD 14 PE	Negative	**IgG2a PE**
HLA ABC FITC	Positive	**IgG1 FITC+IgG1 PE**
HLA DR PE	Negative	**IgG2a PE**

Table 2.1 – Flow cytometry antibody markers used to label adipose-derived mesenchymal stem cells.

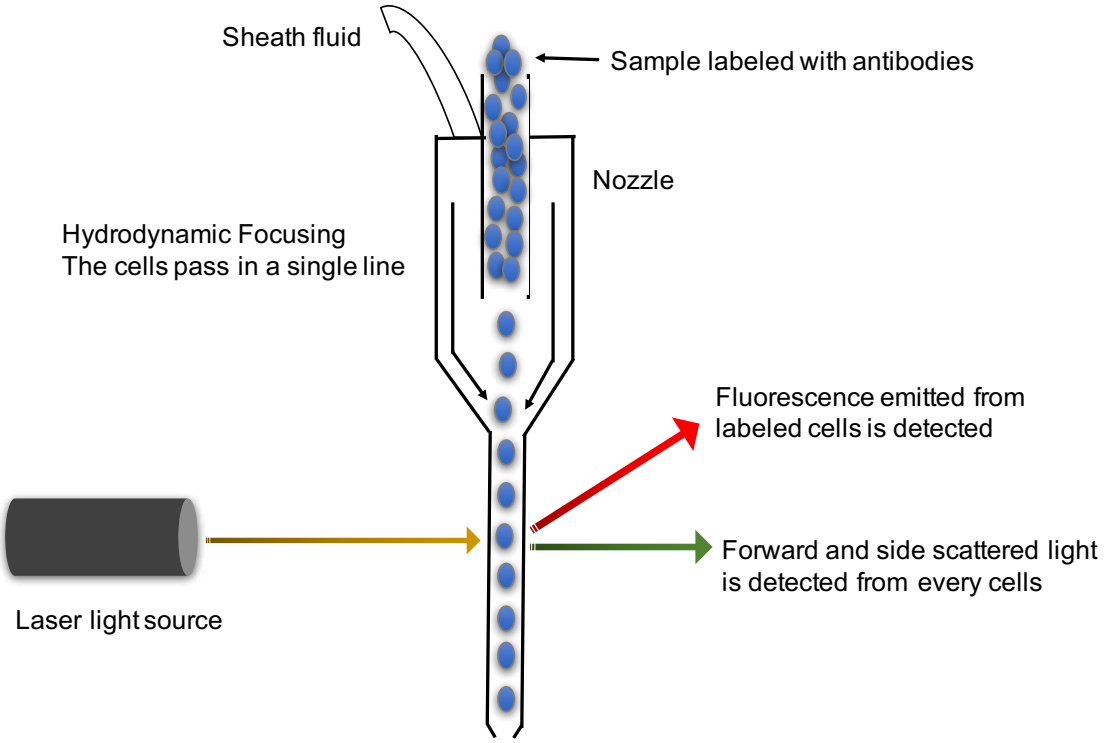

Diagram 2.2 – Flow cytometry principle. Cell suspension go through nozzle and cells get sorted in a single line before light reflects on them, and the labeled cells emit fluorescence, whilst forward and side scatters detected from all cells that pass through reflecting cell size and density respectively.

2.9 Generation of conditioned media

We sought to test the Conditioned media (CM) produced by the ASCs to assess whether the bandages prevented the cells from releasing paracrine factors or if storage temperature had any effect on the number of paracrine factors produced. CM that contains all possible secreted factors by ASCs such as exosomes, microvesicles, growth factors, and cytokines were collected. CM collected the following storage at 4°C and 15°C. The collected CM was centrifuged to remove debris and stored at -80°C until use to give an analysis of the level of growth factors and cytokines released during storage. ASCs were cultured in a reduced serum media until encapsulation, where they were washed a few times with PBS and encapsulated in SFM media followed by 3 days storage, thus, we expect no serum contamination to have affected our cultures.

2.10 Cell lysis within scaffold

Cell lysis is the breakage of the cell membrane and the release of cell components to the environment. One common method used for cell lysis is freeze-thawing, which involves freezing cells (in the absence of a cryo-protectant) followed by thawing cells at room temperature. This method elicits the cells to swell due to ice crystal formation during freezing, which then contracts during thawing, thus, cells will break releasing their components into the media (lysate). Following encapsulated ASCs storage at 4°C and 15°C, the encapsulated cells were placed at -80°C for two hours, to allow for cell lysis within alginate and the release on their components into the media for the formation of lysate. Followed by 30 minutes thawing at room temperature to allow the bandage to return to room temperature before use in scratch-wound. During thawing, the medium incubated with the bandage contains the released components of the lysed cells, which is referred to as cell lysate. In the following experiments, cells lysis used ± their lysate.

2.11 Mechanical-wound assay

In vitro scratch assay is the simplest and most economical method to investigate cell migration and/or proliferation in response to a physical assault/wound. This mechanical wound assay is one of the most common method of measuring cells behaviour *in vitro*. The assay includes the introduction of a physical wound to cells confluent monolayer. Mechanical cell scratching offers a simple, cost-effective method with a variety of approaches used to create scratches such as pipette tips. The methods used in the following experiments was created using the fine end of a sterile 1mL pipette tip (diameter 1.15mm). The scratches were performed on a cell monolayer grown in a 6-well plate (surface area of 9.6cm^2) in a straight line as shown in Diagram 2.3 c. To standardise scratch formation, we (i) used a blue tip to induce the scratch, (ii) used the same area to image the scratch, which is the middle of the well, and (iii) measured the same area size using ImageJ software.

Images of the scratches were taken using Iprasense lens-free microscopy (Cap Alpha, Avenue de l'Europe, 34830 CLAPIERS, France) 6-well cytonote. The cytonote is designed to take time-lapse images of the cells inside the incubator using

a holographic reconstruction algorithm. Iprasense holographic microscopy is a live cell imaging system that can be used inside the incubator. It has a wide field of view (29.4mm^2), with LED 650nm light source and a CMSO 10 Mpix sensor, which makes it the preferred imaging system for our experiments (Diagram 2.3). Following image taken, images were analysed using ImageJ (version 1.49u) software using the Polygon selection tool, the cell-free area was chosen and from the Analyze tab, plugin Measure used to give a reading of the scratch area in µm. The area values were then transferred to a spreadsheet and graphs plotted using Prism 6.0 software. Images at the time (t) = 0, 20, 30, and 40-hours post scratch were analysed using ImageJ and presented after adjusting the Colour Balance and adding the scale bar before correcting the Black & White scale using PhotoScape X 2.9.

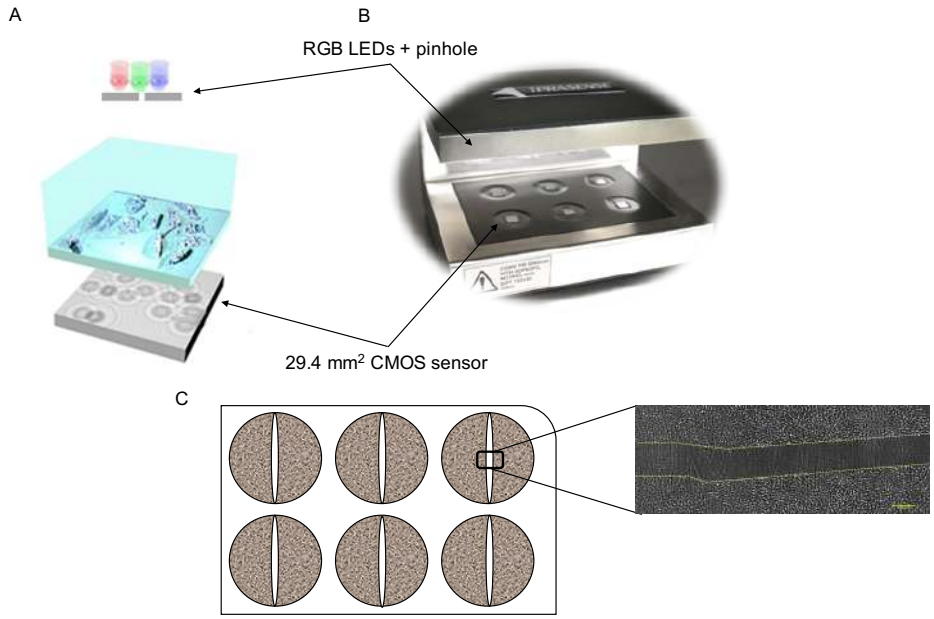

Diagram 2.3 – Iprasense lens-free microscopy. (A) Lens-free microscopy acquisition system, RGB LED and pinhole placed roughly 5cm above the sample where they provide illumination. (B) 6-well plate cytonote used to take time-lapse images inside the incubator via a holographic reconstruction algorithm, the microscope uses CMOS image sensor with image area of 29.4mm^2 (6.4 mm x 4.5 mm). (C) The microscope allows for the imaging and analyzing of the cells monolayer behavior upon wounding. Images (A and B) are taken from the manufacturer guide.

2.12 Assessment of corneal cells collagen production

Following scratch healing, human CSC was stained with Picro-Sirius Red (Sigma-Aldrich, UK) a polyazo dye that is used to determine collagen production, by staining collagen fibers in red, and subsequently dissolved in picric acid to keep the solution stable. The stain was used as previously described by Dapson *et a*l (Dapson et al., 2011), briefly; following three days post-scratch, the plates were gently washed with warm PBS before fixing with 70% ice-cold EtOH (absolute ethanol, VWR, Lutterworth, Leicestershire, UK) for 10 minutes, followed by overnight incubation at 4°C with Sirius red stain and gentle agitation to allow for equilibrium staining of the cells. Plates were washed with double distilled water before adding 1M sodium hydroxide (NaOH) (ThermoFisher, UK) with gentle agitation to allow cells dissociation from the plate, 100µl were aliquoted into 96-well plate and absorbance measured at 490nm. The collagen results were plotted against a Rat Tail Collagen I (First Link Ltd, UK) standard curve made at different concentrations.

2.13 Total protein analysis

Bradford protein assay is a quick analytical procedure used to measure the amount of protein in a sample. The assay is a colorimetric protein assay that measures the shift in absorbance of the Coomassie Brilliant Blue G-250 dye. The colour range from blue (anionic), green (neutral) to red (cationic) depends on the amount of protein present in the sample. Quick Start™ Bradford Protein Assay (Bio-Rad Laboratories Ltd, Watford, Hertfordshire, UK) was used to measure the protein concertation in conditioned media samples.

The protein content within the conditioned media was concentrated prior to mixing with the 1x dye via adding 4x volume of ice-cold 70% EtOH (VWR, UK) stored at -20°C to the conditioned media (i.e. 800µl of EtOH was added to 200µl of conditioned media) and allowed to incubate overnight at -20°C, followed by 10 minutes centrifugation at 10,000xG at 4°C, the protein pellet was allowed to dry at room temperature before resuspending with PBS. According to the manufacturer, 5µl of the concentrated protein was then mixed with 250µl 1x dye and incubated for 20 minutes at room temperature, the mixture was then aliquoted to 96-wells plate and absorbance was then taken at 595nm using VariosKan LUX Multimode Microplate

Reader (ThermoFisher, UK) (Diagram 2.4). The results were plotted against a standard curve made of bovine serum albumin (BSA) protein standard provided by the manufacturer. BSA is a purified protein used as a reference protein to give a relative protein value.

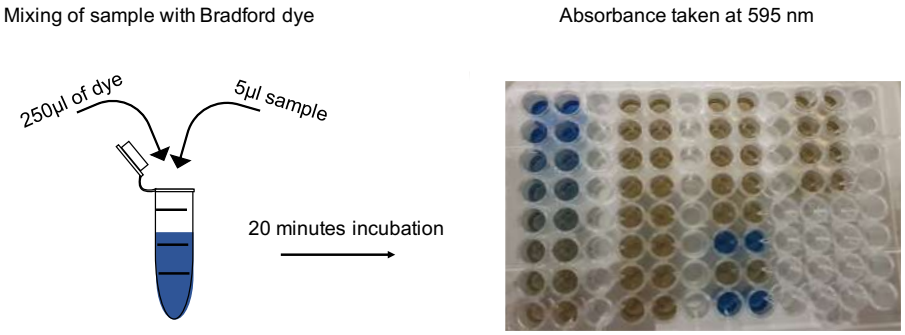

Diagram 2.4 – Bradford protein assay principle. Mixing of the 1x dye with the sample in a ratio recommended by the manufacturer (Left), followed by 20 minutes incubation at room temperature before aliquoting 100µl into 96-wells plate (Right). Absorbance measured at 595nm.

2.14 Enzyme-linked immunosorbent assay

Enzyme-linked immunosorbent assay (ELISA) can detect the antigen present in the sample. To detected the enzyme activity, the immobilised antigen is complexed to an enzyme-linked antibody. With a specific antigen-antibody interaction, the enzyme can be measured. ELISA used to quantify hepatocyte growth factor (HGF), vascular endothelial growth factor (VEGF), and interleukin-1 beta (IL-1ß). Human HGF ELISA kit (ThermoFisher Scientific) used to quantify the presence of HGF, VEGF, and IL-1ß in conditioned media collected from the encapsulated ASCs following 15°C storage following the manufacturer guidelines. Data were plotted and normalised against a standard curve made with each sample. Absorbance measured at 450nm using VariosKan LUX Multimode Microplate Reader.

2.15 Real-time polymerase chain reaction

2.15.1 Primer design

Decorin and Vimentin cDNA transcripts were obtained from the Ensemble genome browser, the specific primers were then designed using the Primer3 (v0.4.0) tool, and Primer-BLAST was then used to cross-reference the primer specificity. These design tools were used as follow:

The Ensemble genome browser is an online database that offers the search of genes of interest from all species. For the purpose of this thesis, the human genome database was used in choosing the appropriate cDNA. Searching for specific genes will result in multiple choices, choosing one of them will show a tab that contains the description of this gene, from the 'Sequence tap', clicking on 'cDNA' shows the different transcript ID of the gene. Clicking on the 'CCDS' tab, Nucleotide Sequence of the transcript gene is shown in a FASTA format, copying a specific sequence length (20 ~ 30 base pair) is desirable and pasting that in 'Primer3' tool to design the primer.

Primer3 tool is an online database that allows the paste of the nucleotide sequence to pick primers. This tool must be set on specific settings to allow for optimal primer choice. 'Pick left primer' and 'pick right primer' were set to the following selections: product size 80 – 200bp, maximal 3' stability is 9, maximal repeat mispriming is 12, pair maximal repeat mispriming is 24.00, maximal template mispriming is 12.00, pair maximal template mispriming is 24.00, minimum primer size is 18bp, optimum primer size is 20bp, maximum primer size is 27bp, minimum primer melting temperature (Tm) 57°C, optimum Tm is 60°C, maximum Tm is 63°C, while the maximum difference allowed between primers Tm is 2°C, minimum primer GC% is 35%, optimum GC% is 60%, maximum GC% is 80%, maximum self-complementarity is 8 and maximum 3' self-complementarity is 3. 'Pick primers' was then selected which showed the sequences of the primer that best resemble the properties chosen. The optimal primer sequence pair was then copied and pasted into the 'Primer-BLAST' tool for primer specificity.

Primer-BLAST: after finding the optimal 5'->3' forward and reverse primer sequence, they were then pasted onto Primer-BLAST and clicked on 'Get primers' to give details of the primers. Primer details include length, Tm, GC%, and Self

complementarity, once optimal details of the forward and reverse primer sequences were found, the primer RNA oligonucleotides were ordered from Eurofins Genomics (Ebersberg, Germany). Upon receiving the primers, they were solubilised in 0.1 µm-filtered RNase-free water (Sigma Aldrich, UK) to 100µM stock concentration. For real-time PCR primers were further diluted via mixing the forward and reverse primers in a 1:1 ratio. To ensure minimal risk of ribonuclease (RNase) contamination, RNase-free filter pipette tips were used.

Decorin, vimentin, a-smooth muscle actin, aldehyde dehydrogenase 3, and lumican primers were used for keratocytes gene expression analysis (Table 2.2). Hepatocyte growth factor, insulin-like growth factor, hypoxia-inducible factor-1A, vascular endothelial growth factor, REX1, tumor necrosis factor-inducible gene 6 protein, and a-smooth muscle actin primers were to measure the gene expression following scratch healing (Table 2.3). GAPDH housekeeping gene was used in all real-time PCR runs.

Gene	Primers 5' → 3'
Decorin	F: CTGCTTGCACAAGTTTCCTG
(DCN)	R: GACCACTCGAAGATGGCATT
Vimentin	F: CCTCCTACCGCAGGATGTT
(VIM)	R: CTGTAGGTGCGGGTGGAC
a-smooth muscle actin	F: CTGAGCGTGGCTATTCCTTC
(aSMA)	R: TTCTCAAGGGAGGATGAGGA
Aldehyde dehydrogenase 3	F: CCCCTTCAACCTCACCATCC
(ALDH3A1)	R: GTTCTCACTCAGCTCCGAGG
Lumican	F: CCTGGTTGAGCTGGATCTGT
(LUM)	R: TAGGATGGCCCCAGGA
GAPDH	F: AGCCGAGCCACATCGCTGAG
(housekeeping gene)	R: TGACCAGGCGCCCAATACGAC

Table 2.2 – Description of primers used in real-time PCR for keratocytes gene expression analysis.

Gene	Primers 5' → 3'
Hepatocyte growth factor	F: GTGAATACTGCAGACCAATGT
(HGF)	R: CCAGAGGCATTGTTTTCTTGC
Insulin-like growth factor-1	F: GCTGGTGGATGCTCTTCAGT
(IGF-1)	R: TTGAGGGGTGGGCAATACAT
Hypoxia-inducible factor-1A	F: CCAGAAGAACTTTTAGGCCGC
(HIF1A)	R: TGTCCTGTGGTGACTTGTCC
Vascular endothelial growth factor	F: AGGAGGGCAGAATCATCACG
(VEGF)	R: CCAGGGTCTCGATTGGATGG
Reduced expression 1	F: CCTCATTCATGGTCCCCGAG
(REX1)	R: CACCCTTCAAAAGTACACCG
Tumor necrosis factor-inducible gene	F: AAGGATGGGGATTCAAGGAT
6 protein (TSG-6)	R: TTTTTCTGGCTGCCTCTAGC
a-smooth muscle actin	F: CTGAGCGTGGCTATTCCTTC
(aSMA)	R: TTCTCAAGGGAGGATGAGGA

Table 2.3 – Description of primers used in real-time PCR for ASC gene expression analysis.

2.15.2 Sample preparation and RNA extraction

Sample preparation: human CSC and keratoconus cultures were harvested following scratch-wound healing. Three wells of the 6-wells plate were pooled together for every condition to harvest enough cells for RNA extraction. The harvested cells, counted in the range of 5×10^5 ~ 1×10^6 proceeded with RNA extraction. Human ASCs were also harvested following storage and use in scratch-healing.

RNA extraction: RNeasy® Mini Kit (QIAGEN, Manchester, UK) was used for RNA purification from cell cultures as directed by the manufacturer. Briefly; the harvested cell pellets were resuspended with 350µL RLT Buffer for sample disruption and homogenizing before transferring suspension to the RNeasy Mini spin column with an equal amount of 70% EtOH and centrifuging at 8000xg for 15 seconds. The flow-through was discarded and 700µl Buffer RW1 was added to the column membrane followed by centrifuging. 500µl of Buffer RPE was added twice to

the column followed by 15 second and 2 minutes centrifugation respectively. At which point, the RNeasy spin column was placed in a new 1.5mL microtube and 50µl RNase-free water was added to the column membrane to yield the RNA. The extracted RNA was either used for cDNA synthesis or stored at -80°C until needed.

2.15.3 cDNA synthesis

RNA samples, extracted in section 2.9.B were thawed on ice and measured for RNA concentration and purity using NanoDrop 2000 spectrophotometer (ThermoFisher, UK). The samples were measured by the 260nm and 280nm ($A_{260/280}$) absorption ratio before diluting RNA samples to 0.1mg/µl concentration using RNase-free water and stored on ice. cDNA synthesis was performed using the RT^2 First Strand Kit (QIAGEN, UK). All the reagents were thawed on ice before mixing 2µl of genomic DNA elimination GE buffer with 8ul RNA sample and water mix and incubated for 5 minutes at 42°C in TC-Plus thermal cycler (Techne, Staffordshire, UK) then immediately returned to the ice. A Reverse-Transcription mastermix containing 4µl 5x buffer BC3, 1µl P2 control, 2µl RE3 reverse transcriptase mix, and 3µl RNase-free water was mixed with the genomic cDNA and returned to the thermal cycler and incubated at 42°C for 15 minutes followed by 2 minutes at 95°C to inactivate the reverse transcriptase. The resulted cDNA was then further diluted with 50ul RNase-free water in a 1.5mL RNase-free sterile microtubes and stored at -20°C until needed for real-time PCR. All reagents used were vortexed briefly before use to ensure thorough mixing of components. The risk of contamination was minimised with the use of RNase-free filter pipette tips.

2.15.4 Real-time polymerase chain reaction

Real-time PCR (RT-PCR), also known as quantitative PCR (qPCR), is a technique used frequently to measure relative cDNA expression levels. Briefly, 7µl of SYBR green mastermix (ThermoFisher, UK). was mixed with 5µl cDNA samples and 2µl forward and reverse primer mix in a 48-well Eco™ PCR reaction plate (Illumina, San Diego, USA). The plates were then sealed using Eco ™adhesive seal (Illumina, USA) and briefly centrifuged to mix and bring all components to the bottom of the well and ensuring no bubbles were present. Plates were then transferred to Eco™ Real-Time PCR System (Illumina, USA) set with 10-minute incubation at 95°C,

followed by 40x cycles of 10 seconds at 95°C, 30 seconds at 60°C and 15 seconds at 72°C to allow for the cDNA denaturation, primers annealing, and transcript elongation. At the end of every cycle, data were collected corresponding to the relative sample fluorescence expression. The increase in the fluorescence level leads to a cycle threshold (Ct) value detection. Ct value is the number of PCR cycles needed to amplify the DNA target to a measurable level. Following PCR cycles, a melting curve is performed for every plate consisting of 15 seconds at 95°C, 15 seconds at 55°C and 15 seconds at 95°C. The data generated from the melting temperature should give a single peak to represent no formation of secondary product in the reaction, including primer-dimer and non-specific misprimers forming. Within the same PCR reaction, all experiments were performed in duplicates.

Standard curves were made for every primer used to measure the primer efficiency, using a 5-fold serial dilution of the cDNA template. The efficiency curves were used to measure primer efficiency using the equation: 'Efficiency (E) = $10^{(-1/\text{slope})}$-1' an efficiency value of 2 was considered 100% amplification efficiency. The relative level of target genes were quantified using the Pfaff mathematical model (Pfaffl, 2001) using the following equation:

$$\text{Fold change} = \frac{(E_{\text{target gene}})^{\Delta Ct\ [\text{target gene}]\ (\text{control-sample})}}{(E_{\text{housekeeping gene}})^{\Delta Ct\ [\text{housekeeping gene}]\ (\text{control-sample})}}$$

2.16 Proteome profiler human XL cytokine array

The human cytokine array kit (R&D Systems, Abingdon Science Park, Abingdon, UK) is a sensitive tool to detect the presence of different cytokines in the samples. The kit can capture antibodies spotted on a nitrocellulose membrane (Diagram 2.9) and a give relative expression of 105 different cytokines within one sample (Table 2.4). Which makes it an easier tool than immunoassays. Following certain steps, the signal produced at the capture spot corresponds to the amount of protein-bound.

Sample preparations: Conditioned media taken from eight conditions used for the kit (Diagram 2.10). These include (i) human CSCs plated in a 6-well plate with SFM, (ii) calcium alginate used with CSC following 15°C storage, encapsulated ASCs (iii) stored at 15°C for 72 hours only, or, followed by (iv) 48 hour storage at 37°C, encapsulated ASCs used with scratch healing for 48-hours with either (v) post 15°C storage, or, (vi) non-stored, non-encapsulated ASCs were also used as (vii) non-stored, or, (viii) following 15°C storage. The supernatant from each sample was centrifuged to remove all debris and diluted with the blocking buffer to a final volume of 1.5 mL then placed on ice to be used with the kit.

Array procedure: The kit was used with cell culture supernatants produced according to the manufacturer's instructions. Briefly; the kit contains four membranes that were placed inside a 4-well multi-dish and incubated with a blocking buffer for 1 hour on a rocking platform. The prepared samples were added to the 4-well multi-dish for overnight incubation at 4°C on a rocking platform. The membranes were then washed with a 1X washing buffer prepared by mixing 20mL wash buffer with 480mL PBS for 10 minutes on a rocking platform for a total of three washes. During membrane washing steps, the 4-well multi-dish was also washed with tap water to prepare for the next steps. Detection Antibody Cocktail was prepared by diluting the Human XL Cytokine Detection Antibody Cocktail with 200µL PBS, followed by mixing 30µL of the detection antibody cocktail with 1.5mL of 1X Array Buffer 4/6 that was prepared by mixing 4mL of Array Buffer 4 to 8mL of array buffer 6. After the wash, 1.5mL of Detection Antibody Cocktail mixed with 1X Array Buffer 4/6 was incubated with each membrane in the 4-well multi-dish for 1 hour at room temperature on a rocking platform. Followed by washing steps and 2mL of 1X Streptavidin-HPR was added to the membranes for 30 minutes at room temperature on a rocking platform. 1X Streptavidin-HPR was diluted in Array Buffer 6 in a 1:2000 dilution before use. Followed by washing steps, 1mL Chemi Reagent Mix was pipetted evenly onto each membrane and incubated for 1 minute at which point the membranes were protected from light. Chemi Reagent Mix was prepared by mixing Chemi reagent 1 and 2 in a 1:1 ratio freshly before use. The membranes were protected from light and placed in a wash buffer until visualisation using Amersham™ Imager 600 (GE Healthcare Life Sciences, Buckinghamshire, UK). Using ImageJ, the produced membrane images were analysed for pixel intensity, choosing the same circle width to mark all captured

antibodies spots, under the Analyze tab, Measure plugin was used to measure the pixel intensity and plotted in an Excel spreadsheet and graphs processed using Prism 6.0.

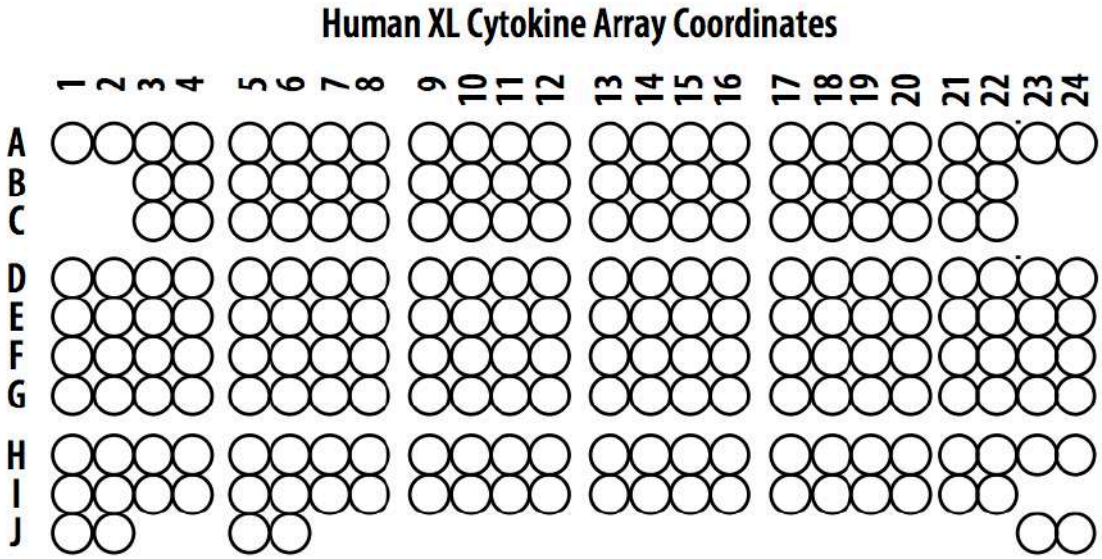

Diagram 2.5 – Human XL cytokine array membrane coordinates

Coordinate	Analyte/Control	Coordinate	Analyte/Control
A1 – A2	Reference spot	C1 – C2	-
A3 – A4	Adiponectin	C3 – C4	ENA-78
A5 – A6	Apolipoprotein A-I	C5 – C6	Endoglin
A7 – A8	Angiopoietin	C7 – C8	Fas Ligand
A9 – A10	Angiopoietin-1	C9 – C10	FGF basic
A11 – A12	Angiopoietin-2	C11 – C12	FGF-7
A13 – A14	BAFF	C13 – C14	FGF-19
A15 – A16	BDNF	C15 – C16	Fit-3 ligand
A17 - A18	CC-C5/C5a	C17 - C18	G-CSF
A19 – A20	CD14	C19 – C20	GDF-15
A21 – A22	CD30	C21 – C22	GM-CSF
A23 – A24	Reference spot	C23 – C24	-
B1 – B2	-	D1 – D2	GROa
B3 – B4	CD40 ligand	D3 – D4	GH
B5 – B6	CHI3L1	D5 – D6	HGF
B7 – B8	CF D	D7 – D8	ICAM-1
B9 – B10	CRP	D9 – D10	IFN-y
B11 – B12	Cripto-1	D11 – D12	IGFBP-2
B13 – B14	Cystatin C	D13 – D14	IGFBP-3
B15 – B16	Dkk-1	D15 – D16	IL-1a
B17 - B18	DPPIV	D17 - D18	IL-1b
B19 – B20	EGF	D19 – D20	IL-1ra
B21 – B22	Emmprin	D21 – D22	IL-2
B23 – B24	-	D23 – D24	IL-3

Coordinate	Analyte/Control	Coordinate	Analyte/Control
E1 – E2	IL-4	G1 – G2	Leptin
E3 – E4	IL-5	G3 – G4	LIF
E5 – E6	IL-6	G5 – G6	Lipocalin-2
E7 – E8	IL-8	G7 – G8	MCP-1
E9 – E10	IL-10	G9 – G10	MCP-3
E11 – E12	IL-11	G11 – G12	M-CSF
E13 – E14	IL12 P70	G13 – G14	MIF
E15 – E16	IL-13	G15 – G16	MIG
E17 - E18	IL-15	G17 - G18	MIP1a/MIP1b
E19 – E20	IL-16	G19 – G20	MIP-3a
E21 – E22	IL-17A	G21 – G22	MIP-3b
E23 – E24	IL-18 Bpa	G23 – G24	MMP-9
F1 – F2	IL-19	H1 – H2	Myeloperoxidase
F3 – F4	IL-22	H3 – H4	Osteopontin
F5 – F6	IL-23	H5 – H6	PDGF-AA
F7 – F8	IL-24	H7 – H8	PDGF-AB/BB
F9 – F10	IL-27	H9 – H10	Pentraxin-3
F11 – F12	IL-31	H11 – H12	PF4
F13 – F14	IL-32	H13 – H14	RAGE
F15 – F16	IL-33	H15 – H16	RANTES
F17 - F18	IL-34	H17 - H18	RBP-4
F19 – F20	IP-10	H19 – H20	Relaxin-2
F21 – F22	I-TAC	H21 – H22	Resistin
F23 – F24	Kallikrein 3	H23 – H24	SDF-1a

Coordinate	Analyte/Control	Coordinate	Analyte/Control
I1 – I2	Serpin E1	J1 – J2	Reference spot
I3 – I4	SHBG	J3 – J4	-
I5 – I6	ST2	J5 – J6	Vitamin D BP
I7 – I8	TARC	J7 – J8	CD31
I9 – I10	TFF3	J9 – J10	TIM-3
I11 – I12	TfR	J11 – J12	VCAM-1
I13 – I14	TGF-a	J13 – J14	-
I15 – I16	Thrombospondin-1	J15 – J16	-
I17 - I18	TNF-a	J17 - J18	-
I19 – I20	uPAR	J19 – J20	-
I21 – I22	VEGF	J21 – J22	-
I23 – I24	-	J23 – J24	Negative control (Background)

Table 2.4 – Human XL cytokine array coordinates.

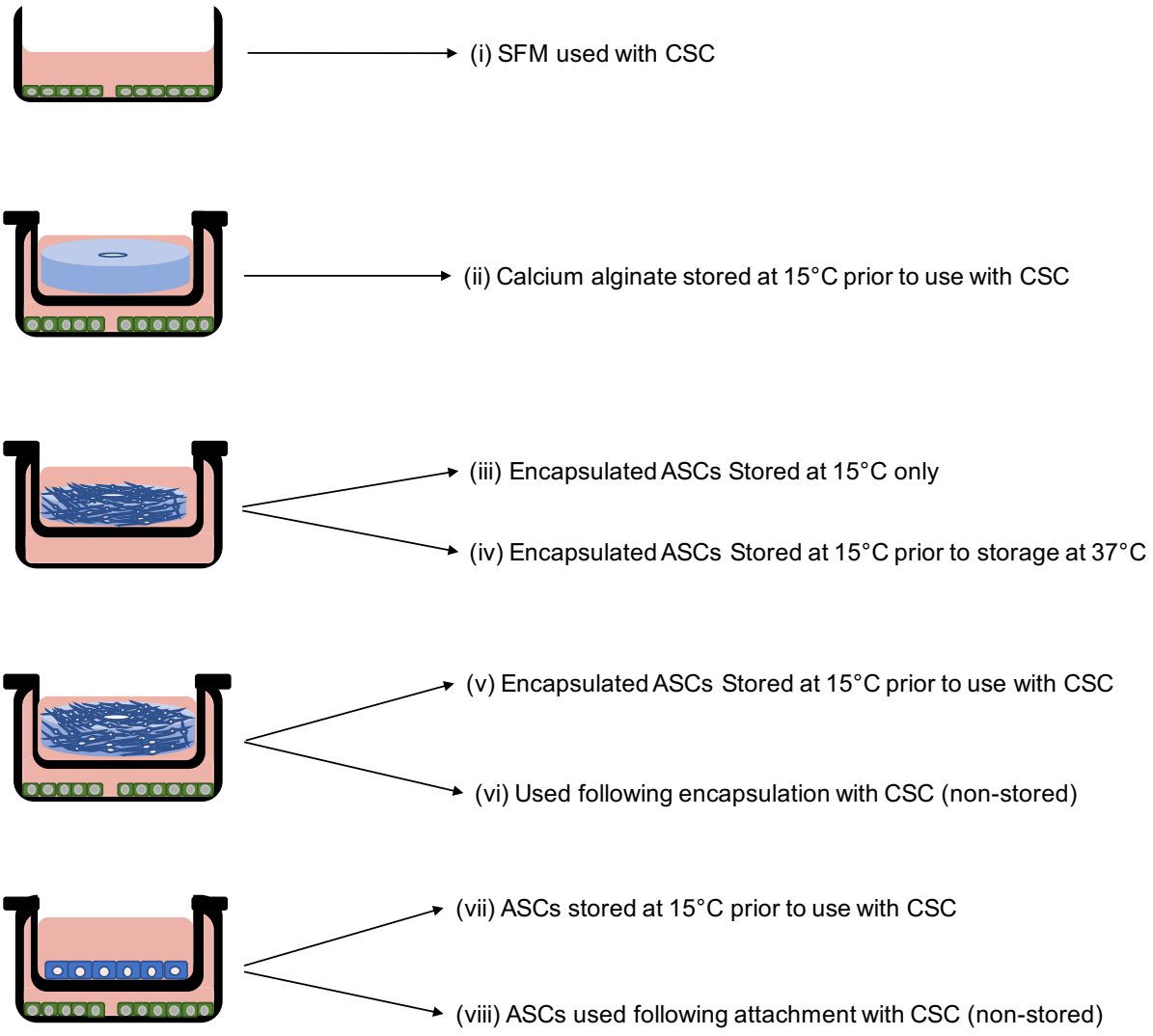

Diagram 2.6 – The conditions used for the Human Cytokine XL Array Kit. (i) CSC used with SFM, (ii) calcium alginate used with CSC following 3 days storage at 15°C, (iii) encapsulated ASCs stored at 15°C for 3 days, (iv) prior to storing at 37°C without CSC, encapsulated ASCs used with CSC (v) post storage at 15°C and (vi) immediately following encapsulation, non-encapsulated ASCs attached to the transwell insert and used with CSC (vii) post storage at 15°C and (viii) immediately following attachment. CSC: corneal stromal cells; SFM: Serum-free DMEM:F12; Calcium alginate: VLVG alginate; ASCs: adipose-derived mesenchymal stem cells.

2.17 Statistical analysis

Unless otherwise stated in the thesis, statistical analysis was performed using GraphPad Prism, Version 6.0. Data are expressed as the mean of values from at least three separate donors ± SEM. Statistical comparisons were made using one-way or two-way repeated-measures ANOVA, and Tukey's multiple comparisons tests, excluding comparison of two single variables for which paired two-tailed *t*-test were used. Values of p> 0.05 were considered significant (*, $p < 0.05$; **, $p < 0.01$; ***, $p< 0.001$; ****, $p<0.0001$).

Chapter 3. Stem cells bandages formation: Effect of cells encapsulated in alginate on *in vitro* corneal stromal scratch wound closure

3.1 Introduction

Corneal damage can range in severity between superficial (cellular) and deep stromal damage. Depending on the damage grade, the treatment method can range. Superficial corneal abrasions that damage the epithelial cells can be healed within a few days using antibiotics. Deeper abrasions may require antibiotics, steroids, and painkillers to help heal the eye. Severe abrasions, on the other hand, even with treatment, can still affect vision by forming a scar. Stem cells have been tested as therapeutic cells that can heal various diseases. Adipose-derived stem cells (ASCs), present a promising choice for corneal therapy for they can be easily obtained from fat tissues, are known to be environmentally responsive in wound repair, and able to secret paracrine factors and extracellular molecules that have immunomodulatory (Aggarwal and Pittenger, 2005), angiogenic (Watt et al., 2013), trophic (Roddy et al., 2011) and anti-fibrotic activity (Dong et al., 2015). Thus, we hypothesise that stem cell bandages can help heal these scars and improve vision.

3.2 Aims

This chapter will explain the preliminary experiments taken to determine the optimal approaches in investigating the formation and effect of stem cell bandages containing alginate encapsulated human ASCs on *in vitro* human corneal cell cultures. Herein, we explain the steps taken in (i) determining the optimal seeding density of corneal cells, (ii) media used to culture cells, and (iii) methods used in assessing cell migration and proliferation. We also show (iv) the encapsulation optimisation of ASCs and (v) the types of alginate used for the encapsulation that is suitable for scratch assay and image analysis using time-lapse and ImageJ software. As well as (vi) the hypothermic procedure used to store the cells and (vii) the adaptability made to the model to improve reproducibility. These optimisation steps allowed the formation of stem cell bandages. These bandages maintained their viability and functional ability during hypothermic storage and *in vitro* wound healing.

HGF is an important protein responsible for cell motility, proliferation and morphogenesis, thus we also tested its production level

3.3 Results

3.3.1 A choice of cell migration assay and media effect on corneal stromal cells cultures

To start our experiments, human corneal cells (CSCs) were isolated and expanded from healthy corneal donors (see isolation procedure in chapter 2 2.1). To measure cell migration, few adjustments were needed to optimise the scratch procedure. Starting with the seeding density of the cells to accommodate the wells and expand to near confluency, without being over confluent. Cells were seeded at a range of densities in a 6-well plate with 5% media for 24 hours, at which point the cells were in their fibroblastic active form. Followed by 72 hours of starvation via supplementing the cells with serum-free media (SFM) (DMEM: F12 supplemented with 5g/L ascorbic acid, 1% Insulin-Transferrin-Selenium and 1% penicillin-streptomycin) to induce their in-active form. Over- or under- confluent wells were not used in the experiments, for they presented non-uniform scratches, and gave inconsistent scratch measurements across technical and biological repeats (Figure 3.1). During the 72 hours incubation, the cells were expected to have minimal proliferation. To reach the optimum monolayer confluency, different seeding densities were measured including $5x10^5$ cells/well (Figure 3.1 A), $1.5x10^5$ cells/well (Figure 3.1 B) and $2.5x10^5$ cells/well (Figure 3.1 C). Hence, the initial seeding density of $2.5x10^5$ cells/well was preferred as the optimal seeding density.

A

Over confluency

Microscope

Iprasense

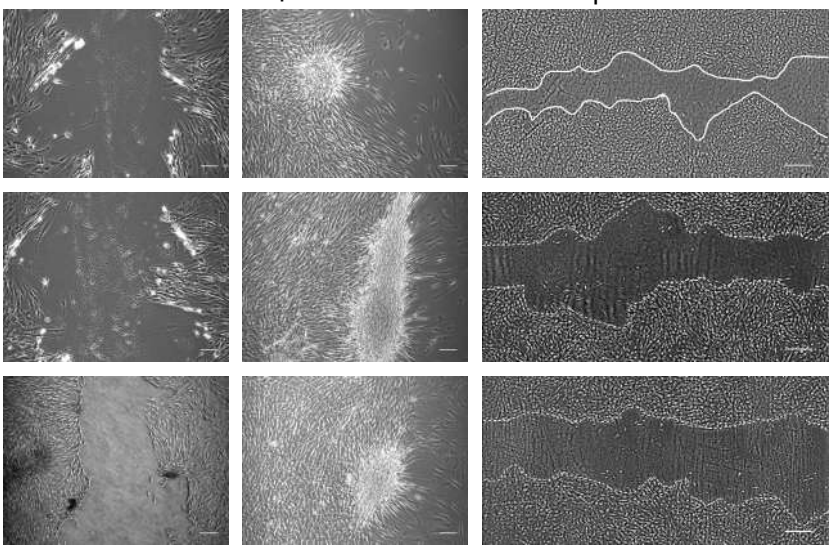

B

Under confluency

Microscope

Iprasense

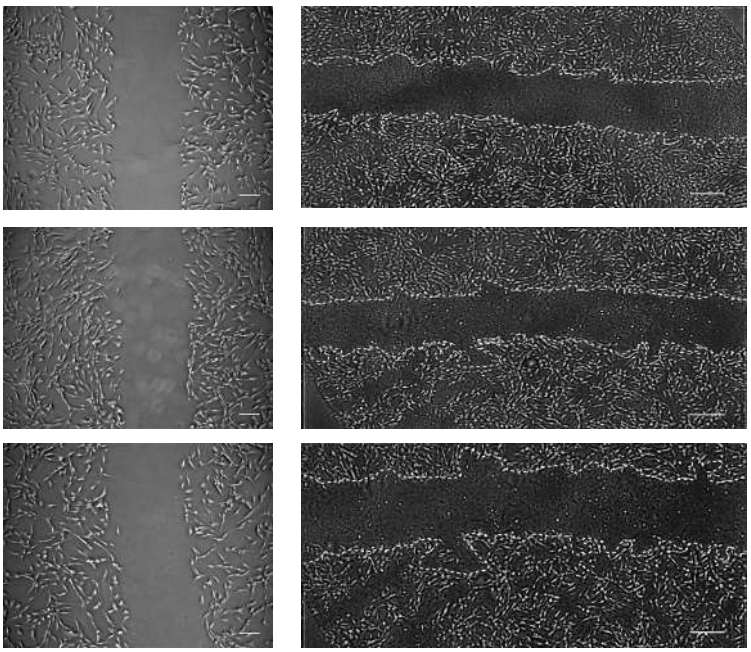

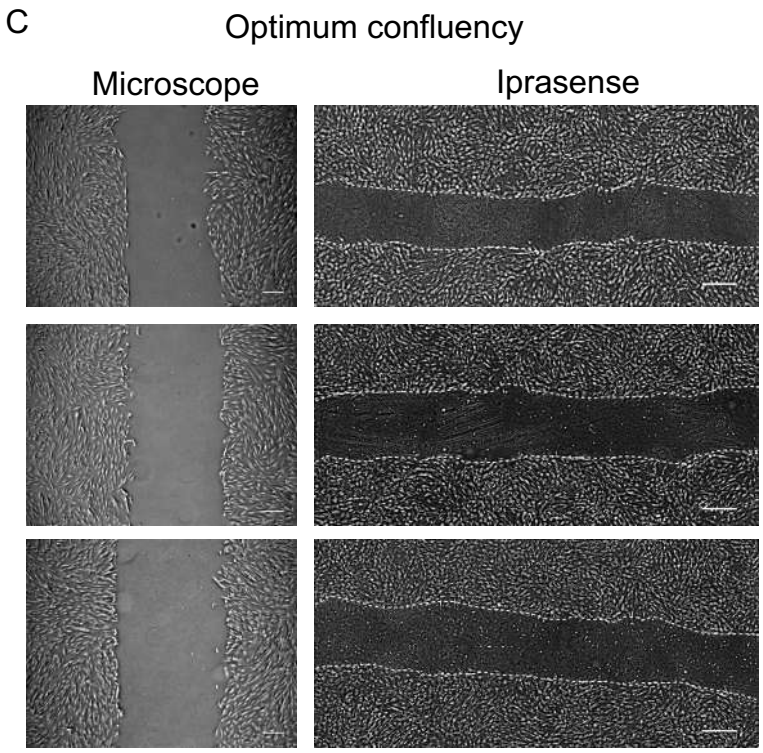

Figure 3.1 – Effect of the seeding density on scratch uniformity presenting cell images of (A) over confluent ($5x10^5$ cells/well), (B) under confluent ($1.5x10^5$ cells/well), and (C) the optimum confluency ($2.5x10^5$ cells/well) that is used in the subsequent experiments. Two types of microscopes are used to take images, an inverted microscope using Leica software (Left) and Iprasense lensless imaging using Horus software (Right). n = 3 repeats. Scale bars of microscope images = 220µm, and Iprasense images = 300µm.

CSC cultures were used to optimise the incubation time following scratch to determine the optimum time needed to allow the cells to cover the full scratch (cell-free) area. Following 72 hours of cell starvation, scratch assays were performed on the cells and incubated with either SFM or 5% media for 48 hours (Figure 3.2 A). SFM was used with all subsequent CSC experiments, therefore, they were used as a negative control, while 5% media used as a positive control, where the presence of serum is expected to activate CSC to fibroblasts to migrate and proliferate. The cultured plates were imaged using Iprasense time-lapse microscopy in a 1-hour interval without disruption.

As we expected, significant differences were found between the two conditions following time 20h, 30h ($p < 0.0001$) and 40h ($p = 0.0002$) (Figure 3.2 B). This

indicated the time it takes for the cells to cover the cell-free area; therefore, it was decided that 48 hours of culture (following scratch induction) mark the end of each experiment. Using Alamar blue assay, we determined cell density at time 48 hours compared to time 0 (Ctrl) (Figure 3.2 C) an increase in cell number was found with the 5% media ($p = 0.0309$). Indicating 5% media induced the cells to proliferate to cover the wound area, which is achieved via cells differentiating into their active fibroblastic form.

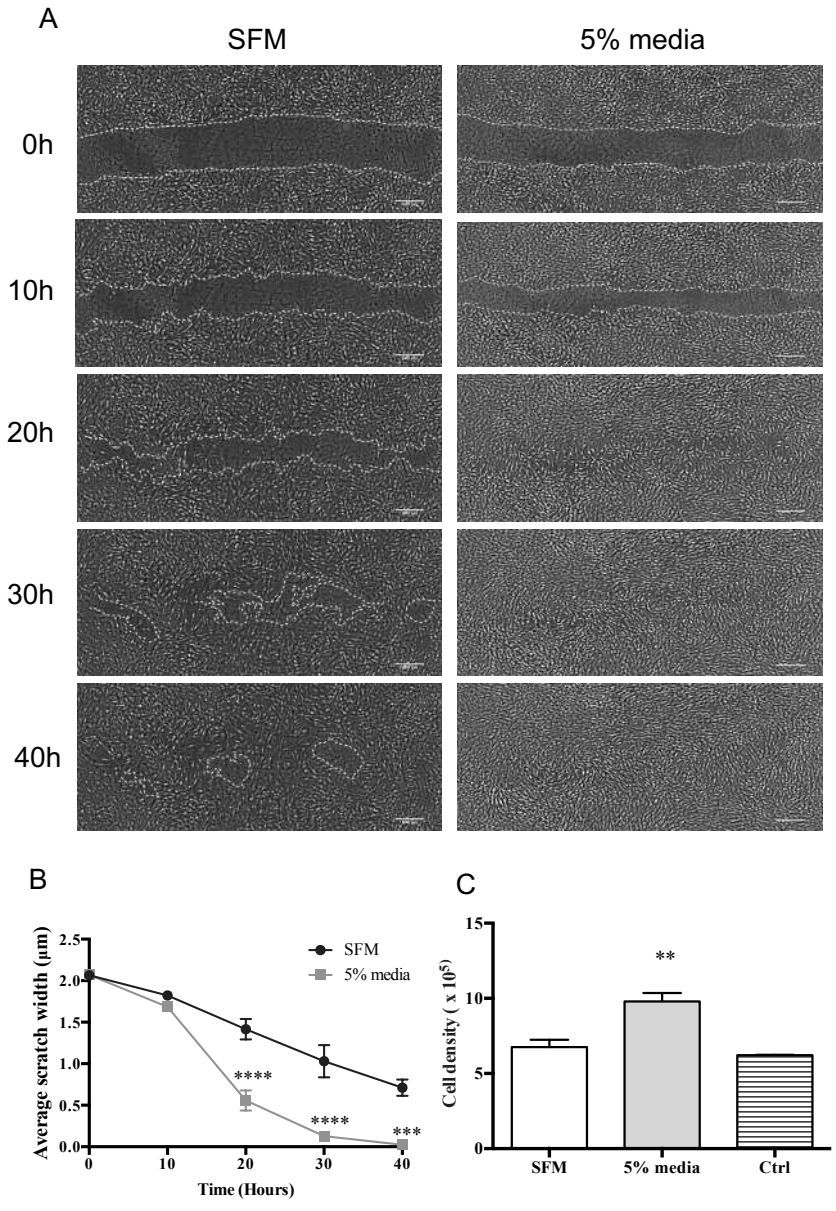

D

Time (Hours)	SFM	5% Media
0	100	100
10	89.83239473	81.438376
20	70.75146893	27.0114659
30	54.94253768	6.202255888
40	37.07073254	1.202824965

Figure 3.2 – Media effect on CSCs cultures. Comparing Serum-free media (SFM) and 5% media (DMEMF12 supplemented with 5% FBS). (A) Representing scratch migration assay, (B) average scratch width, (C) cell number at time 48 for SFM and 5% media, while time 0 for Ctrl, and (D) percentage wound closure. Scale bar = 300μm, values are expressed as means ± SEM of at least n=3, (****, $p < 0.0001$; ***, $p < 0.001$; **, $p < 0.01$).

3.3.2 Formation of stem cells bandages: cell encapsulation in 3D biomaterial

To test stem cell bandages, we tested two types of alginate sources, Sigma-Aldrich and NovaMatrix alginate (Table 3.1). Both of the providers extracted sodium alginate from the brown algae cell wall and supplied it in a powder format in different levels of purity. While there seemed to be differences in the appearance of the powder, from the datasheet, the major differences were found in the viscosity, purity, and composition of the G and M acid block copolymers ratio.

	Sigma (S)	NovaMatrix (N)
Powder appearance	Off-white to light brown	White to off-white
Solution appearance	Light brow to yellow	Colourless
Viscosity	4 – 12 mPa/s	< 20 mPa/s
pH	N/A	5.5 – 8.8
Composition	Primarily D-mannuronic acid residues	Primarily Guluronic acid residues
Purity	N/A	Ultrapure
Shelf life	N/A	5 years
Storage conditions	2 – 8 °C	2 – 8 °C

Alginate composition

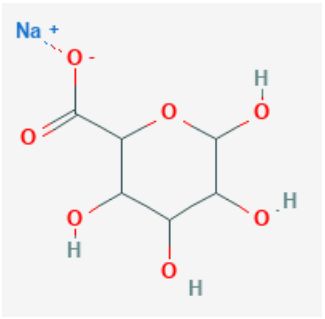

Table 3.1 – Comparison between Sigma and NovaMatrix alginates (image adapted from https://pubchem.ncbi.nlm.nih.gov/compound/5102882#section=Top).

We adapted Swioklo's encapsulation method and further adjusted it to suit our system (encapsulation procedure is explained in detail in chapter 2. 2.6). Following bandage ± cell formation, we sought to determine its effect on CSC cultures. S. (Sigma) and N. (NovaMatrix) alginates ± $1x10^6$ cells were used immediately following formation, a condition referred to as (non-stored). From the scratch images (Figure 3.5 A, B), the presence of bandage + ASCs (S. and N. alginates) within the co-culture showed an improvement in CSC area coverage compared to the bandage - ASCs (S. and N. alginates). This improvement showed significance at 30 and 40 hours in S. ($p = 0.023$ and 0.011 respectively) and N. ($p = 0.006$ and 0.0009 respectively) alginates (Figure 3.5 C). However, compared to the 0-hour cell number (ctrl) (Figure 3.5 D) there was no significant increase in CSCs proliferation, thus these cells were mostly migrating into the scratched cell-free area (as shown in our

development experiments Figure 3.2). Upon comparing all these conditions, no significant differences were found between the two alginates.

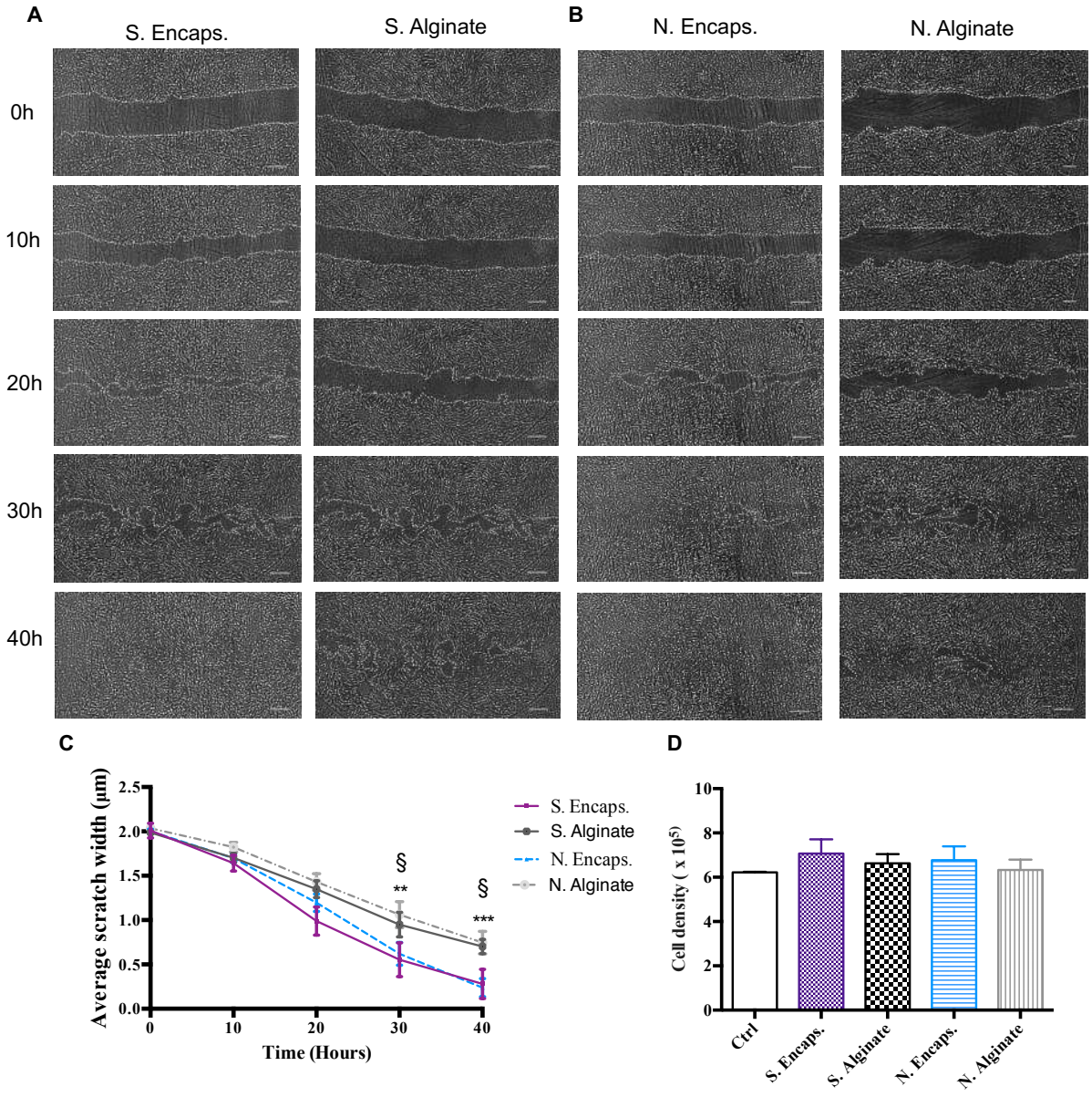

E

Time (Hours)	S. Encaps.	S. Alginate	N. Encaps.	N. Alginate	SFM
0	100	100	100	100	100
10	81.69821345	85.59131728	84.83644374	89.48036646	89.83239473
20	49.79913212	67.77276819	59.73258326	70.29389912	70.75146893
30	28.20143779	47.75834416	31.01474136	52.30109544	54.94253768
40	14.27614064	35.20327455	12.10979343	36.71236533	37.07073254

Figure 3.3 – Comparison of the non-stored conditions. Scratch images of the (A) S. (Sigma) and (B) N. (NovaMatrix) alginates at times 0, 10, 20, 30 and 40 hours. (C)

Average scratch width, (D) cell number, and (E) percentage wound closure. Scale bar = 300μm, values are expressed as means ± SEM of at least n=3, using 2way ANOVA, asterisks represent significance between the N. alginate and N. Encaps (***, $p < 0.001$; **, $p < 0.01$), while symbols represent significant between S, alginate and S. Encaps. (§, $p < 0.5$). S. represent Sigma alginate; N. represent NovaMatrix alginate; ctrl represents time 0-hour cell number.

3.3.3 Assessment of hypothermically stored ASCs on corneal stromal cell culture

3.3.3.1 Hypothermic storage effect on viable cell recovery

For efficient cell therapy, it is important to avoid the use of serum and for the stored cells to be adapted to a serum-free condition. Therefore, we encapsulated ASCs and stored them at 4°C and 15°C in SFM for 72 hours using both S. and N. alginates before counting the cells (Figure 3.4). Although no significant differences were found between the different alginates, there were differences when comparing the different temperatures within the same type of alginate. At 4°C, stored cells showed a significant drop in cell number yielding 54.3% ± 7.8% and 64% ±3.4% viable cells in both S. and N. alginates respectively, when compared to non-stored conditions (ASCs released following encapsulation) significant difference shown ($p = 0.0027$ and 0.0041 respectively). Whereas at 15°C, cells achieved a viable cell recovery of 75% ± 2.4% and 77% ± 2.9% in S. and N. alginates respectively. When compared to the non-stored conditions, significant differences were found in the N. alginate ($p = 0.04$) but not in the S. alginate. Therefore, and corresponding to Swioklo *et al*, 15°C storage was again shown to be the optimal storage condition, which also corresponded with the minimum acceptable specification of cell viability (70% viable cells following storage) set by the FDA (Administration), and this result could not be achieved without alginate encapsulation. The difference in cell viability between our experiment and Swioklo's is attributed to the use of growth media that contains 2% serum whilst our experiment did not contain serum.

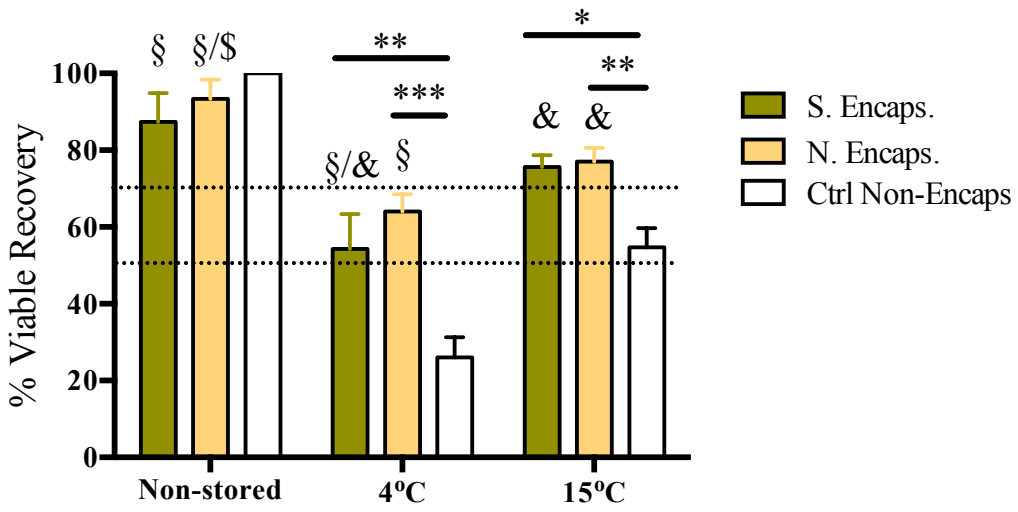

Figure 3.4 – Storage effect on viable cell recovery. ASCs released immediately following encapsulation (non-stored) or stored at 4 and 15°C either encapsulated or non-encapsulated (Ctrl), for 72 hours before assessing percentage of viable cells recovered. Values are expressed as means ± SEM of n=3, asterisks represent significant differences between control and temperature differences with the different alginate type (***, $p < 0.001$; **, $p < 0.01$; *, $p < 0.05$) and symbols represent differences between temperatures of the same alginate (§, $p < 0.01$; &, $p < 0.5$).

3.3.3.2 Hypothermically stored bandages effect on CSC scratches

Following a viable cell recovery assessment, we aimed to assess the possibility of paracrine factors released from the bandages using scratch wound assay. We stored both types of alginates at 4°C (Figure 3.5) ± ASCs before assessing their effect on CSC culture. Surprisingly, no significant differences were found when comparing S. alginate ± ASCs (Figure 3.5 A, C), where both conditions showed similar area coverage over time. N. alginate ± ASCs showed significant differences at 30 and 40 hours ($p = 0.0042$ and 0.0148 respectively) post scratch (Figure 3.5 B, C). Upon comparing both alginates, significant differences were found between S. Encaps. and N. at 20 and 30 hours post scratch ($p = 0.025$ and < 0.0001 respectively), whilst S. Alginate showed significantly faster wound coverage compared to N. Alginate at 30 hours ($p = 0.0046$) and N. Encaps. at 40 hours ($p = 0.0015$). N. Encaps showed a significant increase in cell proliferation compared to N. Alginate ($p = 0.0383$) (Figure 3.5 D).

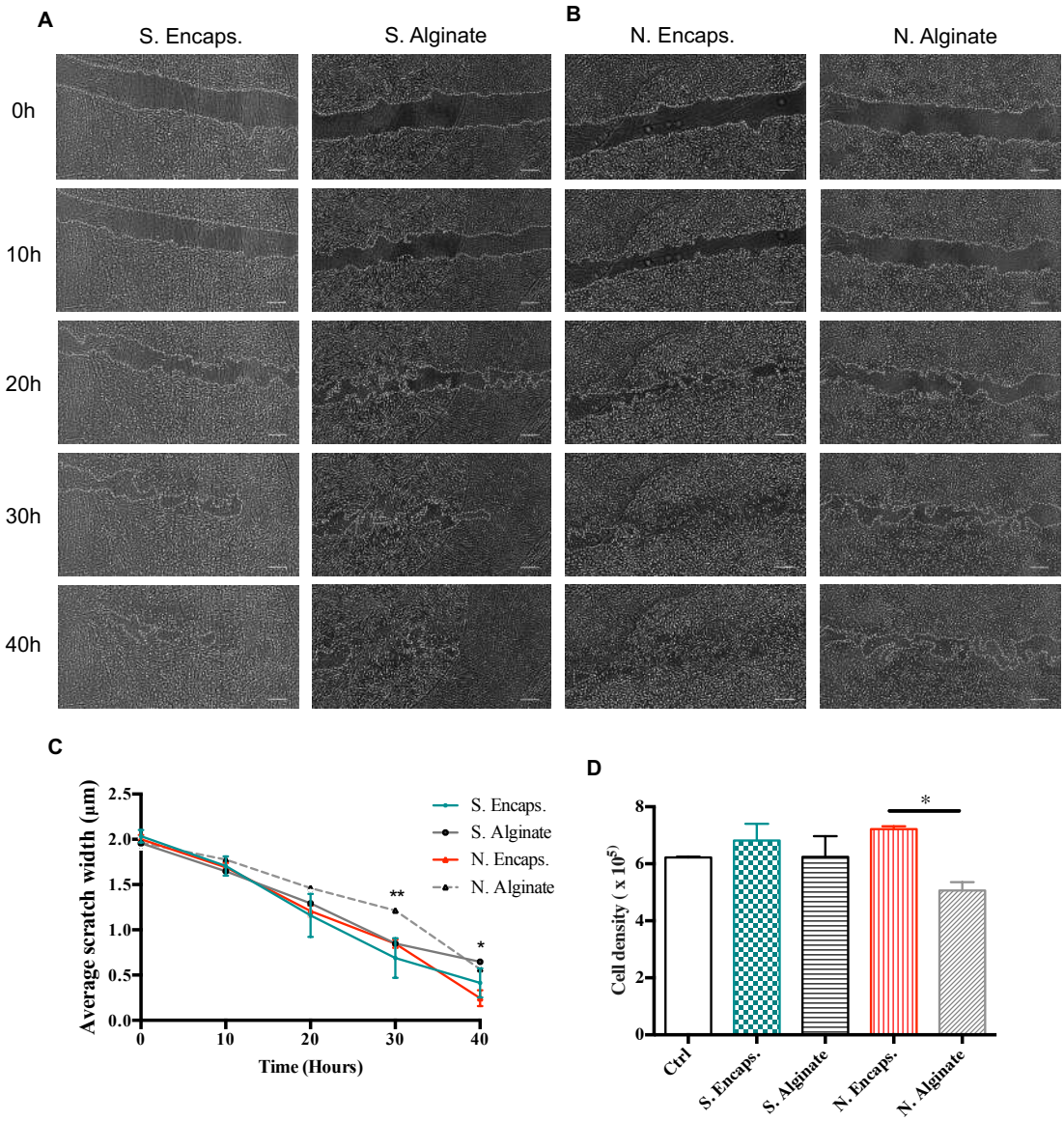

E

Time (Hours)	S. Encaps.	S. Alginate	N. Encaps.	N. Alginate	SFM
0	100	100	100	100	100
10	83.5371172	84.05481802	84.56866255	90.47747724	89.83239473
20	55.78751849	65.43229828	60.38956215	74.35161473	70.75146893
30	32.92712167	42.52496771	42.25491349	61.73361512	54.94253768
40	19.7598764	32.09181836	12.16991261	29.23586167	37.07073254

Figure 3.5 – Hypothermic storage effect at 4°C on corneal stromal culture. S. and N. Alginates ± ASCs. Scratch images of (A) S. and (B) N. alginates, (C) average scratch width, (D) cell density, and (E) percentage scratch closure. Values are expressed as means ± SEM of at least n=3, (**, $p < 0.01$; *, $p < 0.05$). Scale bar = 300µm.

Similarly, both alginates ± ASCs were stored at 15°C for 72 hours (Figure 3.6). Where S. Encaps. showed an enhanced wound coverage at time 30 hours ($p = 0.0463$) (Figure 3.6 A, C). Unexpectedly, N. alginate showed a significant delay in area coverage 20, 30, and 40 hours post scratch ($p < 0.0001$) (Figure 3.6 B, C). This difference is also shown when compared to S. alginate ($p < 0.0001$). On the other hand, the presence of ASCs with the N. alginate presented an enhanced wound coverage, as well as a significant increase in cell proliferation (Figure 3.6 D) compared to S. and N. alginates, where the latter showed a small reduction in cell density compared to control.

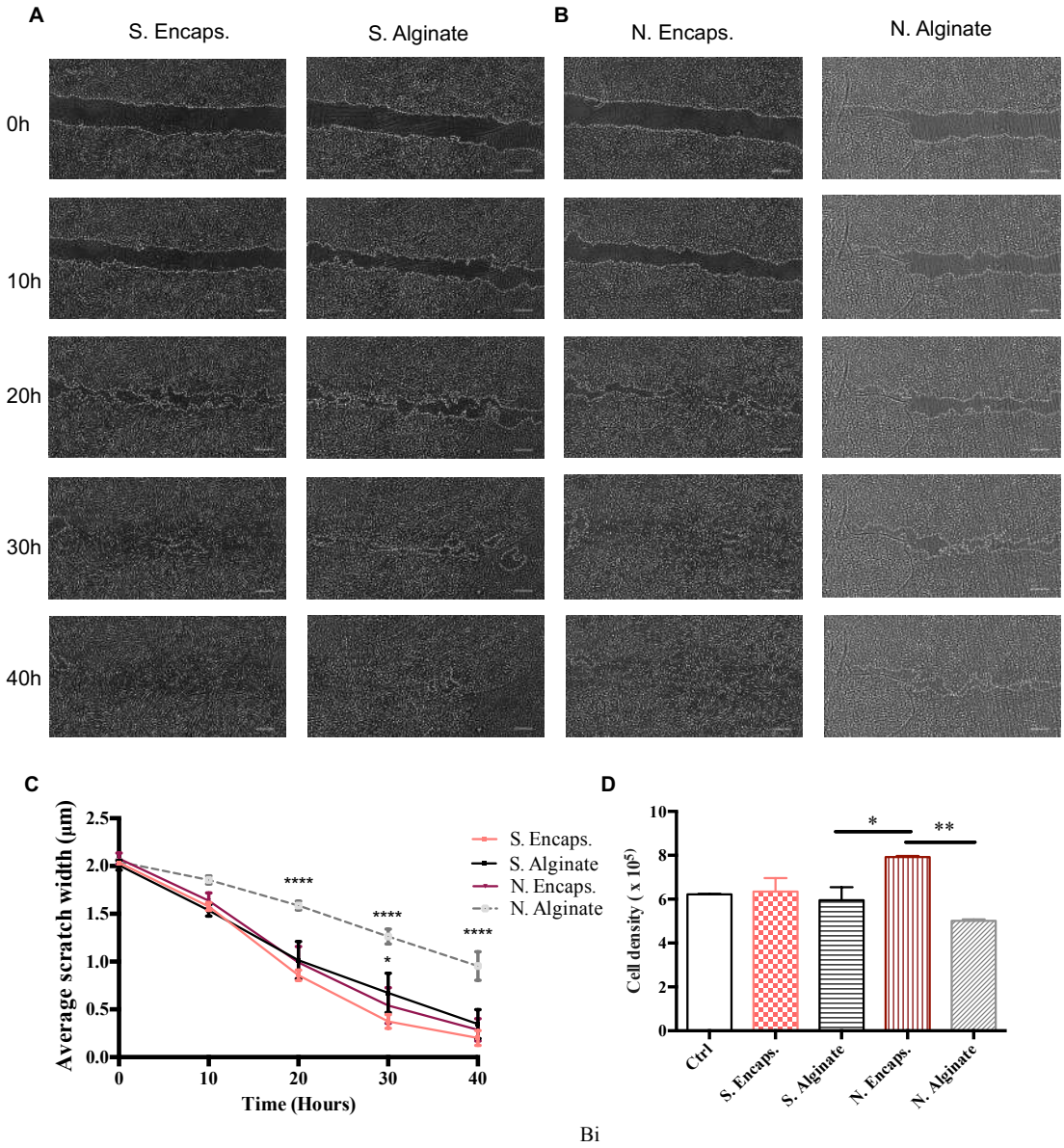

Bi

E

Time (Hours)	S. Encaps.	S. Alginate	N. Encaps.	N. Alginate	SFM
0	100	100	100	100	100
10	77.45314883	76.67395547	78.89253634	90.6730273	89.83239473
20	42.13011347	50.70229797	47.42793869	77.57457737	70.75146893
30	18.34201136	33.38349459	25.59013208	61.72007122	54.94253768
40	9.859734452	17.09513986	13.64367217	46.73877113	37.07073254

Figure 3.6 – Hypothermic storage effect at 15°C on corneal stromal culture. S. and N. alginates ± ASCs stored at 15°C for three days. Shown scratch images of (A) S. and (B) N. alginates, (C) average scratch width, (D) cell density, and (E) percentage

scratch closure. Values are expressed as means ± SEM of at least n=3, (****, $p < 0.0001$; **, $p < 0.01$; *, $p < 0.05$), Scale bar = 300µm.

From the data, differences were found at times 20 and 30 hours post-scratch in the bandage + ASCs condition, thus we compared these time points (Figure 3.7 A). Whilst no significant differences were found when comparing non-stored and storage at 15°C for S. and N. Encaps. S. Encaps following 15°C storage showed a significant increase in wound recovery compared to S. Encaps following 4°C at times 20 and 30 hours post scratch ($p = 0.029$ and 0.0217 respectively). This reduction in wound area suggested that 15°C storage affected ASCs and in turn affect CSC. culture via growth factor(s) release. Whereas N. Encaps following 4°C storage showed a delay in wound coverage at time point 30 hour compared to S. Encaps following 15°C storage ($p < 0,0001$), N. Encaps following 15°C storage ($p = 0.0052$), and S. Encaps non-stored (used immediate following encapsulation) ($p = 0.0081$), which could be due to the reduced ASCs cells number before starting the experiment. So far, S. Encaps following 15°C storage presented the best temperature and alginate type to be used for initiating therapy. This effect of scratch healing can be attributed to the alginate composition since the only difference between N. Encaps and S. Encaps is the type of alginate used.

Our data suggest that Encaps. ASCs stored at 15°C for 3 days improve CSCs scratch wound, whereas alginate controls did not show this effect, suggesting that encapsulated ASCs can produce soluble factor(s). We can assume that the amount of these factor(s) produced is relative to the number of (live) ASCs cell number. Thus, we normalized the measured effect (wound closure) to the number of live ASCs found within the alginate at the end of the experiment. After applying this normalisation step we found that non-stored Encaps. (Figure 3.7 B, C) showed the slowest cell response compared to the other conditions.

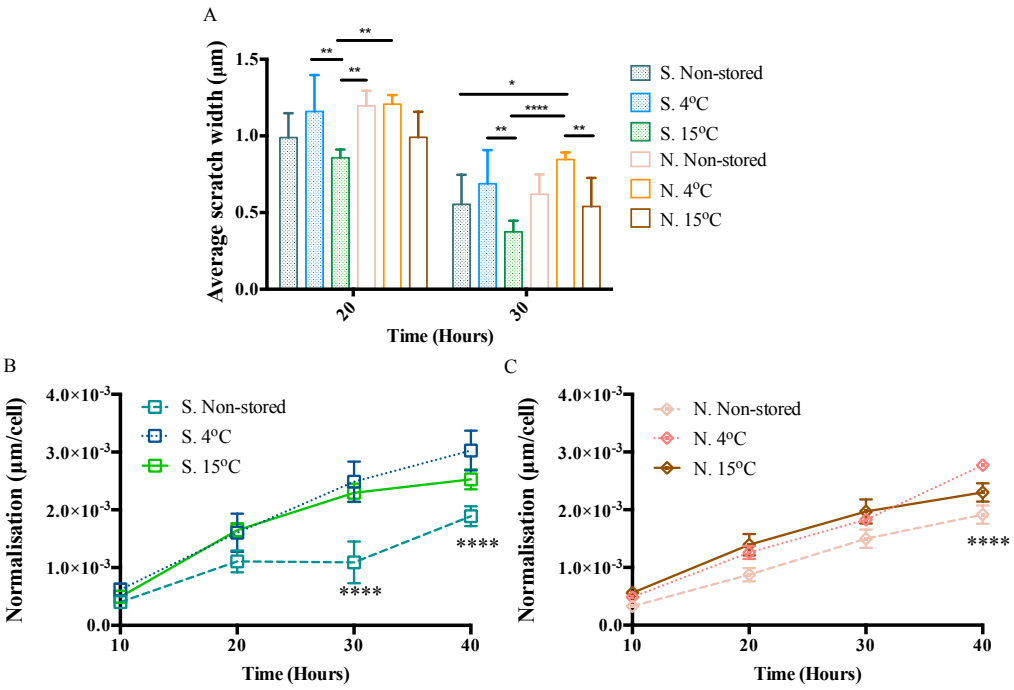

Figure 3.7 – Migration speed per cell. (A) comparison of S. and N. alginates at times 20 and 30 hours post scratch. ASCs cell number normalized to CSCs number following 48 hours for both (B) S. alginate, and (C) N. alginate. Values are expressed as means ± SEM of at least n=3, (****, $p < 0.0001$; **, $p < 0.01$; *, $p < 0.05$).

3.3.4 Assessment of ASCs cell surface marker expression

Following the assessment of ASCs' effect of CSC culture, we sought to assess if ASCs maintained their phenotypic markers following culture with CSC. Flow cytometry analysis performed and compared non-stored ASCs grown in culture without alginate (Figure 3.8 A) to encapsulated ASCs in S. or N. alginates either used with CSC for 48 hours (Figure 3.8 B) or without CSC culture (Figure 3.8 C). ASCs were assessed for size (forward scatter) and granularity (side scatter) following release from encapsulation. When comparing the two types of alginates (Figure 3.8 B, C), a similar profile was found in cell size and granularity compared to normally grown ASCs. Upon assessing ASCs-associated markers (Figure 3.8 D), CD 90 and CD73 were slightly lower in the S. (74.1% and 70.1%) alginate compared to the and N. alginate (76.6% and 73.2%). Of the markers that have a key role in cell adhesion and cell-cell interaction, CD166 were slightly less expressed in N. alginate (84.6%) than S. alginate (90.2%), while CD29 expression was faintly less in S. alginate (77%) than N. alginate (79.8%). The expression of negative markers CD45

and CD14 remained unchanged for S. alginate (1.5% and 1.9%) and N. alginate (1.3% and 1.4%). While human leukocyte markers (HLA) -ABC and -DR were slightly higher in S. alginate (56.4% and 25.2%) compared to N. alginate (50.8% and 18.2%). Thus, both alginates do not affect cell expression of surface markers.

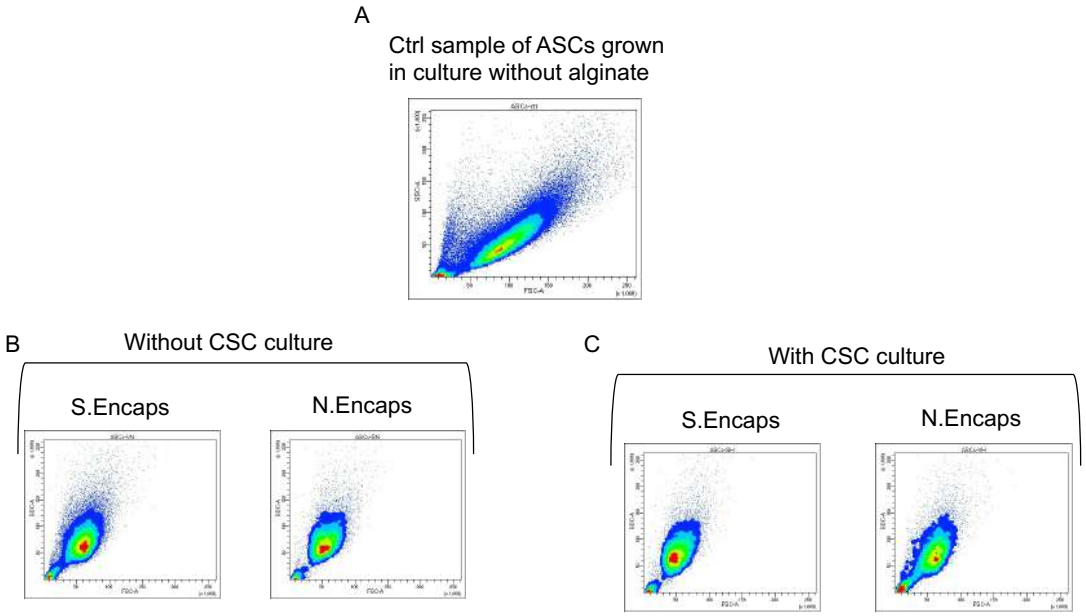

D

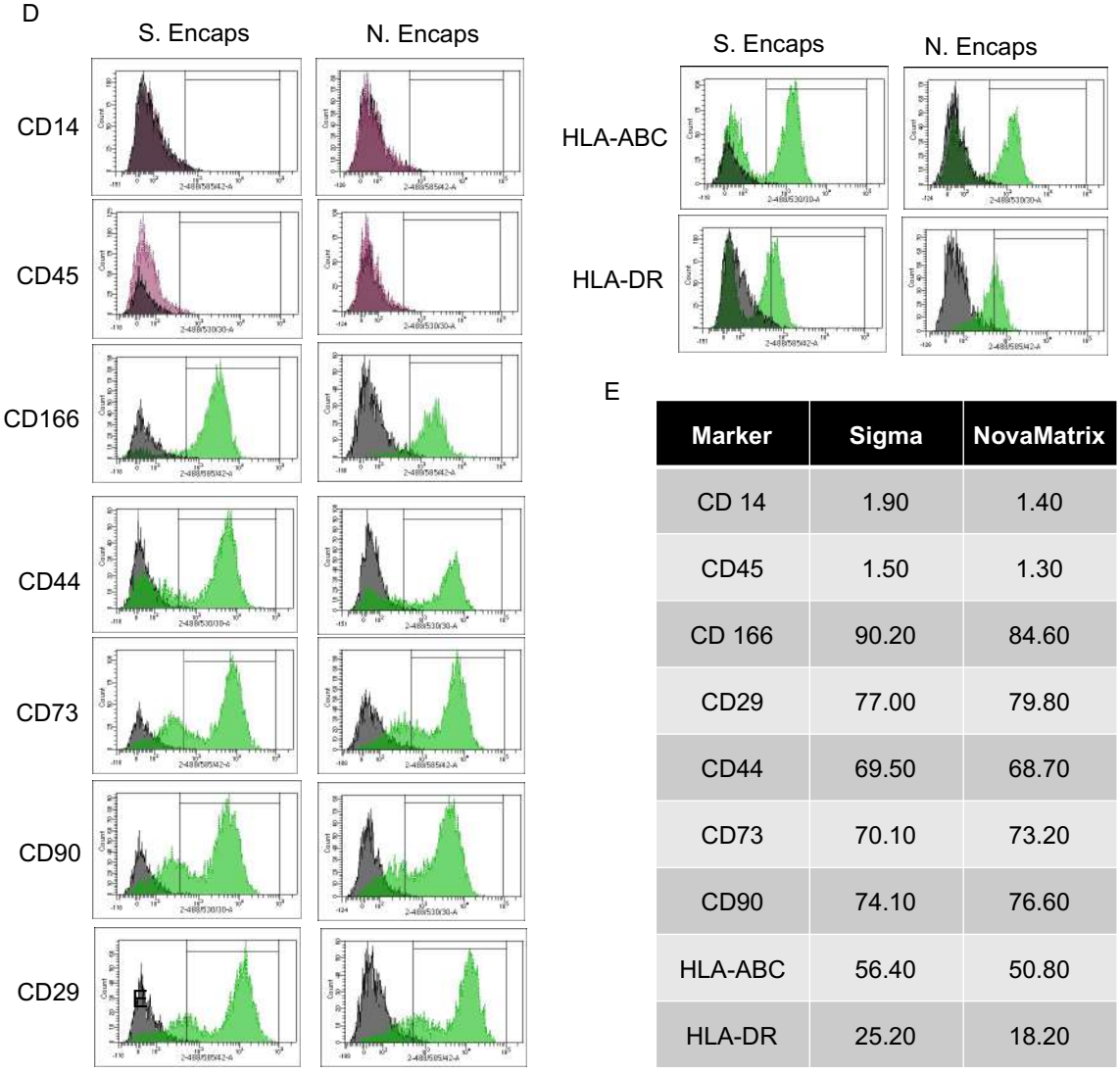

E

Marker	Sigma	NovaMatrix
CD 14	1.90	1.40
CD45	1.50	1.30
CD 166	90.20	84.60
CD29	77.00	79.80
CD44	69.50	68.70
CD73	70.10	73.20
CD90	74.10	76.60
HLA-ABC	56.40	50.80
HLA-DR	25.20	18.20

Figure 3.8 – Assessment of granularity, size, and immunophenotype of encapsulated ASCs following culturing with CSC scratch wound. ASCs were grown in culture at 37°C assessed for (A) size and granularity. Encapsulated ASCs in Sigma (S.) and NovaMatrix (N.) alginates without (B) and with (C) CSCs culture without CSCs culture. (D) Immunophenotype markers were assessed after use with CSCs culture. (E) Table represent the percentage of expression of cell surface markers from 2 separate donors. Abbreviations: FSC, forward scatter; SSC, side scatter; HLA, human leukocytes antigen; CSCs, corneal stromal cells.

3.3.5 Effect of cell encapsulation in different alginate matrices on HGF and VEGF secretion

The following results were compiled by a Master student's project (Tam Jeewon) and included here to further test Sigma and NovaMatrix alginates in terms of the effect on growth factors production. To quantify the hepatocyte growth factor (HGF) and vascular endothelial growth factor (VEGF), Enzyme-Linked Immune-Sorbent Assay (ELISA) was used. ELISA was performed using conditioned media collected from the encapsulated ASCs following 15°C storage (Figure 3.9 A). Using 7 different types of alginate to form the bandages including Sigma, VLVG, LV, MVG, VLVM, LVM, and MVM. These alginates differ in viscosity and M/G monomers ratio; thus, they were chosen for this comparison. VLVG alginate is the NovaMatrix alginate we have been using in the previous experiments. VLVG, very low viscosity alginate with a minimum of 60% guluronate monomers; LVG, low viscosity alginate with a minimum of 60% guluronate monomers; MVG, medium viscosity alginate with a minimum of 60% guluronate monomers; VLVM, very low viscosity alginate with a minimum of 50% mannuronate monomers, LVM, low viscosity alginate with a minimum of 50% mannuronate monomers; MVM, medium viscosity alginate with a minimum of 50% mannuronate monomers. Sigma (S.) alginate presented the highest level of HGF produced on day 3 compared to adherent cells and VLVG (N.) alginate. Whilst VEGF levels were slightly higher in VLVG (N.) alginate than S. alginate (Figure 3.9 B). To determine the effect of cell number of HGF and VEGF secretion, data were normalised to cell number (Figure 3.9 C). Data normalisation showed that S. alginate produced significantly the highest level of HGF protein compared to adherent culture and N. alginate. Whereas VEGF levels were significantly higher in encapsulated cells compared to adherent cultures (Figure 3.9 D).

Following the previous observation, to determine the effect of S. alginate on cells production of HGF, ASCs culture were grown in a monolayer and alginate gels (Sigma, VLVG (N.) and VLVM) were placed in a transwell system (Figure 3.10) It was found that cells produced a high level of HGF with the S. Alginate compared to N. Alginate. This observation suggested that S. Alginate may contain impurities that increase the cells' secretion of HGF. This may explain the increase in scratch wound recovery over time compared to N. Alginate.

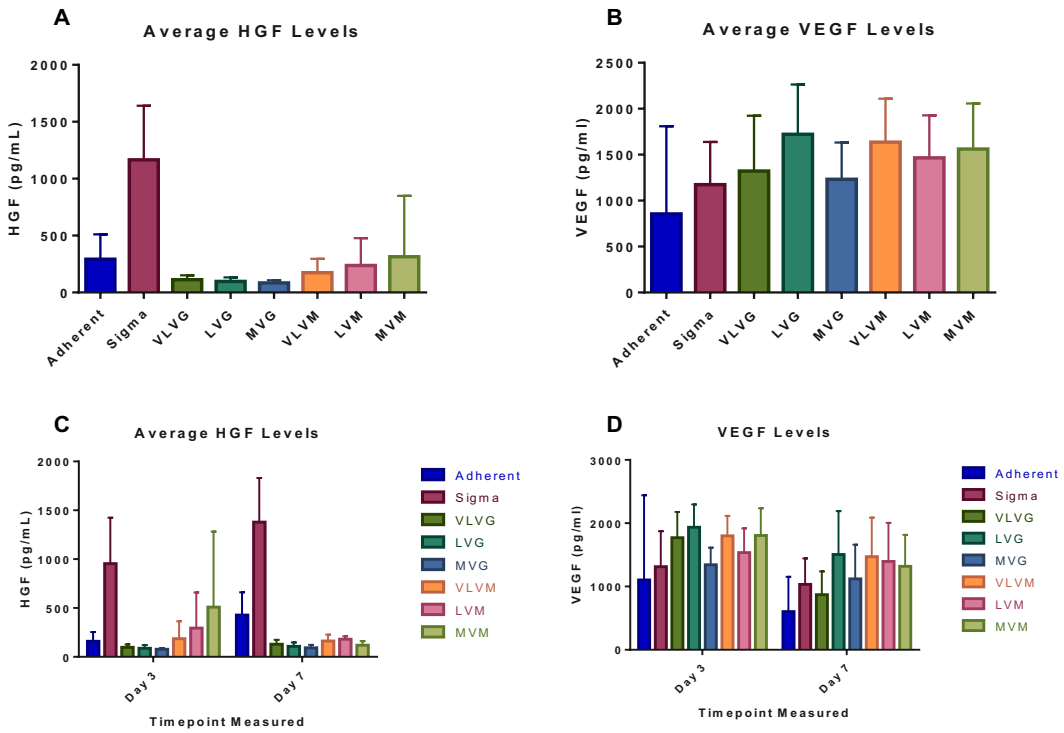

Figure 3.9 – The effect of different alginate matrices on HGF and VEGF protein production. Encapsulated ASCs stored at 15°C were assessed for (A) HGF, and (B) VEGF production over 7 days' time course. Similarly, ASCs production of (C) HGF and (D) VEGF represented on days 3 and 7. N =2. VLVG alginate is the NovaMatrix alginate we have been using in the previous experiments. Abbreviates, VLVG, very low viscosity alginate with 60% guluronate monomers; LVG, low viscosity alginate with 60% guluronate monomers; MVG, medium viscosity alginate with 60% guluronate monomers; VLVM, very low viscosity alginate with 50% mannuronate monomers, LVM, low viscosity alginate with 50% mannuronate monomers; MVM, medium viscosity alginate with 50% mannuronate monomers.

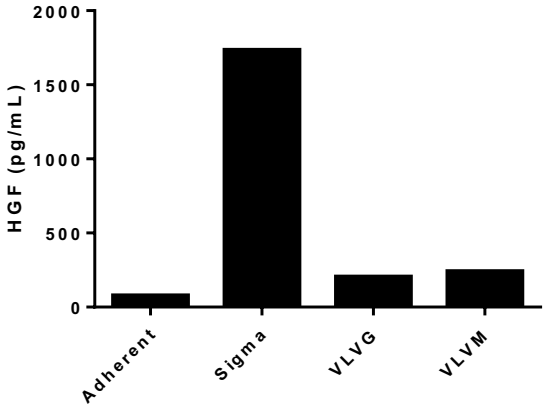

Figure 3.10 – ASCs production of HGF in proximity with cell-free gels. N = 2.

HGF and VEGF levels were further measured in response to inflammatory stimulation. ASCs were cultured with interleukin-1 beta (IL-1ß), an inflammatory cytokine activated by macrophages. IL-1ß is involved in many cellular events, such as cell differentiation, apoptosis, and proliferation. In the cornea, IL-1ß stimulates neutrophil activation and inflow, which leads to corneal haze (Barbosa et al., 2010, Kaur et al., 2009). Our results show, upon stimulating ASCs with IL-1ß (Figure 3.14 A), HGF levels were upregulated compared to non-stimulated cultures ($p = 0.0007$), similarly, although not significant (Figure 3.14 B), VEGF levels were also upregulated.

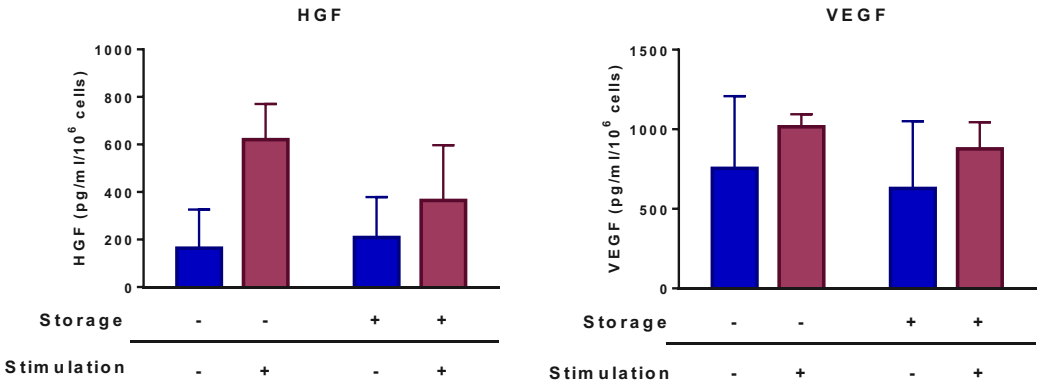

Figure 3.11 – IL-1ß stimulation on ASCs increase the production of (A) HGF and (B) VEGF. n = 2. Blue; adherent ASCs, Red; ASCs bandages.

3.4 Discussion

Biomaterial selection is one of the key factors in determining the success of translational therapy (Mount et al., 2015). The biomaterial needs to becompatible with the cells encapsulated within, i.e. allowing cells survival during transportation (Dash et al., 2018). For the cells to survive, they need to maintain nutrients exchange by taking in fresh nutrients and excreting waste, for that the biomaterial design must allow this exchange. Biomaterials function as carriers of cells, therefore, regardless of delivery method, they should maintain the cells inside the barrier whilst allowing the cells to produce factors in response to the environment (Shen et al., 2008). This is an important feature of a biomaterial. A key aspect of many approaches to stem cell therapy is the cells ability to sense the environmental cues and produce factors in response to these cues (Ruprecht et al., 2017). For example, in an injury penetrating to the corneal stroma, depending on the severity of the wound, the cells at the wound site would release signals whilst undergoing apoptosis. These signals are usually sensed by adjacent cells to start differentiating, migrating and proliferating to close the wound (Jester et al., 1999b). Therefore, if a biomaterial were to be applied to the injury site, the cells within the biomaterial must sense these cues and start producing growth factor(s) to aid in wound closure. Therefore, the biomaterial should be compatible with the cells within and the host tissue. To comply with this condition, a biomaterial must undergo various adjustments to serve in a specific application without causing any complications.

Cell migration is essential to many biological processes, such as tissue remodelling, immune response and wound healing (Ridley et al., 2003). Cell migration requires the cells to be active and to move in a specific direction via sensing environmental cues (Mak et al., 2016). These cues (mechanical and chemical signals) can polarise and differentiate the cells to an active, motile morphology, thus, able to migrate in the direction of these cues (Swaney et al., 2010). Cell polarisation is essential in defining the leading and trailing ends, via allocating proteins, which allow the cells to move in the right direction (Etienne-Manneville, 2008). *In vitro*, cell migration is demonstrated using time-lapse microscopy as cells can take up to several hours to make a small movement. Therefore, in this study, to measure *in vitro* cells migration, scratch assay was chosen as a low-cost, easy to perform, robust albeit relatively simplistic (in terms of

wound healing biology) assay (Cory, 2011). A scratch assay can give an accurate measure of cells' behaviour under the effect of specific and well controlled conditions. Taking images at the start of the experiments, following the formation of a scratch and then taking images at different time points (time lapse), or an image at the end of the experiment, results in information on the speed of cell migration (once proliferation is accounted for).

Although the scratch assay is a good method to measure migration it has limitations. Cells not only migrate but they proliferate, and the scratch assay does not easily differentiate between migration and proliferation. Scratch assay also has a technical issue where it requires a uniform scratch across all used cells or conditions to give a relatively accurate measure of area closure over time (Liang et al., 2007, Jonkman et al., 2014). Upon *in vivo* cell injury, cells usually release signals that alert the body and are recognised by either cellular receptors to initiate a pro-inflammatory response or by extracellular sources to stimulate inflammatory response (Rock and Kono, 2008). Thus, the advantage of a scratch assay is having an injury response model, therefore, it is a suitable method for our research.

Calcium alginate can be extracted from seaweed which makes it a naturally existent polymer. It has been used in drug delivery (Cong et al., 2017), wound dressings (Aderibigbe and Buyana, 2018), and protein and enzyme immobilisation (Gombotz, 1998). Alginate as a wound dressing material maintains a moist environment, reduce bacterial infection, and induce wound healing. Thus, this material would be best suited for the entrapment and delivery of cells. Depending on the cross-linker used, alginates can be controlled in releasing drug dosage inside the wound, which makes them appealing for pharmaceutical applications (Lee and Mooney, 2012). For this, alginate hydrogels can be used to deliver cells into the injury site to induce the resident cells in regenerating the tissue. Alginate hydrogels have been used in cultivating corneal endothelial and limbal stem cells, where it suggested that alginate can aid in corneal regeneration (Wright et al., 2012, Liang et al., 2011). It has also been found that alginate maintains ASCs viability and functional ability during short-term hypothermic storage (Swioklo and Connon, 2016, Swioklo et al., 2016). This ability of alginate is a key feature in the formation of stem cells bandages. As such, alginate was used to encapsulate cells in a 3D environment in all subsequent experiments.

Although calcium alginate is a suitable biomaterial for the formation of stem cell bandage, it is still important to determine the source of alginate (Sanchez et al., 2013). The structure is dependent on the guluronic and mannuronic acid formation, which is also dependent on the source (Augst et al., 2006). Therefore, we tested two types of alginate sources, the first was purchased from Sigma-Aldrich (extracted from *Macrocystis pyrifera*, referred to as S.) a low molecular weight, non-purified, high M acid content. The second is NovaMatrix ultrapure, low molecular weight, and high G acid content alginate purchased from FMC Biopolymer (extracted from *Laminaria hyperborea,* referred to as N.). Both of the providers extracted sodium alginate from the brown algae cell wall and supplied it in a powder format in different levels of purity. While there seemed to be differences in the appearance of the powder, from the datasheet, the major differences were found in the viscosity, purity, and composition of the G and M acid block copolymers ratio.

We then sought to determine the cell encapsulation method. In our lab, Swioklo *et al* encapsulated $1x10^6$ adipose-derived stem cells (ASCs) in 0.5mL alginate hydrogel discs (Swioklo et al., 2016). The authors crosslinked alginate gels with 102mM calcium chloride, to produce a gelled disc that contains cells. The formed disks were transferred inside a 2ml cryovials with growth medium. The growth medium is a reduced serum growth medium (MesenPro RS) supplemented with 2mM GlutaMAX and 1% v/v antibiotic-antimycotic.

The two alginate materials were found here to preserve ASCs viability when used with a secondary cell population, shown by the cell number counted upon release. In our system, the encapsulated cells were separated from the CSCs culture by using a transwell system, which serves as a physical barrier that prevents direct contact between CSCs and alginate (Rohrschneider et al., 2015). Additionally, we used serum-free media, with three days' serum starvation prior to starting the experiment, this would induce the cells to deactivate to an inactive form (Foster et al., 2015). Previously, it was shown that serum absence from culture media induce partial retrieval of the native keratocyte phenotype from corneal fibroblasts. This upturn was expressed by the increase of keratocyte markers such as kertocan, lumican, and SLRPs (Beales et al., 1999, Brown et al., 1999, Foster et al., 2015). SFM incubation with CSCs fibroblasts was shown to allow the cells to partially return to their keratocytes phenotype, thus, allowing the cells to return to their inactive form

(West-Mays and Dwivedi, 2006), at which point, the cells were about 90% confluent. This was evident when comparing the average time it took for the cell to cover the cell-free area when compared to cells cultured with serum media, as such, serum-free cultured cells showed a slower area coverage. Thus, the beneficial effect seen is from having ASCs in culture.

One of the key aspects of successful stem cell therapy is the scaffolds' ability to maintain cell viability and ability to release growth factors (Ashimova et al., 2019, Nicodemus and Bryant, 2008). Another important condition is the transportation of therapeutic cells, from the manufacturing site to the clinic where it can take from days to weeks (Swioklo and Connon, 2016). Therefore, we sought to test alginate ability in maintaining cell survivability during storage. Swioklo *et al* investigated alginate ability to maintain ASCs viability and morphology during three days of storage at temperatures ranging from 4°C to 23°C (Swioklo et al., 2016). Upon comparing the various temperatures, 15°C storage marked the best temperature in maintaining cell survivability when compared to non-encapsulated cells. Upon cell release, our results correspond to the results found by Swioklo, therefore, we used it with CSCs culture. Data suggested that storing cells at 15°C prior to using with CSCs culture to enhance area coverage over time when compared to 4°C and non-stored conditions in both alginate types. In support of this, we assessed ASCs-associated surface markers by flow cytometry, where they were maintained during encapsulation in both types of alginates following culture with CSCs. These results showed Sigma and NovaMatrix alginate to maintain ASCs' size and granularity. ASCs' surface marker expression profile was mostly similar between cells encapsulated in Sigma and NovaMatrix alginates following culture with CSCs (Mildmay-White and Khan, 2017). In which cells expressed CD29, CD44, CD73, CD90, and MHC class I but not MHC class II, CD14, and CD45. Thus, support our belief that alginate can be used as a bandage to immobilise the cells without affecting their function.

To treat corneal opacity, MSCs were previously tested for the production of HGF and VEGF, where it was found that MSCs produce HGF in response to inflammatory cytokine IL-1ß (Weng J, 1997b, Weng J, 1997a). It was also found that the addition of HGF to a corneal wound can restore corneal transparency by inhibiting myofibroblastogenesis (Miyagi et al., 2018). Authors also found that HGF

decreases inflammatory cytokines level in a corneal epithelial injury model whilst promoting cell proliferation (Torricelli et al., 2016). Therefore, evidence suggests that high HGF levels in the cornea can restore corneal transparency while reducing inflammatory cytokines. In our results, there was no change in VEGF levels, however, the increase in HGF level was associated with the presence of Sigma alginate and not the ASCs themselves. HGF levels were also higher in response to IL-Iß stimulation compared to non-stimulated cells. Therefore, this effect was considered as undesirable in stem cell therapy, since the focus of the therapy is the ASCs' ability to produce growth factors in response to the environmental cues.

In conclusion, this chapter tested the possibility of using ASCs in corneal therapy focusing on comparing two types of alginates Sigma and NovaMatrix alginates. We show the importance of using alginate biomaterial to encapsulate and store ASCs before use in therapy, where they maintain ASCs viability and functional ability during storage. ASCs were also able to maintain the immune surface markers in both alginates. Sigma alginate showed superiority over NovaMatrix alginate in improving CSCs scratch wound closure. This ability was also shown following storage at 4°C and 15°C for 72 hours. Upon further testing this, Sigma alginates were found to induce ASCs secretion of HGF and VEGF, which may explain the effect we have presented in the Sigma alginate condition. Although it is important to have HGF in corneal wound healing, having HGF secreted via the effect of alginate would defy the purpose of safe cell therapy. Alginate offer cells cytoprotection during storage by reducing cellular edema and osmotic shock while having involvement in solute and ion diffusion throughout the matrix (Golmohamadi and Wilkinson, 2013). As a material, it demonstrated biocompatibility, reproducibility, and importance in cell therapy. As such, our model of NovaMatrix alginate bandages presented a promising method of therapy.

Chapter 4. Hypothermically stored alginate encapsulated ASCs enhance corneal stromal cells scratch wound closure via release of paracrine factors

4.1 Introduction

A considerable body of evidence suggests that mesenchymal stem cells (MSCs), have a beneficial effect on corneal injury (Arnalich-Montiel et al., 2008, Espandar et al., 2012, Alio del Barrio et al., 2015), especially through their ability to produce paracrine factors (Ratajczak et al., 2012, Al-Jaibaji et al., 2019). Adipose-derived mesenchymal stem cells (ASCs) have been shown to produce various cytoprotective and angiogenic factors that aid in cell therapy including vascular endothelial growth factor (VEGF) (Kinnaird et al., 2004, Rehman et al., 2004), insulin-like growth factor (IGF-1) (Togel et al., 2007), monocyte chemoattractant protein (MCP-1) (Kwon et al., 2014), transforming growth factor- B (TGF-ß) (Boomsma and Geenen, 2012), hepatocyte growth factor (HGF) (Rehman et al., 2004), and interleukin-6 (IL-6) (Kwon et al., 2014). It has been shown that MSCs reduce inflammation in alkali burn corneas via reducing CD68+ cells of macrophage and monocyte lineages and downregulating VEGF, tumor necrosis factor-a (TNF-a) and macrophage inflammatory protein -1a (MIP-1a) (Yao et al., 2012). Moreover, MSCs growing on the nanofiber scaffold transferred onto alkali-induced oxidative injury showed a reduction in neovascularization and inflammatory cell infiltration (Cejkova et al., 2013). Tumor necrosis factor-a stimulated gene-6 (TSG-6) secretion by MSCs was shown to promote corneal epithelial wound recovery in diabetic mice via the activation of local epithelial cells (Di et al., 2017). These studies suggest that MSCs produce various paracrine factors that would benefit specific treatments and may be used for specific cell therapy.

4.2 Aims

Our findings in the previous chapter suggest that alginate preserves cells functional state during hypothermic storage. Hypothermically stored ASCs bandages were shown to have a favorable effect on corneal stromal cells (CSC) and so we are closer to the formation of stem cell bandages. However, many more tests are

required to evaluate and improve the construction of stem cell bandages. We sought to assess different conditions using scratch assay including (i) ASCs ability in healing CSCs without the bandage, (ii) encapsulation of different densities of ASCs, (iii) conditioned media (CM) production from the bandages, (iv) effect of CM + bandages, (v) effect of ASCs lysis (death) and lysate (formed CM during cell lysis), (vi) effect of different cell bandages including human dermal fibroblasts (hDF) corneal stromal-mesenchymal stem cells (CSF) and keratoconus cells (KC) compared to ASCs bandages. Followed by assessment of (vii) CSC and ASCs key markers using qPCR, (viii) protein production using Bradford assay, (viiii) collagen production using Sirius red, and lastly (x) the paracrine factors produced by ASCs bandages using human XL cytokine array kit. Our presented results in this chapter elucidate the beneficial effect of ASCs bandages in healing CSC *in vitro* via the production of paracrine factors including HGF, TSG-6, IL8, MCP-1, thrombospondin-1, among other factors that regulate inflammation and wound healing.

4.3 Results

4.3.1 ASCs improves corneal stromal cells scratch closure in an indirect co-culture

As we want to form bandages, we require a scaffold to maintain the viability and function of the cells. However, even without a scaffold, it is known that ASCs do indeed improve wound recovery, which has been shown in many *in vitro* and *in vivo* studies (Almaliotis et al., 2015, Aluri et al., 2017, Arnalich-Montiel et al., 2008). Therefore, it is indispensable to measure ASCs' effect on CSCs without the use of a scaffold. To do that, we plated ASCs on a transwell insert either without storage (non-stored) or following 72-hours storage at 4°C and 15°C. The cells were left to attach to the membrane for 2-hours at 37°C and 5% CO_2 with SFM. Two hours following incubation, the transwells were carefully washed to remove dead cells and incubated with fresh SFM before placing with scratched CSCs cultures (as described in chapter 2 2.5). Since the cells were plated on the transwell membrane, we were unable to use Iprasense holographic time-lapse microscopy to follow cell movements. Instead, we used Leica light microscopy, with images were manually taken at 0-, 24-, and 48-hours following scratch.

The presence of ASCs improved area coverage (Figure 4.1 A, B), storage seemed to play an important aspect in this. Following 15°C storage, at 24 hours, an increase in area coverage was found compared to non-stored and 4°C stored cells ($p = 0.0001$ and $p > 0.0001$ respectively). This difference continued to 48 hours when compared to non-stored ($p = 0.0157$). No difference was found upon comparing CSC cell density at 48-hour post scratch (Figure 4.1 C). Interestingly, this disparity was seen despite the fact that 15°C stored ASCs density were far less than non-stored cells. At 48-hours, 15°C stored ASCs were counted to be $1.89x10^5$ cells/mL (37.8%) compared to non-stored ASCs $3.96x10^5$ cells/mL (79.2%) and to 4°C stored ASCs $0.86x10^5$ cells/mL (17.2%). Upon normalizing ASCs number to CSCs scratch wound percentage (Figure 4.1 D), significant differences were found between non-stored and 15°C at times 24 and 48 hours ($p = 0.0479$ and <0.0001) and to 4°C stored (<0.0001). This suggests that although storage has a certain effect on cells in improving their production of paracrine factors, ASCs cell number present another important aspect in cell therapy, and adjusting this can lead to enhanced therapy.

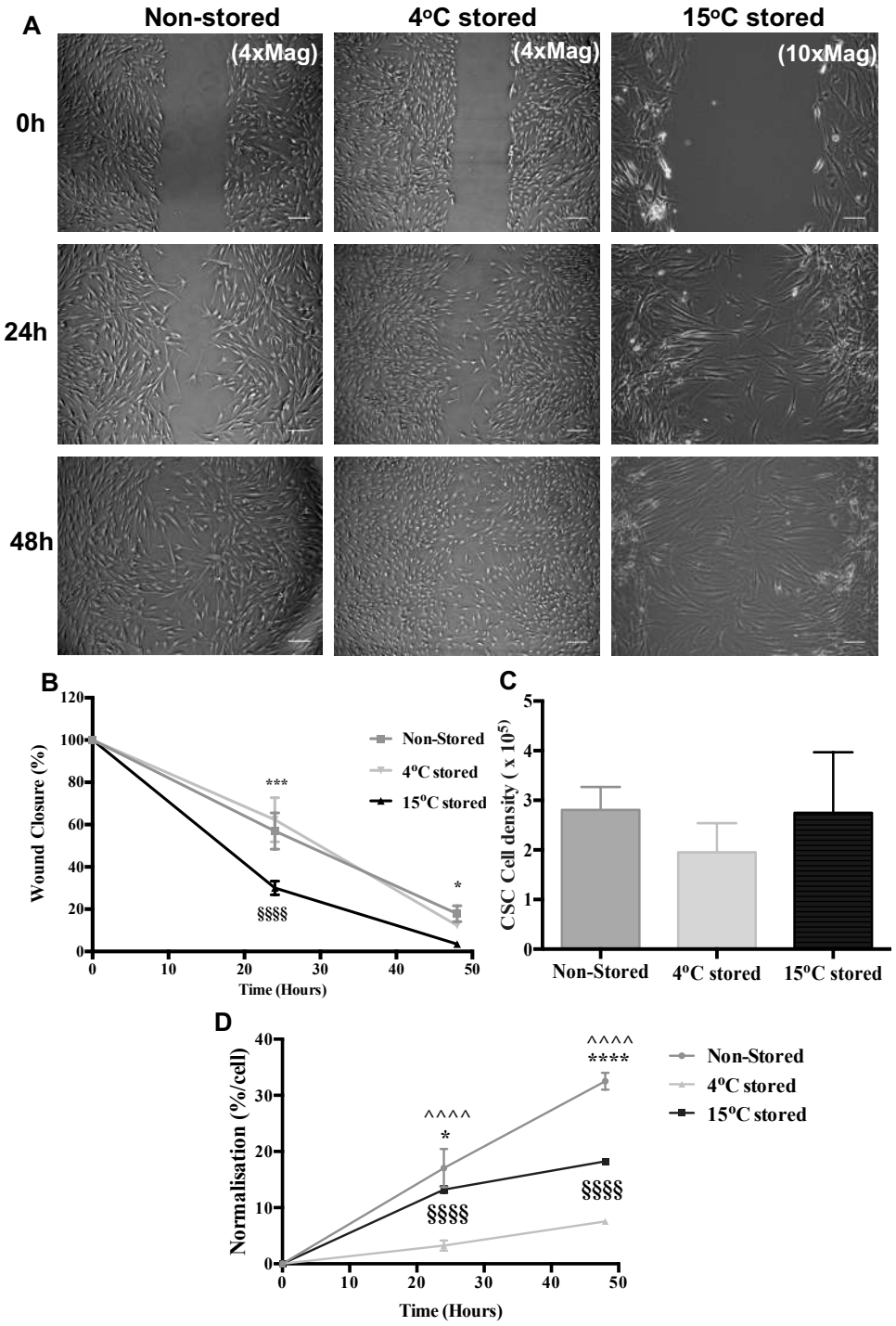

Figure 4.1 – Wound closure analysis of non-encapsulated ASCs. ASCs were used immediately following plating on a transwell membrane or following 72-hours storage at 4°C and 15°C. (A) Scratch images taken using light microscopy at times 0-, 24-, and 48 –hours. (B) Wound closure percentage over time. (C) CSCs cell density at 48-hours. (D) ASCs cell number normalized to CSCs scratch area. Values are presented as mean ± SEM from three separate keratocytes donors, asterisks represent significance between non-stored and 15°C stored conditions (****, p <

0.0001; ***, $p < 0.001$; *, $p < 0.05$), while symbols represent significance between 15°C and 4°C stored ASCs (§§§§, $p < 0.0001$) and 4°C and non-stored (^^^^, $p < 0.0001$). Scale bar = 220μm for the non-stored and 4°C stored and 110μm for the 15°C stored. Non-stored and 4°C stored images taken using 4x magnification, while 15°C images taken using 10x magnification.

4.3.2 Encapsulated ASCs density determines area coverage speed

Although in the previous chapter we encapsulated the same number of ASCs ($1x10^6$ cells), we still needed to measure the effect of cell density on CSCs. We expect with more ASCs in culture the faster the area will be covered by CSCs i.e. dose-response. Thus, we encapsulated a range of ASCs densities (10,000 cells, 100,000, cells and 500,000 cells) in alginate and used that with scratched CSCs (Figure 4.2 A). ASCs were used immediately following encapsulation (i.e. without storage). In agreement with our speculations (Figure 4.2 B), the more cells encapsulated, the faster the area covered by CSCs, where encapsulating $1x10^6$ cells showed significant improvement in area coverage compared to all other densities at 24 hours ($p > 0.0001$). This significance persisted to 48 hours when compared to $0.01x10^6$ cells encapsulated ($p = 0.0004$). Significant increase in CSCs cell number with the $1x10^6$ cells ASCs following scratch healing compared to $0.01x10^6$ cells and $0.1x10^6$ cells ($p = 0.0355$ and 0.0365 respectively), which supports our theory of the more cells we have in culture the better effect seen (Figure 4.2 C).

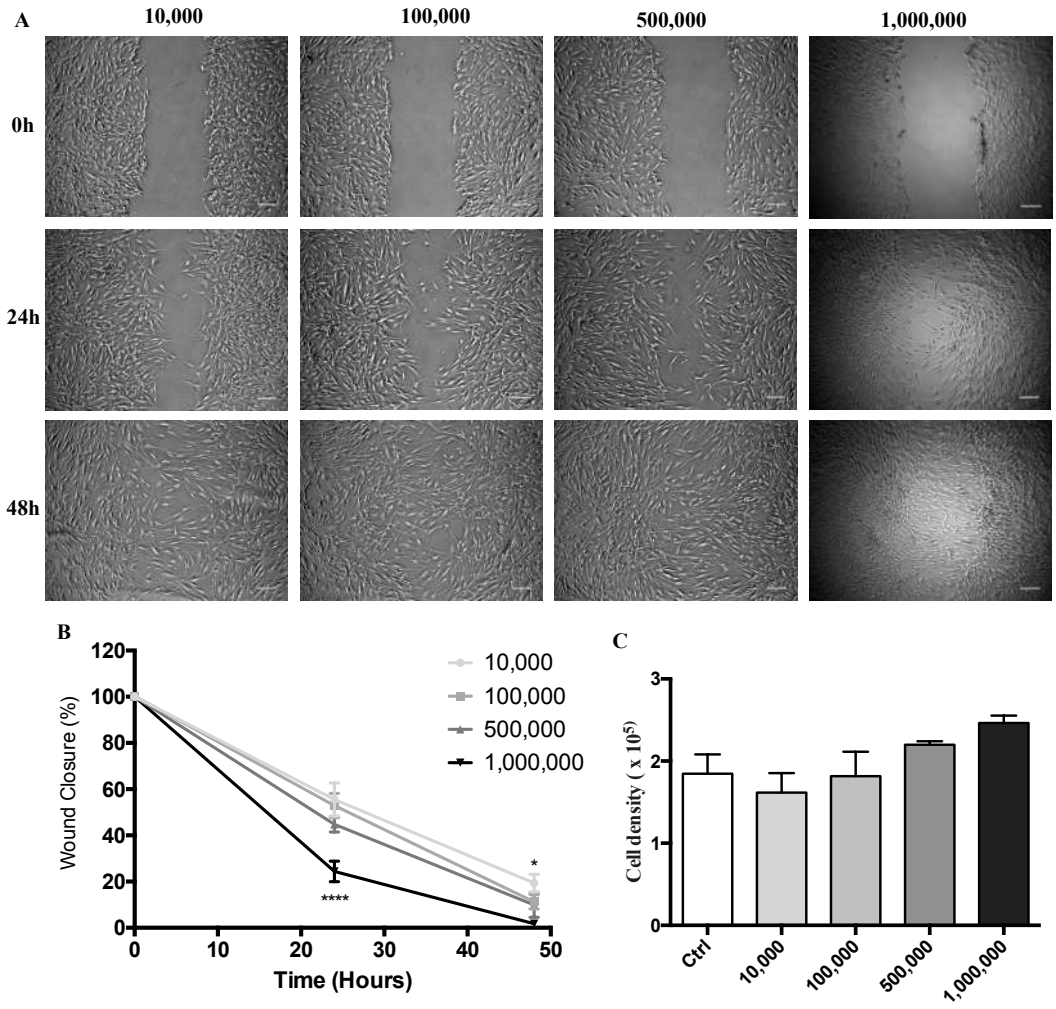

Figure 4.2 – Wound closure analysis of ASCs cell dilution. ASCs were used immediately following encapsulation. (A) Scratch images taken using light microscopy at times 0-, 24-, and 48 –hours. (B) Wound closure percentage over time. (C) CSCs density at 48 hours. Values are presented as mean ± SEM from three separate keratocytes donors, asterisks represent significance between 1x10^6 cells and 0.01x10^6 cells (****, $p < 0.0001$; *, $p < 0.05$). Scale bar = 220μm. The difference in images is due to technical issues.

4.3.3 Conditioned media enhances area coverage

In our system, to determine ASCs' suitability as a bandage, we need to test the release of therapeutic soluble factors. It is expected that encapsulated ASCs secrete a cocktail of factors into the media, thus, we needed to know the storage effect on these factors. With the assumption that ASCs in culture can improve healing

because they are environmentally responsive, we sought to test the conditioned media (CM) produced from the encapsulated ASCs. ASCs were encapsulated and stored at 4°C and 15°C for 72-hours with SFM without disruption, at which point, the media were collected and considered as CM (explained in chapter 2 2.9). This CM was taken from the encapsulated cells and the alginate controls. Two concentrations were used with CSC scratches, 50% CM diluted in 50% SFM, and 100% CM. These two concentrations were used with the assumption that ASCs produce paracrine factors during storage and so the more CM used the greater the effect on CSC scratch closure will be seen.

CM taken from 4°C stored ASCs bandages showed a significant increase in area coverage compared to alginate only CM (Figure 4.3 A, B, C). 20-hours following scratch induction, CSC incubated with CM taken from 50% Encaps. showed a significant increase in area coverage compared to CM taken from 50% alginate ($p = 0.0297$), similarly, 100% Encaps. showed a significant decrease in the cell-free area compared to 100% alginate ($p > 0.0001$). This significance persisted at times 30- and 40-hours post scratch for both 50% CM ($p = 0.0001$) and 100% conditioned media ($p < 0.0001$ and 0.0001 respectively). Upon comparing 50% and 100% CM taken from ASCs bandages, differences were shown at times 20- and 30-hour post scratch ($p = 0.0010$ and 0.0282 respectively). These results suggest that the CM taken from stored ASCs bandages to contains factors released from the cells that can aid in wound recovery.

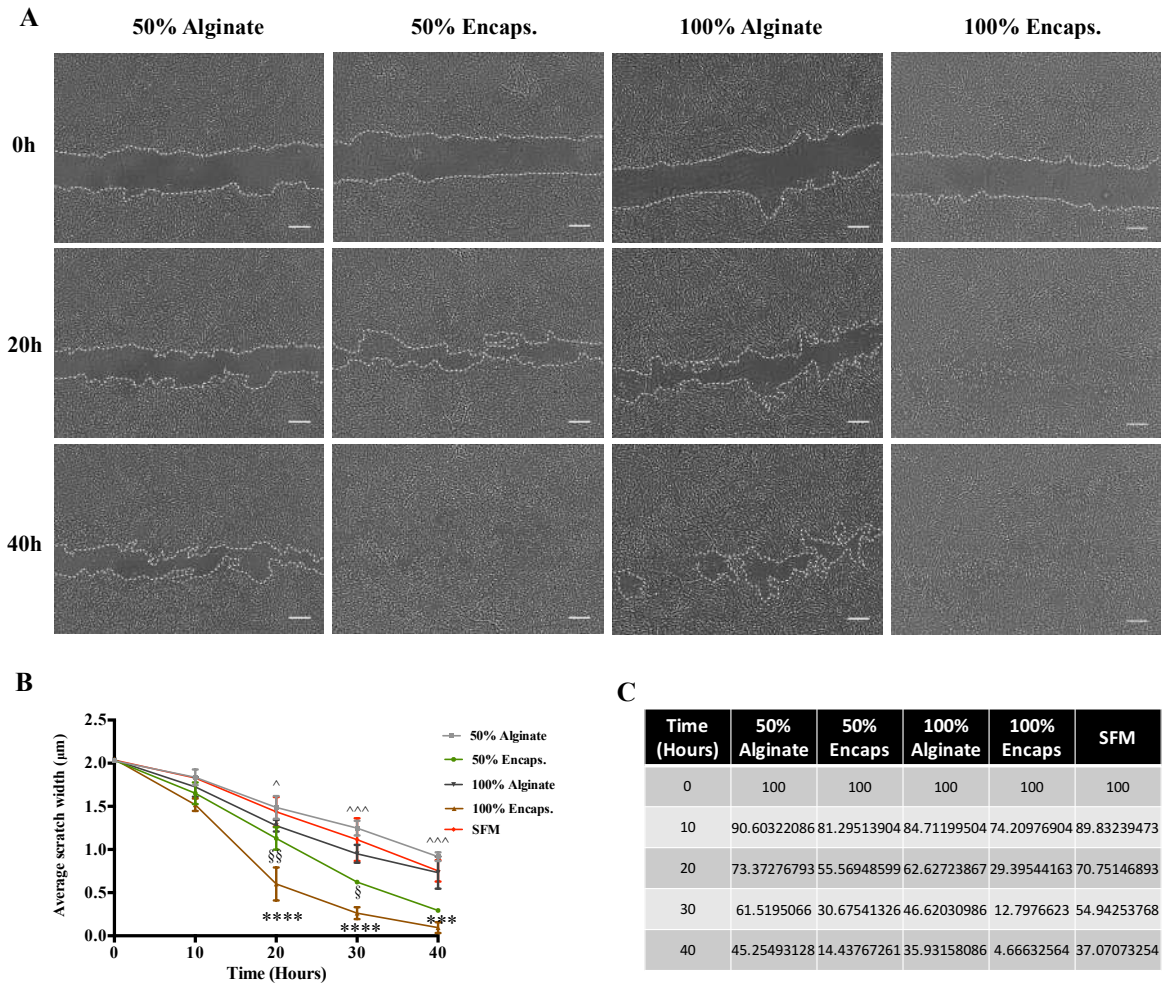

C

Time (Hours)	50% Alginate	50% Encaps	100% Alginate	100% Encaps	SFM
0	100	100	100	100	100
10	90.60322086	81.29513904	84.71199504	74.20976904	89.83239473
20	73.37276793	55.56948599	62.62723867	29.39544163	70.75146893
30	61.5195066	30.67541326	46.62030986	12.7976623	54.94253768
40	45.25493128	14.43767261	35.93158086	4.66632564	37.07073254

Figure 4.3 – Wound closure analysis of conditioned media taken from 4°C stored alginate +/- ASCs. Condition media were either diluted with SFM or used without dilution. (A) Scratch images taken using Iprasense at times 0-, 20-, and 40 –hours. (B) Average scratch width (C) Percentage wound closure. Values are presented as mean ± SEM from three separate keratocytes donors, asterisks represent significance 100% Encaps. and 100% alginate (****, $p < 0.0001$; ***, $p < 0.001$), while (^) symbol represent significance between 50% Encaps. and 50% alginate (^^^, $p < 0.001$; ^, $p < 0.05$). The (§) symbol represents significance between 100% Encaps. and 50% Encaps. (§§, $p < 0.01$; §, $p < 0.5$). Scale bar = 300µm. Alginate, bandage – ASCs; Encaps, bandage + ASCs.

CM taken form 15°C stored alginate encapsulated ASCs also showed significant improvement in wound coverage (Figure 4.4 A, B, C). 50% conditioned media showed a significant increase in area coverage compared to conditioned

media taken from alginate controls at times 30- and 40-hours post scratch (p = 0.0079 and 0.0145 respectively). Whereas 100% conditioned media taken from encapsulated cells also showed significant difference at times 20-, 30-, and 40-hours post scratch (p = 0.0015, 0.0002 and 0.0085 respectively). Whilst 50% and 100% conditioned media taken from encapsulated cells showed significant difference at time 20 hours post scratch (p = 0.0114). From the graph, although not significant, there seems to still be a difference between the two conditions.

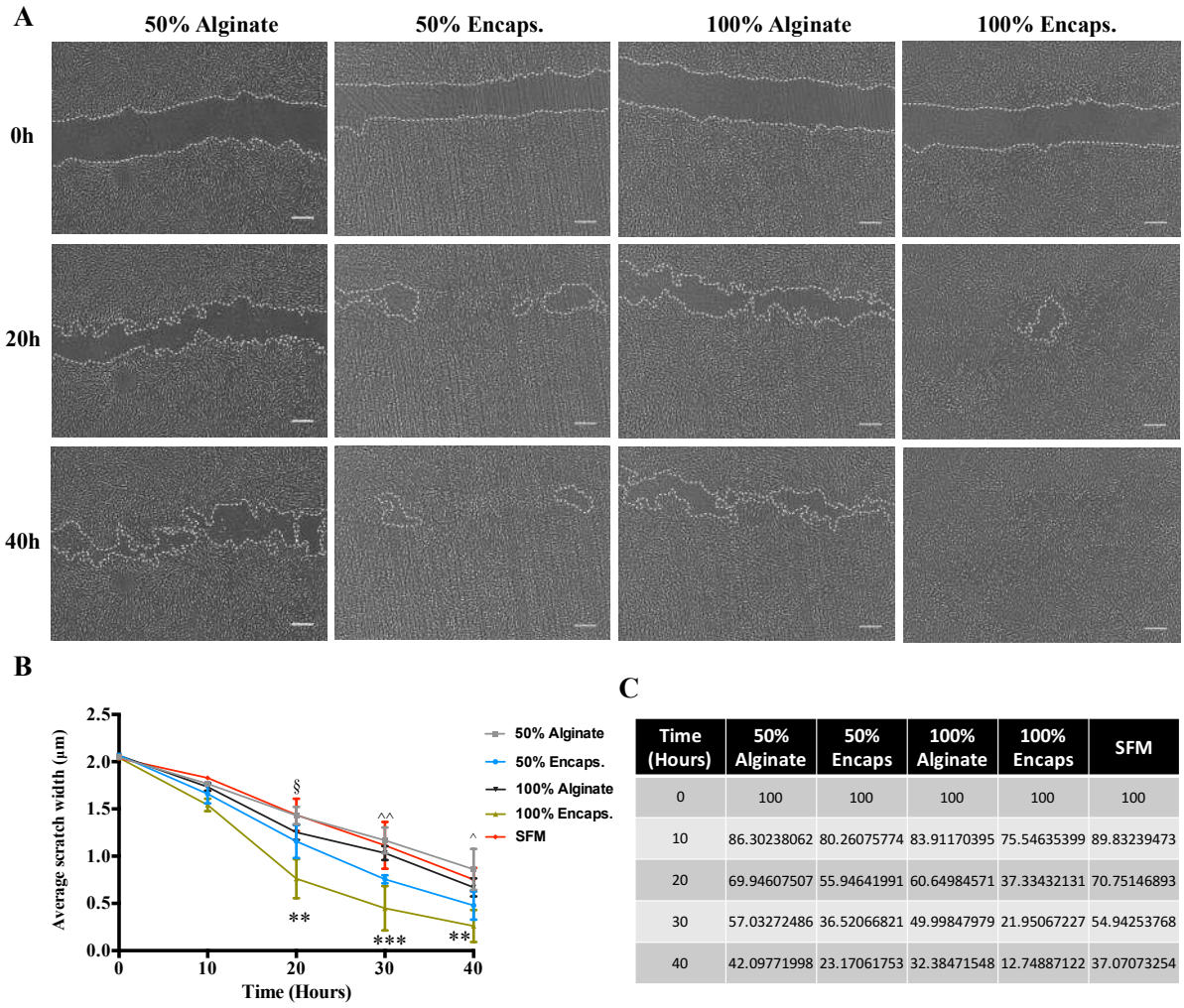

C

Time (Hours)	50% Alginate	50% Encaps	100% Alginate	100% Encaps	SFM
0	100	100	100	100	100
10	86.30238062	80.26075774	83.91170395	75.54635399	89.83239473
20	69.94607507	55.94641991	60.64984571	37.33432131	70.75146893
30	57.03272486	36.52066821	49.99847979	21.95067227	54.94253768
40	42.09771998	23.17061753	32.38471548	12.74887122	37.07073254

Figure 4.4 – Wound closure analysis of conditioned media taken from 15°C stored alginate +/- ASCs. Condition media were either diluted with SFM or used without dilution. (A) Scratch images taken using Iprasense at times 0-, 20-, and 40 –hours. (B) Average scratch width. (C) Percentage wound closure. Values are presented as mean ± SEM from three separate keratocytes donors, asterisks represent significance 100% Encaps. and 100% alginate (***, p < 0.001; **, p < 0.01), while (^)

symbol represent significance between 50% Encaps. and 50% alginate (^^, $p < 0.01$; ^, $p < 0.5$). The (§) symbol represents significance between 100% Encaps. and 50% Encaps. (§, $p < 0.05$). Scale bar = 300μm. Alginate, bandage – ASCs; Encaps, bandage + ASCs.

To determine which storage temperature improves cell production of growth factor, we compared 50% and 100% CM taken from 4°C and 15°C. However, no significant differences were found between the conditions. Next, we sought to determine the possibility of using double-conditioned CM. It was interesting to test whether the co-culture used up all the beneficial factors within the CM during scratch healing. If so, then it is expected to see no effect on CSC or a reverse effect because the double-conditioned CM will contain the waste produced from the co-cultured cells during scratch healing.

Following the use of 100% CM with CSCs healing, we collected that media and used it again with another population of scratched CSC. Double-conditioned CM should contain all the growth factors released from ASCs bandages during storage, adding to that, the growth factors released during scratch recovery. The downside of this is that this Double-conditioned CM contains all the factors produced by the two cell populations, and we have not explored the effect of CSC CM alone.

We used 15°C storage 100% CM with CSC for 48-hours, followed by another 48 hours of scratch healing with another CSC scratch culture (Figure 4.5 A). Interestingly, significant differences were found between the Double-conditioned CM from bandages ± ASCs (Figure 4.5 B &C). At 20-hours post-scratch, a significant increase in wound coverage was seen over time ($p = 0.0203$) which persisted to times 30-, and 40-hours post scratch ($p = 0.0017$ and 0.0005 respectively). This, however, when compared to 100% CM showed the disadvantage of using double-conditioned CM, where the latter showed a significant delay on area coverage at times 20-, 30-, and 40-hours post scratch ($p = 0.0006$, 0.0020 and 0.0105 respectively). This may suggest that the most active factors are from the ASCs rather than CSC since ASCs' growth factors would have been used during culture with first CSCs.

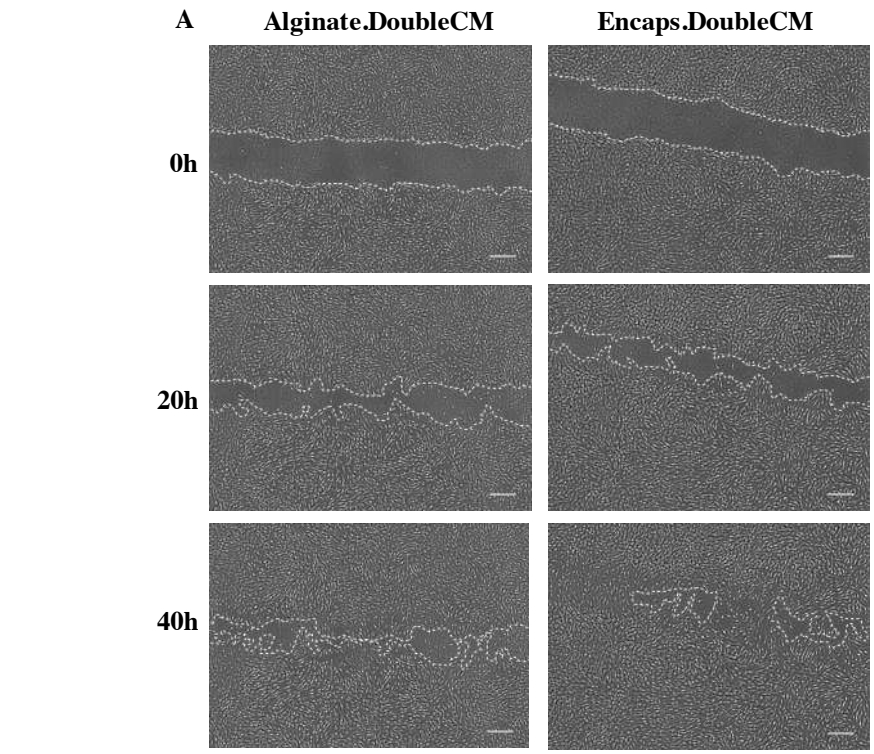

B

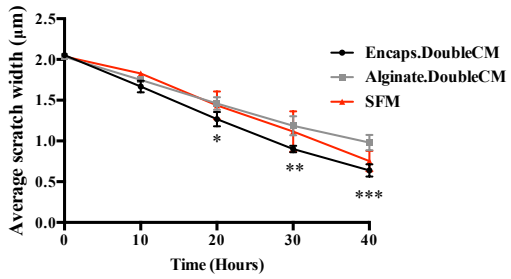

C

Time (Hours)	Alginate. DoubleCM	Encaps. DoubleCM	SFM
0	100	100	100
10	85.97840051	81.15864045	89.83239473
20	71.66229635	61.66704625	70.75146893
30	58.24554184	43.86046189	54.94253768
40	48.15147782	31.07046718	37.07073254

Figure 4.5 – Wound closure analysis of double conditioned media taken from 15°C stored alginate +/- ASCs. A) Scratch images taken using IPRASENS at times 0-, 20-, and 40 –hours. B) Average scratch width. (C) Percentage wound closure. Values are presented as mean ± SEM from three separate keratocytes donors, asterisks represent significance between conditions (***, $p < 0.001$; **, $p < 0.01$; *, $p < 0.05$). Scale bar = 300µm.

4.3.4 Combination of 15°C stored encapsulated ASCs conditioned medium with ASCs bandages have improved effect on corneal scratch wounds

Following CM assessment, and determining the effect of 100% CM, we wanted to assess whether this CM caused an additive effect. ASCs bandages stored at 15°C with SFM for 72 hours were used with their formed CM. Upon incubating ASCs

bandages plus their formed CM with CSC scratch wound, the combinative effect was seen on CSC scratch closure (Figure 4.6 A). Comparing the combination of ASCs bandages with CM (Encaps.Combi) and the ASCs - bandage with their CM (Alginate.Combi) (Figure 4.6 B &C), significant differences were seen at times 20, 30 and 40 hours post scratch (p = 0.0121, 0.0032 and 0.0058 respectively). Upon comparing Encaps.Combi to ASCs bandages and to CM only, no significant differences were found. This experiment, however, was made using only 2 technical repeats and the results would need to be further validated.

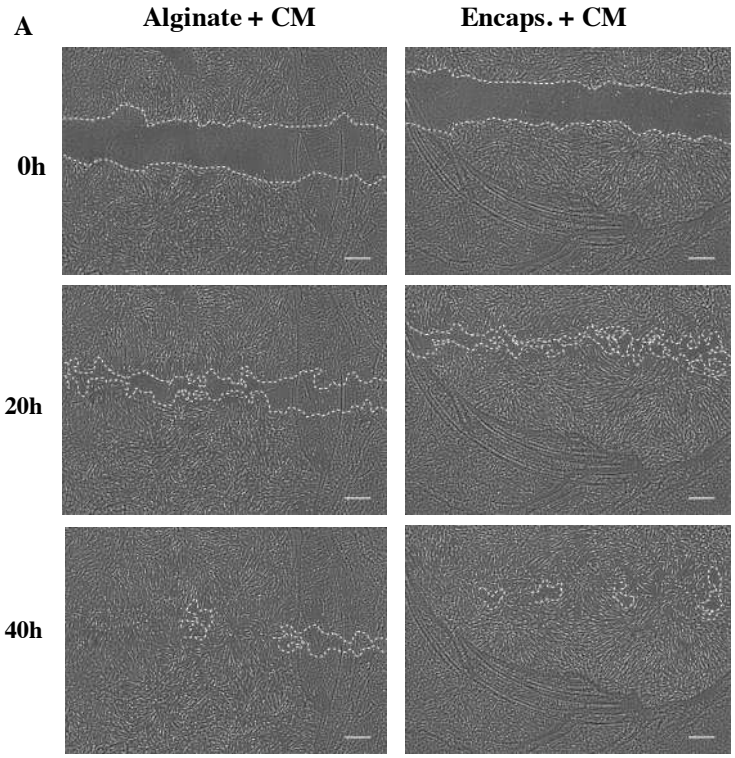

B

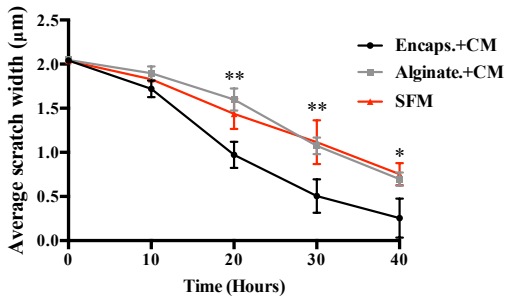

C

Time (Hours)	Alginate + CM	Encaps + CM	SFM
0	0	100	100
10	92.6520271	84.24924207	89.83239473
20	78.10746731	47.69766783	70.75146893
30	52.42325876	24.80781353	54.94253768
40	34.09269802	12.57842644	37.07073254

Figure 4.6 – Wound closure analysis of combined conditioned media and alginate +/- ACs following 15°C stored. (A) Scratch images taken using Iprasense at times 0-, 20-, and 40 –hours. (B) Average scratch width. (C) Percentage wound closure. Values are presented as mean ± SEM from three separate keratocytes donors,

asterisks represent significance between conditions (**, $p < 0.01$; *, $p < 0.05$), scale bar = 300μm.

4.3.5 Cell lysis within alginate slightly improves wound area coverage

Having the cells alive inside the gel means they can respond to the environmental cues. However, we wanted to assess whether growth factors are released from the encapsulated ASCs during culture with CSCs (in response to co-culture, i.e. active response to injury) or during storage (passage response) but are suppressed inside the gel then released over time upon return to normal therma. And so, we sought to assess the cell lysis effect within the scaffold using the freeze-thaw cycle, assuming that this would release all GF from within the ASCs).

Following 72-hour storage at 4°C and 15°C, encapsulated ASCs were incubated at -80°C for 2-hours followed by 30 minutes incubation at room temperature, to allow the gels to thaw at room temperature before using with CSC culture. At which point, the cells were released and incubated with live/dead staining to assess cell survival where the cells showed an average of 98% dead cells. For the freezing process, the encapsulated cells were washed and incubated with fresh SFM to remove any possible growth factors present and released during storage. The formed SFM following freezing were considered as lysate for they contain all the contents of the lysed cells. Thus, we compared gels containing cells that had been frozen (cell lysis) plus media (lysate) to gels containing cells that had been frozen without media (Figure 4.7 and 4.8).

At 4°C storage (Figure 4.7 A, B &C), a significant difference was found between the two conditions, where the presence of lysate (ASCs lysis plus lysate) in culture presented improvement in wound coverage significantly shown at times 20-, 30-, and 40-hours post scratch ($p = 0.005$, 0.0032 and 0.0268 respectively). Upon comparing it with live cells, cell lysis plus lysate showed improvement of wound coverage significantly shown at times 20- and 30-hours post scratch ($p = 0.0253$ and 0.0227 respectively). Interestingly, live cells showed a similar effect to lysed cells (without lysate), which can be explained by (i) the number of live cells inside the gel before use with CSCs being low, (ii) growth factors within gel released during storage to be the main source and not from the cells during culture with CSCs, or (iii) ASCs require time to adjust upon return to normal therma to start releasing growth factors.

Following 15°C storage (Figure 4.8 A, B &C), no significant differences were found upon comparing ASCs lysis plus lysate to ASCs lysis without lysate. However, from the graph, there seems to be a slight difference between the two conditions. Where ASCs lysis plus lysate showed improvement in CSCs scratch wound closure compared to ASCs lysis without lysate. Upon comparing ASCs lysate plus lysis and ASCs lysate without lysis to encapsulated ASCs, the latter still presented an improved wound recovery. This could be attributed to the cells themselves being able to release growth factors in response to the environment.

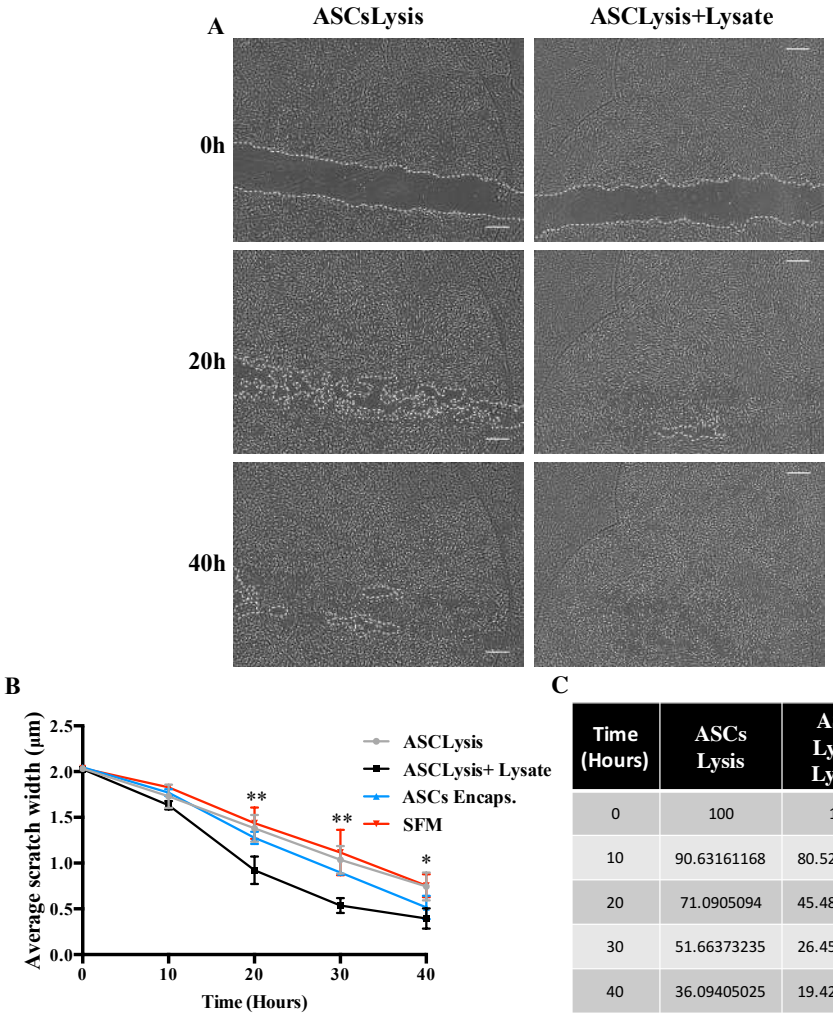

C

Time (Hours)	ASCs Lysis	ASCs Lysis+ Lysate	Encaps. ASCs	SFM
0	100	100	100	100
10	90.63161168	80.52292461	86.53511798	89.83239473
20	71.0905094	45.48379311	62.43107708	70.75146893
30	51.66373235	26.45936222	43.82554642	54.94253768
40	36.09405025	19.42103077	25.16327479	37.07073254

Figure 4.7 – Wound closure analysis of In-scaffold lysis, taken from 4°C stored encapsulated ASCs. Encapsulated ASCs were incubated at -80°C for two hours before thawing at room temperature and incubating with scratch wound. (A) Scratch images taken using Iprasense at times 0-, 20-, and 40 –hours. (B) Average scratch width. (C) Percentage wound closure. Values are presented as mean ± SEM from three separate keratocytes donors, asterisks represent significance between

conditions (**, p < 0.01; *, p < 0.05). Scale bar = 300μm. ASCsLysis, following thawing, encapsulated ASCs incubated with fresh SFM before placing with scratch wounds; ASCLysis + Lysate, following thawing, encapsulated ASCs and their formed lysate incubated with scratch wounds.

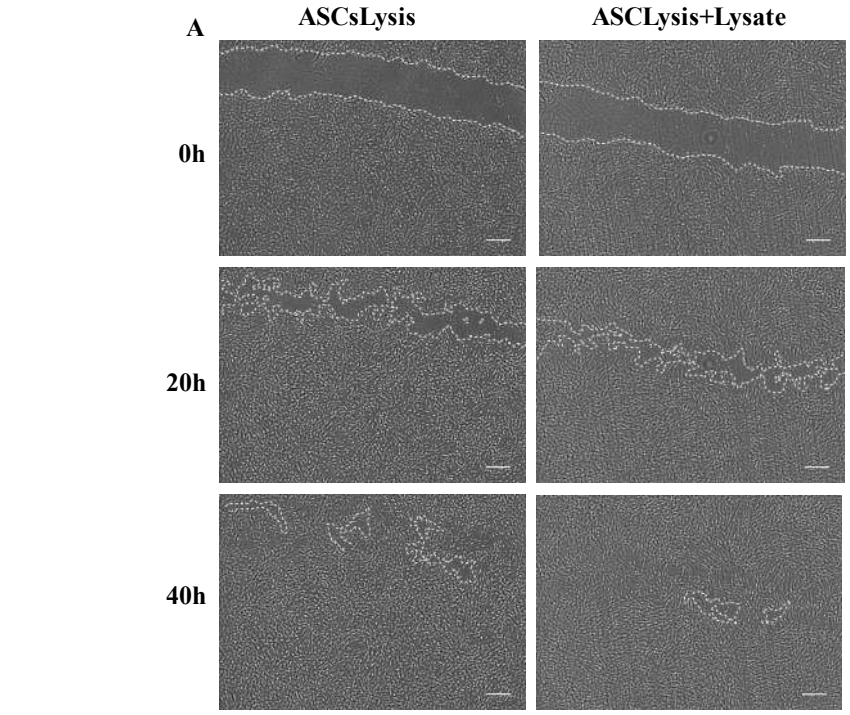

B

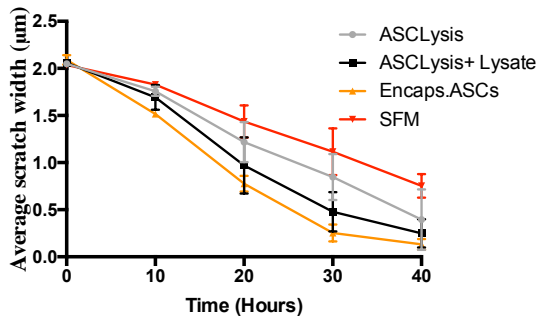

C

Time (Hours)	ASCs Lysis	ASCs Lysis+ Lysate	Encaps. ASCs	SFM
0	100	100	100	100
10	85.77807296	82.09673522	79.43707323	89.83239473
20	59.31898973	46.96426761	39.88720645	70.75146893
30	41.28026535	23.18804652	13.64608496	54.94253768
40	19.0883818	12.10000676	4.741656273	37.07073254

Figure 4.8 – Wound closure analysis of In-scaffold lysis, taken from 15°C stored encapsulated ASCs. Encapsulated ASCs were incubated at -80°C for two hours before thawing at room temperature and incubating with scratch wound. (A) Scratch images taken using Iprasense at times 0-, 20-, and 40 –hours. (B) Average scratch width. (C) Percentage wound closure. Values are presented as mean ± SEM from three separate keratocytes donors, Scale bar = 300μm. ASCsLysis, following thawing, encapsulated ASCs incubated with fresh SFM before placing with scratch wounds; ASCLysis + Lysate, following thawing, encapsulated ASCs and their formed lysate incubated with scratch wounds.

4.3.6 Assessment of ASCs specificity

The following part will discuss the possibility of encapsulating different types of cells and assessing them in healing CSC scratch wounds.

4.3.7 Encapsulated human dermal fibroblasts bandages used as a negative control for CSCs scratch wound healing

For stem cell bandages, we assessed the possibility of using ASCs in healing scratch wounds because of their well-known regenerative properties, however, other cell types have also been used in wound recovery. Human dermal fibroblasts (hDF) are normally responsible for skin wound healing (Froget et al., 2003, Tracy et al., 2016), thus, we wanted to assess their use in corneal recovery.

Alginate encapsulated hDF were used either immediately following encapsulation (non-stored) or 3 days storage at 4°C and 15°C with CSCs scratch wounds. Although hDF are usually used in healing skin wounds, in our system encapsulated hDF slowed CSCs scratch wound closure (Figure 4.9 A, B &C). Where there seemed to be a similar delay in corneal cell migration into the cell-free area in all used conditions (non-stored, 4°C and 15°C stored encapsulate hDF). Upon comparing encapsulated hDF to alginate only controls there was no significant difference in scratch wound healing, however, encapsulated hDF still presented a delay in wound closure. Whereas encapsulated ASCs presented significant improvement compared to encapsulated hDF. Comparing non-stored encapsulated hDF to non-stored encapsulated ASCs significant differences were found at times 30- and 40-hour post scratch ($p = 0.0146$ and <0.0001 respectively), similarly, when comparing 4°C stored cells ($p = 0.0331$ and <0.0001), and 15°C stored cells ($p= 0.0090$ and 0.0039 respectively). These results suggested the importance of using ASCs with corneal injuries. Looking at Alginate alone results we see there is an effect from Alginate alone on CSC scratch wound, from this experiment however, there is no significant difference which can indicate hDF to promote CSC, this however could not be confirmed due to the lack of appropriate experiment of hDF only control.

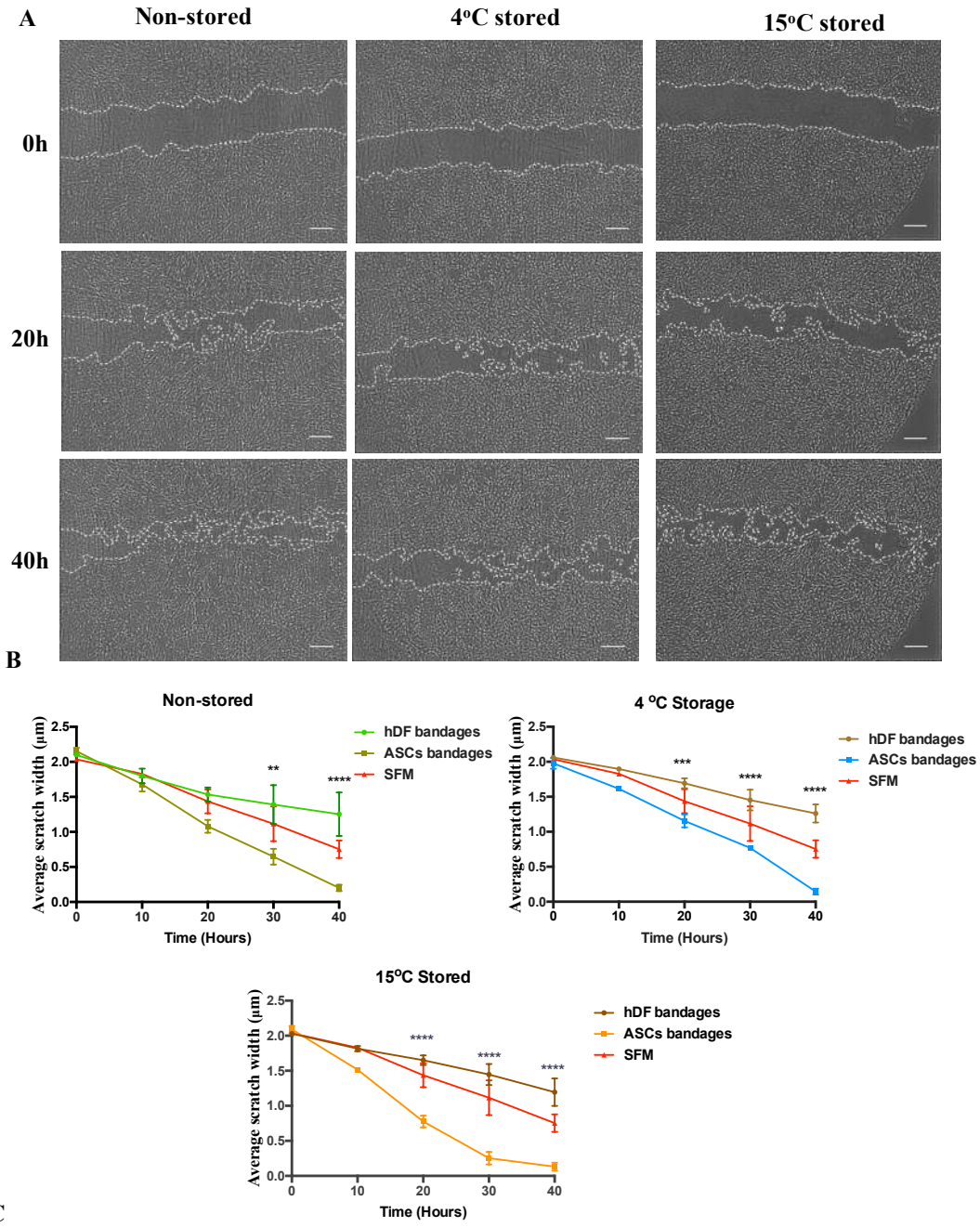

Time (Hours)	Non-Stored hDF	Non-Stored ASCs	4°C Stored hDF	4°C Stored ASCs	15°C Stored hDF	15°C Stored ASCs	SFM
0	100	100	100	100	100	100	100
10	85.75333184	78.13118194	92.00348966	81.82428254	89.41940506	72.53508148	89.83239473
20	73.11509375	50.31418161	82.10339975	58.5926144	81.35175857	37.012002	70.75146893
30	66.03392464	30.18385353	70.50705363	39.05894691	71.24436658	11.90677761	54.94253768
40	59.49126883	9.279878252	61.22677584	7.430192092	58.84651036	6.245047377	37.07073254

Figure 4.9 - Wound closure analysis of encapsulated human dermal fibroblasts (hDF). hDF were used immediately following encapsulation or following 72 hours

storage at 4°C and 15°C. (A) Scratch images taken using Iprasense at times 0-, 20-, and 40 –hours. (B) Average scratch width. (C) Percentage wound closure. Values are presented as mean ± SEM from three separate keratocytes donors asterisks represent significance between bandages (****, $p < 0.0001$; ***, $p < 0.001$, **, $p < 0.01$). Scale bar = 300μm.

4.3.8 Encapsulated corneal-derived mesenchymal-like stromal cells bandages improves corneal scratch area closure

It has been suggested that corneal stromal fibroblast (CSF) are in fact mesenchymal-like stem cells (Eslani et al., 2017, Vereb et al., 2016, Branch et al., 2012, Pinnamaneni and Funderburgh, 2012). Thus, we wanted to determine the possibility of using these cells in CSCs scratch healing. Hence, we encapsulated CSF and used them either immediately following encapsulation (non-stored) or following 72 hours storage at 15°C (Figure 4.10 A, B &C) with our standard scratch assay. Although the presence of these cells did improve wound closure, there was no difference when compared to alginate only controls. No differences were found upon comparing encapsulated CSF to encapsulated ASCs in the non-stored condition and the 15°C stored cells. However, there was a slight improvement of area closure in the 15°C stored encapsulated ASCs compared to encapsulated CSF.

A

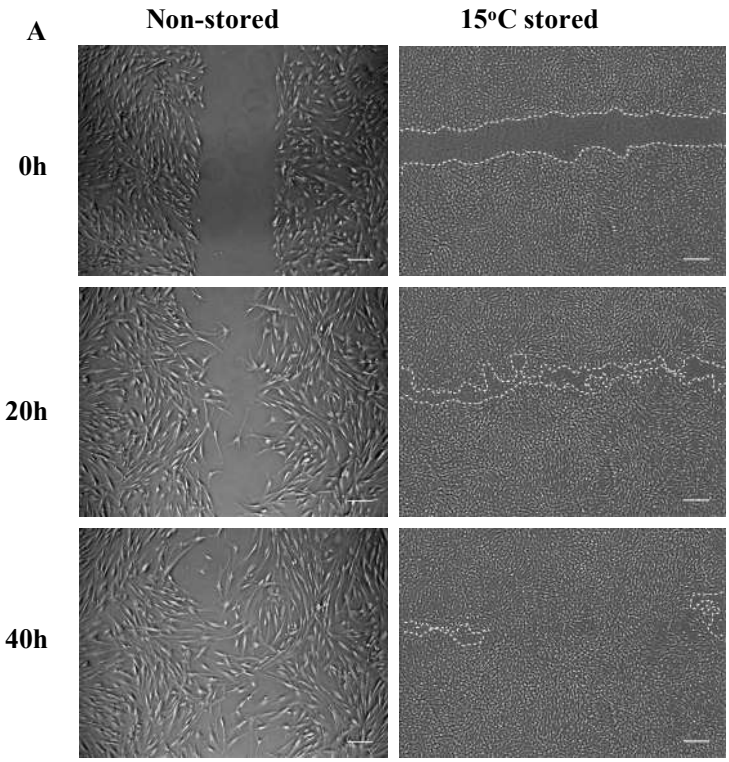

B

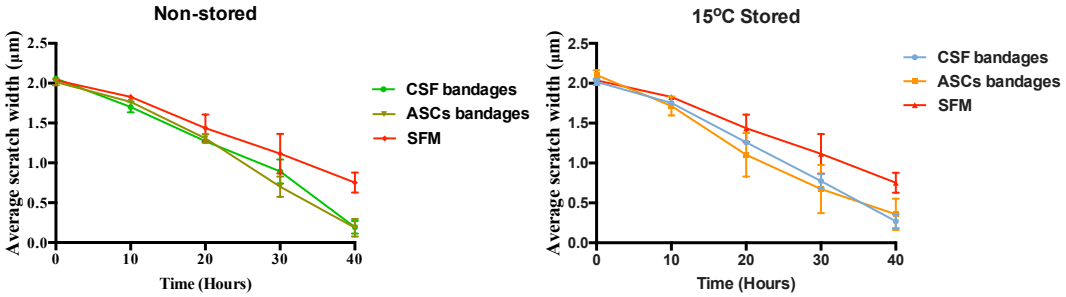

C

Time (Hours)	Non-Stored CSF	Non-Stored ASCs	15°C Stored CSF	15°C Stored ASCs	SFM
0	100	100	100	100	100
10	82.72314343	78.13118194	86.90368731	72.53508148	89.83239473
20	61.83004392	50.31418161	62.50073856	37.012002	70.75146893
30	43.37750084	30.18385353	38.22205016	11.90677761	54.94253768
40	9.411863258	9.279878252	13.40905716	6.245047377	37.07073254

Figure 4.10 – Wound closure analysis of encapsulated corneal stromal fibroblasts (CSF). CSF were used immediately following encapsulation or following 72 hours storage at 15°C. (A) Scratch images taken using Lica microscopy for the non-stored and Iprasense holographic microscopy at times 0-, 20-, and 40 –hours. (B) Average scratch width. (C) Percentage wound closure. Values are presented as mean ± SEM

from three separate keratocytes donors. Scale bar = 110μm for the non-stored and 300μm for the 15°C stored.

4.3.9 Human keratoconus bandages for CSC scratch wounds

Keratoconus (KC) is a progressive eye disease where the cornea loses its typical curved shape and thins to a cone-like shape (McMonnies, 2009). KC cells are extracted from the corneal stromal layer for they lack healthy keratocytes (McKay et al., 2017b). Therefore, we thought it interesting to assess the effect of diseased cells on healthy cells. As before, we compared two conditions, non-stored and 15°C stored KC bandages (Figure 4.11 A, B &C). In both conditions, a decrease in wound area were found, at approximately 30-hours post scratch however, the wound area increased in size, where there seemed to be a change in healthy cells morphology and more cells dying and detaching. Although this was not detected in other experiments, this result suggested that there could be factors released from the diseased cells that have a negative effect on the healthy cells, or, the lack of fresh media affected both cultures. seeing as we did not add fresh media to the duration of the incubation time, we expect that there was a competition between the two cell types for the nutrients in the media and so there was a decrease in healthy cells. Although the presence of KC improved cell coverage when compared to alginate only control, significantly shown at time 30-hour ($p = 0.0185$), they were still slower than ASCs. Upon comparing non-stored encapsulated KF to non-stored encapsulated ASCs, differences were found at time 40-hour post scratch ($p = 0.0106$), whereas 15°C stored ASCs showed significant improvement in scratch closure at times 30- and 40-hour ($p = 0.0058$ and 0.0012 respectively).

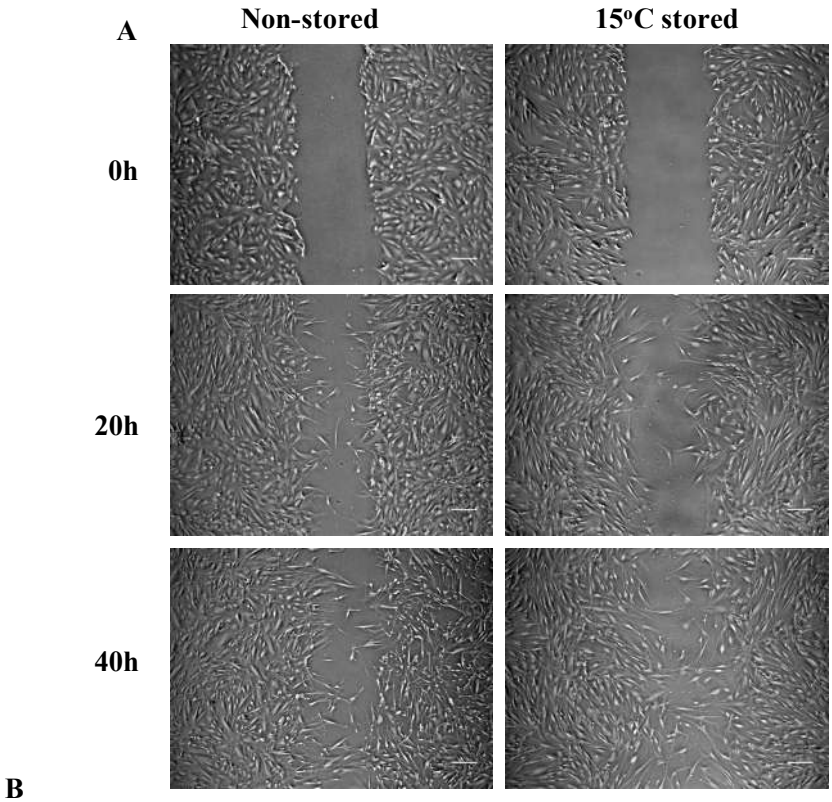

B

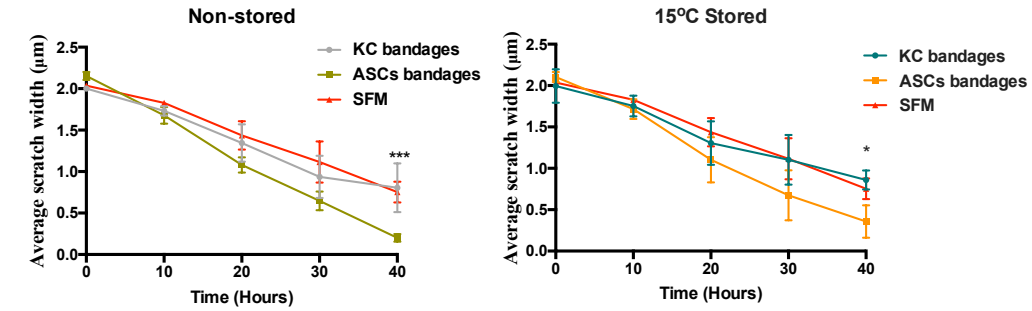

C

Time (Hours)	Non-Stored KC	Non-Stored ASCs	15°C Stored KC	15°C Stored ASCs	SFM
0	100	100	100	100	100
10	86.62735	78.13118194	88.38814039	72.53508148	89.83239473
20	67.27039833	50.31418161	69.09847053	37.012002	70.75146893
30	46.86629333	30.18385353	59.15486639	11.90677761	54.94253768
40	40.23944667	9.279878252	44.97025316	6.245047377	37.07073254

Figure 4.11 – Wound closure analysis of KC bandages. KC were used immediately following encapsulation or following 72 hours storage at 15°C. A) Scratch images taken using light microscopy at times 0-, 20-, and 40 –hours. B) Wound closure percentage. (C) Percentage wound closure. Values are presented as mean ± SEM

from three separate keratocytes donors asterisks represent significance between bandages (***, $p < 0.001$; *, $p < 0.05$). Scale bar = 220μm.

4.4 Cells expression markers

Following the experiments with Encapsulated ASCs, CSCs markers were analyzed at the gene transcription level and compared to the serum-free controls. Primer efficiency was calculated from the efficiency curves using 'Efficiency $=10^{(-1/slope)}$ -1'equation. The efficiency value of 2 represents 100% efficiency. Primer efficiency values for the genes used with CSCs (Figure 4.12 A-G) and ASCs (Figure 4.13 A-H) showed a good correlation coefficient.

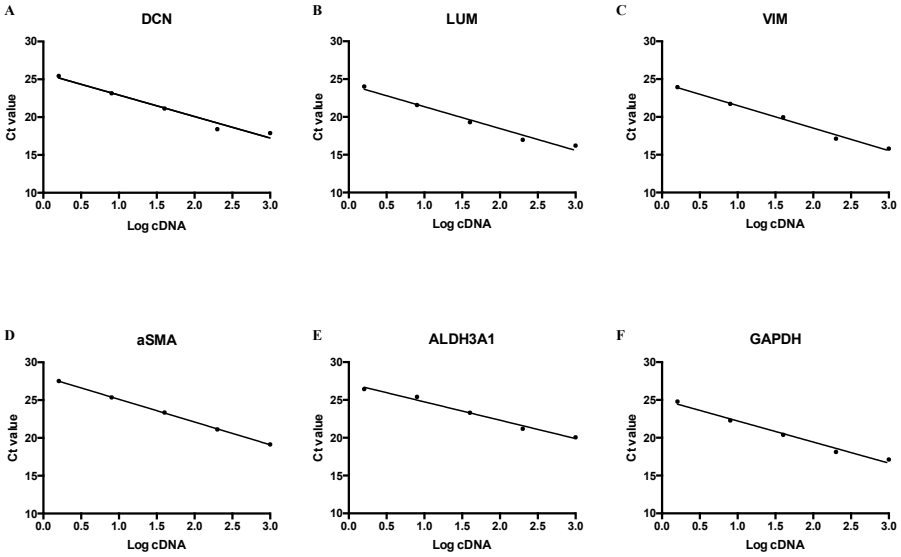

G

Gene	Efficiency	R^2
DCN	2.24	0.971
LUM	2.21	0.9755
VIM	2.16	0.99088
aSMA	2.15	0.99968
ALDH3A1	2.58	0.9853
GAPDH	2.28	0.9831

Figure 4.12 – Primer efficiency curves for (A) DCN, (B) LUM, (C) VIM, (D) aSMA, (E) ALDH3A1, (F) GAPDH. 5-fold dilutions were performed on cDNA pooled from all samples. Log cDNA concentrations plotted against Ct values and efficiency calculated (G). Data expressed as mean of duplicated values form a single experiment.

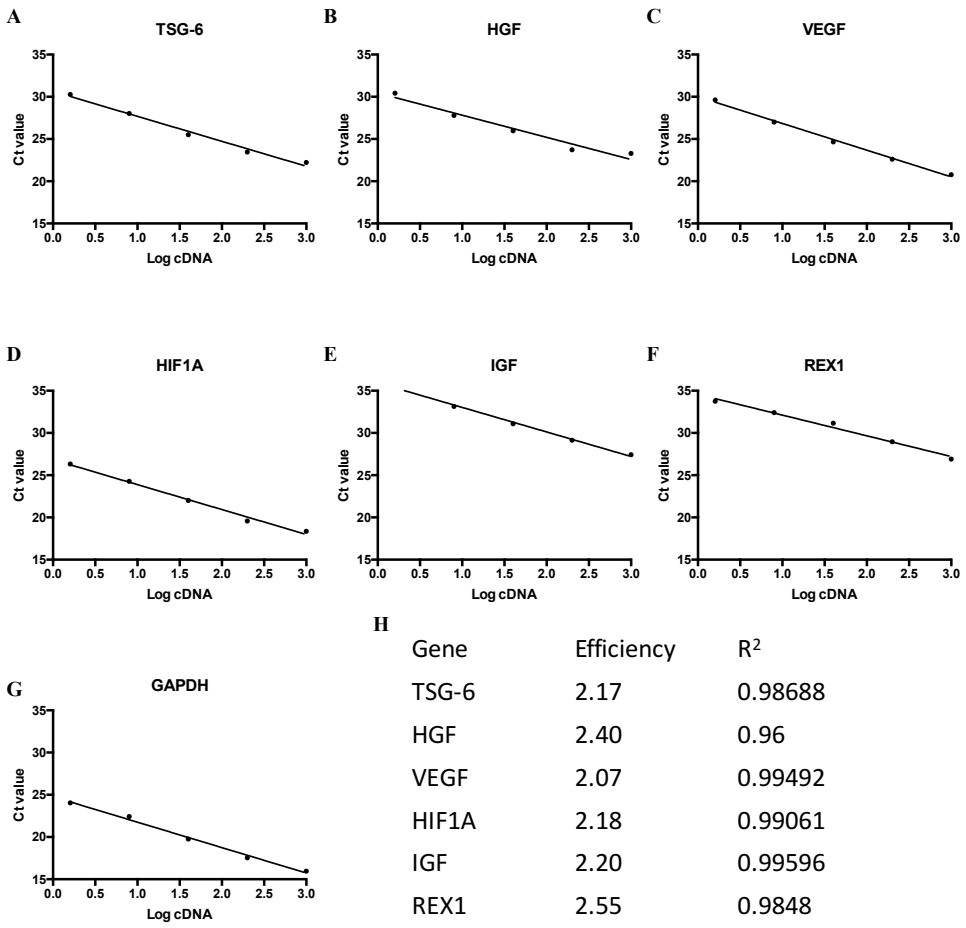

H

Gene	Efficiency	R^2
TSG-6	2.17	0.98688
HGF	2.40	0.96
VEGF	2.07	0.99492
HIF1A	2.18	0.99061
IGF	2.20	0.99596
REX1	2.55	0.9848
GAPDH	2.14	0.99274

Figure 4.13 – Primer efficiency curves for (A) TSG-6, (B) HGF, (C) VEGF, (D) HIF1A, (E) IGF, (F) REX1, (G) GAPDH. 5-fold dilutions were performed on cDNA pooled from samples. Log cDNA concentrations plotted against Ct values and efficiency calculated (H). Data expressed as mean of duplicated values form a single experiment.

CSC gene expression data were normalised to scratched cells incubated with SFM (Ctrl) (Figure 4.14). Results showed a clear decrease in CSCs gene expression levels (DCN, LUM, VIM, and aSMA) when cultured with encapsulated ASCs. Particularly, the following storage, where DCN expression was significantly reduced following exposure to ASCs previously-stored at 4°C and 15°C ($p = 0.0005$ and 0.0286 respectively). Whereas corneal crystalline gene expression ALDH3A1 was significantly enhanced following exposure at 15°C stored ASCs compared to the control, non-stored, and 4°C stored Encaps ($p = 0.0049$, 0.0060 and 0.0337

respectively). As such, encapsulated ASCs seemed to be affected by storage to produce paracrine factors that reduce corneal cell gene levels.

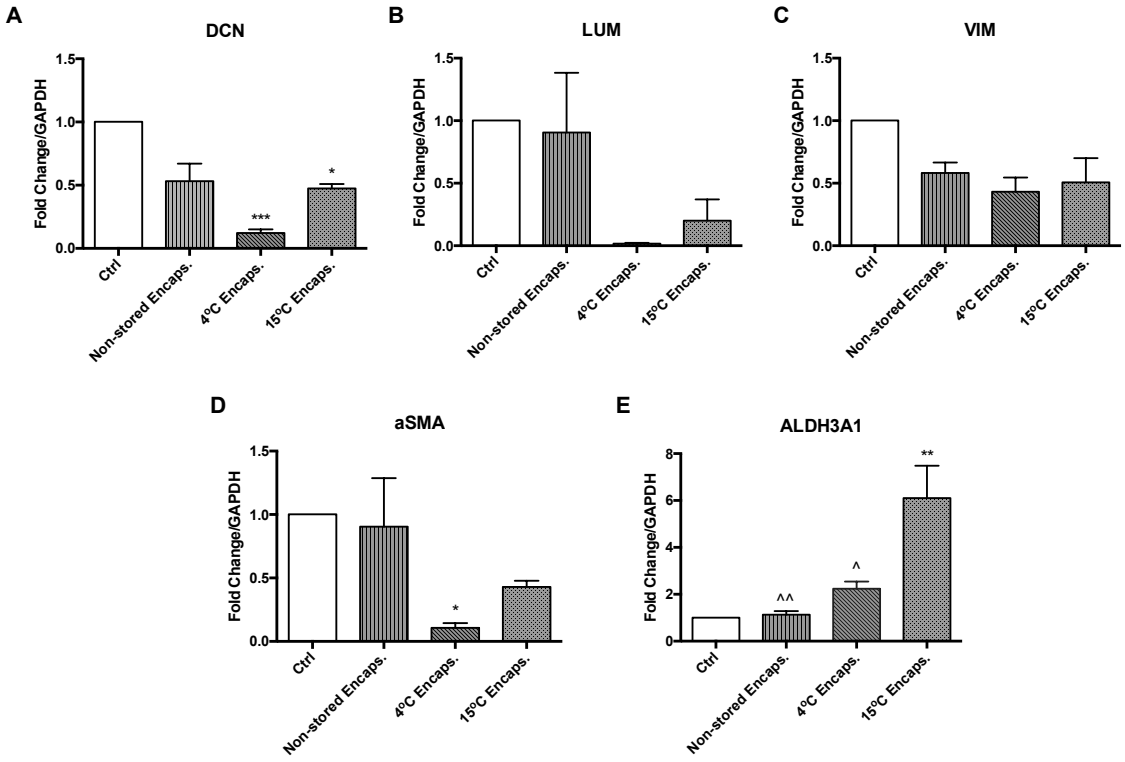

Figure 4.14 – Corneal stromal cells marker expression at the gene transcription level. Key corneal stromal markers, Decorin (DCN) (A), lumican (LUM) (B), vimentin (VIM) (C), aSMA (D) and ALDH3A1 (E) expressions were assessed. Values are presented as mean ± SEM of three separate donors, asterisks represent significance between conditions and control sample (***, $p < 0.001$; **, $p < 0.01$; *, $p < 0.05$), symbols represent difference between 15°C storage and other conditions (^^, $p < 0.01$; ^, $p < 0.5$).

Furthermore, ASCs markers were analyzed at the gene transcription level and normalised to normal ASC culture controls. (Figure 4.15). Comparing ASCs bandages following storage to following scratch healing. Results showed that storage decreased anti-inflammatory gene coding TSG-6 and HGF gene expression while increasing VEGF, aSMA ($p = 0.0374$, and 0.0172), IGF, and HIF1A gene expressions. Whereas, healing increase TSG-6 ($p = 0.0441$) and HGF gene expression, whilst reducing VEGF, HIF1A, aSMA, and IGF gene expression. ASCs also expressed high levels of REX1 gene responsible for stem cell phenotype ($p = 0.0497$) (Figure 4.15 G). These results suggest that encapsulated ASCs have an

active role in wound repair and that these cells may be affected by CSC presence in a bidirectional signaling pathway.

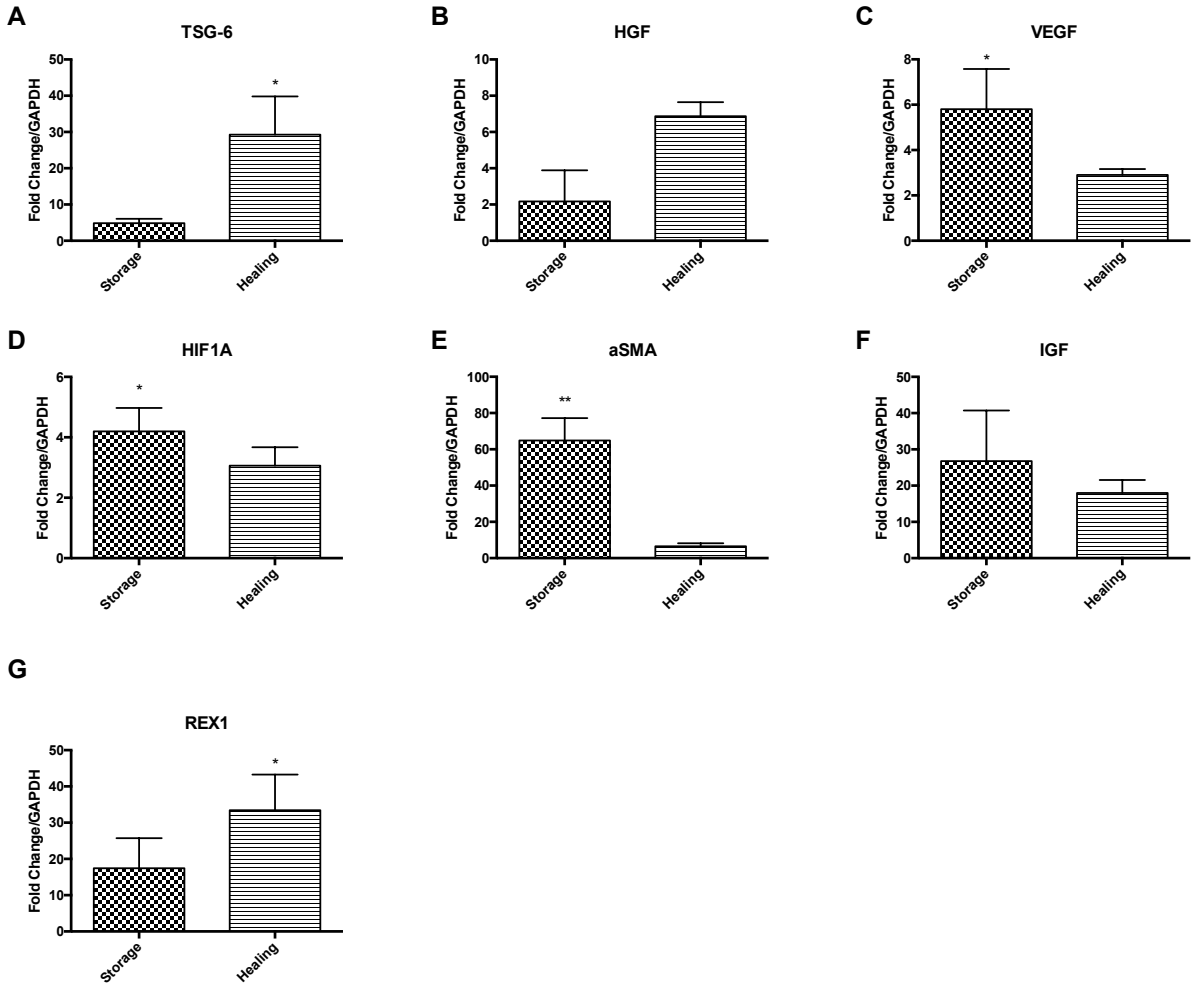

Figure 4.15 – Adipose derived stem cells marker expression at the gene transcription level. Key ASCs markers, TNF-stimulate gene-6 (TSG-6) (A), hepatocyte growth factor (HGF) (B), vascular endothelial growth factor (VEGF) (C), hypoxia inducible factor 1 subunit alpha (HIF1A) (D), insulin like growth factor (IGF) (E), and REX1 (F) expressions were assessed. Values are presented as mean ± SEM of three separate donors. (**, $p < 0.01$;*, $p < 0.05$).

4.5 Assessment of soluble protein concertation within the media

Bradford assay was performed on conditioned media produced following each experiment to determine soluble protein concentrations produced. The experiments were made in the presence of CSC except for 15°C Encaps-storage and 4°C Encaps-storage where the CM was taken following 72h storage (Figure 4.16).

Results were plotted against a standard curve made of bovine serum albumin (BSA) protein standard provided by the manufacturer (Figure 4.16 A).

To start with (Figure 4.16 B), CSC cultured with SFM had a 6 ± 2.6-fold increase in protein concentration over 48-hours culture. whereas 15°C and 4°C Encaps-storage had 7.4 ± 4.5- and 12.9 ± 3-fold increase in protein concentration over 48-hour culture. Upon comparing the encapsulated ASCs to alginate controls stored at 15°C and 4°C, 8.5 ± 5.1- and 13. 5 ± 1.5-fold increase in protein concentration was found. This increase implies that ASCs had an effect on CSC cultures via the production of paracrine factors and this production of factors was enhanced upon culturing with CSC. We also measured the protein concentrations of the encapsulated ASCs dilution (10,000, 100,000 and 500,000 cells), non-encapsulated Non-stored (Non-stored, 15°C and 4°C stored NE) ASCs, and the ASCs + CM at 48-hour culture with CSC scratch wound (Figure 4.16 C). Although no significant differences were found between the conditions and the SFM controls, there seems to be a trend in protein concentration in relation to the increase in ASCs number. Non-encapsulated ASCs also had a similar effect, where non-stored and 15°C stored ASCs had an increase in protein concentration compared to 4°C stored. This can be attributed to ASCs cell number as mentioned before (section 4.3.1) being lower in the 4°C stored. This suggests that cell number play a vital role in paracrine factors production.

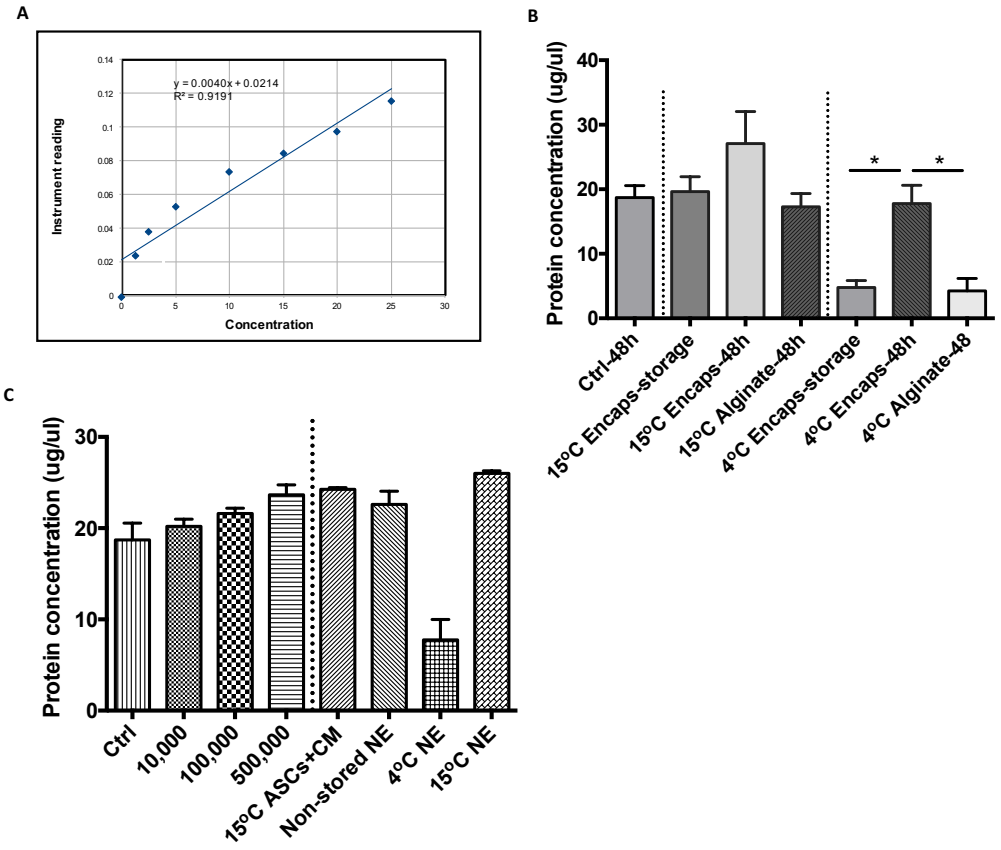

Figure 4.16 – Soluble protein concentrations. (A) Values plotted against standard curve made of bovine serum albumin. Comparing (B) the media taken following 72h storage and protein concentration at time 48h, (C) media taken from ASCs dilution, and non-encapsulated (NE) ASCs following 48 hours incubation of non-stored and following 4°C and 15°C storage. Values are presented as mean ± SEM of three separate keratocytes donors, asterisks represent significance (*, $p < 0.05$). Ctrl, serum-free media at time 48 hours taken following CSCs scratch wound healing.

4.6 Assessment of collagen production

Sirius red assay was performed on CSCs cultures following scratch healing. The stained materials were imaged and absorbance measured at 490nm and compared to SFM control samples. Absorbance results were plotted against a Rat Tail Collagen I (First Link Ltd, UK) standard curve made at different concentrations (Figure 4.17 A). In general, results suggested a trend between different conditions. A 5.9 ± 0.7 mg increase in collagen amount produced from the CSCs when cultured in the presence of non-stored encapsulated ASCs compared with the amount of collagen produced from SFM control group (Figure 4.17 B, Bi). Moreover, 11.9 ± 9.7

and 17 ± 6.2 mg increase in collagen amount from the CSCs found when cultured in the presence of 15°C and 4°C stored encapsulated ASCs. However, upon comparing the alginate only groups to the SFM control we see similar increases in collagen production i.e. a 1.0 ± 0.7 mg increase in collagen amount with the non-stored alginate alone, 13.1 ± 10 mg fold increase with the 15°C stored alginate alone and 13.9 ± 10.5 mg increase with the 4°C stored alginate alone. Interestingly, when comparing the Encapsulated ASCs to the alginate control conditions, we found an increase in collagen amount in the non-stored and the 4°C stored by 4.8 ± 0.0 mg and 3.0 ± 4.3 mg and a decrease in the 15°C stored by 1.1 ± 0.5 mg. Upon normalizing collagen amount to cell number, alginate only showed an increase in collagen production compared to ASCs encapsulated groups, which can indicate that alginate can have an effect on cell production on collagen. This effect may be driven by alginate ability to sequester ions from the media and so CSC becomes non-motile thus produce collagen (Figure 4.17 C).

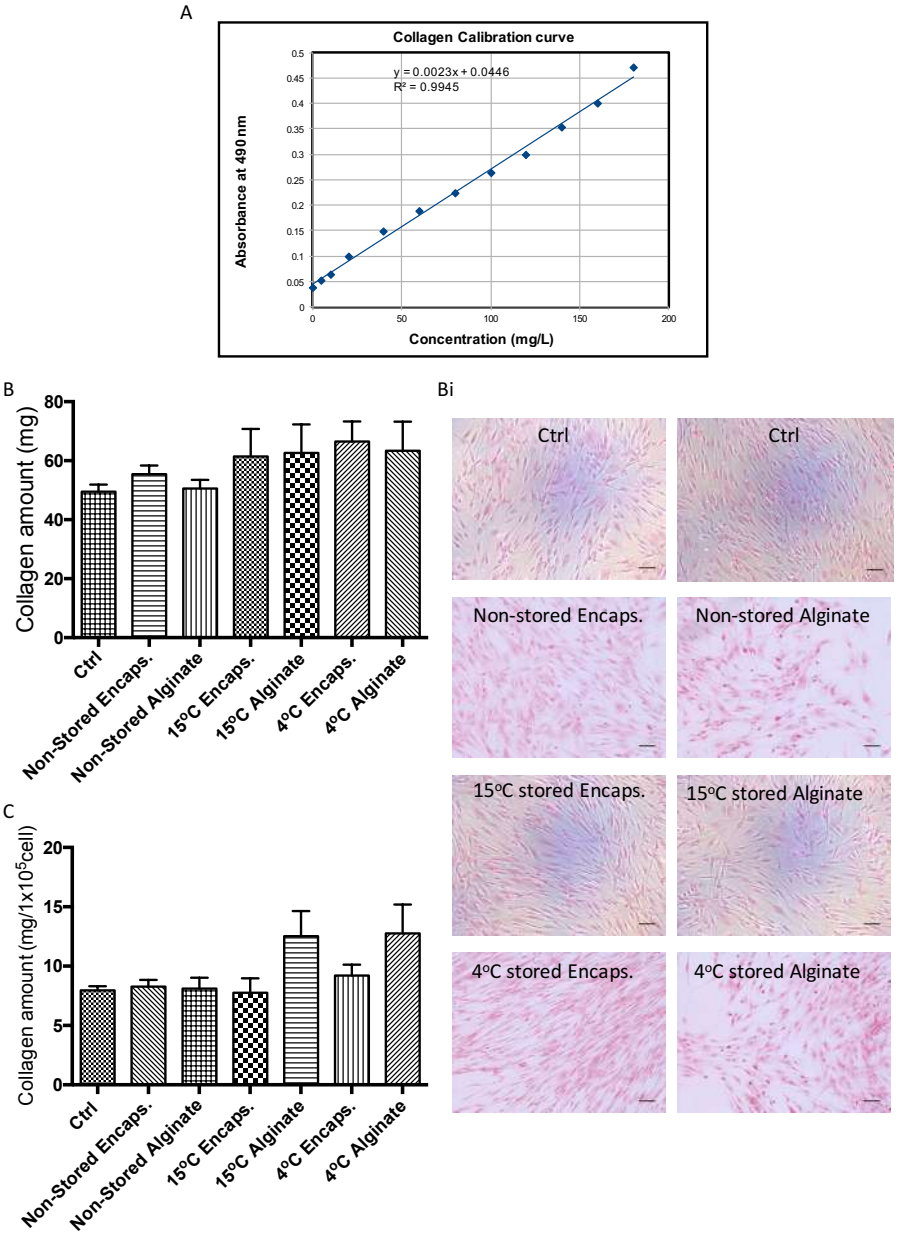

Figure 4.17 – Assessment of collagen amount. (A) Values plotted against standard curve made of Rat Tail Collagen I, (B) total collagen amount of each condition, (Bi) representative images of collagen stained CSCs cultures taken at 48 hours. (C) Collagen amount normalised to cell number. Values are presented as mean ± SEM of three separate keratocytes donors, Scale bar = 100μm. Ctrl, serum-free cultures.

4.7 Proteome profiler human XL cytokine array

To assess which factors were produced by the ASCs, a Human XL Cytokine Array (R&D Systems, Abingdon Science Park, Abingdon, UK) was used to detect 109 different soluble growth factors, cytokines, chemokines and other soluble

proteins within the 8 different conditioned media (Diagram 4.1). The detected protein levels were expressed relative to an internal (by the manufacturer) positive control for each sample, which allowed for a direct semi-quantitative comparison between samples. Cells were treated with SFM labeled as ‘CSC’, plus alginate only, labeled as ‘CSC + alginate’, non-encapsulated ASCs either non-stored or stored at 15°C in the presence of CSCs, labeled as ‘Non-Stored Non Encaps’ and ‘15°C Non-Encaps’, non-stored or 15°C stored encapsulated ASCs, labeled as ‘Non-Stored Encaps’ and ‘15°C Encaps’. Lastly, conditioned media were taken from encapsulated ASCs following 15°C storage for 72 hours, labeled as ‘15°C Storage’, and double stored encapsulated ASCs (encapsulated ASCs stored at 15°C for 72 hours followed by storage at 37°C for 48 hours), labeled as ‘2x Storage’, which represented the storage effect on ASCs (Figure 4.18).

Cultured CM was generated for each condition. 0.5mL CM was taken following each experiment and analysed with the array kit, ImageJ used to quantify the dot blots. Of the 109 soluble factors on the array, 30 were detected. Most of the tested angiogenic factors, including angiogenin, VEGF, and MCP-1 were detected in the CSC, CSC + alginate (Figure 4.18 and 4.19), and 15°C Encaps conditioned media. Furthermore, these conditions produced significantly high levels of chemotactic factor growth-related oncogene (GROa) and stromal cell-derived factor-1 (SDF-1). Whilst most of the IL family proteins were not detected, except for IL-6 and IL-8 and a small amount of IL-17A and IL-18 Bpa. Most of the detected factors were upregulated in the 2x storage condition when compared to the 15°C storage, which may indicate that encapsulated ASCs produce more factors upon return to culture condition. However, for technical issues 15°C storage CM were used following a cycle of freeze-thawing at -80°C, thus, the shown result for this condition is unreliable. On the other hand, non-encapsulated ASCs conditioned media showed no difference in the detected paracrine factors levels when compared to the other conditions.

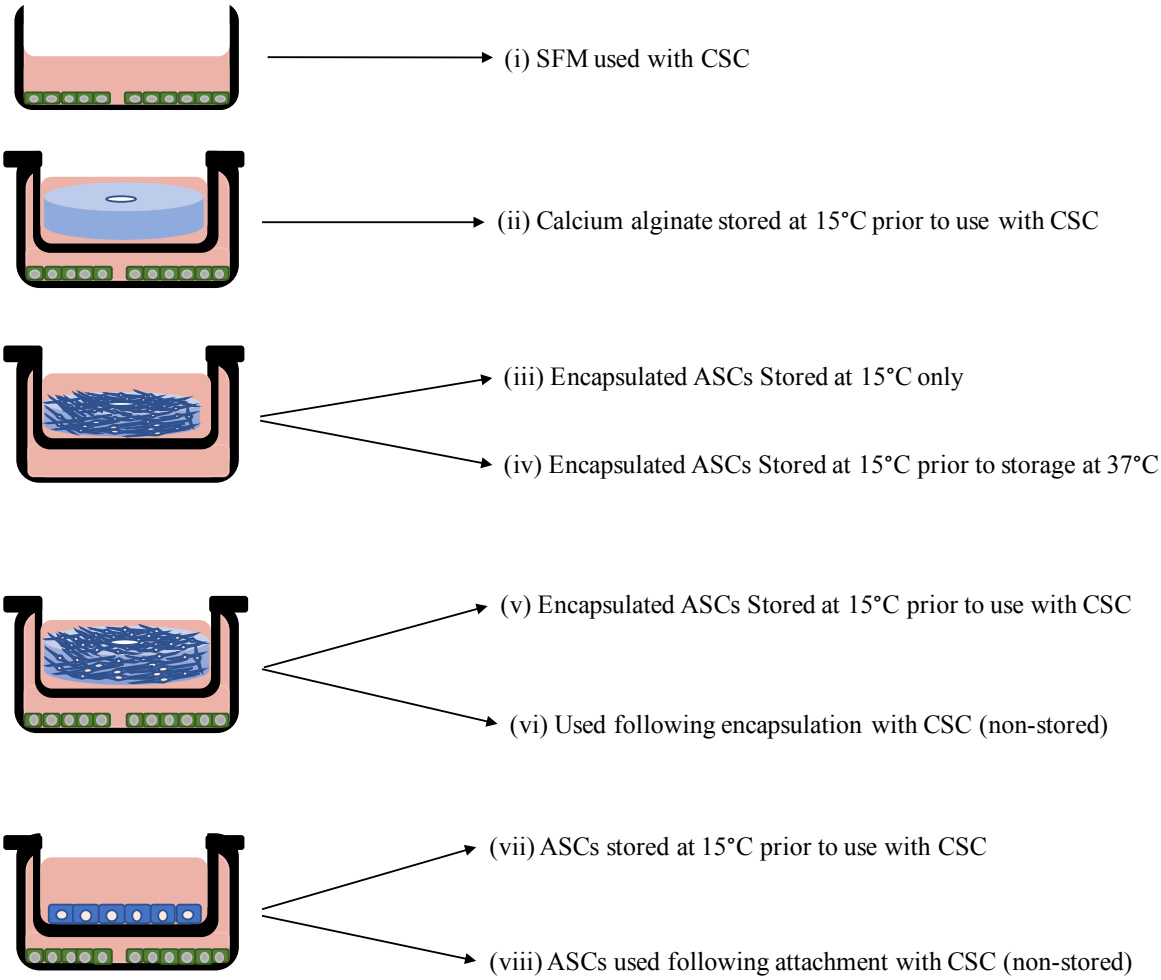

Diagram 4.1 – Schematic of the conditions used for the Human XL Cytokine Array kit.

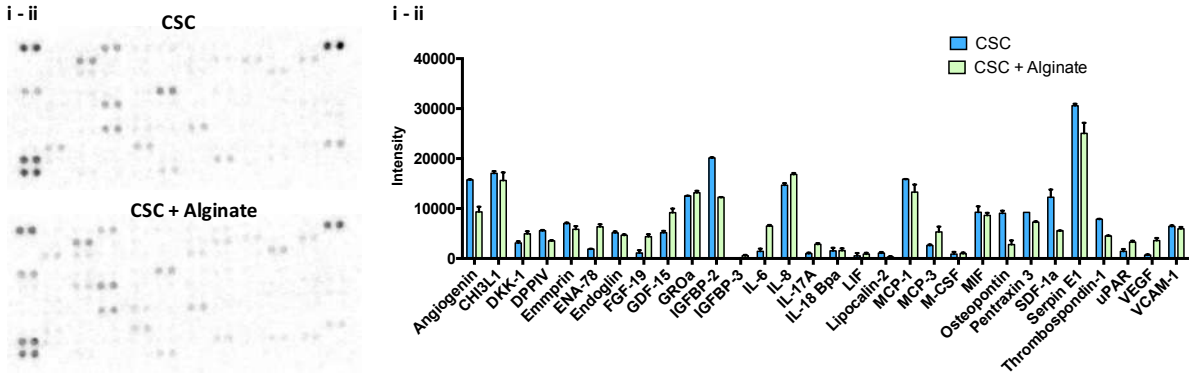

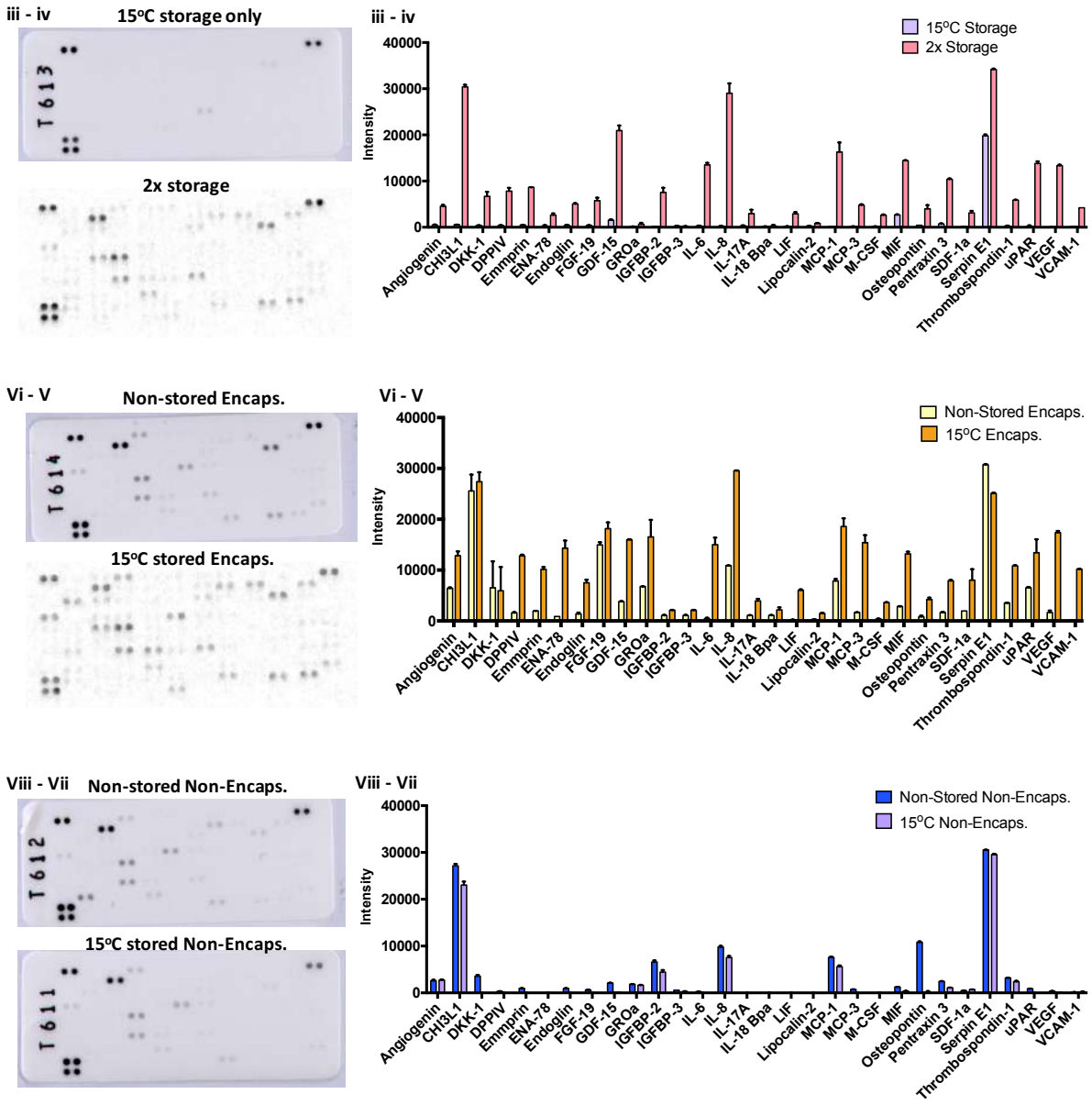

Figure 4.18 – Cells production of paracrine factors. A Human XL Cytokine Array kit was used to measure the relative number of paracrine factors produced by the encapsulated cells at 48 hours in (A, Ai) the CSC and CSC+ alginate, (B, Bi) 15°C stored ASCs and 15°C+37°C stored ASCs, (C, Ci) Non-stored and 15°C stored non-encapsulated ASCs, and (D, Di)non-stored and 15°C stored ASCs used with CSCcultures. Values are presented as mean ± SEM of two technical repeats, asterisks represent significance (****, $p < 0.0001$; ***, $p < 0.001$; **, $p < 0.01$; *, $p < 0.05$).

Angiogenin

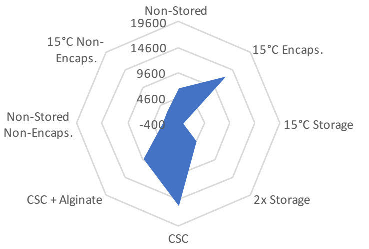

Chitinase-3-like protein 1 (CHI3L1)

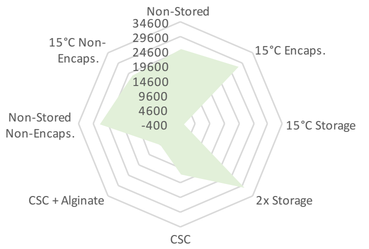

Dickkopf-related protein 1 (DKK-1)

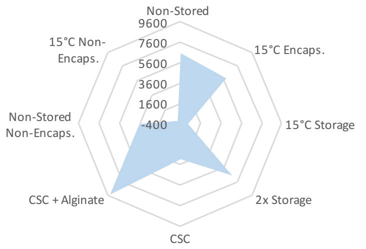

Dipeptidyl peptidase-4 (DPP4)

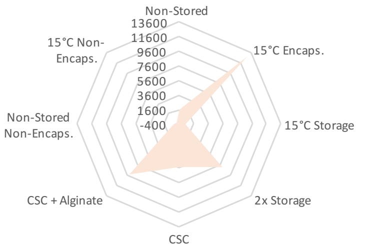

Extracellular matrix metalloproteinase inducer (EMMPRIN)

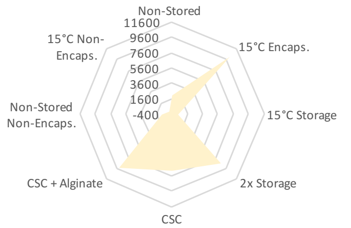

CXC motif chemokine 5 (CXCL5 or ENA78)

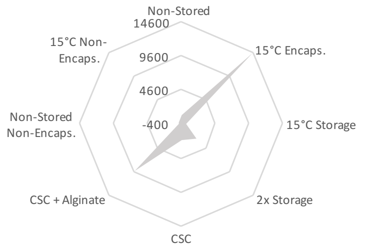

Endoglin (CD105)

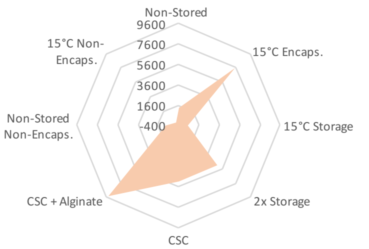

Fibroblast growth factor 19 (FGF-19)

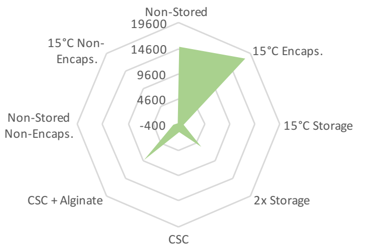

Growth/differentiation factor 15 (GDF15))

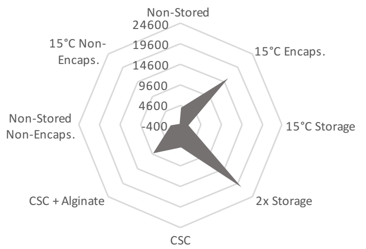

Chemokine (CXC motif) ligand 1 (GROa)

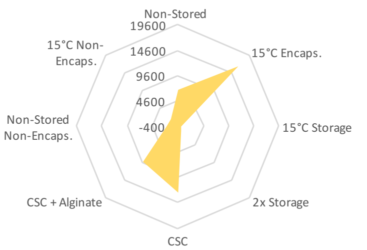

Insulin-like growth factor-binding protein 2 (IGFBP-2)

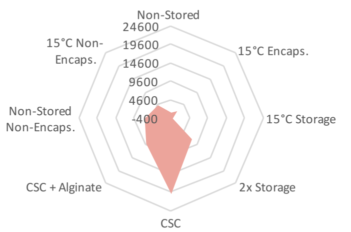

Insulin-like growth factor-binding protein 3 (IGFBP-3)

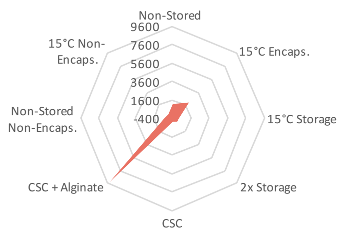

Interleukin 6 (IL-6)

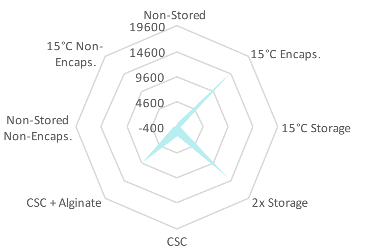

Interleukin 8 (IL-8)

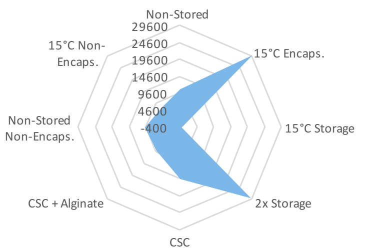

Interleukin 17A (IL-17A)

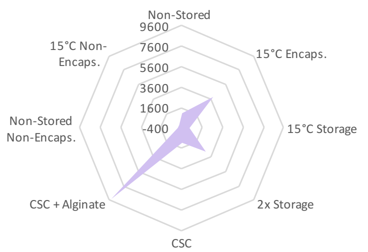

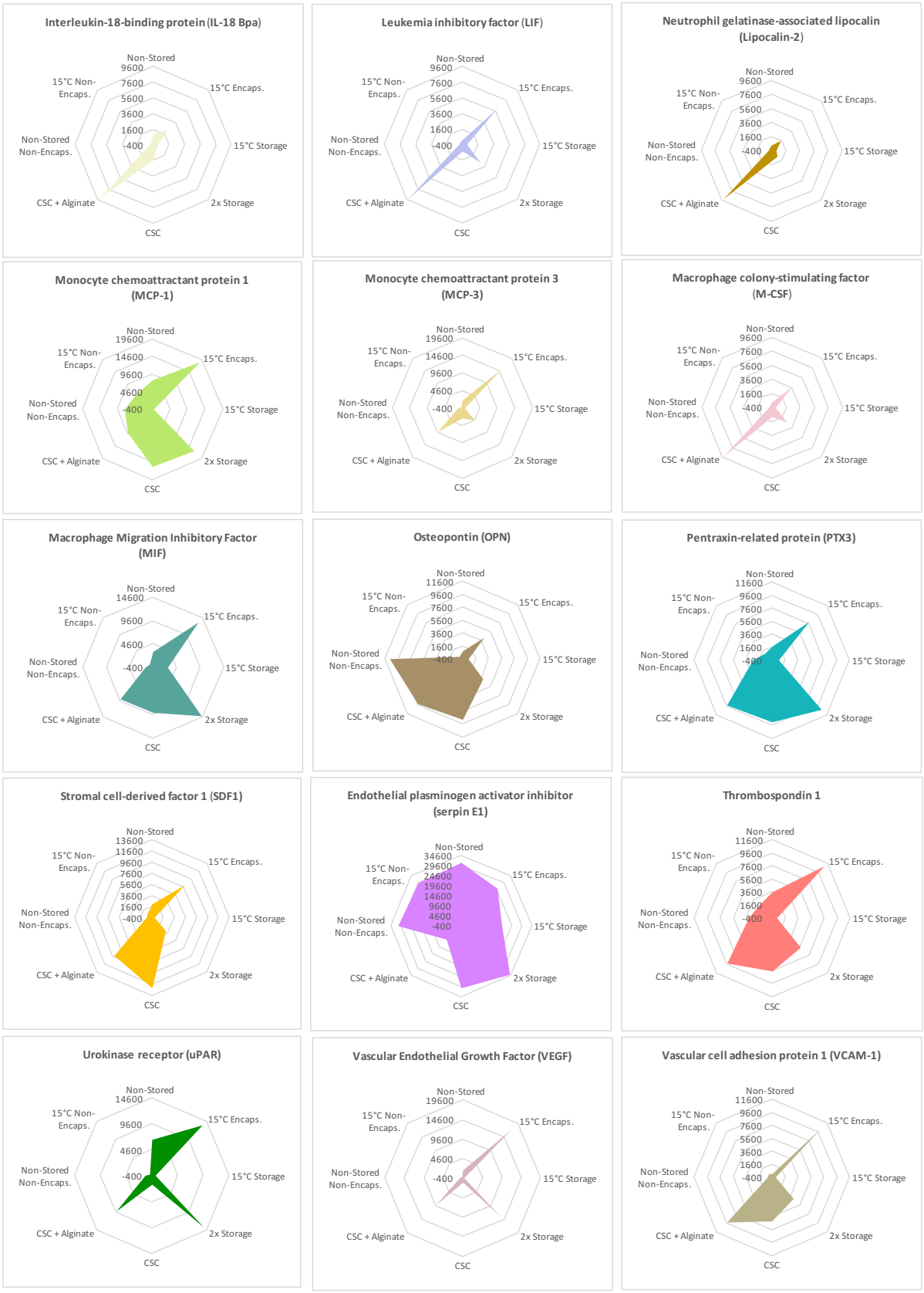

Figure 4.19 – Spider Radar plot of all 30 markers showing the difference in marker intensity between the different conditions.

4.8 Discussion

This chapter explored the effect of ASCs bandages on *in vitro* primary CSC cultures. Cell transplantation is becoming an important concept for the modern pharmaceutical industry. ASCs, although they have limitless potential in medicine, they still hold major concerns in clinical settings. Testing the functional activity of the cells is the first step in producing pharmaceutical therapy. Therefore, measuring ASCs' affect and their production of paracrine factors, i.e HGF, IGF, VEGF, IL, and many other factors that could affect wound closure has been used to investigate the effect of this potential therapy. The search for the best conditions/parameters to store ASC for optimum clinical effect is still ongoing (Patrikoski et al., 2019). For example, storage temperature and duration, cell condition, number, and type must be adjusted to produce a product.

We tested ASCs' ability to 'heal' corneal scratch wounds. ASCs were either stored (at 4°C or 15°C) for 72 hours or non-stored (used following normal culture at 37°C). 15°C storage showed significant improvement in wound closure compared to non-stored and 4°C stored cells. These are encouraging results similar to the previous chapter where 15°C storage enhanced the cells to produce paracrine factors. Thus, we suggest storage to be a hypoxic condition. Hypoxia induces ASCs to enhance their potential in producing factors (Zachar et al., 2011, Chung et al., 2009, Riis et al., 2017). Literature showed cells to retain or enhance their ability following storage in hypoxic conditions using different wound models (Riis et al., 2017, Schive et al., 2017, Chung et al., 2009). However, we needed to further validate this theory in terms of stem cell bandages.

Cell number is an important factor for stem cells bandage formation (Bohari et al., 2011). We assumed that cell numbers play a role in the observed rate of wound healing, where the more cells we have the more paracrine factors produced and the faster the closure of the scratch wound. To test this, we encapsulated and compared a range of ASCs cell numbers (10,000, 100,000, 500,000 and 1,000,000 cells). Storage can lead to cell loss (Angel et al., 2016), thus, cells were used immediately following gel formation. Our data suggest ASCs ability to produce paracrine factors to be in proportion to their number. This, however, was only done with normal culture

(i.e. non-stored cells), the question arises whether we see the same effect following storage. Storage at 15°C does enhance the cells to become more active and to enhance their ability to affect wound closure, as was seen in the previous chapter. Hence, we expect to see an additive effect of storage and cell number; however, we did not further test this theory.

Cell-free therapy is gaining much interest in therapy. CM contains all the elements produced by the cells during storage such as cytokines, chemokines, and growth factors (Dowling and Clynes, 2011). It has been investigated in various wound models including heat shock (Mahat and Lis, 2017), cell differentiation (Yang et al., 2014), and regenerative medicine (Pawitan, 2014) where they found it to be an effective treatment. CM that contains the factors produced by ASCs were tested and used in the healing of various diseases (Shan et al., 2018, Lee et al., 2014, Lee et al., 2016, Yang et al., 2010). Therefore, CM as a therapeutic tool has become popular in recent years. CM produced from our ASCs bandages were shown to improve CSC wound healing. Double CM, a condition we used to test whether beneficial factors produced during wound healing remain when used again with different cultures showed a reduction in wound healing. This reduction can be due to the waste materials present in the media or the beneficial factors present used during the first wound healing, both of which can show the importance of using fresh CM (Mahat and Lis, 2017).

Since CM showed improvement in wound closure, the next question we asked whether this CM coupled with the bandages can present us with better wound coverage. Interestingly, no differences were observed compared to using bandages on its own. *In vitro* studies of ASCs-derived CM showed enhanced wound closure and fibroblast migration (Stojanovic and Najman, 2019, Ong et al., 2017). Our data support other published data in that ASCs bandages and CM improve wound healing, however, to our knowledge, no other investigations have been done on using both bandages + CM in wound healing. Although we show no significant difference in combining the two conditions, this would need to be further investigated. Also, we did not generate CM from cells during normal culture, which limits our data interpretation and should be added in future experiments.
To test whether ASCs have an active effect on wounds rather than a passive effect, we induced cell death within the bandages.

According to our knowledge, no published data were found aimed at assessing the effect of dead ASCs bandages on wound healing. Many *in vitro* and *in vivo* studies focused on finding new cell-free ASCs based therapies, utilizing cell secretome where they found it to promote wound healing (Stojanovic and Najman, 2019, Kober et al., 2016, Park et al., 2018, Lombardi et al., 2019). In our experiment, dead-ASCs bandages + their CM (lysate) improved scratch wound closure, this, however, fell short when compared to having live cells in cultures. Thus, support our hypothesis that ASCs able to actively release paracrine factors in response to the signals present in the culture. This is also supported by the gene expression data showing that CSCs can influence ASCs' behavior.

We then sought to assess the role of ASCs and whether we can replace them with an alternative cell type. We tested hDF, CSF, and KC bandages in healing CSC wounds. When compared to ASCs, hDF presented a major delay in wound healing, while CSF and KC presented a delay in wound recovery. Interestingly, KC bandages impeded wound closure following 30 hours which merits further investigation.

Stored encapsulated ASCs modulate the expressions of keratocytes-characteristic ECM components (decorin, lumican) corneal myofibroblasts marker (vimentin, aSMA) and corneal crystalline (ALDH3A1) expressions. Decorin and lumican belong to small leucine-rich proteoglycan family (SLRPs) which mainly aid in collagen fibrillogenesis and tissue hydration. The binding of SLRPs to collagen fibrils affects collagen matrix assembly and in turn, can affect corneal transparency. The significant increase in ALDH3A1 is particularly interesting in the 15°C stored group since ALDH3A1 maintains corneal transparency (Jester J.V. et al., 1999) and protects the cornea from harmful UV-induced lipid peroxidation. It has been shown *in vivo* and *in vitro* that ALDH is mainly produced by inactive keratocytes rather than their activated, fibroblastic phenotype (Stagos et al., 2010, Pei et al., 2006). As was seen in the previous chapter, 15°C stored ASCs cultured with CSC were found to increase cell proliferation, evident by CSC cell number following scratch healing. As such, ASCs seem to maintain corneal cells inactive keratocyte phenotype while aiding in therapy.

At the same time, ASC markers were analyzed following 15°C storage and culturing with CSC. ASCs phenotypic marker REXI showed an increase in expression following incubation with CSCs. Similarly, TSG-6 and HGF markers that are usually produced in response to injury showed upregulation in expression during

incubation with CSC. Whereas, hypoxia presenting markers VEGF, HIF1A, and aSMA were upregulated during storage. Which suggest that storage is a hypoxic environment that induces the cells to become highly active, this also corresponds to the literature (Lakatos et al., 2016, Liu et al., 2017, Han et al., 2016) Thus, our data indicated that the cells used after storage can exhibit an augmented wound healing compared to non-stored cells.

Soluble protein concentration can give a good indication of the amount of protein present in the culture at a specific time point. Interestingly, ASCs bandages showed a significant increase insoluble protein production following 72-hour storage at 15°C. This production in soluble factors indicates that at 15°C, the cells remain active within the gel compared to 4°C storage where the cells are in a relatively dormant state. May also explain the reason why we found more viable cells following 15°C storage compared to 4°C storage. At 15°C cells are actively producing factors that aid in maintaining viability compared to the dormant state the cells are in during 4°C storage. Interestingly, the cells remained in their activated state following return to normal culture condition and incubation with a secondary population, similar to what was found before (Hung et al., 2007).

An important structural protein is collagen, CSCs predominately secret collagen type I and V, which are the main collagen fibrils in the cornea. Collagen fibrils run parallel with one another, this arrangement along with their uniform diameter is the main reason for corneal transparency (Meek and Boote, 2004). Our data suggest that storage affects CSCs collagen production, although not significant. Upon normalizing the data to cell number, CSCs with alginate only were shown to produce marginally more collagen than all the other conditions. It is suggested that CSCs increase collagen production in non-motile cultures when incubated with retinoic acid (Gouveia and Connon, 2013). Which suggests that CSC incubated with alginate remain in-active, hence, explaining the delay found in the scratch wound healing of this condition. We suggest that CSC produce collagen while delaying cells migration and proliferation in closing the wound. This however, need to be further investigated in future experiments.

It has been shown that ASCs produce many paracrine factors in response to injury in ocular and nonocular cell types (Alio Del Barrio et al., 2017, Chung et al., 2009, Lee et al., 2014, Shan et al., 2018, Yang et al., 2010). These factors able to promote epithelialization while reducing neovascularization, scarring, and

inflammation (Bray et al., 2014, Song et al., 2018, Eslani et al., 2018). This cocktail of factors, however, is not fully understood. Research is lacking in the limits of the different factors produced by the ASCs in response to injury. Therefore, in an attempt to explore these factors, we decided to test a random set of growth factors, cytokines, and chemokines. Whilst this may present a good indication of what the cells produce, it does not give a definitive answer to all the factors produced by the cells.

Pre-conditioning MSCs by subjecting them to hypoxia have been found to induce the heart to be more resistant to lethal ischemic attacks, which is found in an ischemic myocardium module (Murry et al., 1986). This method was adapted into cell therapy with the aim of increasing cell viability (Dzobo et al., 2018). Various other studies showed that pre-conditioning MSCs in hypoxic situations induces MSCs expression of proangiogenic and pro-survival factors, such as angiopoietin-1, VEGF and hypoxia-inducible factor-1 (HIF-1) (Mirotsou et al., 2011, Rehman et al., 2004, Thangarajah et al., 2009, Hsiao et al., 2013).

It has been shown that ASCs produce many inflammatory cytokines and chemokines including MCP-1, IL-6, and IL-8 (Pourgholaminejad et al., 2016, Kyurkchiev et al., 2014) that aid in corneal wound healing (Roddy et al., 2011, Ma et al., 2006b). It has been shown that IL-6 and IL-8 regulate immune cell infiltration during wound healing whilst inducing fibroblasts and keratocytes migration (Oh et al., 2009, Oh et al., 2008). Our data show upregulation in IL-8 in all conditions and significantly in the 15°C Encaps. Whereas IL-6 levels were upregulated in the 15°C Encaps and the 2x Storage conditions. When compared to 2x conditions, data suggest that ASCs do indeed produce IL-6 and IL-8. MCP-1 is an important chemokine that regulates macrophage recruitment (Yu et al., 2016). Our data show significantly high expression of these proteins in the 15°C Encaps condition compared to the non-stored condition. Interestingly, epithelial neutrophil-activating protein 78 (ENA-78) a chemoattractant of neutrophil function (Fillmore et al., 2003), extracellular matrix metalloproteinase inducer (EMMPRIN) a protein that stimulates fibroblasts to synthesize matrix metalloproteinase (Huet et al., 2011) were highly expressed in the 15°C Encaps treatment.

An antiangiogenic factor, Thrombospondin-1 (TSP-1) was found to be produced by corneal epithelium (Sekiyama et al., 2006). TSP-1 was also found to be produced underneath the corneal epithelium (Schlotzer-Schrehardt et al., 2007,

Chen et al., 2012). In our experiment, TSP-1 was produced in all conditions, however, it was upregulated in the 15°C Encaps, which suggest that ASCs highly expressed the antiangiogenic factor to induce corneal wound healing. An angiogenic factor, VEGF, usually increases endothelial growth, migration, proliferation, differentiation, and vascular permeability (Ma et al., 2006a, Hui-Kang et al., 2009). VEGF key role in inflammation is determined by promoting B-cell and monocyte chemotaxis production and vascular leakage (Ferrara et al., 2003). VEGF is undesirable in corneal therapy, research found the use of anti-VEGF antibodies to show therapeutic success (Chang et al., 2012, Devarajan et al., 2019). Although not favourable, we found VEGF, to be produced at 15°C Encaps, 2x storage, which can indicate that ASCS produce VEGF. However, we also found VEGF produced in the CSC+Alginate group, which can indicate that VEGF is produced in the effect of alginate. Whereas, there was no production of VEGF in the non-stored group, which lead to the assumption of VEGF production to be related to storage. The key mediator of hypoxia is hypoxia-inducible factor (HIF), which can regulate various genes, including VEGF (Ramakrishnan et al., 2014). Thus, support our hypothesis that storage is hypoxia-inducible situation.

Serpine e1 level expresses the rate at which the cornea heals (Sun et al., 2015, Deng et al., 2006). Serpine e1 key role is suggested to be in modulating cell migration and matrix reconstruction. We found serpine e1 to be activated in all conditions except CSC+ alginate. Serpine e1 expression is TGFß1 mediated (Samarakoon et al., 2009, Johnsen et al., 2002), which in turn is expressed in the wounded cornea, thus we can expect it to be produced in wound healing. However, we found Serpine e1 expressed in the 2x storage group, which was not a wound healing group. Hence, further study is warranted to investigate the effect of Serpine e1 during wound healing.

In conclusion, our findings so far elucidate the effect of hypothermically stored ASCs bandages in CSC wound healing by the production of paracrine factors that aid in wound recovery whilst maintaining normal keratocytes phenotype. Such effects of ASCs bandages may not be limited to healthy CSC. Considering that ASCs bandages and their production of paracrine factors are important for other diseases, such as keratoconus and deep corneal injuries/scratches. Thus, these data suggest the possible beneficial use of ASCs bandages for the *in vivo* corneal wound healing.

Chapter 5. Effect of stem cells bandages on keratoconus fibroblasts scratch-wounds

5.1 Introduction

Keratoconus (KC) is a bilateral and asymmetrical corneal disorder characterized by thinning of corneal stroma, which results in the corneal protrusion that leads to myopic shift and astigmatism (Romero-Jimenez et al., 2010, Zadnik et al., 1996, Zadnik et al., 2002). Presently, it is considered a multifactorial disorder caused by environmental and genetic factors (Bawazeer et al., 2000, Wachtmeister et al., 2009, Fabre et al., 2009). Although KC is considered as a non-inflammatory disease, inflammatory factors including interleukins and matrix metalloproteinases have a role in KC development (Balasubramanian et al., 2012, Lema et al., 2009, Kaiserman and Sella, 2019). KC treatment depends on the severity of the disease, ranging from spectacles and contact lenses to keratoplasty. The shortage of corneal donors is the main issue in treating KC.

To solve this, cell therapy is used. KC usually produces a thinner irregular extracellular matrix (ECM) that contains collagen type3 and pro-fibrotic marker compared to the healthy stromal cells (McKay et al., 2015, Sharif et al., 2019). KC also changes the cellular metabolism that correlates to an increase in oxidative stress (McKay et al., 2017a). Thus, the cornea appears thin and opaque. ASCs bandages are a developing treatment that aims to improve the cornea, however, there still insufficient evidence to determine its benefits in KC treatment.

Although a great amount of research is being conducted into the use of mesenchymal stem cells (MSCs) in KC treatment, it is still insufficient. MSCs ability to release growth factors in response to the environment is one of the key therapeutic features of these cells. It has been shown that MSCs release hepatocyte growth factor (HGF), transforming growth factor beta 1 (TGF-ß1), platelet-derived growth factor (PDGF), among many others (Boomsma and Geenen, 2012, Lee et al., 2011, Lee et al., 2015) to improve various diseases. These factors although not fully understood, were found to promote cell migration, proliferation, and extracellular matrix protein production (Jiang et al., 2017). There is still insufficient evidence in the

use of ASCs in KC treatment. Thus, our ASCs bandages can help advance the treatment of KC *in vitro* and possibly in the clinic.

5.2 Aims

In the present chapter, we investigate the effect of adipose-derived mesenchymal stem cells (ASCs), as a stem cell bandage, on the corneal KC wound healing model. Diseased cells behave differently to healthy/normal cells, including their production of paracrine factors. Thus, investigating our bandages' ability to affect their KC will provide us with an in-depth understanding of the usage and limitation of our bandages. Using *in vitro* model of human-derived KC, our previously described scratch wound assay was used to measure the effect of hypothermically stored ASCs bandages on (i) KC cell migration/proliferation, (ii) soluble protein concertation and (iii) collagen deposition. We show that ASCs bandages the ability to secret paracrine factors regardless of storage temperature, which improved KC wound closure. In addition, stored cells stimulated KC survival compared to non-stored cells, which lead to an improvement in wound closure. Our findings in this chapter elucidate the beneficial effect of ASCs bandages in healing KC *in vitro* via the production of paracrine factors. Although we did not test the factors produced, from the previous finding, we expect factors including HGF, TSG-6, IL8, MCP-1, thrombospondin-1, to improve wound healing.

5.3 Results

5.3.1 ASCs bandages effect on keratoconus cultures

To explore ASCs bandages' effect on KC cultures, we cultured ASCs bandages immediately the following formation and compared that with serum-free DMEM:F12 (SFM) and alginate only controls (Figure 5.1 A &B). As shown in the figure, ASCs bandages showed increase in wound closure at times 20, 30 and 40-hours post scratch when compared to SFM ($p < 0.0001$, 0.0001, and 0.0009 respectively) and when compared to alginate ($p < 0.0001$, 0.0001, and 0.0074 respectively) cultures.

We also assessed the effect of hypothermically stored ASCs bandages on KC culture. As we found in the previous chapter, 15°C is the optimum temperature for cells survival and for enhancing cells functional ability, we assessed this on KC

scratch wounds (Figure 5.1 A &C). Similar to the previous observation, ASCs bandages improved cells scratch wound closure significantly shown at times 20, 30, and 40-hours post scratch when compared to SFM ($p = 0.0005$, <0.0001, and 0.0001 respectively) and when compared to alginate cultures ($p = 0.0001$, <0.0001, and <0.0001 respectively).

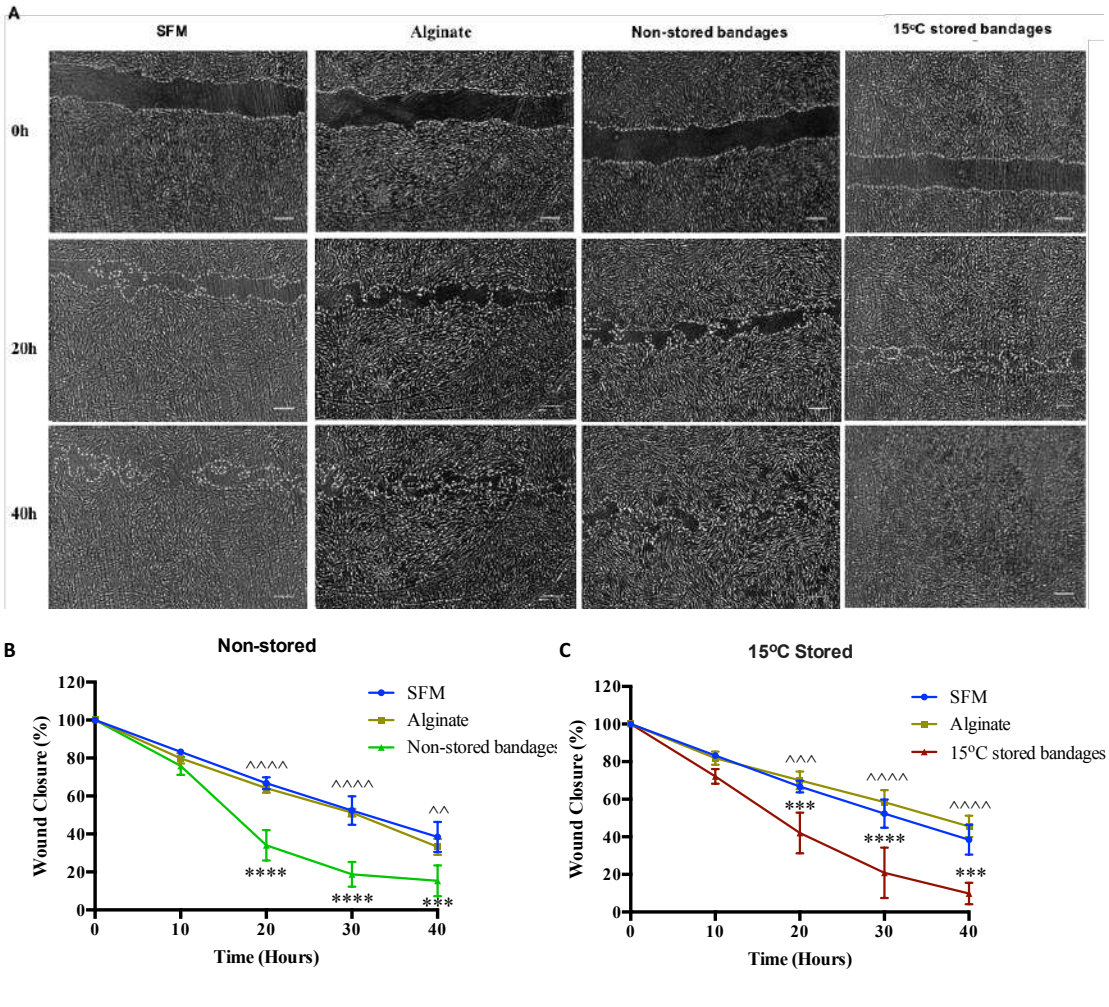

D

Time (Hours)	SFM	Alginate	Non-stored bandage	15°C Stored bandage
0	100	100	100	100
10	89.83239473	79.81871667	75.81346667	72.18942
20	70.75146893	64.18318	34.06266	42.05753
30	54.94253768	51.25793333	18.79689333	20.886708
40	37.07073254	33.25612333	15.30699833	9.881723

Figure 5.1 – Keratoconus wound closure. (A) Wound closure images taken using Iprasense lensless holographic microscope at times 0-, 20-, and 40-hours post scratch. (B) Scratch wound closure percentage of non-stored bandages, (C) scratch

wound closure percentage of 15C stored bandages, and (D) wound closure valuse. Wound closure percentage measured by dividing the scratch area at time 0 hour with scratch area at subsequent times and multiplied by 100. Values are presented as mean ± SEM from three separate Keratoconus donors, asterisks represent significance between bandages and SFM (****, $p < 0.0001$; ***, $p < 0.001$), while symbols represent significance between bandages and Alginate (^^^^, $p < 0.0001$; ^^^, $p < 0.001$; ^^, $p < 0.01$). Scale bar = 300μm. SFM, serum free DMEM:F12; Alginate, bandages without cells; non-stored and 15C stored bandages, bandages + ASCs either used immedicably following formation or following 3 days storage.

5.3.2 ASCs bandages conditioned medium effect on keratoconus cultures

SFM cultured with 15°C stored bandages with and without ASCs was used to generate conditioned media (CM) as before (Chapter 4). 100% CM was used with KC scratch cultures (Figure 5.2). CM taken from encapsulated cells showed significant improvements in scratch closure compared to gel only CM significantly shown at times 10, 20-, 30-, and 40-hours post scratch ($p = 0.0149$, 0.0222, 0.0033, and 0.0319 respectively).

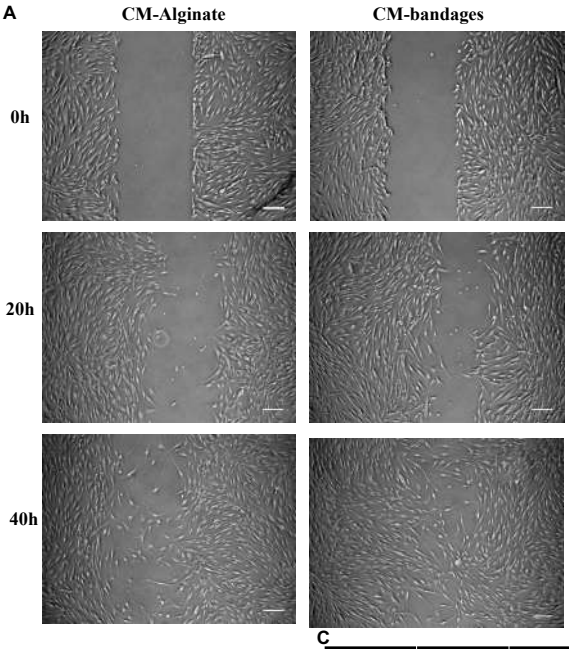

B

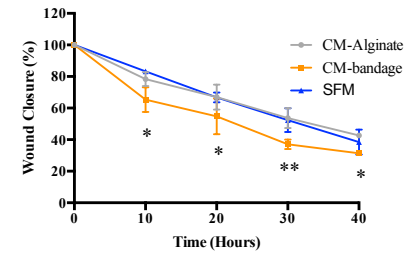

C

Time (Hours)	SFM	CM-Alginate	CM-bandage
0	100	100	100
10	89.83239473	78.33333333	65.33333333
20	70.75146893	66.90096	54.79672
30	54.94253768	53.66666667	37
40	37.07073254	42.65608667	31.34917

Figure 5.2 – Conditioned media effect on Keratoconus cultures. CM taken from 15°C stored alginate with and without cells following 3 days storage. (A) Images taken using light microscopy at times 0-, 20-, and 40-hour post scratch. (B) Wound closure percentage and (C) values measured by dividing the scratch area at time 0 hour with scratch area at subsequent times and multiplied by 100. Values are presented as mean ± SEM from three separate Keratoconus donors, asterisks represent significance between conditions (****, $p < 0.0001$; ***, $p < 0.001$). Scale bar = 220μm. SFM, serum free media; CM-Alginate, CM taken from gel only cultures; CM-bandage, CM taken from ASCs bandages.

5.3.3 Combination of ASCs bandages and their generated conditioned medium effect on keratoconus cultures

Upon comparing the CM scratch coverage to ASCs bandages scratches coverage, no significant differences were found between the two conditions. Nonetheless, from the graph (Figure 5.3), we see faster wound coverage with the encapsulated ASCs condition.

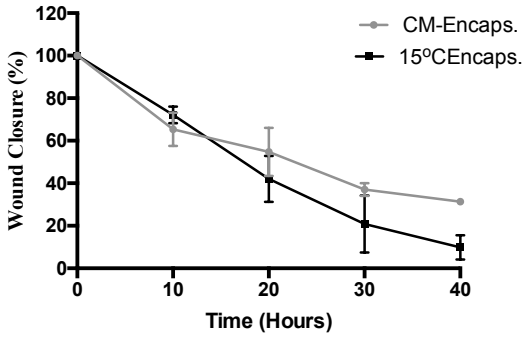

Figure 5.3 – Comparison of encapsulated ASCs and the conditioned media used with Keratoconus scratch wounds.

Thus, we sought to investigate the combined effect of encapsulated ASCs and their generated CM (Figure 5.4). Comparing ASCs+CM with alginate+CM, significant difference was found at time 30-hour post scratch (p = 0.0271). When compared to encapsulated ASCs without CM however, no differences were found between the cultures.

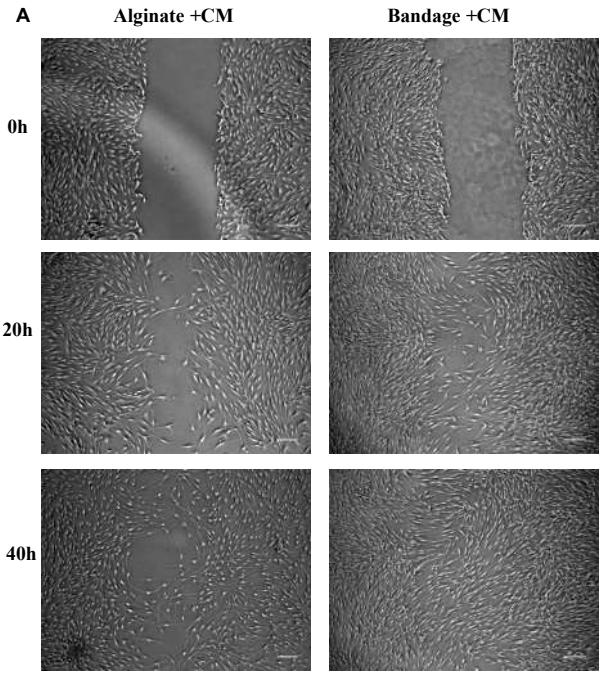

B

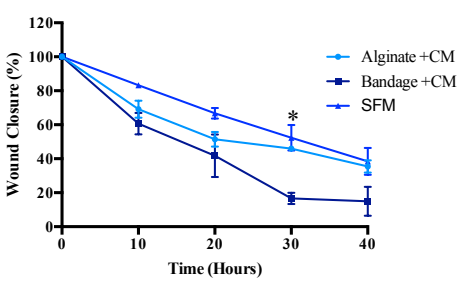

C

Time (Hours)	SFM	Alginate + CM	Bandage + CM
0	100	100	100
10	89.83239473	69.10272	60.68065
20	70.75146893	51.49863333	41.70049333
30	54.94253768	45.94838	16.66148333
40	37.07073254	35.42572	14.95567633

Figure 5.4 – comparison between Combi-Encaps. (ASCs bandage + CM) and Combi-Alginate (alginate + CM) used with Keratocoic cells scratch wounds. (A) Images taken using light microscopy at times 0-, 20-, and 40-hour post scratch. (B) Wound closure percentage and (C) values measured by dividing the scratch area at time 0 hour with scratch area at subsequent times and multiplied by 100. Values are presented as mean ± SEM from three separate Keratoconus donors, asterisks represent significance between conditions (*, $p < 0.05$). Scale bar = 220μm. Combi-Alginate, gel conditioned media used with alginate; Combi-Encaps, encapsulated ASCs conditioned media used with encapsulated ASCs cultures.

5.3.4 Corneal stromal cells bandages effect on keratoconus cultures

Next, we sought to investigate corneal stromal cells (CSCs) bandages effect of KC cultures (Figure 5.5). Comparing non-stored and 15°C stored encapsulated CSCs, a significant difference was shown at time 40-hour post scratch ($p = 0.0459$).

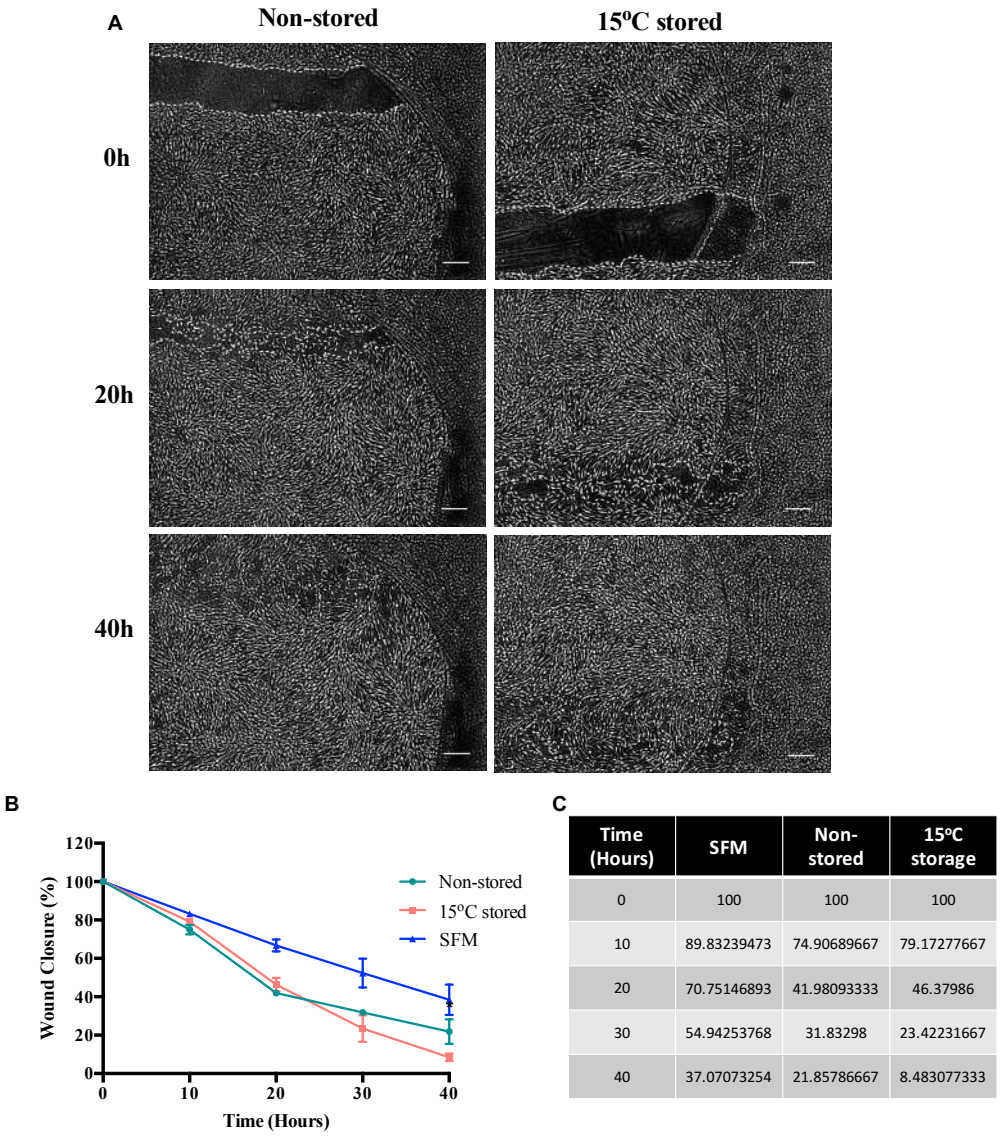

Time (Hours)	SFM	Non-stored	15°C storage
0	100	100	100
10	89.83239473	74.90689667	79.17277667
20	70.75146893	41.98093333	46.37986
30	54.94253768	31.83298	23.42231667
40	37.07073254	21.85786667	8.483077333

Figure 5.5 – Corneal stromal cells effect of Keratoconus cultures used either immediately following encapsulation (Non-stored) or 3 days following 15°C storage (15°C stored). Images taken using Iprasense lensless holographic microscope at times 0-, 20-, and 40-hours post scratch. Wound closure percentage measured by dividing the scratch area at time 0 hour with scratch area at subsequent times and multiplied by 100. Values are presented as mean ± SEM from three separate Keratoconus donors, asterisks represent significance between conditions (*, $p < 0.05$). Scale bar = 300μm.

5.3.5 Human keratoconus bandages effect on keratoconus cultures

We then assessed the effect of KC bandages on another KC culture either immediately the following formation or after 3 days of storage at 15°C (Figure 5.6).

Surprisingly, the negative effect was seen from the non-stored KC conditions when compared to 15°C storage where it showed improvement in wound closure at times 30- and 40-hours post scratch (p = 0.0017 and 0.0003 respectively). This suggests that non-stored KC are in a way defected but when stored they are modified or corrected by the storage temperature.

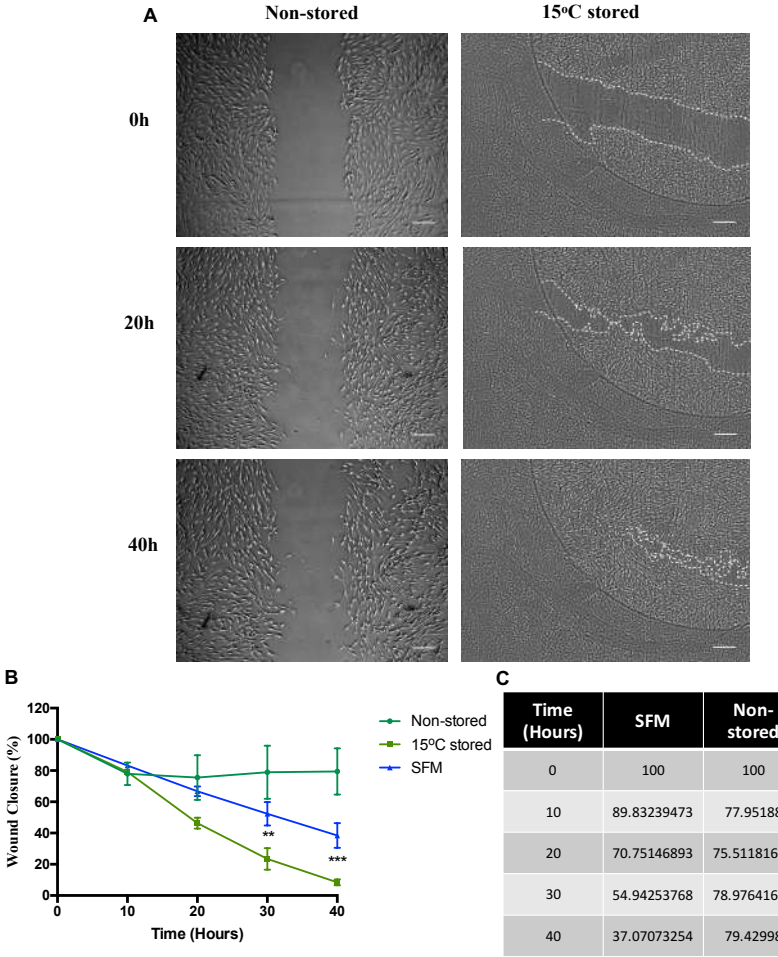

C

Time (Hours)	SFM	Non-stored	15ºC storage
0	100	100	100
10	89.83239473	77.95188	79.17277667
20	70.75146893	75.51181667	46.37986
30	54.94253768	78.97641667	23.42231667
40	37.07073254	79.42998	8.483077333

Figure 5.6 – Encapsulated Keratoconic cells effect on Keratoconus cultures used either immediately following encapsulation (Non-stored) or 3 days following 15°C storage (15°C stored). (A) Images taken using light microscopy for the non-stored condition and Iprasense lensless holographic microscope for the 15°C stored at times 0-, 20-, and 40-hours post scratch. (B) Wound closure percentage and (C) values measured by dividing the scratch area at time 0 hour with scratch area at subsequent times and multiplied by 100. Values are presented as mean ± SEM from three separate Keratoconus donors, asterisks represent significance between conditions (***, p < 0.001; **, p < 0.01). Scale bar = 220µm and 300µm.

5.3.6 Total protein production assessment

Next, we sought to assess the soluble protein concentration within the culture following scratch healing (Figure 5.7). Comparing 15°C stored ASCs bandages with bandage +CM and SFM cultures. A significant difference was found between the ctrl and bandage +CM cultures ($p = 0.0427$).

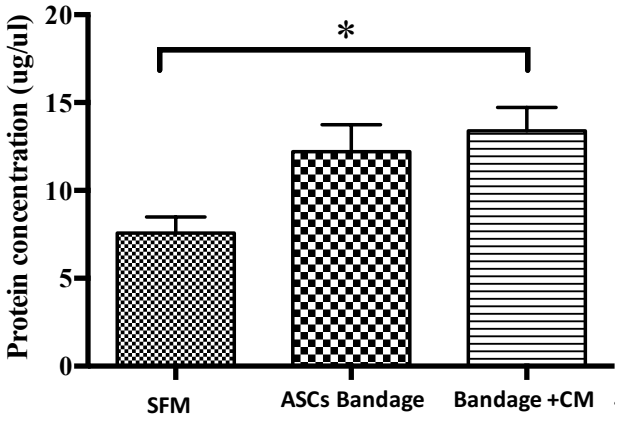

Figure 5.7 – Soluble protein concentration taken using following scratch healing using Bradford protein assay. Values are presented as mean ± SEM from three separate repeats, asterisks represent significance between conditions (*, $p < 0.05$).

5.3.7 Collagen production

Subsequently, we assessed collagen production using Sirius Red staining on the KC cultures following scratch healing of the SFM, alginate, only and ASCs bandages (Figure 5.8 A, Ai). No differences were found between the conditions. We then measured the KC cell number (Figure 5.8 B), similarly, no differences were found between conditions. Upon normalizing CSC cell number to collagen amount (Figure 5.8 C), although no differences were found between cultures, from the graph, alginate cultures showed an increase in collagen amount compared to SFM and ASCs bandages.

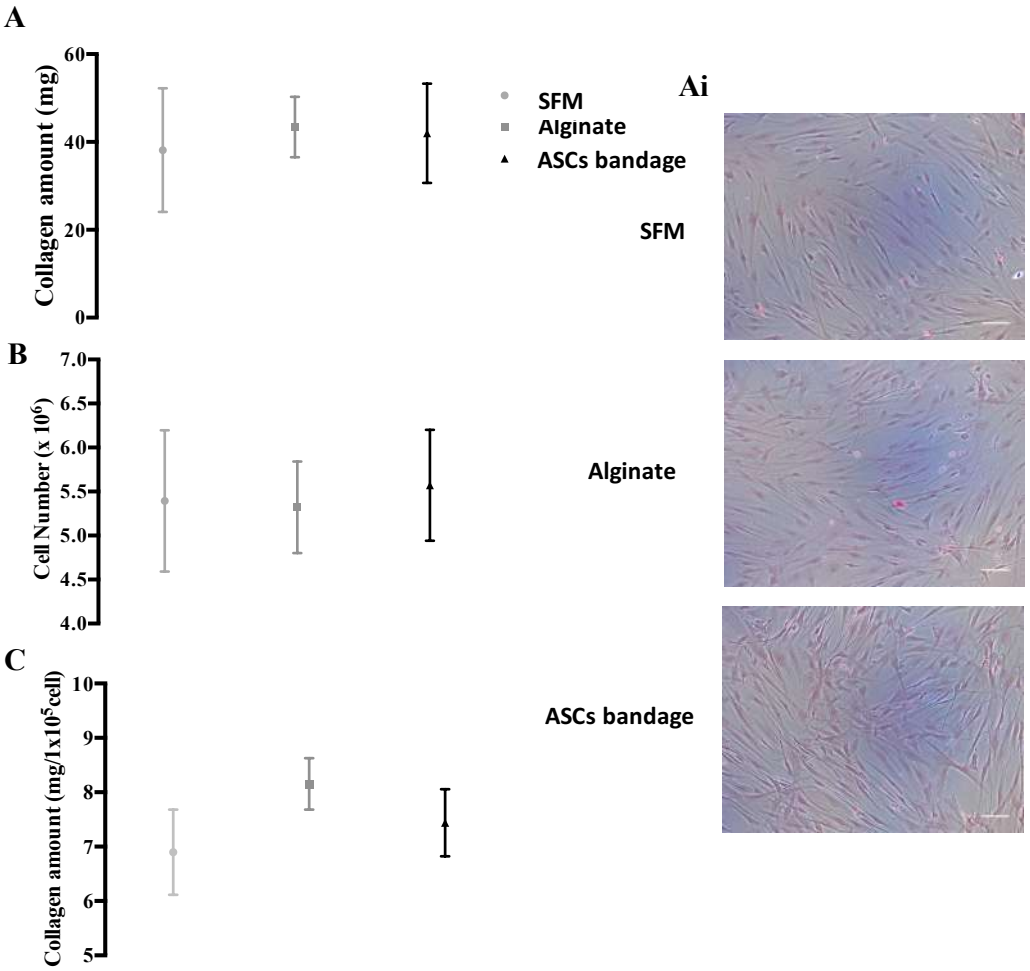

Figure 5.8 – Assessment of Keratoconus collagen amount (A, Ai), cell number (B), and normalized collagen amount to cell number (C). Scale bar = 100μm.

5.4 Discussion

MSCs have been used in the treatment of many diseases as therapeutic cells due to their ability to secret immunomodulatory molecules, influence endogenous production of extracellular matrix proteins, and enhance endogenous cell proliferation (Pinnamaneni and Funderburgh, 2012). In corneal therapy, MSCs have also been shown to improve corneal transparency via the production of paracrine factors (Mittal et al., 2016, Basu et al., 2014). Several studies suggested MSCs and ASCs can promote corneal wound healing via their ability to release paracrine factors (Kern et al., 2006, Gnecchi et al., 2005, Zeppieri et al., 2017). Such factors have been seen to promote corneal stromal cells migration, proliferation, and expression of extracellular matrix proteins. ASCs has also been shown to improve

visual parameters of patients with advanced KC (Alio Del Barrio and Alio, 2018). This chapter entails the use of ASCs bandages on diseased cultures whereas the previous chapter discussed the use of ASCs bandages on healthy cultures. Diseased cells behave differently than normal/healthy cells, including their production of different paracrine factors. Thus, showing our bandages effect on these cells provide us with an in-depth understanding of what our bandages can be used for. Our results showed ASCs bandages promoting KC wound healing via the release of paracrine factors. This ability of ASCs was present following storage at 15°C. Upon testing collagen deposition, no differences were found between the conditions, this could be attributed to the culture period of our scratch being too short. These results correspond to our findings in the previous chapters.

ASCs CM was previously shown to promote cell migration, proliferation, and wound healing (Yoon et al., 2010, Watson et al., 2010). Moreover, in a corneal injury mouse model, MSCs CM was found to improve corneal epithelium regeneration (Jiang et al., 2017). Thus, we tested CM taken following 3 days of storage at 15°C, where it showed an improvement in wound closure. We also found that combining encapsulated ASCs with their CM enhanced wound closure, in contrast, to stand-alone CM that contains growth factors released during storage. Soluble protein levels were enhanced within the media following scratch healing of bandage +CM. compared to control samples. This difference is minor when compared to ASCs bandages. The similarity found between these conditions suggests that ASCs actively respond to the injury via sensing signals produced by KC and react by producing paracrine factors that aid in wound healing. These factors can include but are not limited to HGF, IGF, TGF-ß, and KGF.

Studies demonstrated that mesenchymal-like stem cells are present in the human limbus area (Polisetty et al., 2008, Hertsenberg and Funderburgh, 2015). These corneal mesenchymal stromal cells (CSC) were shown to have decrease antiangiogenic properties *in vivo* and to reduce corneal neovascularization (Eslani et al., 2017). Therefore, we assessed CSC bandage ability in improving KC scratch wound with and without storage. Our result showed no difference between non-stored and stored CSC bandages, where both conditions enhanced KC wound closure. When compared to ASCs, no difference was found between the two cell types. This corresponds to research by Holan *et al*, where authors compared MSCs,

ASCs, and limbal stem cells in a rabbit alkali injured eye (Holan et al., 2015). They found all cell types were able to reduce neovascularization, improve re-epithelization while suppressing inflammation.

Although KC is diseased cells, we sought to investigate their effect on another KC population. Since both cell populations were diseased, we expected to see no effect on wound closure or a negative effect. Similar to our expectation, non-stored KC bandages showed a negative effect on wound closure, where there was no change in the scratch size. Surprisingly, however, 15°C stored KC bandage showed improvement in wound closure comparable to the use of ASCs. It has been suggested that storage stimulates ASCs ability to express enhanced levels of growth factors (Kaita et al., 2019). Moreover, we showed cells stored at 15°C prior to using with a scratch assay to improve cells' ability to produce growth factors. Thus, it would seem that storage also enhanced KC to produce beneficial growth factors that aid in wound closure. We also expect that storage affected KC gene expression which reduced their ability to produce harmful factors, this, however, needs further testing and understanding.

It has been suggested that cryopreservation affects the cell cycle (following thaw). Devine *et al* suggested that cryopreserved marrow and leukemia cell lines maintain these alterations in the cell cycle following 48-hours after return to normal temperature (Devine et al., 2018). In another study, authors stored a retinal pigment epithelial cell line at 4°C, 16°C and 37°C for 7 days (Pasovic et al., 2017). Cells stored at 4°C showed minimal changes in gene expression comparable to non-stored cells, whereas cells stored at 16°C and 37°C showed larger changes in gene expression. Interestingly, changes in hypoxic markers were shown at 16°C and 37°C storage. This suggests that hypothermic storage at 15°C also affects cell cycle and in turn their gene expression and so increases their value in therapy. We suggest that storage affected cells cycle, thus, presented us with improved wound recovery. However, our data suggested that the improvement seen following 15°C storage is comparable to non-stored cells. This can be attributed to the recovered cell number, where a reduction in ASCs cell number was seen following storage. Hence, we suggest two main factors affect ASCs' ability in wound healing, these being their number and storage temperature.

In conclusion, this chapter suggests that our bandages can be used in future therapies of KC diseases, and this would benefit the patient when there is a limited supply of corneal donors. 15°C stored encapsulated ASCs improved KC wound healing comparable to the non-stored cells. This improvement can be attributed to the storage effect on cell cycle and gene expression, where the cells showed improvement in the production of paracrine factors. ASCs' production of paracrine factors attributed to their ability to sensing environmental cues. These factors including but not limited to HGF, IGF, KGF, and TGF-ß that improve adherent cells' ability in migration and proliferation to close the wound. Thus, ASCs bandages provide great potential in KC wound treatment.

Chapter 6. Multipotent adult progenitor cell bandages for corneal stromal cell scratch-wounds

6.1 Introduction

Multipotent adult progenitor cells (MAPCs) have been investigated in various diseases, including bone repair and myelodysplasia (Martens et al., 2017, Roobrouck et al., 2017, Plessers et al., 2016), graft vs host disease (Maziarz et al., 2015), ischaemic stroke (Hess et al., 2017), and acute myocardial infarction (Penn et al., 2012). However, it has not been tested on the ocular surface or the cornea, hence, we sought to test MAPCs bandages on corneal recovery. It is suggested that the immnunomodulatory effects produced by MAPCs are released in response to wounding (Ravanidis et al., 2015, Reading et al., 2013). This effect is postulated to be driven by the cells' ability to produce growth factors, such as hepatocytes growth factors (HGF), tumor necrosis factor-inducible gene 6 (TSG-6), and transforming growth factors-ß1 (TGF-ß1). There is still not enough evidence to support the use of MAPCs, thus, we aimed to assess their effect on corneal wounds to give us an idea of their future therapeutic value.

6.2 aims

This chapter discusses the possible use of commercial MAPCs® as bandages. We assessed (i) their expansion and morphology, (ii) viability following hypothermic storage at 4°C and 15°C, followed by (iii) effect on *in vitro* corneal stromal cells (CSC) scratch wound, and their (iv) collagen levels using Sirius red staining. To our knowledge, this is the first report that shows MAPCs favorable effect on corneal wounds. The results obtained showed the benefit of incorporating MAPCs into future corneal therapy.

6.3 Results

6.3.1 MAPCs expansion and morphology assessment

As described in Methods Section (Chapter 2. 1.5) the received frozen MAPCs® vials (ReGenesys, Belgium) were thawed and seeded in a cell-binding flask, in a

2000 cell/cm^2 density, which was recommended by the supplier, and cultured at 37°C for 72 hours with XF media. XF (Xenobiotic-free) media were also recommended by the supplier to be the optimum media that can be used in growing the cells, whilst maintaining their stem cell phenotypic morphology. Prior to this study, MAPCs properties were tested by Crabbè *et al* (Crabbè et al., 2016) and compared to MSCs cultures, where both cell types were isolated from three shared donors. The authors found that compared to MSCs, MAPCs show faster doubling potential with smaller fibroblastic-like cells.

Following 72 hours of culture, MAPCs showed high proliferative potential with 80% confluency. At which point, cells were assessed for their morphology using phase-contrast microscopy, where the cells showed small, spindle-shaped fibroblastic-like morphology (Figure 6.1). This shape is similar to what was found by the supplier in a previous study (LoGuidice et al., 2016, Reyes and Verfaillie, 2001), therefore, no further validations were required in regards to morphology, stem cells markers and differentiation potential. Following 3 days in culture, cell viability was tested with live/dead staining and showed an average of 95 ± 1% of viable cells.

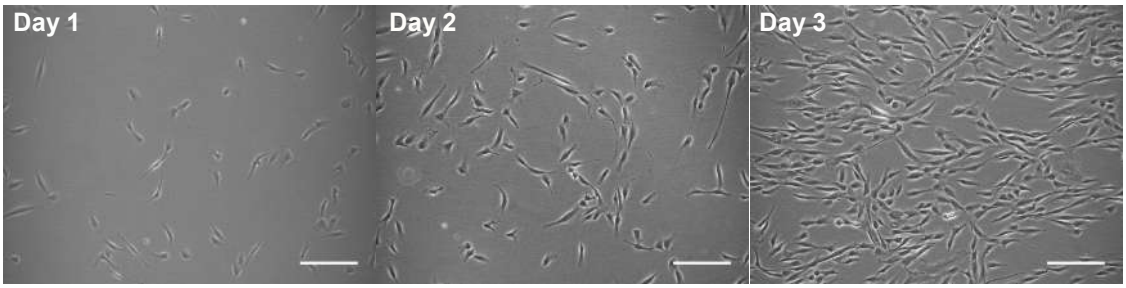

Figure 6.1 – Bright field images of MAPCs morphology. Images taken 72 hours following seeding, showing spindle shaped fibroblastic-like cells. This morphology was seen an all MAPCs expansion cultures (n=3), and, in correspondence with the literature, is considered normal MAPC morphology, therefore, no further validations were taken in terms of phenotyping. Scale bar = 200µm.

6.3.2 Alginate encapsulation effect on MAPCs viability

Calcium alginate was used to form MAPCs bandages and measure the hypothermic storage effect on cell function and viability. 1 x 10^6 cells were encapsulated in 1.2% w/v VLVG alginate in ring shape molds (encapsulation and

storage procedure explained in detail in chapter 2. 2.6) and stored at 4°C and 15°C in XF media for 72 hours. Encapsulated cell recovery was compared to non-encapsulated cells stored and treated in the same manner to eliminate any possible differences between the conditions.

MAPCs bandages stored at 15°C showed similar viable cell yield to cells stored at 4°C (~ 66%), whilst the non-encapsulated cells stored at 4°C showed reduced cell viability (~40%) compared to non-encapsulated cells stored at 15°C, where the latter showed similar viability to encapsulated cells (Figure 6.2 A). Following cell viability assessment, cells were tested for attachment efficiency, via culturing the released cells at 37°C for 24 hours and stained with Alamar blue. Following cell reattachment, significant differences were seen when comparing the previously encapsulated cells to non-encapsulated cells, suggesting encapsulation preserves cell functionality (Figure 6.2 B). Further normalisation was taken to measure overall cell functionality by multiplying cell viability values by cells' attachment efficiency. This showed significant differences between the encapsulated cells and non-encapsulated cells, further suggesting the importance of alginate in maintaining cell function (Figure 6.2 C) following storage. Although not significant, storing encapsulated cells at 15°C showed a better cell function than 4°C, whilst significant differences were shown between non-encapsulated cells stored at 4°C and 15°C. Cell morphology was also examined using light microscopy, were the cells adopted a spindle-shaped fibroblastic-like morphology, indistinguishable to non-stored cells (Figure 6.2 D). They also displayed high proliferative potential following 24 hours of culture.

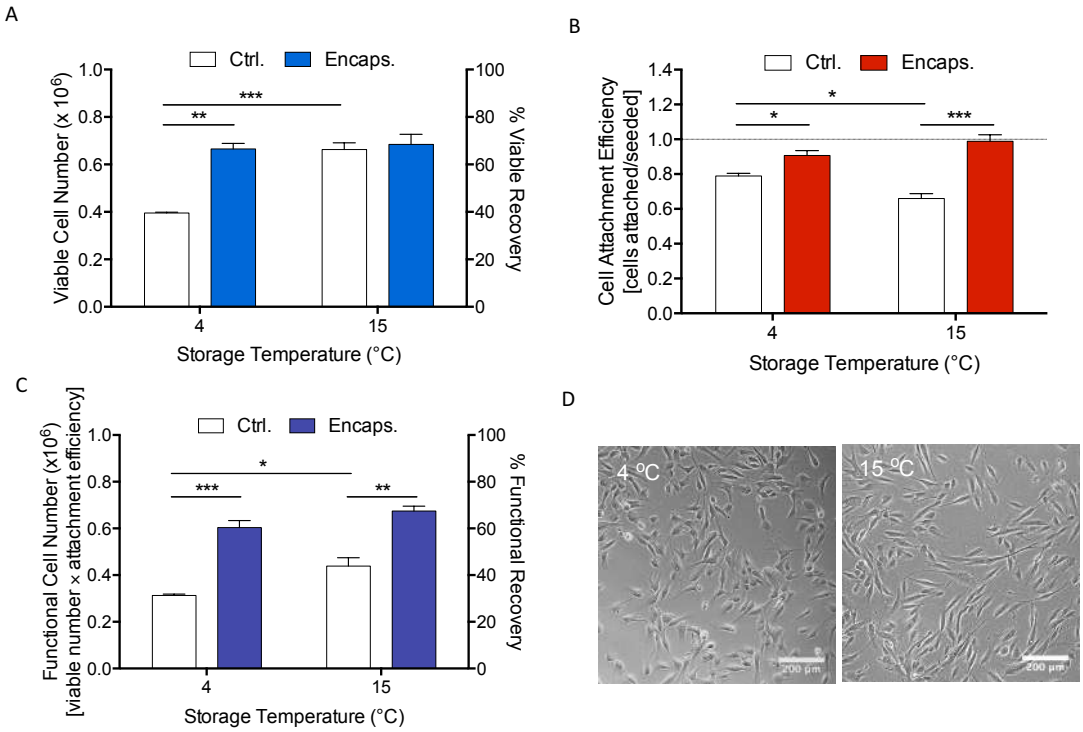

Figure 6.2 – Alginate encapsulation effect on MAPCs. MAPCs encapsulated in alginate (Encaps.) were compared to non-encapsulated MAPC (Ctrl.) following 72 hours of hypothermic storage at 4°C and 15°C. (A) Cells were released from encapsulation following 72 hours of storage before measuring viable recovery, and (B) attachment efficiency. (C) MAPCs functional cells number was also calculated via dividing viable cell recovery by the attachment efficiency. (D) MAPCs morphology was also assessed upon release and return to culture following 42 hours. Values are expressed as means ± SEM from n=3 with asterisks indicating significance from control values (***p < 0.001; **p < 0.01; * < 0.05), scale bar = 200µm.

6.3.3 Encapsulated MAPCs effect on in vitro corneal scratch-wound regeneration

Encapsulated MAPCs effect was tested on corneal stromal cells (CSCs) using the scratch-wound assay. CSC monolayers were serum-starved for 72-hours prior to scratching with 1mL pipette tip, at which point, the cells were grown in a confluent monolayer. The scratched cells were incubated with the following conditions; serum-free medium (SFM), alginate only (Alginate), and MAPCs bandages (Figure 6.3). Time-lapse images were taken for the duration of 48-hours following the scratch with a 1-hour interval, while ImageJ was used to measure the scratch width on time (t) =

0, 10, 20, 30, and 40 hours post-scratch. Experiments were repeated with 3 separate biological donors of CSCs and two technical repeats for each, whilst, three vials of MAPCs were received from the collaborator, each vial was used for a separate CSC donor.

The effect of MAPCs bandages on CSC was examined directly following their formation (non-stored). From the graphs, Non-stored MAPCs bandages had an augmented scratch closure compared to Alginate and SFM only (Figure 6.3 A&B). 20 hours post-scratch, CSC showed significant decrease in scratch width with the effect of MAPCs bandages compared to Alginate ($p = 0.0002$), this effect persisted following 30 and 40 hours post-scratch ($p < 0.0001$ and < 0.0001 respectively). Meanwhile, SFM showed a significant difference to Alginate at time points 20, 30, and 40 hours ($p = 0.0012$, 0.0036, and 0.0025 respectively) where it had faster-wound closure. SFM also displayed slower scratch-wound recovery compared to MAPCs bandages at time points 30 and 40 hours ($p = 0.0393$ and 0.0117 respectively).

Hypothermic storage of the MAPCs bandages was tested following 4°C storage for 72 hours (Fig 6.3 A&C). MAPCs bandages showed significant scratch closure at time points 20, 30, and 40 hours when compared to Alginate ($p = 0.0373$, 0.0021 and 0.0007 respectively). Surprisingly, however, no significant differences were found when compared to SFM. Whereas storage at 15°C for 72 hours (Fig 6.3 A&D) showed a significant wound closure at time points 20, 30 and 40 hours when compared to Alginate ($p = 0.0004$, <0.0001 and <0.0001 respectively), Interestingly significant differences were found between SFM and MAPCs bandages at time point 30 hours ($p= 0.0288$). Thus, storing MAPCs at 15°C prior to using with CSC did affect their ability to improve wound closure.

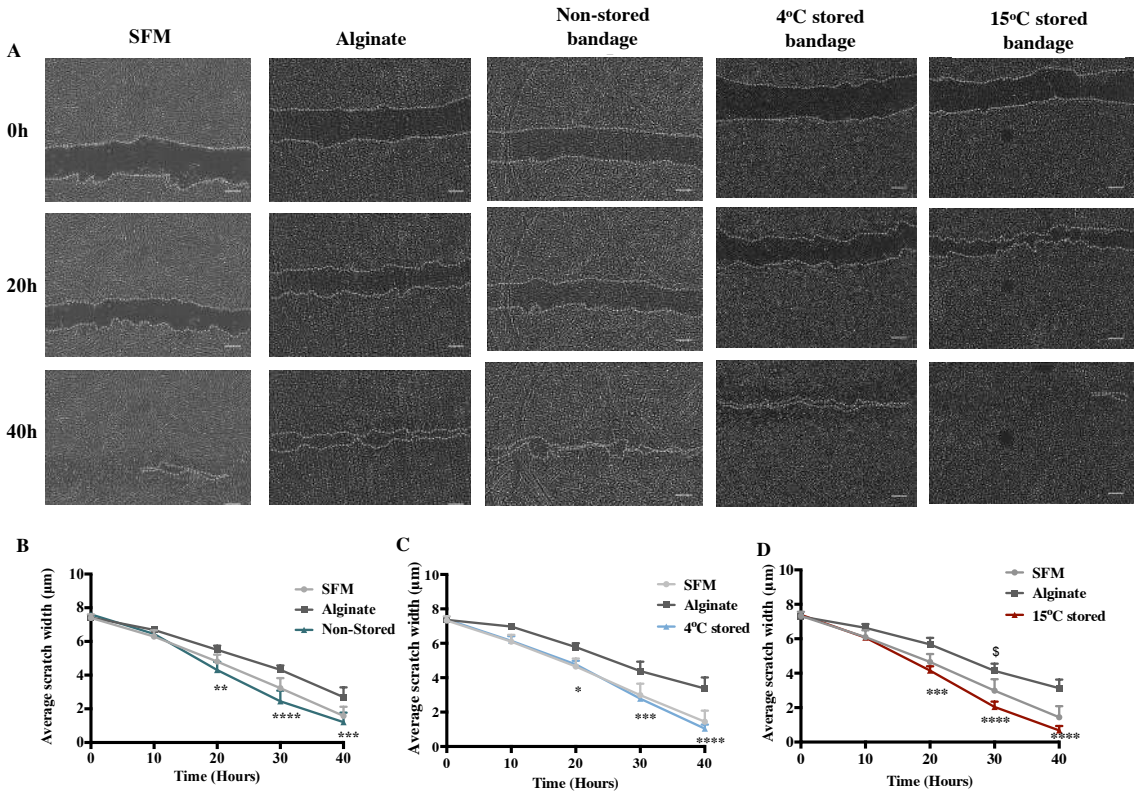

E

Time (Hours)	SFM	Alginate	Non-stored	4°C storage	15°C storage
0	100	100	100	100	100
10	89.83239473	90.2468741	84.77022011	83.19104675	82.1769285
20	70.75146893	74.28158858	56.40275556	64.61386277	56.26766769
30	54.94253768	58.4928743	31.80806083	37.71729114	27.74437148
40	37.07073254	37.1387765	15.58263046	13.98659725	9.347396422

Figure 6.3 – Effect of non-stored and hypothermically stored at 4°C and 15°C MAPCs bandages on CSC cultures. (A) Representative images of the scratch taken using Iprasense time-laps holographic microscope at time points 0, 20, and 40 hours post-scratch. Comparison of the scratch wound closure over time of (B) non-stored, (C) 4°C stored, and (D) 15°C stored bandages, and (E) scratch percentage values. Significant differences presented for the comparison of Alginate and Encaps in each graph. SFM, serum-free DMEM:F12; Alginate, VLVG alginate; Non-stored, MAPCs bandages used following formation; 4°C and 15°C stored, MAPCs bandages used following 72 hours of hypothermic storage. Values are expressed as means ± SEM from n=3, (****p < 0.0001; ***p < 0.001; **p< 0.01), Scale bar = 300µm.

Although CSCs were all shown to have improved wound healing when co-cultured with MAPCs bandages (rather than Alginate alone), there are also differences when compared together (Figure 6.4). For example, 20- and 30-hours post scratch, significant wound closure was seen in the presence of the 15°C stored bandages when compared to non-stored bandages ($p = 0.0427$ and 0.0091 respectively). At 40-hour post scratch, differences were found when compared with 4°C stored bandages ($p = 0.0471$). These results suggest that 15°C storage increases the amount of soluble factors available to the CSC as measured by scratch-wound closure, which supports our previous chapters.

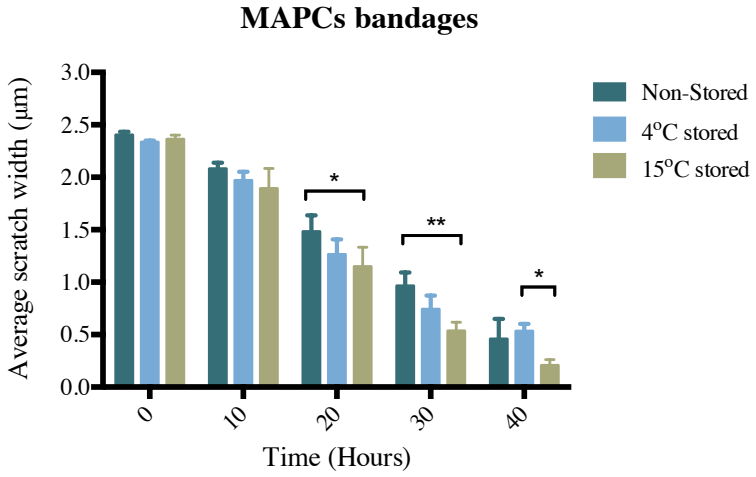

Figure 6.4 – Comparison of MAPCs bandages following use in CSCs scratch-recovery of the non-stored, 4°C and 15°C storage. (**p < 0.01; * < 0.05).

Following scratch closure, we counted the MAPCs cell number using live/dead staining and subsequently used to normalise the scratch closure data (Figure 6.5). Average scratch width values were divided by the total remaining MAPCs cell number for every condition and subtracted from time 0 values, to the present rate of which individual MAPCs effect CSC wound closure. From the graph, significant differences were found between the non-stored and 4°C stored at times 20, 30, and 40 hours post scratch ($p = 0.0312$, 0.0035, and 0.0368 respectively) with speed of migration of 0.0000019, 0.0000029, and 0.0000033 µm/cell/hour respectively. Whilst 15°C seems to be slower at time 20 hours 0.0000016 µm/cell/hour, 30 hours 0.0000024 µm/cell/hour, and 40 hours 0.0000021 µm/cell/hour. This is an indication that although there are less average cells alive after 4°C storage (5x10^5 ± 0.89

cells), they can show similar healing potential on a per-cell basis to those stored at 15°C prior to incubation with scratch 7.4 x 10^5 ±0.69 cells and non-stored 7.6 x 10^5 ±0.87 cells. This supports our previous suggestion that hypothermic storage can influence cells to produce a greater amount or more potent factors that affect CSCs culture within the scratch assay.

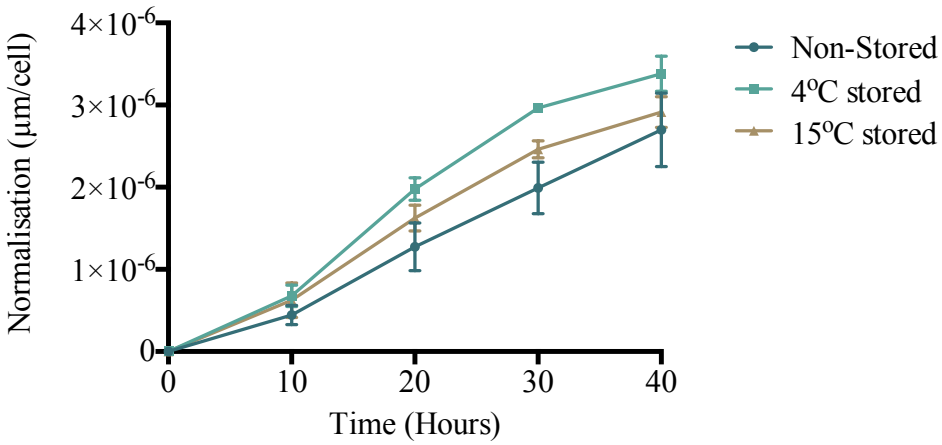

Figure 6.5 – Normalisation of the recovered MAPCs cell number following scratch recovery to CSC scratch healing over time, the graph represents the speed which MAPC cell affect CSC scratch-wound closure.

6.3.4 Corneal stromal cell proliferation and collagen production following scratch wound recovery in presence of bandages

CSC cell number was measured following scratch closure; the cells were lifted and stained with Trypan blue and counted using Countess FL automated cell counter (Figure 6.6 A). CSC cell number was counted for all conditions stated previously to determine whether the cells migrated or proliferated. From the initial seeding density 2 x 10^5 cells/well, CSC cultured with SFM showed a slight increase in cell number (2.1 x10^5 ± 0.17 cells/well), while there was a decrease in cell number in the Alginate condition (1.4 x10^5 ± 0.32 cells/well), whilst a sharp increase in cell number was noticed in the MAPC bandages condition when they were hypothermically stored prior to co-culture at 4°C and 15°C (2.95 x10^5 ± 0.23 and 4.17 x10^5 ± 0.5 cells/well respectively), compared to non-stored (2.1 x10^5 ± 0.42 cells/well). Thus, CSCs showed an approximate doubling in proliferation when co-

cultured with 15°C stored bandages. following scratch wound healing compared with non-stored.

72-hours post-scratch wound, the plates with CSC were stained with Picro-Sirius red staining to measure collagen deposition (Figure 6.6 B). Total collagen amount measured in the SFM condition was found to be 48.2mg ± 3.0, whereas CSC cultured with 5% media (5% FBS added to the media) were found to be 84.0mg ± 8.5. CSC cultured with 15°C stored MAPC bandages showed an increase in collagen deposition to 62.5mg ±19.4, similar to 4°C 61.0mg ±13.1 and higher than non-stored 56.3mg ±15.4. In comparison, Alginate condition showed an even higher collagen deposition amount to 67.2mg ±15.6 in the non-stored condition and 63.9mg ±21 in the 4°C storage and 57.1mg ±24.4 when stored at 15°C prior to using. However, no significant differences were found among all the groups.

The total collagen amount was normalized to CSC cell number, to measure single-cell collagen deposition by dividing total collagen amount to final cell number (Figure 6.6 C). From the graph, significant differences were found among the treatment groups when compared to Alginate (different to what was found in Chapter 4, which can be attributed to the difference in the type of plate used for the experiments), while there was a drop-in collagen amount produced by cells in the 15°C stored bandages and the 5% media.

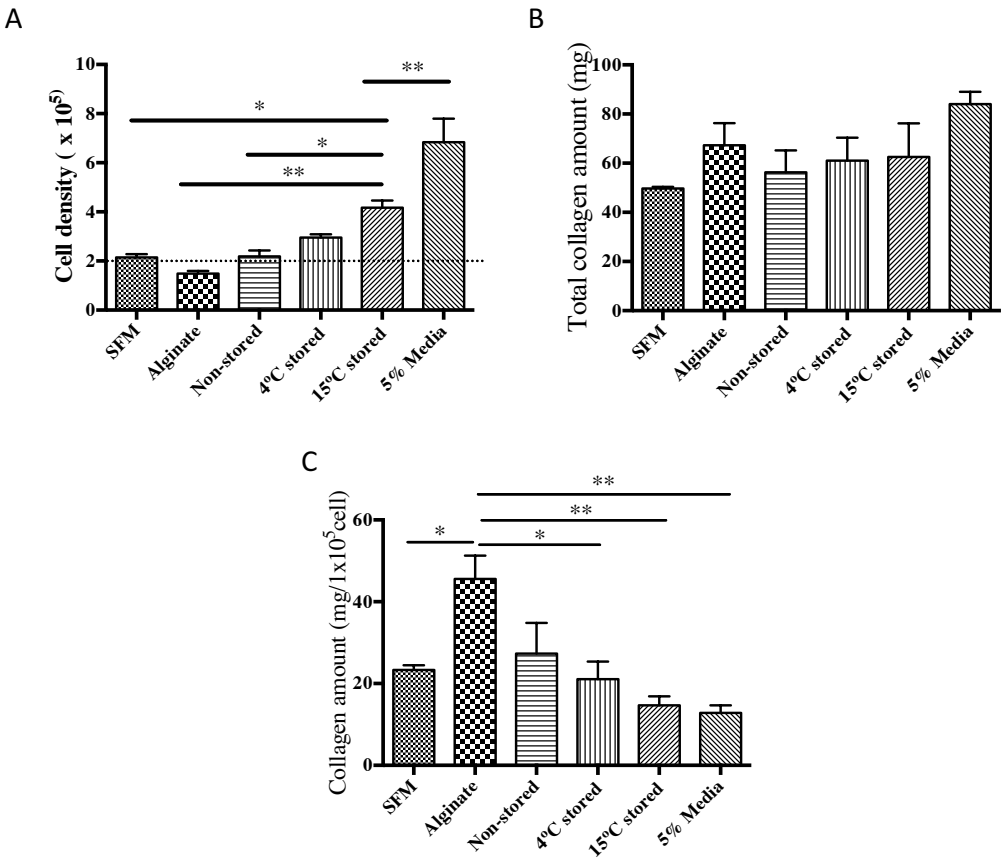

Figure 6.6 – (A) CSC Cell density, and (B) total collagen amount taken following scratch recovery, and (C) collagen amount normalized to cell number to represent the amount of collagen produced per cell. 5% media, 5% FBS DMEM:F12. Values are expressed as means ± SEM from n=3, (***p < 0.001; **p < 0.01; * < 0.05).

6.4 Discussion

MAPCs therapeutic value appears to be dependent upon the method of delivery that allows for optimal retention of the functional viability whilst maintaining their ability in producing supposed paracrine factors (i.e. HGF, PDGF, TGFß, etc.). So far, MAPCs have shown significant value in the clinical treatment of multiple sclerosis (Singh et al., 2017), acute ischemic stroke (Hess et al., 2017), hind limb ischemia (Aranguren et al., 2011), bone repair (LoGuidice et al., 2016), and myelodysplastic syndrome (Roobrouck et al., 2017). MAPCs therapeutic abilities were shown to be driven by their immunoregulatory effectors and their secretion of paracrine factors (Kovacsovics-Bankowski et al., 2015). Although MAPCs are similar to MSCs, until now, they have not been tested in corneal injures (*in vitro* or otherwise).

We investigated the ability of alginate in maintaining MAPCs viability and function following hypothermic storage at 4°C and 15°C. Previously, we and others showed that alginate preserves MSCs viability and functional recovery following ambient and hypothermic storage, it was also found that changes in temperature can affect cell viability (Cesselli et al., 2009, Weissman et al., 2001). Here, we found alginate to preserve MAPCs during 72 hours of hypothermic storage at 4°C and 15°C. Alginate also maintained MAPCs phenotype when returned to normal culture conditions, where they presented spindle-shaped fibroblastic like cells with high proliferative potential, this was indeed in agreement with the literature (Reading et al., 2013, Boozer et al., 2009, Crabbè et al., 2016).

Although many studies were conducted on MAPCs they were not researched on corneal injuries. Thus, we tested the MAPCs bandages' effect on CSC scratch wound healing. From the data, we found that MAPCs bandages produce some (as of yet) undefined factors that significantly improved scratch closure. Storage at 15°C prior to using in co-culture presents a faster scratch closure. An intriguing observation is the 4°C storage, which showed an enhanced wound closure potential following normalization to cell number. Although we note a decrease in MAPCs cell number following 72-hour storage at 4°C, the cells, however, appear to display high activity in producing paracrine factors and so are able to speed the scratch wound closure.

As has been shown in chapter 3 and 4, alginate presence in the culture seems to attenuate the wound recovery rate while increasing collagen amount produced by the CSC. We expect this to be attributed to the ion exchange reaction between the alginate and the SFM. Alginate contains calcium ions that may react with the sodium ions from the media, thus, effecting CSC proliferation (Tong et al., 2017, Lee and Mooney, 2012). The increase in ion absorption may have caused the alginate to swell and slowly dissolve in the media, which might explain the negative effect seen with the alginate only treatment used with CSC culture. It is also suggested that the subsequent increase in calcium ions may influence cell migration and proliferation (Lee et al., 2018).

Collagen is one of the main components of the cornea, which is also produced by the corneal fibroblasts in response to wound recovery. Depending on the wound severity, collagen deposition can be delayed (Ljubimov et al., 1998, Nakayasu et al.,

1986). Within the present system, collagen deposition is delayed across the conditions that showed high cell proliferation, it is suggested that alginate improves collagen deposition in damage site (Wang et al., 2015, Lee et al., 2009). Although no significant difference was found between alginate and MAPCs bandages in regards to collagen amount, normalisaing data to cell number gave a significant increase in alginate condition compared to all other conditions, this delay can prove useful in wound healing. Considering in corneal wound healing, we usually want the cells to heal the injury without causing scar formation, therefore, if there was high collagen production at the injury site without having partial or almost full recovery can cause the formation of scars and loss of corneal transparency. As detailed alginate alone decreases cell proliferation, it has been observed that non-motile corneal stromal cells are associated with high collagen amounts (Gouveia and Connon, 2013). This may explain the increased collagen production in the presence of alginate

In conclusion, these results provide compelling evidence that alginate can preserve MAPCs during hypothermic storage without losing their viability and functional recovery. Also, our initial data support the potential of using MAPC therapy in corneal wounds. However, it is still unknown the exact mechanism in which MAPC affects the corneal cells. Therefore, further work needs to validate and test the growth factors produced by MAPC and their importance in wound healing.

Chapter 7. Summary of wound healing data

The effect of different bandages formation was investigated on the wound healing of the human corneal stromal cells (CSC). Conditions were either with non-stored (Figure 7.1) or stored for 72-hour at 4°C (Figure 7.2) and 15°C (Figure 7.3). The storage was made in tightly sealed plates at 4°C and 15°C with serum-free media (SFM) and to prevent direct contact we used a Transwell® system.

We compared two types of alginates, Sigma and NovaMatrix alginates. Sigma alginate showed improvement in scratch wound closure in all conditions, however, it was shown to induce ASCs to produce hepatocyte growth factor (HGF) and ascular endothelial growth factor (VEGF), thus, for the safety of cell therapy we decided to use NovaMatrix alginate in all experiments.

Many conditions were evaluated and compared to ASCs bandages in healing CSC scratch wounds, including conditioned media (CM) taken from the bandages stored at 4°C and 15°C, other conditions including CSC bandages, human dermal fibroblast (hDF) bandages, keratoconus (KC) bandages, and MAPC bandages. We also measured ASCs lysis (cell death within bandage) effect and their formed lysate, and the combination of ASCs bandages +CM. Compared to all those conditions, ASCs bandages showed its superior effect in healing CSC scratch wounds.

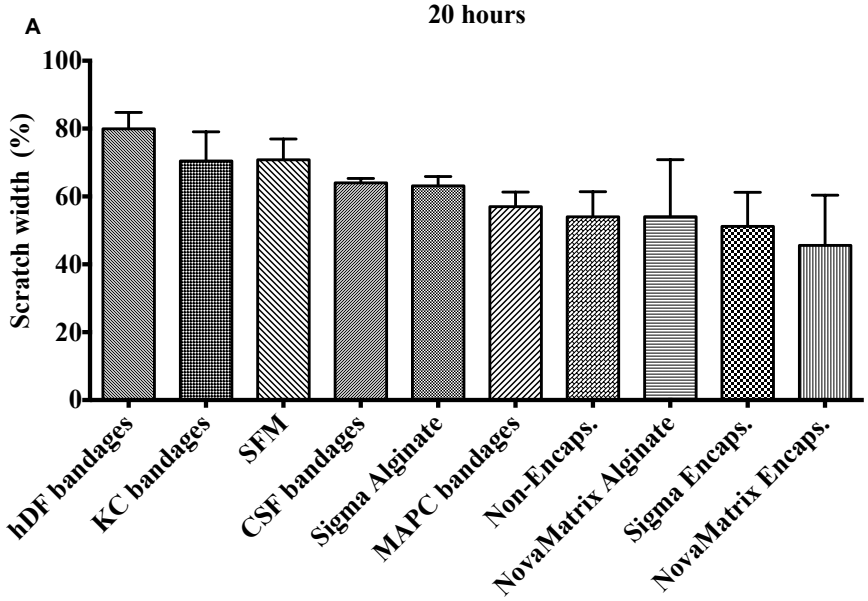

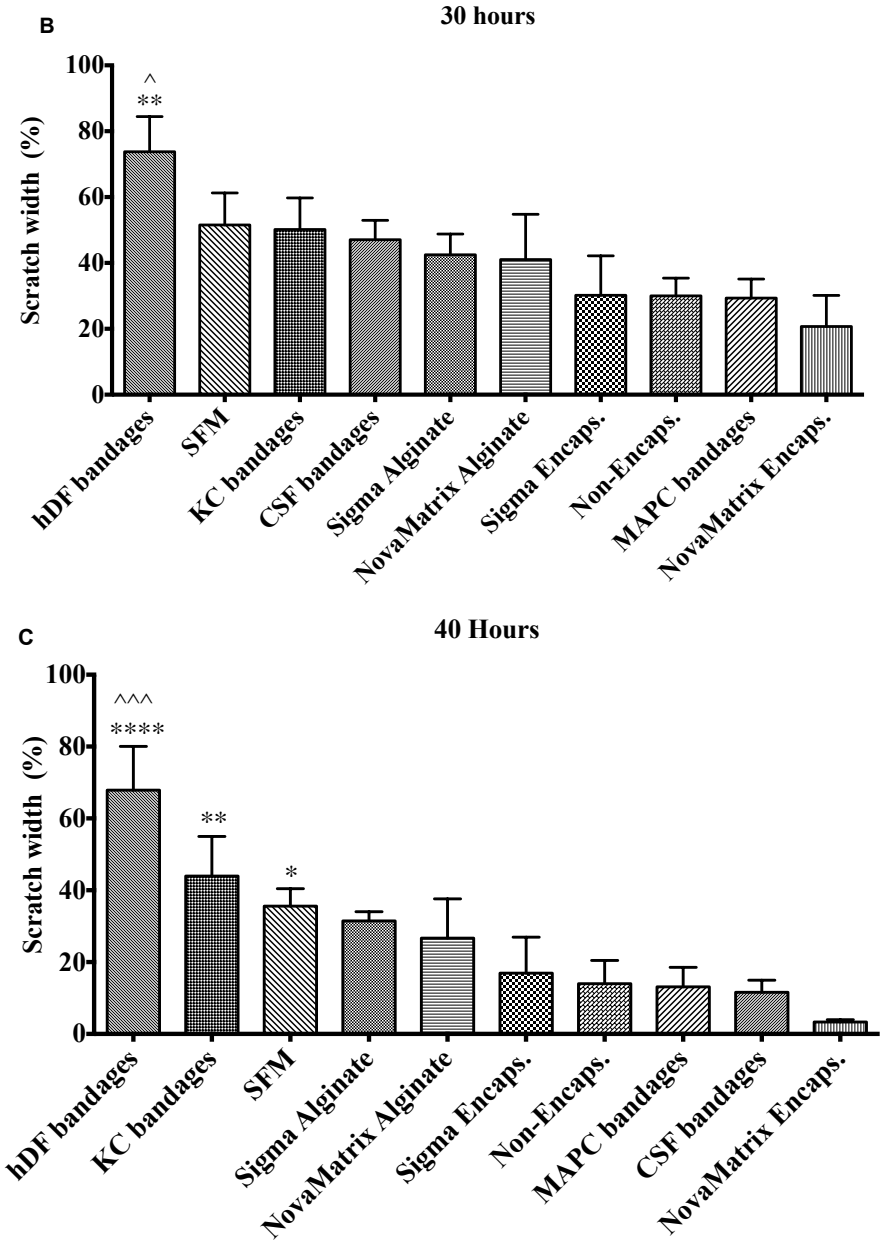

Figure 7.1 – Non-stored conditions used in wound healing. Represented at times (A) 20-, (B) 30-, and (C) 40- hours post scratch. Values are presented as mean ± SEM from three separate keratocytes donors, asterisks represent significance between NovaMatrix Encaps. and all other conditions (****, $p < 0.0001$; **, $p < 0.01$; *, $p < 0.5$), while symbols represent significance between Non-Encaps and all other conditions (^^^, $p < 0.001$; ^, $p < 0.5$). NovaMatrix Encaps., ASCs bandages.

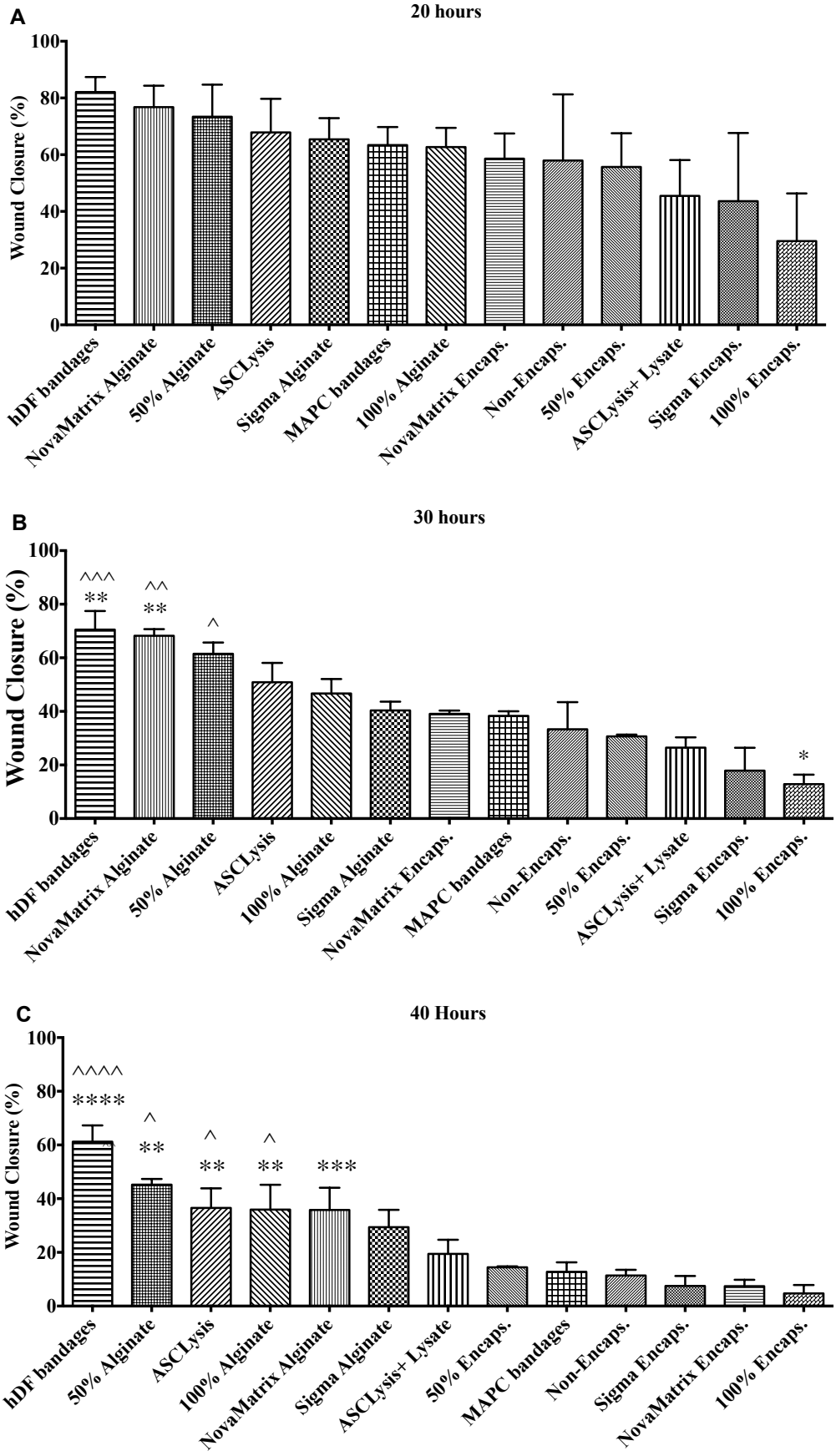
A
20 hours
Wound Closure (%)
100
80
60
40
20
0
hDF bandages
NovaMatrix Alginate
50% Alginate
ASCLysis
Sigma Alginate
MAPC bandages
100% Alginate
NovaMatrix Encaps.
Non-Encaps.
50% Encaps.
ASCLysis+ Lysate
Sigma Encaps.
100% Encaps.
B
30 hours
Wound Closure (%)
^^^
**
^^
**
^
*
hDF bandages
NovaMatrix Alginate
50% Alginate
ASCLysis
100% Alginate
Sigma Alginate
NovaMatrix Encaps.
MAPC bandages
Non-Encaps.
50% Encaps.
ASCLysis+ Lysate
Sigma Encaps.
100% Encaps.
C
40 Hours
Wound Closure (%)
^^^^
****
^
**
^
**
^
**
***
hDF bandages
50% Alginate
ASCLysis
100% Alginate
NovaMatrix Alginate
Sigma Alginate
ASCLysis+ Lysate
50% Encaps.
MAPC bandages
Non-Encaps.
Sigma Encaps.
NovaMatrix Encaps.
100% Encaps.

Figure 7.2 – 4°C stored conditions used in wound healing. Represented at times (A) 20-, (B) 30-, and (C) 40- hours post scratch. Values are presented as mean ± SEM from three separate keratocytes donors, asterisks represent significance between NovaMatrix Encaps. and all other conditions (****, p < 0.0001; ***, p < 0.001; **, p < 0.01; *, p < 0.5), while symbols represent significance between Non-Encaps and all other conditions (^^^^, p < 0.0001; ^^^, p < 0.001; ^^, p < 0.01; ^, p < 0.5). NovaMatrix Encaps., ASCs bandages.

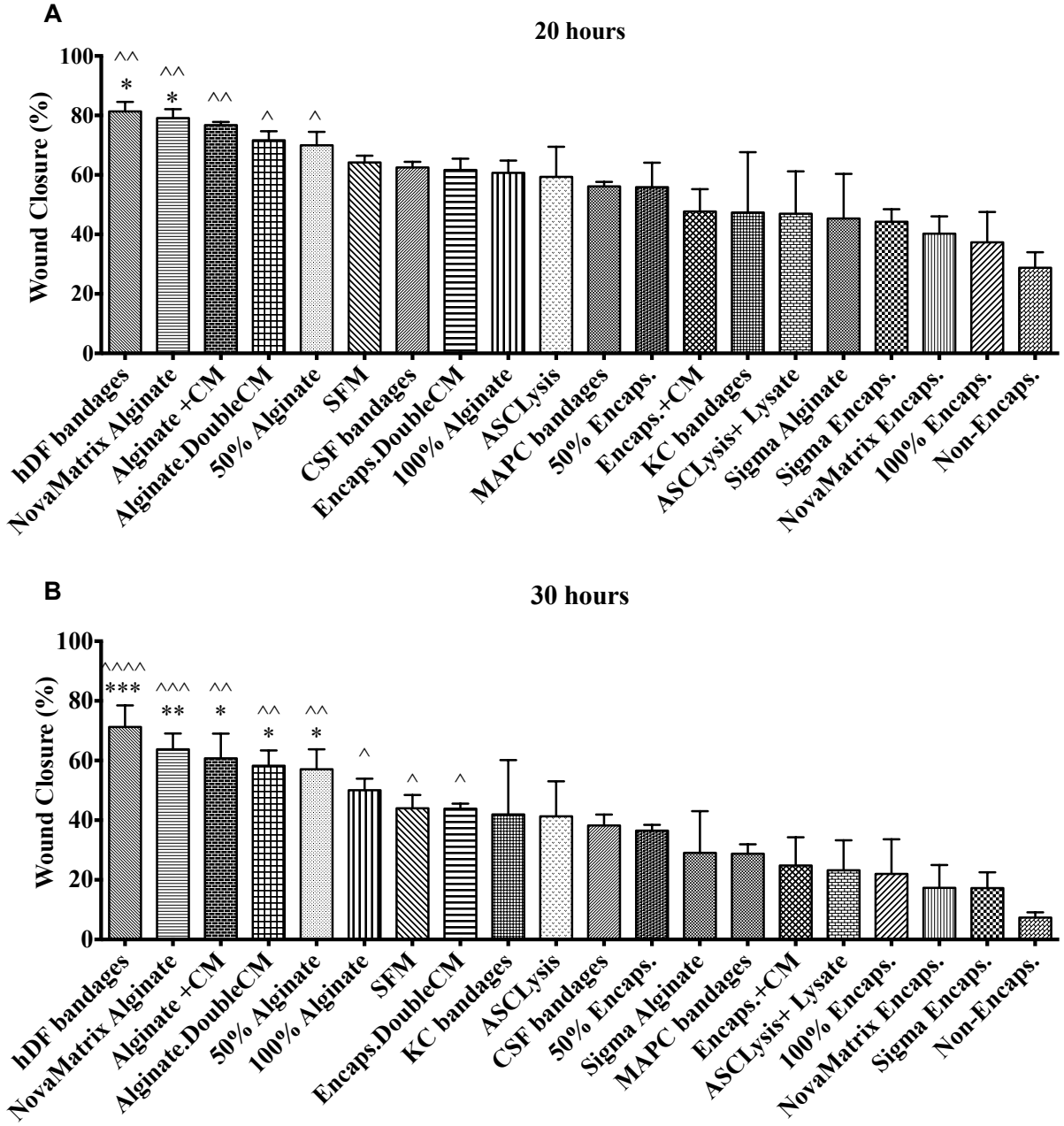

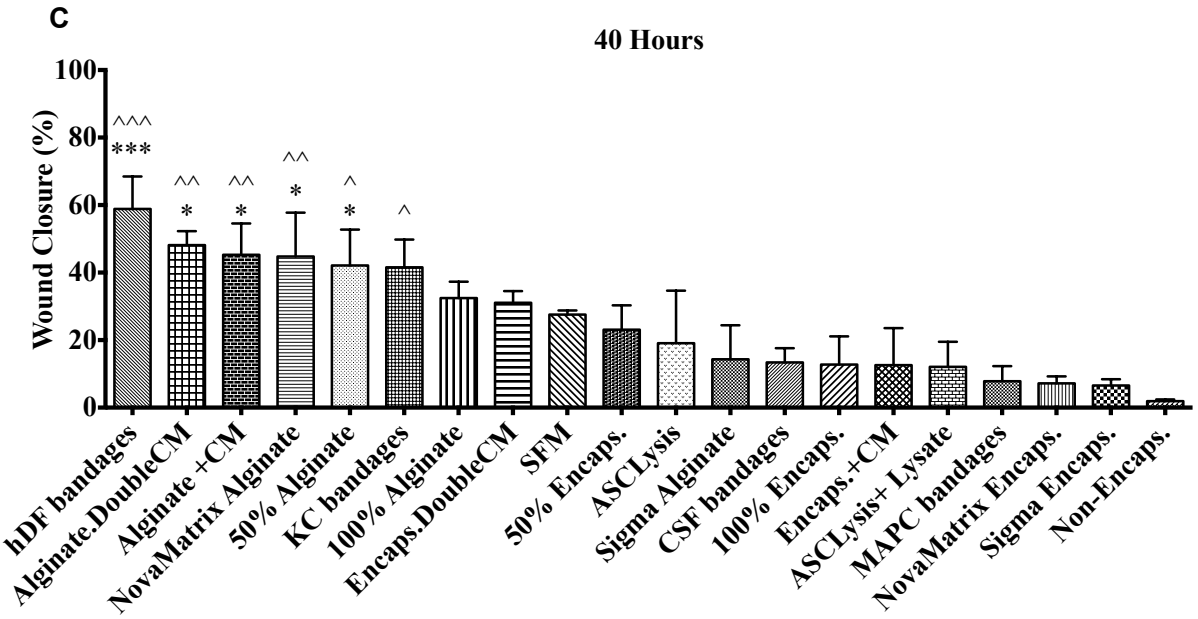

Figure 7.3 – 15°C stored conditions used in wound healing. Represented at times (A) 20-, (B) 30-, and (C) 40- hours post scratch. Values are presented as mean ± SEM from three separate keratocytes donors, asterisks represent significance between NovaMatrix Encaps. and all other conditions (****, $p < 0.0001$; ***, $p < 0.001$; **, $p < 0.01$; *, $p < 0.5$), while symbols represent significance between Non-Encaps and all other conditions (^^^^, $p < 0.0001$; ^^^, $p < 0.001$; ^^, $p < 0.01$; ^, $p < 0.5$). NovaMatrix Encaps., ASCs bandages.

The combined treatment of hypothermically stored ASCs bandages with CSC scratch wound has been shown to increase paracrine factors release to a level that is not achievable when ASCs used without alginate or without storage. In addition, this activity appeared to be enhanced when ASCs in the presence of a secondary population. Supportive effects between ASCs and CSCs have not been previously reported in regards to hypothermic storage and alginate, thus, these studies highlight a significant consideration to make for the potential of combined efficiency of hypothermic storage and alginate in stem cells bandages.

Within the groundwork examination of encapsulated ASCs, we found their importance as bandages for *in vitro* corneal wound healing. This healing ability was mainly driven by their ability to produce a cocktail of growth factors, such as HGF, TGF-ß1, and IGF among many others. Thus, we then wanted to measure their effect in an *in vivo* corneal model.

Chapter 8. Proof of concept: Delivery of hypothermically stored ASCs bandages to the ocular surface

8.1 Introduction

Chemical injuries (including acid and alkali burns) are one of the common eye injuries affecting many people. These injuries vary in severity from minor, affecting the corneal surface to major that penetrate deep into the corneal layers and lead to inflammation, scarring, and blindness (Wagoner, 1997). Therefore, they are considered an emergency that requires immediate assessment and treatment (Singh et al., 2013). Treatments aim to restore corneal epithelium, reduce inflammation, ease pain, and prevent bacterial infection (Salzman and O'Malley, 2007, Fish and Davidson, 2010). The treatment method depends on the severity of the injury. Amniotic membrane (AM) can be transplanted to the injured cornea for grade I, III, and IV injuries (Clare et al., 2012). It can act as a bandage contact lens or a basement membrane for re-epithelialisation and corneal healing (Shimmura et al., 2001, Bouchard and John, 2004). For the most severe injuries limbal stem cell (LSC) transplantation can be used to improve the reconstruction of the ocular surface (Liang et al., 2009, Kim et al., 2003). Corneal transplantation to treat severe thinning, neovascularisation, corneal perforation, or descemetocele (ulcers) (Baradaran-Rafii et al., 2013, Alio et al., 2002). Thus, we found it interesting to investigate our adipose-derived mesenchymal stem cells (ASCs) bandages' ability in healing corneal chemical burns. As a bandage, ASCs can be placed as a contact lens on the eye and release paracrine factors in response to the environmental cues.

8.2 Aims

So far, we have shown that alginate bandages are effective in preserving ASCs during storage. ASCs bandages were able to deliver therapeutic factors to a secondary population *in vitro*, without direct contact with the cells. Therefore, we sought to investigate these bandages as a therapeutic contact lens for the delivery of therapeutic factors to the ocular surface *in vivo*.

8.3 Material and methods

8.3.1 ASCs encapsulation, storage and assessment of viable cells recovery

This study was performed in collaboration with Dr. Stephen Swioklo, Atelerix Ltd. and Dr. Alex Shortt, UCL. Dr. Swioklo designed the experiment and prepared the materials. Dr. Shortt performed the animal study. I was responsible for analysing the corneas post mortem and interpretation of the results.

Human ASCs derived from adipose tissue of healthy donors, were encapsulated in 1.2% w/v calcium alginate. ASCs bandages were stored at 15°C for 3 days in a sealed cryovial with a growth medium. Viable cell recovery was assessed using live-dead staining to count the number of viable cells. Attachment efficiency was measured using methylene blue staining after 24 hours of cells return to culture. While functional recovery was measured by multiplying attachment efficiency by viable cell recovery.

8.3.2 Delivery of stored, encapsulated ASCs to the ocular surface

Human ASCs (as described in chapter 2 2.3) were encapsulated in 1.2% (w/v) calcium alginate discs (as described in chapter 2 2.3) containing 20 x 10^6 cells/mL and stored at 15°C for 3 days in serum-free medium (SFM). Bandages were transported within an insulated box under temperature-monitored conditions. At UCL the bandages were cut down to a diameter of 3.5mm (1 mm thickness) using a biopsy punch to form a therapeutic contact lens, which resulted in approximately 60,000 cells transferred to the eye.

12 Adult male NSG (NOD/SCID/Gamma) mice aged 8 to 12 weeks were divided into two groups, those receiving an ASCs bandage, and those receiving a bandage without cells. Under combined topical and general anesthesia, the left cornea and limbus were treated with 20% ethanol for 3 minutes before debridement of the corneal and limbal epithelium. Eyes were washed with HBSS. An 8-0 proline tarsorrhaphy suture were pre-placed then a 3.5mm diameter gel were placed over the cornea and limbus, the lids were shut and suture tied. The suture was removed after 4 days and the lids opened, at which point, the bandages were found degraded and fragments could be seen on the cornea. Seven days following injury, eyes were imaged under terminal anesthesia before sacrificing the animals and eyes

enucleated. Eyes were fixed in 4% (w/v) paraformaldehyde and mounted in OCT. 15µm sections were cut for subsequent H&E staining and immunohistochemistry studies. Animal care and handling were in-line with ARVO Statement for Use of Animals in Ophthalmic and Vision Research.

8.3.3 Hematoxylin and Eosin staining

Hematoxylin is a deep blue-purple stain that stains the cells nucleic acid, while, Eosin is a pink stain that stains cytoplasm and extracellular matrix. Which makes this an optimal stain to visualise animal tissue sections (Fischer et al., 2008). Hematoxylin can stain the tissue when combined with metal cations, which will be positively charged cations and so, will bind to negatively charged nucleic acids, thus, stain blue. Eosin, on the other hand, is negatively charged anionic and react with amino groups in the cytoplasm, thus, stain pink.

H&E staining procedure was performed as described by Fischer *et al*, briefly, 15µm frozen cryosections of the enucleated eyes were dehydrated at room temperature before washing with 95% and 70% EtOH for 2 minutes and marking the edge of the slide with ImmEdge™ hydrophobic barrier pen (Vector laboratories LTD, Peterborough, UK). Sections were stained with hematoxylin stain (Sigma-Aldrich, UK) for 2.5 minutes followed by a wash and 2 dips in acid alcohol solution, a differentiation solution made by mixing 1% HCl (Fluka analytical, Bucharest, Romania) with 70% EtOH. Ammonia water solution, a blueing solution, made by mixing 0.2% ammonium hydroxide solution (Sigma-Aldrich, UK) in distilled water, was added to the section tissues following a wash for 60 seconds. The sections were then washed with 95% EtOH for 30 seconds before adding Eosin Y solution (Sigma-Aldrich, UK) counterstain for 60 seconds followed by two washes with 95% and 100% EtOH for 5 minutes. The section slides were then cleared and mounted with DPx mountant solution for histology (Sigma-Aldrich, UK) to preserve the stain, and covered with glass coverslip 24 x 50mm (Menzel Gläser, VWR, UK). Images were then taken using Nikon ECLIPSE TS100 (Nikon Instruments Europe BV, Tripolis100, Amsterdam, Netherlands) inverted microscopy using 20x, 10x and 5x magnification using ProgRes® CapturePro (V2.8.8) (Jenoptik, Jena, state of Thuringia, Germany) image analysis software.

8.3.4 Immunocytochemistry

Immunocytochemistry is a semi-automated, rapid technique for determining lymphoid cell phenotype via examining cell surface antigen expression. This technique can define the population of lymphocytes in terms of lineage either T or B cells, monoclonal or polyclonal cells.

The R&D systems protocol was used for staining the frozen cryo-sectioned samples, briefly, the frozen cryosections were allowed to thaw at room temperature before washing with a wash buffer (1X PBS) for 10 minutes to rehydrate the samples. Hydrophobic barrier pen (Vector laboratories LTD, UK) was used to surround the tissue sections before incubating with blocking/incubation buffer containing 2% bovine serum albumin (First link Ltd, Wolverhampton, UK) and 0.1% Triton® X-100 (ThermoFisher Scientific, UK) in PBS for 30 minutes to block non-specific staining between the tissue and primary antibody. Up to 8 sections of each sample were then incubated with primary antibody anti-neutrophil (NIMP-R14) – rat anti-mouse (Abcam, Cambridge, UK) overnight at 4°C in a humidified container to avoid sample dryness. This incubation allows specific binding of the antibody to the tissue whilst reducing non-specific background staining. Sections were washed 3 times for 15 minutes before incubating with IgG anti-rat secondary antibody (1 in 1000 dilution) (Vector Laboratories, Peterborough, UK) and Hoescht 33342 solution (1 in 2000 dilution) (ThermoFisher Scientific, UK) for 60 minutes at room temperature. This was followed by 3 washes with washing buffer for 15 minutes, at which point, the sections were protected from light and mounted in Prolong® Diamond Antifade Mountant (ThermoFisher Scientific, UK) and sections covered with a glass 24 x 50mm coverslip. A Zeiss AxioImager (with Apotome) fluorescence microscope was used to image the cryosections. Negative controls were included in every staining; these were used as described above but without the addition of primary antibody. Neutrophil numbers in the central and corneal periphery were manually calculated from the stained images from at least four sections of the same sample.

8.4 Results

8.4.1 Alginate encapsulation preserves cells during hypothermic storage

Alginate encapsulation preserved cells during hypothermic storage where it showed a significant cytoprotective effect following 72-hours of storage at 15°C. Following 3 days of storage, cells yielded a viable recovery of 86 ± 6% and a functional recovery of 80 ± 3% (Figure 8.1 A). This increase is significantly observed when compared to the control samples where there was a 1,8 ± 0.2-fold increase. Similarly, following 7 days storage, cells presented viable recovery of 68 ± 5% and functional recovery of 63 ± 2.3%, upon comparing to the control samples, a 2.3 ± 0.5-fold increase was detected (Figure 8.1 B).

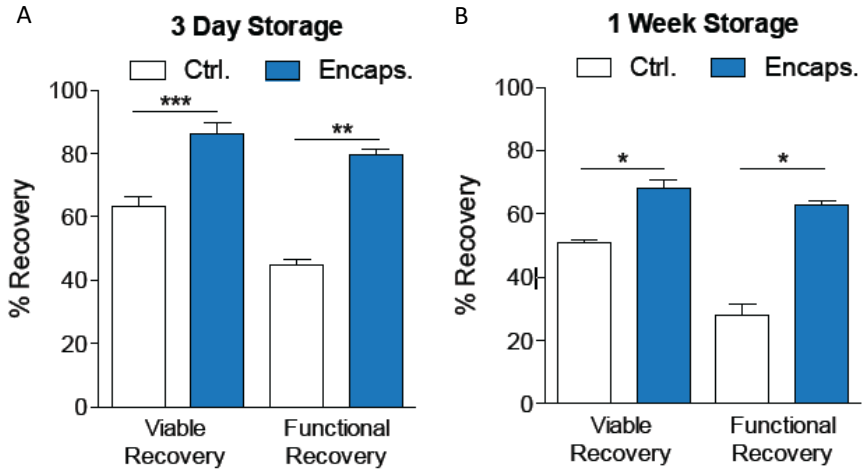

Figure 8.1 – Alginate encapsulation preserves ASCs during hypothermic storage and transport from Newcastle to London. Human ASCs were entrapped in calcium alginate (Encaps.) or in suspension (Ctrl.) for either 3 days (A) or 7 days (B) at 15°C. Data expressed as mean ± SEM of three independent repeats, asterisks represent significance between conditions (***, $p < 0.001$; **, $p < 0.01$; *, $p < 0.5$). Viable recovery, viable cells % following release; functional recovery, attachment efficiency x viable recovery. These results were compiled by Dr Stephen Swioklo, Atelerix Ltd.

8.4.2 Encapsulated ASCs suppress ocular inflammation and promote epithelial wound healing in a mouse chemical injury model

To determine the effect of encapsulated ASCs treatment on corneal chemical burn *in vivo*, we used a NSG (NOD/SCID/Gamma) mice model. Corneal limbal and

epithelial were debrided of cells via treating with 20% EtOH for 3 minutes, and either treated with gel + ASCs containing 20 x 10^6 cells/ mL (treated) or gel – ASCs (untreated control) (Figure 8.2). The corneal injury was induced on the mice's left corneas, while the right corneas served as normal controls. Corneas were harvested on day 7 following injury and were used to assess corneal epithelial layer recovery.

Corneal images taken before enucleation suggested a reduction in corneal haze measured by clinical scoring from microscopy image, in the treated group compared to the untreated groups (Figure 8.3 A). H&E staining presented a reduction in the inflammatory cells infiltration in the corneal stroma in the treated group compared to the untreated group (Figures 8.3B, 8.5, 8.6, and 8.7). Immunohistochemistry staining of anti-neutrophil antibody (NIMP-R14) supported this observation where it showed a decrease in the number of neutrophils infiltrated the cornea in the cell-treated groups (Figure 8.4A, 8.5, 8.6, and 8.7). Moreover, data suggested that the number of neutrophils shown (measured manually via calculating the number of stained neutrophils in the central and peripheral corneas) was higher in the central cornea of the untreated group compared to the treated corneas (Figure 8.4 B). Additionally, aSMA staining showed upregulation in the untreated samples compared to the ASCs treated groups (Figure 8.8). These data suggest that ASCs were able to produce therapeutic factors from within the contact lens to the wound bed.

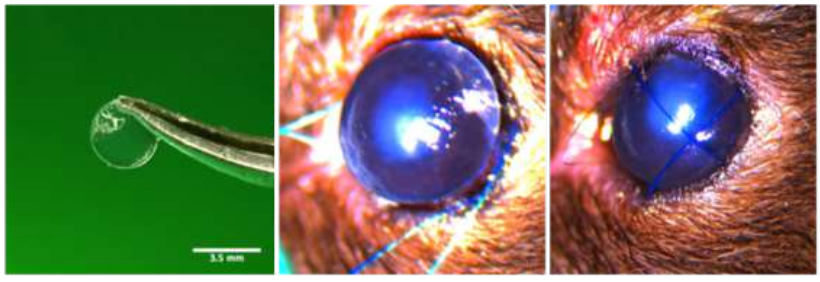

Figure 8.2 – Human ASCs bandages delivery to the ocular surface. 20 x 10^6 cells/mL were encapsulated in alginate (in an approximately 1mm thickness) and stored at 15°C for 3 days. After transport, gels were punched in a 3.5mm diameter (left) and placed directly on the ocular surface (middle) following thorough epithelial debridement and eyelids sutured (right). Scale bar = 3.5mm.

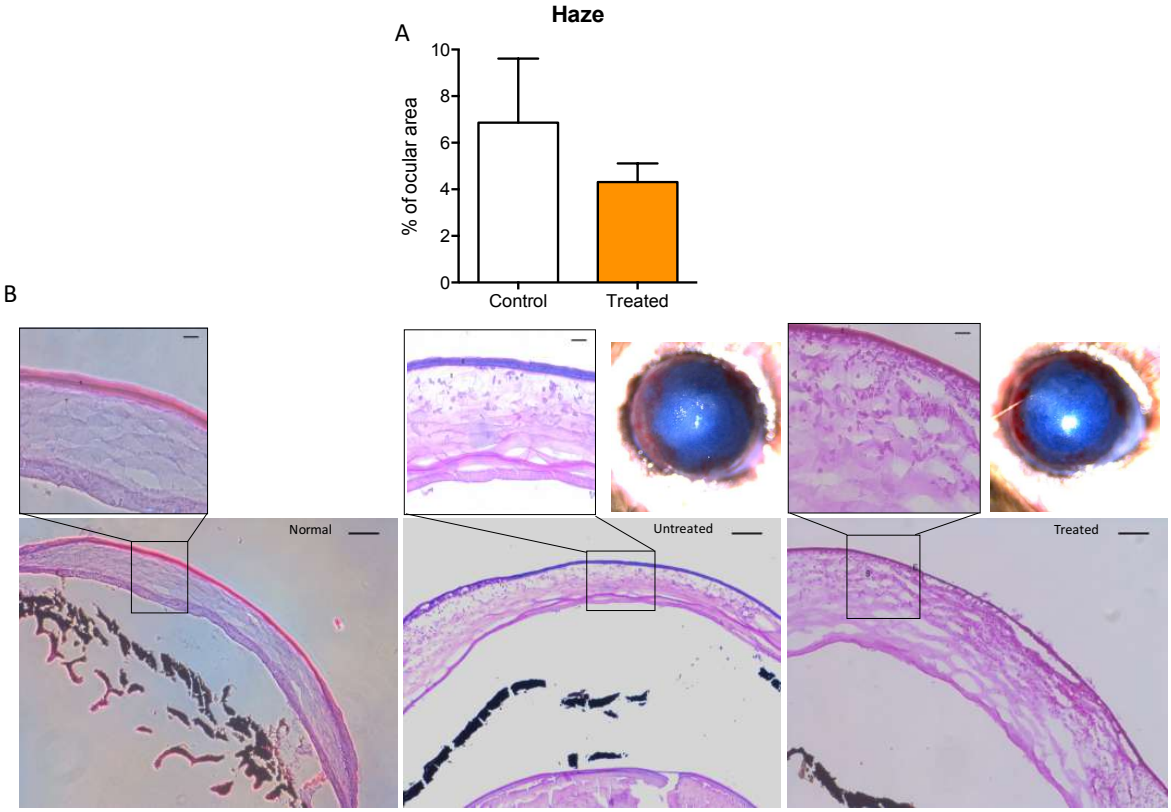

Figure 8.3 – Histological analysis of the cornea. (A) Corneal haze, and (B) H&E staining of the mouse cornea demonstrating corneal inflammation in the untreated (bandages without ASCs) mice compared to the normal (un-injured) and treated (ASCs bandages). N = 7, with 4 treated, 2 untreated and 1 normal samples. S, corneal stromal layer; E, corneal epithelial layer. Scale bar = 50μm.

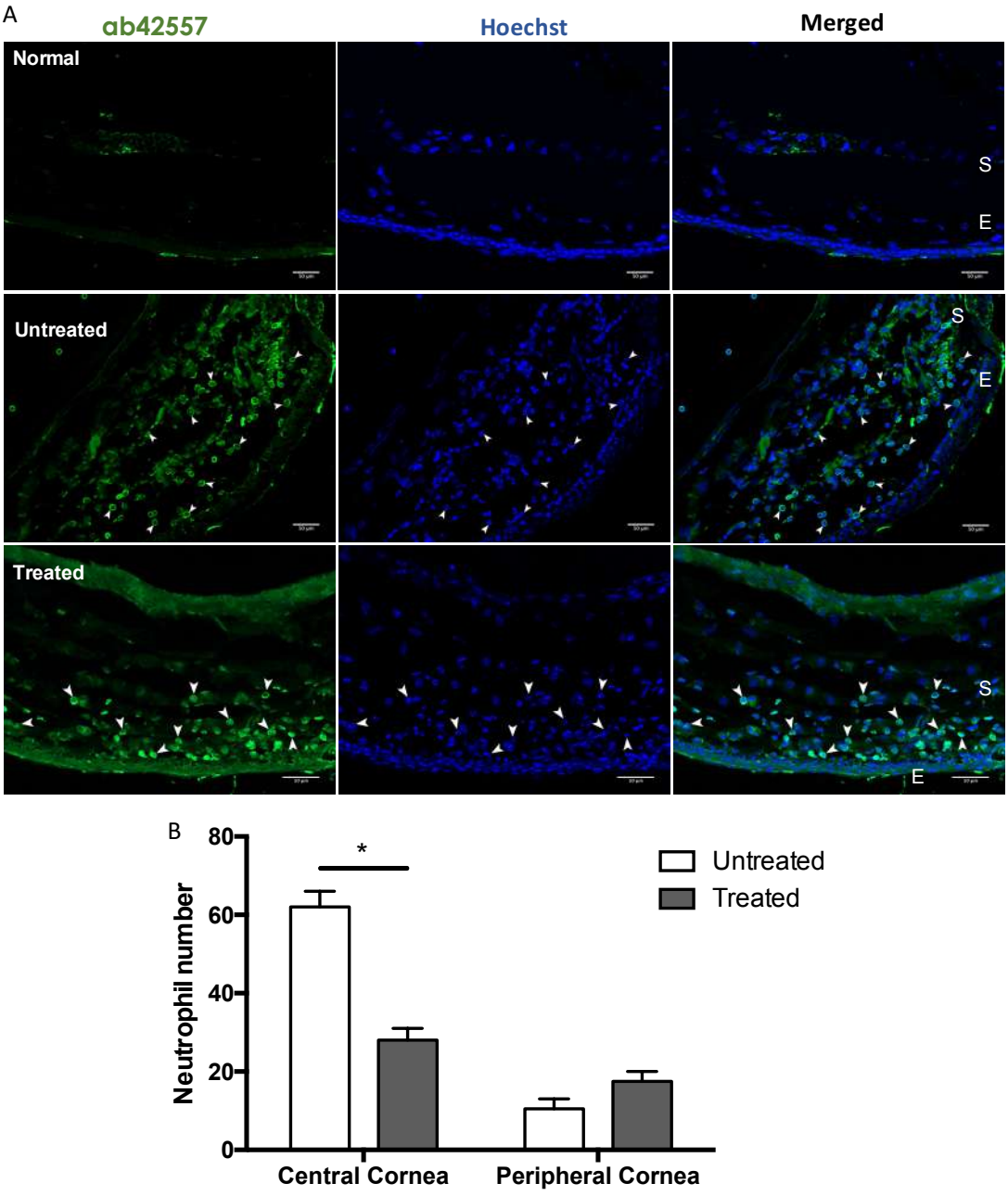

Figure 8.4 – Immunohistochemistry staining for neutrophil. (A) Images revealed intense neutrophil infiltration (arrows) in the untreated groups (bandages without cells) compared to the treated group (ASCs bandages). (B) Neutrophil number counted from the images. S, corneal stromal layer; E, corneal epithelial layer. Images taken using 40x Magnification, scale bar = 50μm.

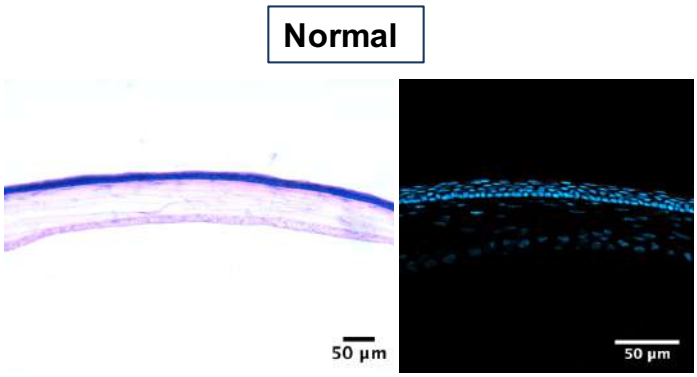

Figure 8.5 - Normal non-injured animal cornea. Data collected and processed in collaboration Dr Stephen Swioklo, Atelerix Ltd.

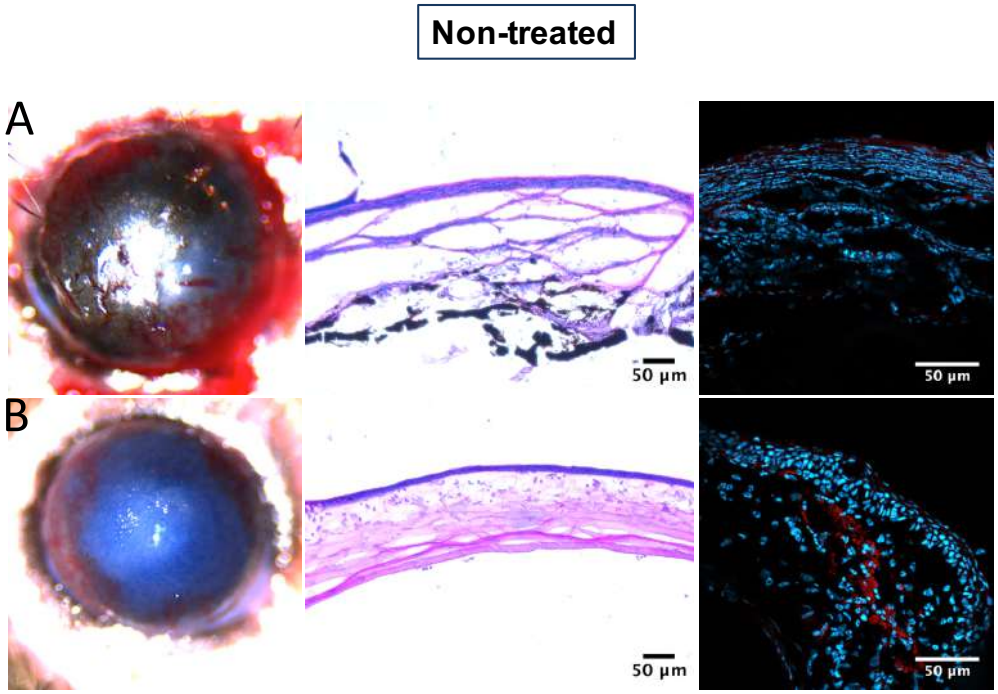

Figure 8.6 –Untreated samples, where bandages were transferred to the cornea. (A) sever injured cornea that were excluded from the study, (B) sample used for the final data processing. Data collected and processed in collaboration Dr Stephen Swioklo, Atelerix Ltd.

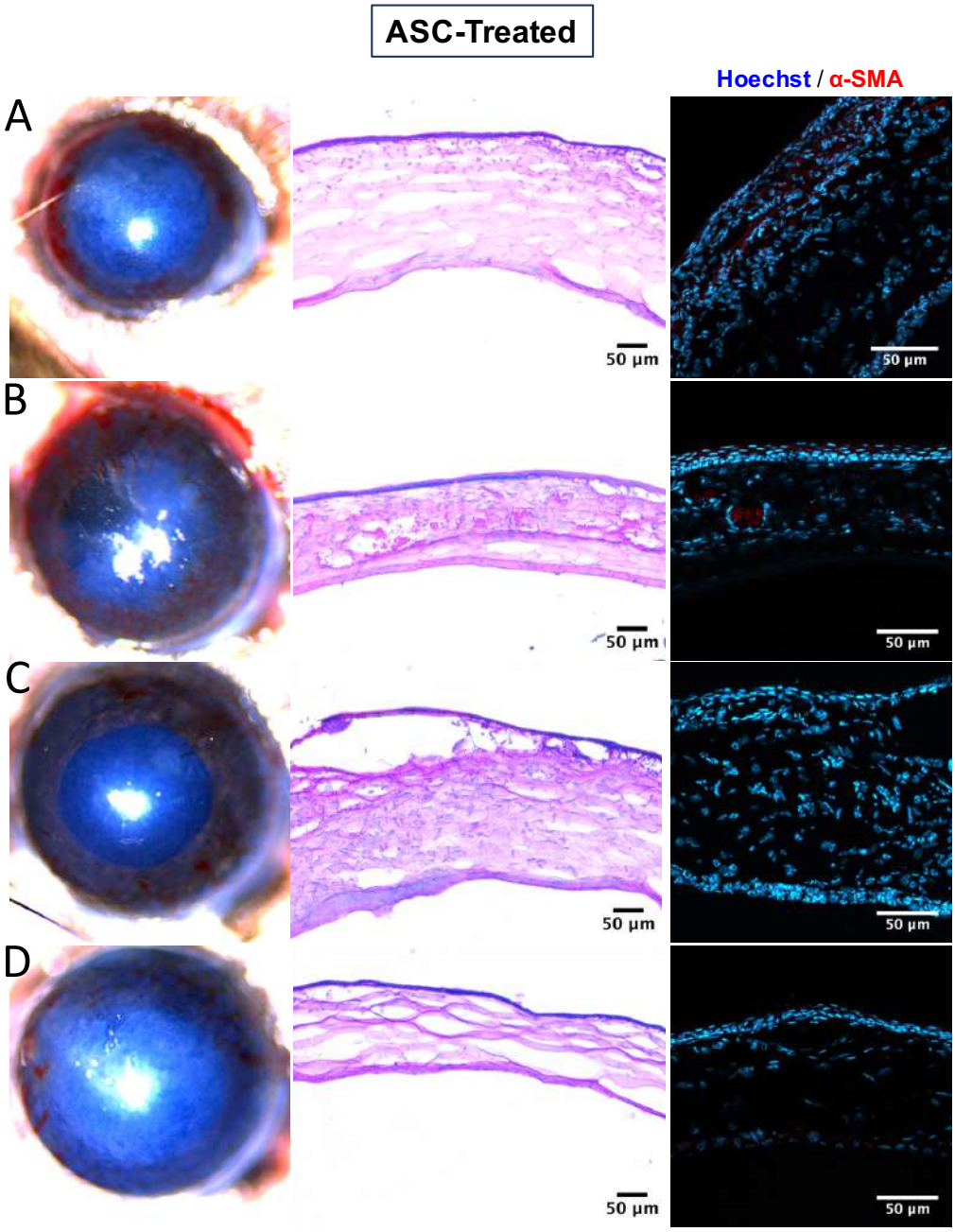

Figure 8.7 – Summary of ASCs bandages treatment. Showing 4 samples that are used in the study. Data collected and processed in collaboration Dr Stephen Swioklo, Atelerix Ltd.

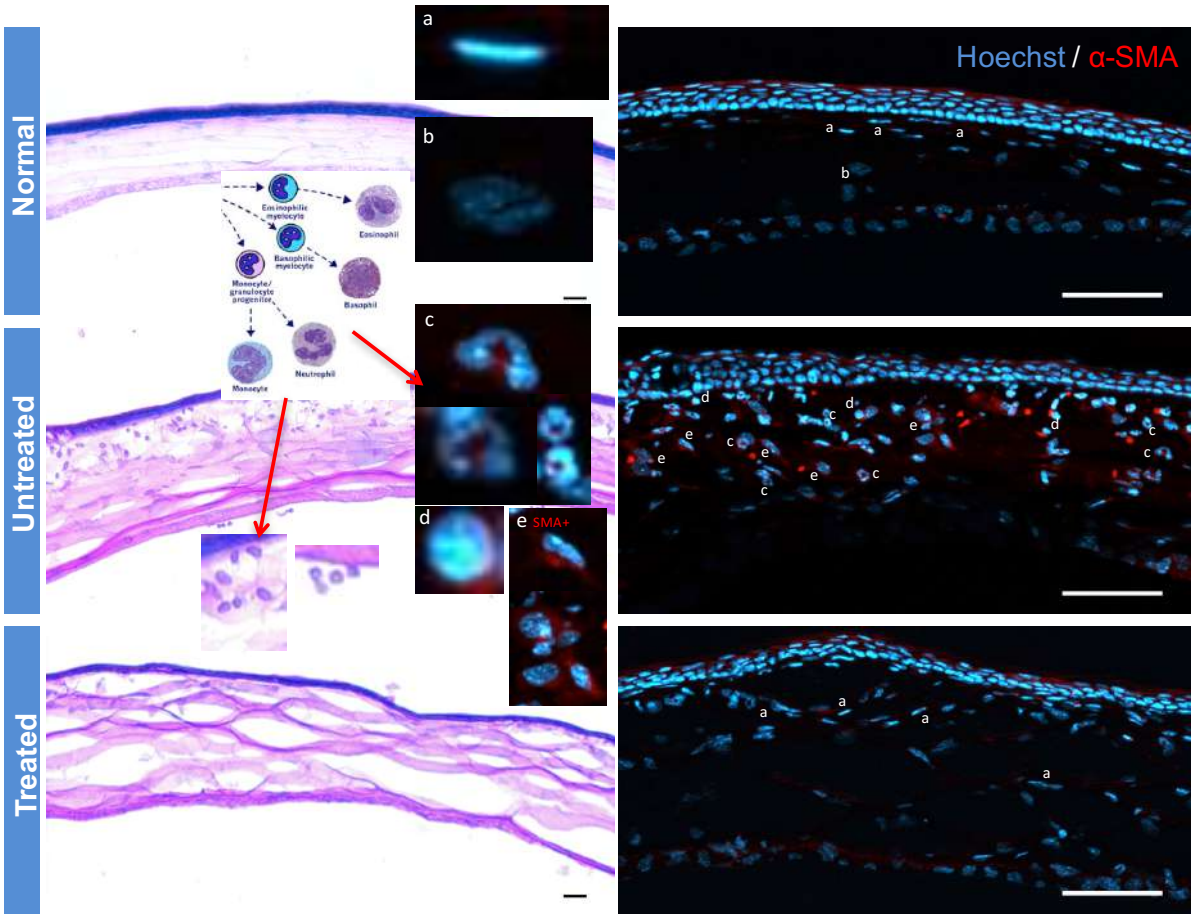

Figure 8.8 – Images showing the type of inflammatory cells infiltrating the cornea as well as a-SMA staining. (a) eosinophil, (b)basophil, (c) neutrophil, and (d) monocytes. Data collected and processed in collaboration Dr Stephen Swioklo, Atelerix Ltd.

8.5 Discussion

Insufficient corneal wound healing can lead to corneal haze, loss in transparency, and vision loss. Various growth factors have been shown to have an important role in corneal epithelial wound healing (Yu et al., 2010). In this study, we show that hypothermically stored, ASCs bandages to reduced inflammatory cells activation and infiltration, following a chemical burn, as evidenced by the higher number of neutrophils in the untreated group. While inflammation is important for normal wound repair processes, persistent and excessive inflammation could lead to complications in corneal healing (Wilson et al., 2001). The increased expression of IL-1ß and aSMA during corneal inflammation can induce corneal stromal keratocytes

apoptosis whilst metalloproteinase expression increases by the keratocytes, which leads to degradation of extracellular matrix (ECM) in the wounded cornea (Wilson et al., 1996, Girard et al., 1991, Ljubimov and Saghizadeh, 2015).

HGF is an important mitogen and motility growth factor that is expressed by corneal epithelial cells, keratocytes, and endothelial cells (Saghizadeh et al., 2005, Weng J, 1997a). Despite the important function of HGF wound healing, its full potential in corneal repair is yet to be fully understood. It has been shown that HGF not only can affect epithelial cells proliferation but also reverse the IL-1ß anti-proliferative effect *in vitro* (Omoto et al., 2017). This suggests that HGF suppresses inflammation in the cornea. Our previous results in chapter 4, showed HGF expression to increase during storage and wound healing *in vitro*. Accordingly, we expect HGF to be one of the main factors in suppressing inflammatory cell infiltration in the injured cornea. Other factors, including IGF, TGF-ß, IL-8, and KGF can also be responsible for suppressing inflammation while improving healing (Lee et al., 2015, Li and Zhao, 2016, Milner and Day, 2003).

In conclusion, the present study despite its limited power (only 4 mice studied for the treated group, 1 for the untreated and 1 for the normal group) shows that application of hypothermically stored ASCs bandages has the potential to be a therapeutic contact lens for the treatment of corneal chemical burns. These preliminary results clearly show corneal wound healing via inflammatory cell reduction. Thus, these data provide new insight into the use of ASCs as a therapeutic contact lens, which could serve as a framework in the development of future cell-based therapies for corneal injuries. Moreover, that such cell-based therapies can be driven exclusively by paracrine factors and that the therapeutic cells need not be in direct contact with the wound but can be entrapped within a hydrogel such as alginate and remain active.

Chapter 9. Conclusion and future directions

9.1 Conclusion

This thesis covers two distinct forms of work in cell therapy, focused on adipose-derived stem cells (ASCs) bandages formation and its effect on a secondary population. The first part of this research focused on the establishment of stem cell bandages comparing two types of alginates, Sigma and NovaMatrix alginates. This important development step with alginate type is a further step towards the goal of stem cell bandage formation. Combined with bandage formation methodology to establish stable bandage that maintains cell viability and functional ability, these bandages were further tested to encompass different types of cells. NovaMatrix alginate displayed stability to encompass these cells while maintaining their viability and functional ability. ASCs bandages, when used in wound healing presented an augmented therapy *in vitro.* When comparing ASCs bandages to conditioned media (CM) therapy, although no significant differences were found between the two, the bandages showed superiority in wound healing. Following this, different cell types were formed as bandages, such as human dermal fibroblasts (hDF), human corneal stromal fibroblasts (CSF), human keratoconus fibroblasts (KC), and multipotent adult progenitor stem cells (MAPC), of which, ASCs bandages presented its superiority. Additionally, hypothermic storage at 15°C displayed the best-tested temperature to store bandages. Storage is a hypoxic environment that can affect the cells positively by making them actively produce paracrine factors. These hypoxic-induced ASCs bandages were also found to reduce immune infiltration when used in an *in vivo* animal model. Thus, supporting the thesis hypothesis.

The second part concerns the testing of proteins and genes produced by the ASCs bandages following scratch healing. This was investigated on the gene level using qPCR and protein level using XL human cytokine array kit. On the gene transcription level, the bandages were shown to increase HGF and TGF-6 levels following healing, which are responsible for wound healing while reducing VEGF, IGF, aSMA, and HIF1A gene levels that are representative of hypoxia. Thus, supporting the hypothesis of storage is a hypoxic induced environment. As for the protein level, 30 different cytokines were found upregulated following wound healing of hypoxia-induced ASCs bandage. These cytokines have a different effect, such as

inflammatory cytokine IL-6, anti-inflammatory cytokine IL-8, macrophage recruitment regulator MCP-1, neutrophil chemoattractant ENA-75, extracellular matrix metalloproteinase inducer EMMPRIN, antiangiogenic factor TSP-1, etc. These factors complement each other with the aim of healing injuries. Thus, ASCs bandages improved scratch wound healing via the production of paracrine factors. These factors were shown to induce the secondary population to migrate and proliferate to close the wound area. It is hoped that some of the unanswered questions of ASCs production of paracrine factors are revealed through the use of a random cytokine array kit. Although only preliminary screening results of one repeat of each condition is described in here, experiments will be going towards the completion of more experimental repeats.

The final section of this thesis highlights the use of hypoxia-induced ASCs bandages on a chemical injury of rat cornea. The bandages were found to reduce neutrophil infiltration, however, for the lack of proper repeats and the small size of this study, no conclusive evidence could be drawn from this. It did, however, indicate that the bandages can be used as therapy if further developed and tested. To our knowledge, this combination of alginate, hypothermic storage, and ASCs has first described in this work thus it added to the literature knowledge of a possible therapeutic bandage.

9.2 Future directions

Few interesting questions were raised from this work that opened up several directions that this work can be guided to. Firstly, alginate improvement; various ways can be used to strengthen the alginate by coupling it with peptide for example, or the use of different materials, such as collagen since the cornea is mainly formed of collagen. The identification of a better material can open up further investigations into the effect and function of the material on cell encapsulation and on a secondary population.

Secondly, there are still many tests to be made on the hypothermic storage. Although hypoxia was attributed to the enhanced beneficial effect seen from the bandages, it was not explicitly tested. Thus, testing hypoxia-induced conditions, such as manipulation of oxygen levels, gene and proteins testing such as hypoxia

inducible factor-1 (HIF-1), and hypoxia response element (HRE), fibroblast growth factor 2 (FGF2), etc. will give a better indication on its effect on the bandages. It is also important to determine the effect of storage or cell recovery at different temperatures on the cells. Thus, testing cell number whilst still inside the bandages would need to be considered for future experiments using live/dead staining.

Thirdly, the future investigation into the effect of bandages on a secondary population using different types of experimental approaches, such as proliferation assay, cell staining for co-culture approach, 3D system, investigating the metabolic interactions, etc. Moreover, an interesting observation in the keratoconus (KC) data is the behavior of the cells following a certain time point where the cells started losing their morphology and detaching from the culture plate. This should be further assessed as to why cells behave this way.

Fourthly, for the animal experiments, for technical issues, only two untreated corneas were included in the results, which were vastly lacking to conclude. Thus, a better experimental design needed following further bandage development. Moreover, the bandages were not tested for the effect of transportation on cells' health and function, which can affect cell viability, thus, would need to be investigated. When ASC-therapy goes into the clinic, various points must be taken into considerations, such as MSCs source, until now there are many different sources which may ultimately give different results; type of material used in bandage formation, where synthetic materials are different from natural materials, also, the FDA must approve the use of hydrogel, which is a taxing and long process; technical challenges, method/technique used to form ASCs bandages; scale up the bandages production; regulatory challenges; clinical challenges and requirements; development cost and time consumed in production. All of these are the key stages in developing ASCs therapy and would be taken under consideration for future bandage improvement.

Finally, although data presented a promising therapy that would be effective for the patient, it would need various regulations to be translated to the clinic. Clinical trials are being conducted on the use of allogenic and autologous MSCs to cure a range of corneal diseases that are considered untreatable by conventional methods. In that regard, numerous *in vivo* studies have demonstrated great promise and potential of MSC-therapy in ocular disorders. This thesis aimed to investigate the

potential of ASCs bandages on corneal cells following hypothermic storage. this research adds to the understanding of literature the benefit of ASCs bandages and the benefit of storage in enhancing cell expression of paracrine factors. ASCs bandages forward testing can potentially lead to healing other diseases such as skin injures. Thus, with more investigations, ASCs bandages can present us with a unique future therapy. ASC-based therapy presents a unique treatment in initiating the healing process of injured tissues. This ability is directed by a succession of complex interactions between the adhesion molecules, growth factors, ECM proteins, and cytokines that are released and expressed by the ASCs. This study contributes to understanding the possible potential of ASCs stem cell bandages in corneal wound healing. Which could have direct application in the development of stem cell bandages for future clinical studies. The results shown in this thesis support the hypothesis that ASCs can be used as bandages and their beneficial effects driven by a paracrine factor mechanism generated from the immobilized cells.

Paper publication

Al-Jaibaji, O., Swioklo, S., Shortt A. Figueiredo F.C., and Connon, C. J. (2020) Hypothermically stored adipose-derived mesenchymal stromal cell alginate bandages facilitate use of paracrine molecules for corneal wound healing. International Journal of Molecular Sciences. 2020. IN SUBMISSION

Al-Jaibaji, O., Swioklo, S. and Connon, C. J. (2019) 'Mesenchymal stromal cells for ocular surface repair', *Expert Opin Biol Ther*, pp. 1-11.

Al-Jaibaji, O., Swioklo, S., Gijbels, K., Vaes, B., Figueiredo, F. C. and Connon, C. J. (2018) Alginate encapsulated multipotent adult progenitor cells promote corneal stromal cell activation via release of soluble factors. *PLoS One*, 13(9), pp. e0202118.

References

Aderibigbe, B. A. and Buyana, B. (2018) 'Alginate in Wound Dressings', *Pharmaceutics,* 10(2).

Administration, U. S. F. a. D. 'Guidance for FDA Reviewers and Sponsors: Content and Review of Chemistry, Manufacturing, and Control (CMC) Information for Human Gene Therapy Investigational New Drug Applications (INDs). Last updated April 2008. Available at http://www.fda.gov/. Accessed May 28,2015.'.

Aggarwal, S. and Pittenger, M. F. (2005) 'Human mesenchymal stem cells modulate allogeneic immune cell responses', *Blood,* 105(4), pp. 1815-22.

Ahmad, S., Osei-Bempong, C., Dana, R. and Jurkunas, U. (2010) 'The culture and transplantation of human limbal stem cells', *J Cell Physiol,* 225(1), pp. 15-9.

Al-Jaibaji, O., Swioklo, S. and Connon, C. J. (2019) 'Mesenchymal stromal cells for ocular surface repair', *Expert Opin Biol Ther*, pp. 1-11.

Alio Del Barrio, J. L. and Alio, J. L. (2018) 'Cellular therapy of the corneal stroma: a new type of corneal surgery for keratoconus and corneal dystrophies', *Eye Vis (Lond),* 5, pp. 28.

Alio del Barrio, J. L., Chiesa, M., Garagorri, N., Garcia-Urquia, N., Fernandez-Delgado, J., Bataille, L., Rodriguez, A., Arnalich-Montiel, F., Zarnowski, T., Alvarez de Toledo, J. P., Alio, J. L. and De Miguel, M. P. (2015) 'Acellular human corneal matrix sheets seeded with human adipose-derived mesenchymal stem cells integrate functionally in an experimental animal model', *Experimental eye research,* 132, pp. 91-100.

Alio Del Barrio, J. L., El Zarif, M., de Miguel, M. P., Azaar, A., Makdissy, N., Harb, W., El Achkar, I., Arnalich-Montiel, F. and Alio, J. L. (2017) 'Cellular Therapy With Human Autologous Adipose-Derived Adult Stem Cells for Advanced Keratoconus', *Cornea,* 36(8), pp. 952-960.

Alio, J. L., Alio Del Barrio, J. L., El Zarif, M., Azaar, A., Makdissy, N., Khalil, C., Harb, W., El Achkar, I., Jawad, Z. A. and De Miguel, M. P. (2019) 'Regenerative Surgery of the Corneal Stroma for Advanced Keratoconus: 1-Year Outcomes', *Am J Ophthalmol,* 203, pp. 53-68.

Alio, J. L., Shah, S., Barraquer, C., Bilgihan, K., Anwar, M. and Melles, G. R. (2002) 'New techniques in lamellar keratoplasty', *Curr Opin Ophthalmol,* 13(4), pp. 224-9.

Almaliotis, D., Koliakos, G., Papakonstantinou, E., Komnenou, A., Thomas, A., Petrakis, S., Nakos, I., Gounari, E. and Karampatakis, V. (2015) 'Mesenchymal stem cells improve

healing of the cornea after alkali injury', *Graefe's Archive for Clinical and Experimental Ophthalmology,* 253(7), pp. 1121-1135.

Alstrup, T., Eijken, M., Bohn, A. B., Moller, B. and Damsgaard, T. E. (2019) 'Isolation of Adipose Tissue-Derived Stem Cells: Enzymatic Digestion in Combination with Mechanical Distortion to Increase Adipose Tissue-Derived Stem Cell Yield from Human Aspirated Fat', *Curr Protoc Stem Cell Biol,* 48(1), pp. e68.

Aluri, H. S., Samizadeh, M., Edman, M. C., Hawley, D. R., Armaos, H. L., Janga, S. R., Meng, Z., Sendra, V. G., Hamrah, P., Kublin, C. L., Hamm-Alvarez, S. F. and Zoukhri, D. (2017) 'Delivery of Bone Marrow-Derived Mesenchymal Stem Cells Improves Tear Production in a Mouse Model of Sj?gren?s Syndrome', *Stem cells international,* 2017, pp. 1-10.

Anderson, R. A. (1977) 'Actin filaments in normal and migrating corneal epithelial cells', *Invest Ophthalmol Vis Sci,* 16(2), pp. 161-6.

Angel, S., von Briesen, H., Oh, Y. J., Baller, M. K., Zimmermann, H. and Germann, A. (2016) 'Toward Optimal Cryopreservation and Storage for Achievement of High Cell Recovery and Maintenance of Cell Viability and T Cell Functionality', *Biopreserv Biobank,* 14(6), pp. 539-547.

Anwar, M. and Teichmann, K. D. (2002) 'Big-bubble technique to bare Descemet's membrane in anterior lamellar keratoplasty', *J Cataract Refract Surg,* 28(3), pp. 398-403.

Aranguren, X. L., Pelacho, B., Penuelas, I., Abizanda, G., Uriz, M., Ecay, M., Collantaes, M., Arana, M., Beerens, M., Coppiello, G., Prieto, I., Perez-Ilzarbe, M., Andreu, E. J., Luttun, A. and Prosper, F. (2011) 'MAPC transplantation confers a more durable benefit than AC133+ cell transplantation in severe hind limb ischemia', *Cell Transplant,* 20(2), pp. 259-69.

Arnalich-Montiel, F., Pastor, S., Blazquez-Martinez, A., Fernandez-Delgado, J., Nistal, M., Alio, J. L. and De Miguel, M. P. (2008) 'Adipose-derived stem cells are a source for cell therapy of the corneal stroma', *Stem Cells,* 26(2), pp. 570-9.

Ashimova, A., Yegorov, S., Negmetzhanov, B. and Hortelano, G. (2019) 'Cell Encapsulation Within Alginate Microcapsules: Immunological Challenges and Outlook', *Front Bioeng Biotechnol,* 7, pp. 380.

Augst, A. D., Kong, H. J. and Mooney, D. J. (2006) 'Alginate hydrogels as biomaterials', *Macromol Biosci,* 6(8), pp. 623-33.

Augusteyn, R. C. (2004) 'alpha-crystallin: a review of its structure and function', *Clin Exp Optom,* 87(6), pp. 356-66.

Auran, J. D., Koester, C. J., Kleiman, N. J., Rapaport, R., Bomann, J. S., Wirotsko, B. M., Florakis, G. J. and Koniarek, J. P. (1995) 'Scanning Slit Confocal Microscopic Observation of Cell Morphology and Movement within the Normal Human Anterior Cornea', *Ophthalmology,* 102(1), pp. 33-41.

Balasubramanian, S. A., Mohan, S., Pye, D. C. and Willcox, M. D. P. (2012) 'Proteases, proteolysis and inflammatory molecules in the tears of people with keratoconus', *Acta Ophthalmologica,* 90(4), pp. e303-e309.

Baradaran-Rafii, A., Eslani, M., Sadoughi, M. M., Esfandiari, H. and Karimian, F. (2013) 'Anwar versus Melles deep anterior lamellar keratoplasty for keratoconus: a prospective randomized clinical trial', *Ophthalmology,* 120(2), pp. 252-9.

Barbosa, F. L., Chaurasia, S. S., Kaur, H., de Medeiros, F. W., Agrawal, V. and Wilson, S. E. (2010) 'Stromal interleukin-1 expression in the cornea after haze-associated injury', *Exp Eye Res,* 91(3), pp. 456-61.

Basu, S., Hertsenberg, A. J., Funderburgh, M. L., Burrow, M. K., Mann, M. M., Du, Y., Lathrop, K. L., Syed-Picard, F. N., Adams, S. M., Birk, D. E. and Funderburgh, J. L. (2014) 'Human limbal biopsy-derived stromal stem cells prevent corneal scarring', *Science translational medicine,* 6(266), pp. 266ra172.

Bawazeer, A. M., Hodge, W. G. and Lorimer, B. (2000) 'Atopy and keratoconus: a multivariate analysis', *Br J Ophthalmol,* 84(8), pp. 834-6.

Beales, M. P., Funderburgh, J. L., Jester, J. V. and Hassell, J. R. (1999) 'Proteoglycan synthesis by bovine keratocytes and corneal fibroblasts: maintenance of the keratocyte phenotype in culture', *Invest Ophthalmol Vis Sci,* 40(8), pp. 1658-63.

Bidarra, S. J., Barrias, C. C. and Granja, P. L. (2014) 'Injectable alginate hydrogels for cell delivery in tissue engineering', *Acta Biomater,* 10(4), pp. 1646-62.

Bizrah, M., Yusuf, A. and Ahmad, S. (2019a) 'Adherence to Treatment and Follow-Up in Patients with Severe Chemical Eye Burns', *Ophthalmol Ther,* 8(2), pp. 251-259.

Bizrah, M., Yusuf, A. and Ahmad, S. (2019b) 'An update on chemical eye burns', *Eye (Lond),* 33(9), pp. 1362-1377.

Bochenek, M. A., Veiseh, O., Vegas, A. J., McGarrigle, J. J., Qi, M., Marchese, E., Omami, M., Doloff, J. C., Mendoza-Elias, J., Nourmohammadzadeh, M., Khan, A., Yeh, C. C., Xing, Y., Isa, D., Ghani, S., Li, J., Landry, C., Bader, A. R., Olejnik, K., Chen, M., Hollister-Lock, J., Wang, Y., Greiner, D. L., Weir, G. C., Strand, B. L., Rokstad,

A. M. A., Lacik, I., Langer, R., Anderson, D. G. and Oberholzer, J. (2018) 'Alginate encapsulation as long-term immune protection of allogeneic pancreatic islet cells transplanted into the omental bursa of macaques', *Nat Biomed Eng,* 2(11), pp. 810-821.

Bohari, S. P., Hukins, D. W. and Grover, L. M. (2011) 'Effect of calcium alginate concentration on viability and proliferation of encapsulated fibroblasts', *Biomed Mater Eng,* 21(3), pp. 159-70.

Boomsma, R. A. and Geenen, D. L. (2012) 'Mesenchymal stem cells secrete multiple cytokines that promote angiogenesis and have contrasting effects on chemotaxis and apoptosis', *PLoS One,* 7(4), pp. e35685.

Boozer, S., Lehman, N., Lakshmipathy, U., Love, B., Raber, A., Maitra, A., Deans, R., Rao, M. S. and Ting, A. E. (2009) 'Global Characterization and Genomic Stability of Human MultiStem, A Multipotent Adult Progenitor Cell', *J Stem Cells,* 4(1), pp. 17-28.

Bor, S., Kalkan, I. H., Celebi, A., Dincer, D., Akyuz, F., Dettmar, P. and Ozen, H. (2019) 'Alginates: From the ocean to gastroesophageal reflux disease treatment', *Turk J Gastroenterol,* 30(Suppl2), pp. 109-136.

Bouchard, C. S. and John, T. (2004) 'Amniotic membrane transplantation in the management of severe ocular surface disease: indications and outcomes', *Ocul Surf,* 2(3), pp. 201-11.

Branch, M. J., Hashmani, K., Dhillon, P., Jones, D. R. E., Dua, H. S. and Hopkinson, A. (2012) 'Mesenchymal Stem Cells in the Human Corneal Limbal Stroma', *Investigative Opthalmology & Visual Science,* 53, pp. 5109-16.

Bray, L. J., Heazlewood, C. F., Munster, D. J., Hutmacher, D. W., Atkinson, K. and Harkin, D. G. (2014) 'Immunosuppressive properties of mesenchymal stromal cell cultures derived from the limbus of human and rabbit corneas', *Cytotherapy,* 16(1), pp. 64-73.

Brewitt, H. (2009) 'Sliding of Epithelium in Experimental Corneal Wounds', *Acta Ophthalmologica,* 57(6), pp. 945-958.

Brown, C. T., Nugent, M. A., Lau, F. W. and Trinkaus-Randall, V. (1999) 'Characterization of proteoglycans synthesized by cultured corneal fibroblasts in response to transforming growth factor beta and fetal calf serum', *J Biol Chem,* 274(11), pp. 7111-9.

Buck, R. C. (1985) 'Measurement of centripetal migration of normal corneal epithelial cells in the mouse', *Invest Ophthalmol Vis Sci,* 26(9), pp. 1296-9.

Buhring, H. J., Battula, V. L., Treml, S., Schewe, B., Kanz, L. and Vogel, W. (2007) 'Novel markers for the prospective isolation of human MSC', *Ann N Y Acad Sci,* 1106, pp. 262-71.

Bunnell, B. A., Flaat, M., Gagliardi, C., Patel, B. and Ripoll, C. (2008) 'Adipose-derived stem cells: isolation, expansion and differentiation', *Methods,* 45(2), pp. 115-20.

Caliari, S. R. and Burdick, J. A. (2016) 'A practical guide to hydrogels for cell culture', *Nat Methods,* 13(5), pp. 405-14.

Carty, F., Corbett, J. M., Cunha, J., Reading, J. L., Tree, T. I. M., Ting, A. E., Stubblefield, S. R. and English, K. (2018) 'Multipotent Adult Progenitor Cells Suppress T Cell Activation in In Vivo Models of Homeostatic Proliferation in a Prostaglandin E2-Dependent Manner', *Front Immunol,* 9, pp. 645.

Cejka, C., Cejkova, J., Trosan, P., Zajicova, A., Sykova, E. and Holan, V. (2016) 'Transfer of mesenchymal stem cells and cyclosporine A on alkali-injured rabbit cornea using nanofiber scaffolds strongly reduces corneal neovascularization and scar formation.', *Histology and histopathology*, pp. 11724.

Cejkova, J., Olmiere, C., Cejka, C., Trosan, P. and Holan, V. (2014) 'The healing of alkali-injured cornea is stimulated by a novel matrix regenerating agent (RGTA, CACICOL20): a biopolymer mimicking heparan sulfates reducing proteolytic, oxidative and nitrosative damage.', *Histology and histopathology,* 29, pp. 457-78.

Cejkova, J., Trosan, P., Cejka, C., Lencova, A., Zajicova, A., Javorkova, E., Kubinova, S., Sykova, E. and Holan, V. (2013) 'Suppression of alkali-induced oxidative injury in the cornea by mesenchymal stem cells growing on nanofiber scaffolds and transferred onto the damaged corneal surface', *Experimental Eye Research,* 116, pp. 312-323.

Cesselli, D., Beltrami, A. P., Rigo, S., Bergamin, N., D'Aurizio, F., Verardo, R., Piazza, S., Klaric, E., Fanin, R., Toffoletto, B., Marzinotto, S., Mariuzzi, L., Finato, N., Pandolfi, M., Leri, A., Schneider, C., Beltrami, C. A. and Anversa, P. (2009) 'Multipotent progenitor cells are present in human peripheral blood', *Circ Res,* 104(10), pp. 1225-34.

Cha, J. and Falanga, V. (2007) 'Stem cells in cutaneous wound healing', *Clin Dermatol,* 25(1), pp. 73-8.

Chai, Q., Jiao, Y. and Yu, X. (2017) 'Hydrogels for Biomedical Applications: Their Characteristics and the Mechanisms behind Them', *Gels,* 3(1), pp. 6.

Chakravarti, S., Magnuson, T., Lass, J. H., Jepsen, K. J., LaMantia, C. and Carroll, H. (1998) 'Lumican regulates collagen fibril assembly: skin fragility and corneal opacity in the absence of lumican', *J Cell Biol,* 141(5), pp. 1277-86.

Chang, J. H., Garg, N. K., Lunde, E., Han, K. Y., Jain, S. and Azar, D. T. (2012) 'Corneal neovascularization: an anti-VEGF therapy review', *Surv Ophthalmol,* 57(5), pp. 415-29.

Chavakis, E., Urbich, C. and Dimmeler, S. (2008) 'Homing and engraftment of progenitor cells: A prerequisite for cell therapy', *Journal of Molecular and Cellular Cardiology,* 45, pp. 514-522.

Chen, B., Wright, B., Sahoo, R. and Connon, C. J. (2013) 'A novel alternative to cryopreservation for the short-term storage of stem cells for use in cell therapy using alginate encapsulation.', *Tissue engineering. Part C, Methods,* 19, pp. 568-76.

Chen, H. C., Yeh, L. K., Tsai, Y. J., Lai, C. H., Chen, C. C., Lai, J. Y., Sun, C. C., Chang, G., Hwang, T. L., Chen, J. K. and Ma, D. H. (2012) 'Expression of angiogenesis-related factors in human corneas after cultivated oral mucosal epithelial transplantation', *Invest Ophthalmol Vis Sci,* 53(9), pp. 5615-23.

Chen, L., Tredget, E. E., Wu, P. Y. and Wu, Y. (2008) 'Paracrine factors of mesenchymal stem cells recruit macrophages and endothelial lineage cells and enhance wound healing', *PLoS One,* 3(4), pp. e1886.

Chen, L., Xu, Y., Zhao, J., Zhang, Z., Yang, R., Xie, J., Liu, X. and Qi, S. (2014) 'Conditioned medium from hypoxic bone marrow-derived mesenchymal stem cells enhances wound healing in mice', *PLoS One,* 9(4), pp. e96161.

Chu, D. T., Nguyen Thi Phuong, T., Tien, N. L. B., Tran, D. K., Minh, L. B., Thanh, V. V., Gia Anh, P., Pham, V. H. and Thi Nga, V. (2019) 'Adipose Tissue Stem Cells for Therapy: An Update on the Progress of Isolation, Culture, Storage, and Clinical Application', *J Clin Med,* 8(7).

Chung, H. M., Won, C. H. and Sung, J. H. (2009) 'Responses of adipose-derived stem cells during hypoxia: enhanced skin-regenerative potential', *Expert Opin Biol Ther,* 9(12), pp. 1499-508.

Clare, G., Suleman, H., Bunce, C. and Dua, H. (2012) 'Amniotic membrane transplantation for acute ocular burns.', *The Cochrane database of systematic reviews*, pp. CD009379.

Colwell, A. S., Beanes, S. R., Soo, C., Dang, C., Ting, K., Longaker, M. T., Atkinson, J. B. and Lorenz, H. P. (2005) 'Increased angiogenesis and expression of vascular

endothelial growth factor during scarless repair', *Plast Reconstr Surg,* 115(1), pp. 204-12.

Cong, Z., Shi, Y., Wang, Y., Wang, Y., Niu, J. e., Chen, N. and Xue, H. (2017) 'A novel controlled drug delivery system based on alginate hydrogel/chitosan micelle composites.', *International journal of biological macromolecules*.

Connon, C. J., Siegler, V., Meek, K. M., Hodson, S. A., Caterson, B., Kinoshita, S. and Quantock, A. J. (2003) 'Proteoglycan alterations and collagen reorganisation in the secondary avian cornea during development', *Ophthalmic Res,* 35(4), pp. 177-84.

Coopman, K. and Medcalf, N. (2014) 'From production to patient: challenges and approaches for delivering cell therapies', *StemBook,* (1-11).

Cory, G. (2011) 'Scratch-wound assay', *Methods Mol Biol,* 769, pp. 25-30.

Cotsarelis, G., Cheng, S.-Z., Dong, G., Sun, T.-T. and Lavker, R. M. (1989) 'Existence of slow-cycling limbal epithelial basal cells that can be preferentially stimulated to proliferate: Implications on epithelial stem cells', *Cell,* 57(2), pp. 201-209.

Crabbè, M. A. E., Gijbels, K., Visser, A., Craeye, D., Walbers, S., Pinxteren, J., Deans, R. J., Annaert, W. and Vaes, B. L. T. (2016) 'Using miRNA-mRNA Interaction Analysis to Link Biologically Relevant miRNAs to Stem Cell Identity Testing for Next-Generation Culturing Development', *Stem Cells Translational Medicine,* 5(6), pp. 709-722.

Crosson, C. E., Klyce, S. D. and Beuerman, R. W. (1986) 'Epithelial wound closure in the rabbit cornea. A biphasic process', *Invest Ophthalmol Vis Sci,* 27(4), pp. 464-73.

da Silva Meirelles, L., Chagastelles, P. C. and Nardi, N. B. (2006) 'Mesenchymal stem cells reside in virtually all post-natal organs and tissues', *J Cell Sci,* 119(Pt 11), pp. 2204-13.

Dapson, R., Fagan, C., Kiernan, J. and Wickersham, T. (2011) 'Certification procedures for sirius red F3B (CI 35780, Direct red 80)', *Biotechnic & Histochemistry,* 86, pp. 133-139.

Dash, B. C., Xu, Z., Lin, L., Koo, A., Ndon, S., Berthiaume, F., Dardik, A. and Hsia, H. (2018) 'Stem Cells and Engineered Scaffolds for Regenerative Wound Healing', *Bioengineering (Basel),* 5(1).

DelMonte, D. W. and Kim, T. (2011) 'Anatomy and physiology of the cornea', *J Cataract Refract Surg,* 37(3), pp. 588-98.

Deng, M., Chen, W. L., Takatori, A., Peng, Z., Zhang, L., Mongan, M., Parthasarathy, R., Sartor, M., Miller, M., Yang, J., Su, B., Kao, W. W. and Xia, Y. (2006) 'A role for the

mitogen-activated protein kinase kinase kinase 1 in epithelial wound healing', *Mol Biol Cell,* 17(8), pp. 3446-55.

Devarajan, K., Ong, H. S., Lwin, N. C., Chua, J., Schmetterer, L., Mehta, J. S. and Ang, M. (2019) 'Optical Coherence Tomography Angiography Imaging to monitor Anti-VEGF treatment of Corneal Vascularization in a Rabbit Model', *Sci Rep,* 9(1), pp. 17576.

Devine, R. D., Sekhri, P. and Behbehani, G. K. (2018) 'Effect of storage time and temperature on cell cycle analysis by mass cytometry', *Cytometry A,* 93(11), pp. 1141-1149.

Di, G., Du, X., Qi, X., Zhao, X., Duan, H., Li, S., Xie, L. and Zhou, Q. (2017) 'Mesenchymal Stem Cells Promote Diabetic Corneal Epithelial Wound Healing Through TSG-6-Dependent Stem Cell Activation and Macrophage Switch', *Invest Ophthalmol Vis Sci,* 58(10), pp. 4344-4354.

Dominici, M., Le Blanc, K., Mueller, I., Slaper-Cortenbach, I., Marini, F. C., Krause, D. S., Deans, R. J., Keating, A., Prockop, D. J. and Horwitz, E. M. (2006) 'Minimal criteria for defining multipotent mesenchymal stromal cells. The International Society for Cellular Therapy position statement', *Cytotherapy,* 8, pp. 315-317.

Dong, L. H., Jiang, Y. Y., Liu, Y. J., Cui, S., Xia, C. C., Qu, C., Jiang, X., Qu, Y. Q., Chang, P. Y. and Liu, F. (2015) 'The anti-fibrotic effects of mesenchymal stem cells on irradiated lungs via stimulating endogenous secretion of HGF and PGE2', *Sci Rep,* 5, pp. 8713.

Dong, Y., Peng, H. and Lavker, R. M. (2018) 'Emerging Therapeutic Strategies for Limbal Stem Cell Deficiency', *J Ophthalmol,* 2018, pp. 7894647.

Dowling, P. and Clynes, M. (2011) 'Conditioned media from cell lines: a complementary model to clinical specimens for the discovery of disease-specific biomarkers', *Proteomics,* 11(4), pp. 794-804.

Dua, H. S., Faraj, L. A., Said, D. G., Gray, T. and Lowe, J. (2013) 'Human corneal anatomy redefined: a novel pre-Descemet's layer (Dua's layer)', *Ophthalmology,* 120(9), pp. 1778-85.

Dua, H. S. and Forrester, J. V. (1987) 'Clinical patterns of corneal epithelial wound healing', *Am J Ophthalmol,* 104(5), pp. 481-9.

Dua, H. S., Miri, A., Elalfy, M. S., Lencova, A. and Said, D. G. (2017) 'Amnion-assisted conjunctival epithelial redirection in limbal stem cell grafting', *Br J Ophthalmol,* 101(7), pp. 913-919.

Dua, H. S. and Said, D. G. (2016) 'Clinical evidence of the pre-Descemets layer (Dua's layer) in corneal pathology', *Eye (Lond),* 30(8), pp. 1144-5.

Dua, H. S., Watson, N. J., Mathur, R. M. and Forrester, J. V. (1993) 'Corneal epithelial cell migration in humans: 'hurricane and blizzard keratopathy'', *Eye (Lond),* 7 (Pt 1), pp. 53-8.

Duran, J. M., Makarewich, C. A., Sharp, T. E., Starosta, T., Zhu, F., Hoffman, N. E., Chiba, Y., Madesh, M., Berretta, R. M., Kubo, H. and Houser, S. R. (2013) 'Bone-derived stem cells repair the heart after myocardial infarction through transdifferentiation and paracrine signaling mechanisms', *Circ Res,* 113(5), pp. 539-52.

Dzobo, K., Thomford, N. E., Senthebane, D. A., Shipanga, H., Rowe, A., Dandara, C., Pillay, M. and Motaung, K. (2018) 'Advances in Regenerative Medicine and Tissue Engineering: Innovation and Transformation of Medicine', *Stem Cells Int,* 2018, pp. 2495848.

Eslani, M., Putra, I., Shen, X., Hamouie, J., Afsharkhamseh, N., Besharat, S., Rosenblatt, M. I., Dana, R., Hematti, P. and Djalilian, A. R. (2017) 'Corneal Mesenchymal Stromal Cells Are Directly Antiangiogenic via PEDF and sFLT-1', *Invest Ophthalmol Vis Sci,* 58(12), pp. 5507-5517.

Eslani, M., Putra, I., Shen, X., Hamouie, J., Tadepalli, A., Anwar, K. N., Kink, J. A., Ghassemi, S., Agnihotri, G., Reshetylo, S., Mashaghi, A., Dana, R., Hematti, P. and Djalilian, A. R. (2018) 'Cornea-Derived Mesenchymal Stromal Cells Therapeutically Modulate Macrophage Immunophenotype and Angiogenic Function', *Stem Cells,* 36(5), pp. 775-784.

Espandar, L., Bunnell, B., Wang, G. Y., Gregory, P., McBride, C. and Moshirfar, M. (2012) 'Adipose-derived stem cells on hyaluronic acid-derived scaffold: a new horizon in bioengineered cornea', *Arch Ophthalmol,* 130(2), pp. 202-8.

Etienne-Manneville, S. (2008) 'Polarity proteins in migration and invasion', *Oncogene,* 27(55), pp. 6970-80.

Fabre, E. J., Bureau, J., Pouliquen, Y. and Lorans, G. (2009) 'Binding sites for human interleukin 1 α, gamma interferon and tumor necrosis factor on cultured fibroblasts of normal cornea and keratoconus', *Current Eye Research,* 10(7), pp. 585-592.

Fares, U., Otri, A. M., Al-Aqaba, M. A. and Dua, H. S. (2012) 'Correlation of central and peripheral corneal thickness in healthy corneas', *Cont Lens Anterior Eye,* 35(1), pp. 39-45.

Fea, A., Bosone, A., Rolle, T. and Grignolo, F. M. (2008) 'Eye injuries in an Italian urban population: report of 10,620 cases admitted to an eye emergency department in Torino', *Graefes Arch Clin Exp Ophthalmol,* 246(2), pp. 175-9.

Feizi, S., Jafarinasab, M. R., Karimian, F., Hasanpour, H. and Masudi, A. (2014) 'Central and peripheral corneal thickness measurement in normal and keratoconic eyes using three corneal pachymeters', *J Ophthalmic Vis Res,* 9(3), pp. 296-304.

Fernandes-Cunha, G. M., Na, K. S., Putra, I., Lee, H. J., Hull, S., Cheng, Y. C., Blanco, I. J., Eslani, M., Djalilian, A. R. and Myung, D. (2019) 'Corneal Wound Healing Effects of Mesenchymal Stem Cell Secretome Delivered Within a Viscoelastic Gel Carrier', *Stem Cells Transl Med,* 8(5), pp. 478-489.

Fernandez-Buenaga, R., Aiello, F., Zaher, S. S., Grixti, A. and Ahmad, S. (2018) 'Twenty years of limbal epithelial therapy: an update on managing limbal stem cell deficiency', *BMJ Open Ophthalmol,* 3(1), pp. e000164.

Ferrara, N., Gerber, H. P. and LeCouter, J. (2003) 'The biology of VEGF and its receptors', *Nat Med,* 9(6), pp. 669-76.

Figueiredo, F. C., Hodge, R., Figueiredo, M. S. and Johnson, R. (2004) 'Newcastle Corneal Transplant Registry: five–year clinical outcomes', *Investigative Ophthalmology & Visual Science,* 45(13), pp. 2911.

Fillmore, R. A., Nelson, S. E., Lausch, R. N. and Oakes, J. E. (2003) 'Differential regulation of ENA-78 and GCP-2 gene expression in human corneal keratocytes and epithelial cells', *Invest Ophthalmol Vis Sci,* 44(8), pp. 3432-7.

Fini, M. E. and Stramer, B. M. (2005) 'How the cornea heals: cornea-specific repair mechanisms affecting surgical outcomes.', *Cornea,* 24, pp. S2-2S11.

Fischer, A. H., Jacobson, K. A., Rose, J. and Zeller, R. (2008) 'Hematoxylin and eosin staining of tissue and cell sections', *CSH Protoc,* 2008, pp. pdb prot4986.

Fish, R. and Davidson, R. S. (2010) 'Management of ocular thermal and chemical injuries, including amniotic membrane therapy', *Curr Opin Ophthalmol,* 21(4), pp. 317-21.

Foster, J. W., Gouveia, R. M. and Connon, C. J. (2015) 'Low-glucose enhances keratocyte-characteristic phenotype from corneal stromal cells in serum-free conditions', *Sci Rep,* 5, pp. 10839.

Foster, J. W., Jones, R. R., Bippes, C. A., Gouveia, R. M. and Connon, C. J. (2014) 'Differential nuclear expression of Yap in basal epithelial cells across the cornea and substrates of differing stiffness', *Exp Eye Res,* 127, pp. 37-41.

Froget, S., Barthelemy, E., Guillot, F., Soler, C., Coudert, M. C., Benbunan, M. and Dosquet, C. (2003) 'Wound healing mediator production by human dermal fibroblasts grown within a collagen-GAG matrix for skin repair in humans. ', *European cytokine network,* 12(1), pp. 60-64.

Funderburgh, J. L., Funderburgh, M. L. and Du, Y. (2016) 'Stem Cells in the Limbal Stroma', *Ocul Surf,* 14(2), pp. 113-20.

Funderburgh, M. L. (2005) 'PAX6 expression identifies progenitor cells for corneal keratocytes', *The FASEB Journal*.

Gain, P., Jullienne, R., He, Z., Aldossary, M., Acquart, S., Cognasse, F. and Thuret, G. (2016) 'Global Survey of Corneal Transplantation and Eye Banking', *JAMA Ophthalmol,* 134(2), pp. 167-73.

Galvez, P., Clares, B., Bermejo, M., Hmadcha, A. and Soria, B. (2014) 'Standard requirement of a microbiological quality control program for the manufacture of human mesenchymal stem cells for clinical use', *Stem Cells Dev,* 23(10), pp. 1074-83.

Gandhi, S. and Jain, S. (2015) 'The Anatomy and Physiology of Cornea in Keratoprostheses and Artificial Corneas.', *Springer*, pp. 19-25.

Gipson, I. K. and Joyce, N. C. (2000) 'Anatomy and cell biology of the cornea, superficial limbus, and conjunctiva', *Principles and Practice of Ophthalmology*, pp. 612-629.

Gipson, I. K. and Kiorpes, T. C. (1982) 'Epithelial sheet movement: protein and glycoprotein synthesis', *Dev Biol,* 92(1), pp. 259-62.

Girard, M. T., Matsubara, M. and Fini, M. E. (1991) 'Transforming growth factor-beta and interleukin-1 modulate metalloproteinase expression by corneal stromal cells', *Invest Ophthalmol Vis Sci,* 32(9), pp. 2441-54.

Gnecchi, M., He, H., Liang, O. D., Melo, L. G., Morello, F., Mu, H., Noiseux, N., Zhang, L., Pratt, R. E., Ingwall, J. S. and Dzau, V. J. (2005) 'Paracrine action accounts for marked protection of ischemic heart by Akt-modified mesenchymal stem cells', *Nat Med,* 11(4), pp. 367-8.

Gnecchi, M., Zhang, Z., Ni, A. and Dzau, V. J. (2008) 'Paracrine mechanisms in adult stem cell signaling and therapy', *Circ Res,* 103(11), pp. 1204-19.

Golmohamadi, M. and Wilkinson, K. J. (2013) 'Diffusion of ions in a calcium alginate hydrogel-structure is the primary factor controlling diffusion', *Carbohydr Polym,* 94(1), pp. 82-7.

Gombotz, W. (1998) 'Protein release from alginate matrices', *Advanced Drug Delivery Reviews,* 31, pp. 267-285.

Gonzalez-Perez, O. (2012) 'Neural stem cells in the adult human brain', *Biol Biomed Rep,* 2(1), pp. 59-69.

Gordon, M. K., Foley, J. W., Birk, D. E., Fitch, J. M. and Linsenmayer, T. F. (1994) 'Type V collagen and Bowman's membrane. Quantitation of mRNA in corneal epithelium and stroma', *J Biol Chem,* 269(40), pp. 24959-66.

Goren, A., Dahan, N., Goren, E., Baruch, L. and Machluf, M. (2010) 'Encapsulated human mesenchymal stem cells: a unique hypoimmunogenic platform for long-term cellular therapy', *FASEB J,* 24(1), pp. 22-31.

Gouveia, R. M. and Connon, C. J. (2013) 'The effects of retinoic acid on human corneal stromal keratocytes cultured in vitro under serum-free conditions', *Invest Ophthalmol Vis Sci,* 54(12), pp. 7483-91.

Gouveia, R. M., Lepert, G., Gupta, S., Mohan, R. R., Paterson, C. and Connon, C. J. (2019) 'Assessment of corneal substrate biomechanics and its effect on epithelial stem cell maintenance and differentiation', *Nat Commun,* 10(1), pp. 1496.

Grant, G. T., Morris, E. R., Rees, D. A., Smith, P. J. C. and Thom, D. (1973) 'Biological interactions between polysaccharides and divalent cations: The egg-box model', *FEBS Letters,* 32(1), pp. 195-198.

Grøndahl, L., Lawrie, G., Anitha, A. and Shejwalkar, A. (2020) 'Applications of alginate biopolymer in drug delivery', pp. 375-403.

Gurtner, G. C., Werner, S., Barrandon, Y. and Longaker, M. T. (2008) 'Wound repair and regeneration', *Nature,* 453(7193), pp. 314-21.

Han, Y. S., Lee, J. H., Yoon, Y. M., Yun, C. W., Noh, H. and Lee, S. H. (2016) 'Hypoxia-induced expression of cellular prion protein improves the therapeutic potential of mesenchymal stem cells', *Cell Death Dis,* 7(10), pp. e2395.

Hay, I. D., Ur Rehman, Z., Moradali, M. F., Wang, Y. and Rehm, B. H. (2013) 'Microbial alginate production, modification and its applications', *Microb Biotechnol,* 6(6), pp. 637-50.

Hertsenberg, A. J. and Funderburgh, J. L. (2015) 'Stem Cells in the Cornea', *Prog Mol Biol Transl Sci,* 134, pp. 25-41.

Hess, D. C., Wechsler, L. R., Clark, W. M., Savitz, S. I., Ford, G. A., Chiu, D., Yavagal, D. R., Uchino, K., Liebeskind, D. S., Auchus, A. P., Sen, S., Sila, C. A., Vest, J. D. and Mays, R. W. (2017) 'Safety and efficacy of multipotent adult progenitor cells in acute ischaemic stroke (MASTERS): a randomised, double-blind, placebo-controlled, phase 2 trial.', *The Lancet. Neurology,* 16, pp. 360-368.

Hocking, A. M. and Gibran, N. S. (2010) 'Mesenchymal stem cells: paracrine signaling and differentiation during cutaneous wound repair', *Exp Cell Res,* 316(14), pp. 2213-9.

Holan, V., Trosan, P., Cejka, C., Javorkova, E., Zajicova, A., Hermankova, B., Chudickova, M. and Cejkova, J. (2015) 'A Comparative Study of the Therapeutic Potential of Mesenchymal Stem Cells and Limbal Epithelial Stem Cells for Ocular Surface Reconstruction', *Stem Cells Transl Med,* 4(9), pp. 1052-63.

Hoogduijn, M. J., Crop, M. J., Peeters, A. M., Van Osch, G. J., Balk, A. H., Ijzermans, J. N., Weimar, W. and Baan, C. C. (2007) 'Human heart, spleen, and perirenal fat-derived mesenchymal stem cells have immunomodulatory capacities', *Stem Cells Dev,* 16(4), pp. 597-604.

Hsiao, S. T., Lokmic, Z., Peshavariya, H., Abberton, K. M., Dusting, G. J., Lim, S. Y. and Dilley, R. J. (2013) 'Hypoxic conditioning enhances the angiogenic paracrine activity of human adipose-derived stem cells', *Stem Cells Dev,* 22(10), pp. 1614-23.

Hu, Y., Qin, C., Zheng, G., Lai, D., Tao, H., Zhang, Y., Qiu, G., Ge, M., Huang, L., Chen, L., Cheng, B., Shu, Q. and Xu, J. (2016) 'Mesenchymal Stem Cell-Educated Macrophages Ameliorate LPS-Induced Systemic Response', *Mediators of Inflammation,* 2016, pp. 1-12.

Huebsch, N. and Mooney, D. J. (2009) 'Inspiration and application in the evolution of biomaterials', *Nature,* 462(7272), pp. 426-32.

Huet, E., Vallee, B., Delbe, J., Mourah, S., Pruliere-Escabasse, V., Tremouilleres, M., Kadomatsu, K., Doan, S., Baudouin, C., Menashi, S. and Gabison, E. E. (2011) 'EMMPRIN modulates epithelial barrier function through a MMP-mediated occludin cleavage: implications in dry eye disease', *Am J Pathol,* 179(3), pp. 1278-86.

Hui-Kang, D., Jesse, H.-C., Lai, J.-Y., Sun, C.-C., Wang, S.-F., Lin, K.-K. and Chen, J.-K. (2009) 'Matrix Revolution: Molecular Mechanism for Inflammatory Corneal Neovascularization and Restoration of Corneal Avascularity by Epithelial stem Cell Transplantation', *The Ocular Surface,* 7(3), pp. 128-144.

Hung, S.-C., Pochampally, R. R., Chen, S.-C., Hsu, S.-C. and Prockop, D. J. (2007) 'Angiogenic Effects of Human Multipotent Stromal Cell Conditioned Medium Activate the PI3K-Akt Pathway in Hypoxic Endothelial Cells to Inhibit Apoptosis, Increase Survival, and Stimulate Angiogenesis', *Stem Cells,* 25(9), pp. 2363-2370.

Hwang, S. J., Cho, T. H., Lee, B. and Kim, I. S. (2018) 'Bone-healing capacity of conditioned medium derived from three-dimensionally cultivated human mesenchymal stem cells

and electrical stimulation on collagen sponge', *J Biomed Mater Res A,* 106(2), pp. 311-320.

Jager, M. J., Gregerson, D. S. and Streilein, J. W. (1995) 'Regulators of immunological responses in the cornea and the anterior chamber of the eye', *Eye (Lond),* 9 (Pt 2), pp. 241-6.

Jester J.V. , Moller-Pedersen T., Huang, J., Sax, C. M., Kays, W. T., Cavangh, H. D., Petroll, W. M. and J., P. (1999) 'The cellular basis of corneal transparency: evidence for 'corneal crystallins'.', *Journal of Cell Science* 112, pp. 613-622.

Jester, J. V., Huang, J., Barry-Lane, P. A., Kao, W. W., Petroll, W. M. and Cavanagh, H. D. (1999a) 'Transforming growth factor(beta)-mediated corneal myofibroblast differentiation requires actin and fibronectin assembly', *Invest Ophthalmol Vis Sci,* 40(9), pp. 1959-67.

Jester, J. V., Petroll, W. M. and Cavanagh, H. D. (1999b) 'Corneal stromal wound healing in refractive surgery: the role of myofibroblasts', *Progress in Retinal and Eye Research,* 18(3), pp. 311-356.

Jiang, Y., Vaessen, B., Lenvik, T., Blackstad, M., Reyes, M. and Verfaillie, C. M. (2002) 'Multipotent progenitor cells can be isolated from postnatal murine bone marrow, muscle, and brain.', *Experimental hematology,* 30, pp. 896-904.

Jiang, Z., Liu, G., Meng, F., Wang, W., Hao, P., Xiang, Y., Wang, Y., Han, R., Li, F., Wang, L. and Li, X. (2017) 'Paracrine effects of mesenchymal stem cells on the activation of keratocytes', *Br J Ophthalmol,* 101(11), pp. 1583-1590.

Johnsen, S. A., Subramaniam, M., Janknecht, R. and Spelsberg, T. C. (2002) 'TGFbeta inducible early gene enhances TGFbeta/Smad-dependent transcriptional responses', *Oncogene,* 21(37), pp. 5783-90.

Jonkman, J. E., Cathcart, J. A., Xu, F., Bartolini, M. E., Amon, J. E., Stevens, K. M. and Colarusso, P. (2014) 'An introduction to the wound healing assay using live-cell microscopy', *Cell Adh Migr,* 8(5), pp. 440-51.

Jun, E. K., Zhang, Q., Yoon, B. S., Moon, J. H., Lee, G., Park, G., Kang, P. J., Lee, J. H., Kim, A. and You, S. (2014) 'Hypoxic conditioned medium from human amniotic fluid-derived mesenchymal stem cells accelerates skin wound healing through TGF-beta/SMAD2 and PI3K/Akt pathways', *Int J Mol Sci,* 15(1), pp. 605-28.

Kachouie, N. N., Du, Y., Bae, H., Khabiry, M., Ahari, A. F., Zamanian, B., Fukuda, J. and Khademhosseini, A. (2010) 'Directed assembly of cell-laden hydrogels for engineering functional tissues', *Organogenesis,* 6(4), pp. 234-44.

Kaiserman, I. and Sella, S. (2019) 'Chronic Ocular Inflammation and Keratoconus', pp. 17-27.

Kaita, Y., Tarui, T., Yoshino, H., Matsuda, T., Yamaguchi, Y., Nakagawa, T., Asahi, M. and Ii, M. (2019) 'Sufficient therapeutic effect of cryopreserved frozen adipose-derived regenerative cells on burn wounds', *Regen Ther,* 10, pp. 92-103.

Karamichos, D., Zareian, R., Guo, X., Hutcheon, A. E., Ruberti, J. W. and Zieske, J. D. (2012) 'Novel in Vitro Model for Keratoconus Disease', *J Funct Biomater,* 3(4), pp. 760-775.

Kaur, H., Chaurasia, S. S., Agrawal, V., Suto, C. and Wilson, S. E. (2009) 'Corneal myofibroblast viability: opposing effects of IL-1 and TGF beta1', *Exp Eye Res,* 89(2), pp. 152-8.

Kern, S., Eichler, H., Stoeve, J., Kluter, H. and Bieback, K. (2006) 'Comparative analysis of mesenchymal stem cells from bone marrow, umbilical cord blood, or adipose tissue', *Stem Cells,* 24(5), pp. 1294-301.

Khan, R. S. and Newsome, P. N. (2019) 'A Comparison of Phenotypic and Functional Properties of Mesenchymal Stromal Cells and Multipotent Adult Progenitor Cells', *Front Immunol,* 10, pp. 1952.

Kheirkhah, A., Raju, V. K. and Tseng, S. C. G. (2008) 'Minimal Conjunctival Limbal Autograft for Total Limbal Stem Cell Deficiency', *Cornea,* 27(6), pp. 730-733.

Kim, I. (2013) 'A brief overview of cell therapy and its product', *J Korean Assoc Oral Maxillofac Surg,* 39(5), pp. 201-2.

Kim, J. Y., Djalilian, A. R., Schwartz, G. S. and Holland, E. J. (2003) 'Ocular surface reconstruction: limbal stem cell transplantation', *Ophthalmol Clin North Am,* 16(1), pp. 67-77.

Kinnaird, T., Stabile, E., Burnett, M. S., Lee, C. W., Barr, S., Fuchs, S. and Epstein, S. E. (2004) 'Marrow-derived stromal cells express genes encoding a broad spectrum of arteriogenic cytokines and promote in vitro and in vivo arteriogenesis through paracrine mechanisms', *Circ Res,* 94(5), pp. 678-85.

Klopsch, C., Skorska, A., Ludwig, M., Lemcke, H., Maass, G., Gaebel, R., Beyer, M., Lux, C., Toelk, A., Muller, K., Maschmeier, C., Rohde, S., Mela, P., Muller-Hilke, B., Jockenhoevel, S., Vollmar, B., Jaster, R., David, R. and Steinhoff, G. (2018) 'Intramyocardial angiogenetic stem cells and epicardial erythropoietin save the acute ischemic heart', *Dis Model Mech,* 11(6).

Kober, J., Gugerell, A., Schmid, M., Zeyda, M., Buchberger, E., Nickl, S., Hacker, S., Ankersmit, H. J. and Keck, M. (2016) 'Wound Healing Effect of Conditioned Media Obtained From Adipose Tissue on Human Skin Cells: A Comparative in Vitro Study', *Ann Plast Surg,* 77(2), pp. 156-63.

Koizumi, J., Inoue, S., Yonekawa, H. and Kunieda, T. (2002) 'Hemosuccus pancreaticus: diagnosis with CT and MRI and treatment with transcatheter embolization', *Abdominal Imaging,* 27(1), pp. 77-81.

Kong, H. J., Alsberg, E., Kaigler, D., Lee, K. Y. and Mooney, D. J. (2004a) 'Controlling Degradation of Hydrogels via the Size of Cross-Linked Junctions', *Adv Mater,* 16(21), pp. 1917-1921.

Kong, H. J., Kaigler, D., Kim, K. and Mooney, D. J. (2004b) 'Controlling rigidity and degradation of alginate hydrogels via molecular weight distribution', *Biomacromolecules,* 5(5), pp. 1720-7.

Kovacsovics-Bankowski, M., Streeter, P. R., Hewett, E., Van't Hof, W. J., J., D. R. and Maziarz, T. R. (2015) 'Multipotent Adult Progenitor Cells (MAPC) Are Immunoprivileged and Demonstrate Immunosuppressive Properties on Activated T Cell Population.', *Blood,* 106(11), pp. 5227.

Krasnodembskaya, A., Song, Y., Fang, X., Gupta, N., Serikov, V., Lee, J. W. and Matthay, M. A. (2010) 'Antibacterial effect of human mesenchymal stem cells is mediated in part from secretion of the antimicrobial peptide LL-37', *Stem Cells,* 28(12), pp. 2229-38.

Kuo, I. C. (2004) 'Corneal wound healing', *Curr Opin Ophthalmol,* 15(4), pp. 311-5.

Kuwabara, T., Perkins, D. G. and Cogan, D. G. (1976) 'Sliding of the epithelium in experimental corneal wounds', *Invest Ophthalmol,* 15(1), pp. 4-14.

Kwon, H. M., Hur, S. M., Park, K. Y., Kim, C. K., Kim, Y. M., Kim, H. S., Shin, H. C., Won, M. H., Ha, K. S., Kwon, Y. G., Lee, D. H. and Kim, Y. M. (2014) 'Multiple paracrine factors secreted by mesenchymal stem cells contribute to angiogenesis', *Vascul Pharmacol,* 63(1), pp. 19-28.

Kyurkchiev, D., Bochev, I., Ivanova-Todorova, E., Mourdjeva, M., Oreshkova, T., Belemezova, K. and Kyurkchiev, S. (2014) 'Secretion of immunoregulatory cytokines by mesenchymal stem cells', *World J Stem Cells,* 6(5), pp. 552-70.

Lagali, N., Germundsson, J. and Fagerholm, P. (2009) 'The role of Bowman's layer in corneal regeneration after phototherapeutic keratectomy: a prospective study using in vivo confocal microscopy', *Invest Ophthalmol Vis Sci,* 50(9), pp. 4192-8.

Lakatos, K., Kalomoiris, S., Merkely, B., Nolta, J. A. and Fierro, F. A. (2016) 'Mesenchymal Stem Cells Respond to Hypoxia by Increasing Diacylglycerols', *J Cell Biochem,* 117(2), pp. 300-7.

Last, J. A., Thomasy, S. M., Croasdale, C. R., Russell, P. and Murphy, C. J. (2012) 'Compliance profile of the human cornea as measured by atomic force microscopy', *Micron,* 43(12), pp. 1293-8.

Lau, K., Paus, R., Tiede, S., Day, P. and Bayat, A. (2009) 'Exploring the role of stem cells in cutaneous wound healing', *Exp Dermatol,* 18(11), pp. 921-33.

Lavker, R. M. and Sun, T. T. (2003) 'Epithelial stem cells: the eye provides a vision', *Eye (Lond),* 17(8), pp. 937-42.

Lee, K. Y. and Mooney, D. J. (2012) 'Alginate: properties and biomedical applications', *Prog Polym Sci,* 37(1), pp. 106-126.

Lee, M. J., Ko, A. Y., Ko, J. H., Lee, H. J., Kim, M. K., Wee, W. R., Khwarg, S. I. and Oh, J. Y. (2015) 'Mesenchymal Stem/Stromal Cells Protect the Ocular Surface by Suppressing Inflammation in an Experimental Dry Eye', *Molecular Therapy,* 23, pp. 139-146.

Lee, M. N., Hwang, H. S., Oh, S. H., Roshanzadeh, A., Kim, J. W., Song, J. H., Kim, E. S. and Koh, J. T. (2018) 'Elevated extracellular calcium ions promote proliferation and migration of mesenchymal stem cells via increasing osteopontin expression', *Exp Mol Med,* 50(11), pp. 142.

Lee, R. H., Oh, J. Y., Choi, H. and Bazhanov, N. (2011) 'Therapeutic factors secreted by mesenchymal stromal cells and tissue repair', *J Cell Biochem,* 112(11), pp. 3073-8.

Lee, S. C., Jeong, H. J., Lee, S. K. and Kim, S. J. (2016) 'Hypoxic Conditioned Medium From Human Adipose-Derived Stem Cells Promotes Mouse Liver Regeneration Through JAK/STAT3 Signaling', *Stem Cells Transl Med,* 5(6), pp. 816-25.

Lee, S. M., Lee, S. C. and Kim, S. J. (2014) 'Contribution of human adipose tissue-derived stem cells and the secretome to the skin allograft survival in mice', *J Surg Res,* 188(1), pp. 280-9.

Lee, W. R., Park, J. H., Kim, K. H., Kim, S. J., Park, D. H., Chae, M. H., Suh, S. H., Jeong, S. W. and Park, K. K. (2009) 'The biological effects of topical alginate treatment in an animal model of skin wound healing', *Wound Repair Regen,* 17(4), pp. 505-10.

Lehrer, M. S., Sun, T. T. and Lavker, R. M. (1998) 'Strategies of epithelial repair: modulation of stem cell and transit amplifying cell proliferation', *J Cell Sci,* 111 (Pt 19), pp. 2867-75.

Leiman, D. A., Riff, B. P., Morgan, S., Metz, D. C., Falk, G. W., French, B., Umscheid, C. A. and Lewis, J. D. (2017) 'Alginate therapy is effective treatment for GERD symptoms: a systematic review and meta-analysis', *Dis Esophagus,* 30(5), pp. 1-9.

Lema, I., Sobrino, T., Duran, J. A., Brea, D. and Diez-Feijoo, E. (2009) 'Subclinical keratoconus and inflammatory molecules from tears', *British Journal of Ophthalmology,* 93(6), pp. 820-824.

LeRoux, M. A., Guilak, F. and Setton, L. A. (1999) 'Compressive and shear properties of alginate gel: effects of sodium ions and alginate concentration', *J Biomed Mater Res,* 47(1), pp. 46-53.

Li, F. and Zhao, S.-Z. (2016) 'Control of Cross Talk between Angiogenesis and Inflammation by Mesenchymal Stem Cells for the Treatment of Ocular Surface Diseases.', *Stem cells international,* 2016, pp. 7961816.

Li, M., Zhao, Y., Hao, H., Han, W. and Fu, X. (2015) 'Mesenchymal stem cell-based therapy for nonhealing wounds: today and tomorrow', *Wound Repair Regen,* 23(4), pp. 465-82.

Li, W., Hayashida, Y., Chen, Y. T. and Tseng, S. C. (2007) 'Niche regulation of corneal epithelial stem cells at the limbus', *Cell Res,* 17(1), pp. 26-36.

Lian, Y., Wang, X., Guo, P., Li, Y., Raza, F., Su, J. and Qiu, M. (2019) 'Erythrocyte Membrane-Coated Arsenic Trioxide-Loaded Sodium Alginate Nanoparticles for Tumor Therapy', *Pharmaceutics,* 12(1).

Liang, C. C., Park, A. Y. and Guan, J. L. (2007) 'In vitro scratch assay: a convenient and inexpensive method for analysis of cell migration in vitro', *Nat Protoc,* 2(2), pp. 329-33.

Liang, L., Sheha, H., Li, J. and Tseng, S. C. (2009) 'Limbal stem cell transplantation: new progresses and challenges', *Eye (Lond),* 23(10), pp. 1946-53.

Liang, Y., Liu, W., Han, B., Yang, C., Ma, Q., Song, F. and Bi, Q. (2011) 'An in situ formed biodegradable hydrogel for reconstruction of the corneal endothelium', *Colloids Surf B Biointerfaces,* 82(1), pp. 1-7.

Lin, W., Xu, L., Zwingenberger, S., Gibon, E., Goodman, S. B. and Li, G. (2017) 'Mesenchymal stem cells homing to improve bone healing', *J Orthop Translat,* 9, pp. 19-27.

Liu, C.-Y., Birk, D. E., Hassell, J. R., Kane, B. and Kao, W. W. Y. (2003) 'Keratocan-deficient Mice Display Alterations in Corneal Structure', *Journal of Biological Chemistry,* 278(24), pp. 21672-21677.

Liu, Y. Y., Chiang, C. H., Hung, S. C., Chian, C. F., Tsai, C. L., Chen, W. C. and Zhang, H. (2017) 'Hypoxia-preconditioned mesenchymal stem cells ameliorate ischemia/reperfusion-induced lung injury', *PLoS One,* 12(11), pp. e0187637.

Ljubimov, A. V., Alba, S. A., Burgeson, R. E., Ninomiya, Y., Sado, Y., Sun, T. T., Nesburn, A. B., Kenney, M. C. and Maguen, E. (1998) 'Extracellular matrix changes in human corneas after radial keratotomy', *Exp Eye Res,* 67(3), pp. 265-72.

Ljubimov, A. V. and Saghizadeh, M. (2015) 'Progress in corneal wound healing', *Progress in Retinal and Eye Research,* 49, pp. 17-45.

LoGuidice, A., Houlihan, A. and Deans, R. (2016) 'Multipotent adult progenitor cells on an allograft scaffold facilitate the bone repair process', *J Tissue Eng,* 7, pp. 2041731416656148.

Lombardi, F., Palumbo, P., Augello, F. R., Cifone, M. G., Cinque, B. and Giuliani, M. (2019) 'Secretome of Adipose Tissue-Derived Stem Cells (ASCs) as a Novel Trend in Chronic Non-Healing Wounds: An Overview of Experimental In Vitro and In Vivo Studies and Methodological Variables', *Int J Mol Sci,* 20(15).

Lu, L., Reinach, P. S. and Kao, W. W. Y. (2016) 'Corneal Epithelial Wound Healing', *Experimental Biology and Medicine,* 226(7), pp. 653-664.

Lukomska, B., Stanaszek, L., Zuba-Surma, E., Legosz, P., Sarzynska, S. and Drela, K. (2019) 'Challenges and Controversies in Human Mesenchymal Stem Cell Therapy', *Stem Cells Int,* 2019, pp. 9628536.

Ma, D. H., Chen, J. K., Zhang, F., Lin, K. Y., Yao, J. Y. and Yu, J. S. (2006a) 'Regulation of corneal angiogenesis in limbal stem cell deficiency', *Prog Retin Eye Res,* 25(6), pp. 563-90.

Ma, Y., Xu, Y., Xiao, Z., Yang, W., Zhang, C., Song, E., Du, Y. and Li, L. (2006b) 'Reconstruction of Chemically Burned Rat Corneal Surface by Bone Marrow-Derived Human Mesenchymal Stem Cells', *Stem Cells,* 24, pp. 315-321.

Mahat, D. B. and Lis, J. T. (2017) 'Use of conditioned media is critical for studies of regulation in response to rapid heat shock', *Cell Stress Chaperones,* 22(1), pp. 155-162.

Mak, M., Spill, F., Kamm, R. D. and Zaman, M. H. (2016) 'Single-Cell Migration in Complex Microenvironments: Mechanics and Signaling Dynamics', *J Biomech Eng,* 138(2), pp. 021004.

Malecaze, F., Simorre, V., Chollet, P., Tack, J. L., Muraine, M., Le Guellec, D., Vita, N., Arne, J. L. and Darbon, J. M. (1997) 'Interleukin-6 in tear fluid after photorefractive keratectomy and its effects on keratocytes in culture', *Cornea,* 16(5), pp. 580-7.

Mansoor, H., Ong, H. S., Riau, A. K., Stanzel, T. P., Mehta, J. S. and Yam, G. H. (2019) 'Current Trends and Future Perspective of Mesenchymal Stem Cells and Exosomes in Corneal Diseases', *Int J Mol Sci,* 20(12).

Martens, A., Ordies, S., Vanaudenaerde, B. M., Verleden, S. E., Vos, R., Van Raemdonck, D. E., Verleden, G. M., Roobrouck, V. D., Claes, S., Schols, D., Verbeken, E., Verfaillie, C. M. and Neyrinck, A. P. (2017) 'Immunoregulatory effects of multipotent adult progenitor cells in a porcine ex vivo lung perfusion model.', *Stem cell research & therapy,* 8, pp. 159.

Maxson, S., Lopez, E. A., Yoo, D., Danilkovitch-Miagkova, A. and Leroux, M. A. (2012) 'Concise review: role of mesenchymal stem cells in wound repair', *Stem Cells Transl Med,* 1(2), pp. 142-9.

Maziarz, R. T., Devos, T., Bachier, C. R., Goldstein, S. C., Leis, J. F., Devine, S. M., Meyers, G., Gajewski, J. L., Maertens, J., Deans, R. J., Van't Hof, W. and Lazarus, H. M. (2015) 'Single and multiple dose MultiStem (multipotent adult progenitor cell) therapy prophylaxis of acute graft-versus-host disease in myeloablative allogeneic hematopoietic cell transplantation: a phase 1 trial', *Biol Blood Marrow Transplant,* 21(4), pp. 720-8.

McKay, T. B., Hjortdal, J., Priyadarsini, S. and Karamichos, D. (2017a) 'Acute hypoxia influences collagen and matrix metalloproteinase expression by human keratoconus cells in vitro', *PLoS One,* 12(4), pp. e0176017.

McKay, T. B., Hjortdal, J., Sejersen, H. and Karamichos, D. (2017b) 'Differential Effects of Hormones on Cellular Metabolism in Keratoconus In Vitro', *Sci Rep,* 7, pp. 42896.

McKay, T. B., Lyon, D., Sarker-Nag, A., Priyadarsini, S., Asara, J. M. and Karamichos, D. (2015) 'Quercetin attenuates lactate production and extracellular matrix secretion in keratoconus', *Sci Rep,* 5, pp. 9003.

McKee, H. D., Irion, L. C., Carley, F. M., Brahma, A. K., Jafarinasab, M. R., Rahmati-Kamel, M., Kanavi, M. R. and Feizi, S. (2014) 'Re: Dua et al.: Human corneal anatomy redefined: a novel pre-Descemet layer (Dua's layer) (Ophthalmology 2013;120:1778-85)', *Ophthalmology,* 121(5), pp. e24-5.

McMonnies, C. W. (2009) 'Mechanisms of rubbing-related corneal trauma in keratoconus', *Cornea,* 28(6), pp. 607-15.

Meek, K. M. and Boote, C. (2004) 'The organization of collagen in the corneal stroma', *Exp Eye Res,* 78(3), pp. 503-12.

Meek, K. M., Dennis, S. and Khan, S. (2003) 'Changes in the Refractive Index of the Stroma and Its Extrafibrillar Matrix When the Cornea Swells', *Biophysical Journal,* 85(4), pp. 2205-2212.

Mei, S. H., Haitsma, J. J., Dos Santos, C. C., Deng, Y., Lai, P. F., Slutsky, A. S., Liles, W. C. and Stewart, D. J. (2010) 'Mesenchymal stem cells reduce inflammation while enhancing bacterial clearance and improving survival in sepsis', *Am J Respir Crit Care Med,* 182(8), pp. 1047-57.

Messina, E., De Angelis, L., Frati, G., Morrone, S., Chimenti, S., Fiordaliso, F., Salio, M., Battaglia, M., Latronico, M. V., Coletta, M., Vivarelli, E., Frati, L., Cossu, G. and Giacomello, A. (2004) 'Isolation and expansion of adult cardiac stem cells from human and murine heart', *Circ Res,* 95(9), pp. 911-21.

Mildmay-White, A. and Khan, W. (2017) 'Cell Surface Markers on Adipose-Derived Stem Cells: A Systematic Review', *Curr Stem Cell Res Ther,* 12(6), pp. 484-492.

Milner, C. M. and Day, A. J. (2003) 'TSG-6: a multifunctional protein associated with inflammation', *Journal of cell science,* 116(Pt 10), pp. 1863-73.

Mirotsou, M., Jayawardena, T. M., Schmeckpeper, J., Gnecchi, M. and Dzau, V. J. (2011) 'Paracrine mechanisms of stem cell reparative and regenerative actions in the heart', *J Mol Cell Cardiol,* 50(2), pp. 280-9.

Mittal, S. K., Omoto, M., Amouzegar, A., Sahu, A., Rezazadeh, A., Katikireddy, K. R., Shah, D. I., Sahu, S. K. and Chauhan, S. K. (2016) 'Restoration of Corneal Transparency by Mesenchymal Stem Cells', *Stem Cell Reports,* 7(4), pp. 583-590.

Miyagi, H., Thomasy, S. M., Russell, P. and Murphy, C. J. (2018) 'The role of hepatocyte growth factor in corneal wound healing', *Exp Eye Res,* 166, pp. 49-55.

Mount, N. M., Ward, S. J., Kefalas, P. and Hyllner, J. (2015) 'Cell-based therapy technology classifications and translational challenges', *Philos Trans R Soc Lond B Biol Sci,* 370(1680), pp. 20150017.

Muller, L. J., Pels, E. and Vrensen, G. F. (2001) 'The specific architecture of the anterior stroma accounts for maintenance of corneal curvature', *Br J Ophthalmol,* 85(4), pp. 437-43.

Muller, L. J., Pels, L. and Vrensen, G. F. J. M. (1995) 'Novel Aspects of the Ultrastructural Organization of Human Corneal Keratocytes', *Investigative Ophthalmology & Visual Science,* 36(13), pp. 2557-2567.

Murry, C. E., Jennings, R. B. and Reimer, K. A. (1986) 'Preconditioning with ischemia: a delay of lethal cell injury in ischemic myocardium', *Circulation,* 74(5), pp. 1124-36.

Nakayasu, K., Tanaka, M., Konomi, H. and Hayashi, T. (1986) 'Distribution of types I, II, III, IV and V collagen in normal and keratoconus corneas', *Ophthalmic Res,* 18(1), pp. 1-10.

Newman, R. E., Yoo, D., LeRoux, M. A. and Danilkovitch-Miagkova, A. (2009) 'Treatment of inflammatory diseases with mesenchymal stem cells', *Inflamm Allergy Drug Targets,* 8(2), pp. 110-23.

Nicodemus, G. D. and Bryant, S. J. (2008) 'Cell encapsulation in biodegradable hydrogels for tissue engineering applications', *Tissue Eng Part B Rev,* 14(2), pp. 149-65.

Oh, J. Y., Kim, M. K., Shin, M. S., Lee, H. J., Ko, J. H., Wee, W. R. and Lee, J. H. (2008) 'The anti-inflammatory and anti-angiogenic role of mesenchymal stem cells in corneal wound healing following chemical injury', *Stem Cells,* 26(4), pp. 1047-55.

Oh, J. Y., Kim, M. K., Shin, M. S., Wee, W. R. and Lee, J. H. (2009) 'Cytokine secretion by human mesenchymal stem cells cocultured with damaged corneal epithelial cells', *Cytokine,* 46(1), pp. 100-3.

Omoto, M., Suri, K., Amouzegar, A., Li, M., Katikireddy, K. R., Mittal, S. K. and Chauhan, S. K. (2017) 'Hepatocyte Growth Factor Suppresses Inflammation and Promotes Epithelium Repair in Corneal Injury', *Molecular therapy : the journal of the American Society of Gene Therapy,* 25(8), pp. 1881-1888.

Ong, H. T., Redmond, S. L., Marano, R. J., Atlas, M. D., von Unge, M., Aabel, P. and Dilley, R. J. (2017) 'Paracrine Activity from Adipose-Derived Stem Cells on In Vitro Wound Healing in Human Tympanic Membrane Keratinocytes', *Stem Cells Dev,* 26(6), pp. 405-418.

Park, S.-R., Kim, J.-W., Jun, H.-S., Roh, J. Y., Lee, H.-Y. and Hong, I.-S. (2018) 'Stem Cell Secretome and Its Effect on Cellular Mechanisms Relevant to Wound Healing', *Molecular Therapy,* 26(2), pp. 606-617.

Pasovic, L., Eidet, J. R., Olstad, O. K., Chen, D. F., Lyberg, T. and Utheim, T. P. (2017) 'Impact of Storage Temperature on the Expression of Cell Survival Genes in Cultured ARPE-19 Cells', *Curr Eye Res,* 42(1), pp. 134-144.

Patrikoski, M., Mannerstrom, B. and Miettinen, S. (2019) 'Perspectives for Clinical Translation of Adipose Stromal/Stem Cells', *Stem Cells Int,* 2019, pp. 5858247.

Pawitan, J. A. (2014) 'Prospect of stem cell conditioned medium in regenerative medicine', *Biomed Res Int,* 2014, pp. 965849.

Pei, Y., Reins, R. Y. and McDermott, A. M. (2006) 'Aldehyde dehydrogenase (ALDH) 3A1 expression by the human keratocyte and its repair phenotypes', *Exp Eye Res,* 83(5), pp. 1063-73.

Peister, A., Mellad, J. A., Larson, B. L., Hall, B. M., Gibson, L. F. and Prockop, D. J. (2004) 'Adult stem cells from bone marrow (MSCs) isolated from different strains of inbred mice vary in surface epitopes, rates of proliferation, and differentiation potential', *Blood,* 103(5), pp. 1662-8.

Pellegrini, G., Ardigo, D., Milazzo, G., Iotti, G., Guatelli, P., Pelosi, D. and De Luca, M. (2018) 'Navigating Market Authorization: The Path Holoclar Took to Become the First Stem Cell Product Approved in the European Union', *Stem Cells Transl Med,* 7(1), pp. 146-154.

Pellegrini, G., Traverso, C. E., Franzi, A. T., Zingirian, M., Cancedda, R. and De Luca, M. (1997) 'Long-term restoration of damaged corneal surfaces with autologous cultivated corneal epithelium', *The Lancet,* 349(9057), pp. 990-993.

Penn, M. S., Ellis, S., Gandhi, S., Greenbaum, A., Hodes, Z., Mendelsohn, F. O., Strasser, D., Ting, A. E. and Sherman, W. (2012) 'Adventitial delivery of an allogeneic bone marrow-derived adherent stem cell in acute myocardial infarction: phase I clinical study', *Circ Res,* 110(2), pp. 304-11.

Petrenko, Y., Chudickova, M., Vackova, I., Groh, T., Kosnarova, E., Cejkova, J., Turnovcova, K., Petrenko, A., Sykova, E. and Kubinova, S. (2019) 'Clinically Relevant Solution for the Hypothermic Storage and Transportation of Human Multipotent Mesenchymal Stromal Cells', *Stem Cells Int,* 2019, pp. 5909524.

Pfaffl, M. W. (2001) 'A new mathematical model for relative quantification in real-time RT-PCR', *Nucleic Acids Res,* 29(9), pp. e45.

Pfister, R. R. (1975) 'The healing of corneal epithelial abrasions in the rabbit: a scanning electron microscope study', *Invest Ophthalmol,* 14(9), pp. 648-61.

Pileggi, A. (2012) 'Mesenchymal stem cells for the treatment of diabetes', *Diabetes,* 61(6), pp. 1355-6.

Pinnamaneni, N. and Funderburgh, J. L. (2012) 'Concise Review: Stem Cells in the Corneal Stroma', *STEM CELLS,* 30, pp. 1059-1063.

Pittenger, M. F., Mackay, A. M., Beck, S. C., Jaiswal, R. K., Douglas, R., Mosca, J. D., Moorman, M. A., Simonetti, D. W., Craig, S. and Marshak, D. R. (1999) 'Multilineage potential of adult human mesenchymal stem cells.', *Science (New York, N.Y.),* 284, pp. 143-7.

Plessers, J., Dekimpe, E., Van Woensel, M., Roobrouck, V. D., Bullens, D. M., Pinxteren, J., Verfaillie, C. M. and Van Gool, S. W. (2016) 'Clinical-Grade Human Multipotent Adult Progenitor Cells Block CD8+ Cytotoxic T Lymphocytes.', *Stem cells translational medicine,* 5, pp. 1607-1619.

Polisetty, N., Fatima, A., Madhira, S. L., Sangwan, V. S. and Vemuganti, G. K. (2008) 'Mesenchymal cells from limbal stroma of human eye', *Mol Vis,* 14, pp. 431-42.

Pourgholaminejad, A., Aghdami, N., Baharvand, H. and Moazzeni, S. M. (2016) 'The effect of pro-inflammatory cytokines on immunophenotype, differentiation capacity and immunomodulatory functions of human mesenchymal stem cells', *Cytokine,* 85, pp. 51-60.

Prockop, D. J. (1997) 'Marrow stromal cells as stem cells for nonhematopoietic tissues.', *Science (New York, N.Y.),* 276, pp. 71-4.

Prockop, D. J., Kota, D. J., Bazhanov, N. and Reger, R. L. (2010) 'Evolving paradigms for repair of tissues by adult stem/progenitor cells (MSCs).', *Journal of cellular and molecular medicine,* 14, pp. 2190-9.

Ramakrishnan, S., Anand, V. and Roy, S. (2014) 'Vascular endothelial growth factor signaling in hypoxia and inflammation', *J Neuroimmune Pharmacol,* 9(2), pp. 142-60.

Ratajczak, M. Z., Kucia, M., Jadczyk, T., Greco, N. J., Wojakowski, W., Tendera, M. and Ratajczak, J. (2012) 'Pivotal role of paracrine effects in stem cell therapies in regenerative medicine: can we translate stem cell-secreted paracrine factors and microvesicles into better therapeutic strategies?', *Leukemia,* 26(6), pp. 1166-73.

Ratner, B. D. and Bryant, S. J. (2004) 'Biomaterials: where we have been and where we are going', *Annu Rev Biomed Eng,* 6, pp. 41-75.

Ravanidis, S., Bogie, J. F. J., Donders, R., Craeye, D., Mays, R. W., Deans, R., Gijbels, K., Bronckaers, A., Stinissen, P., Pinxteren, J. and Hellings, N. (2015) 'Neuroinflammatory signals enhance the immunomodulatory and neuroprotective properties of multipotent adult progenitor cells', *Stem Cell Research & Therapy,* 6, pp. 176.

Reading, J. L., Yang, J. H., Sabbah, S., Skowera, A., Knight, R. R., Pinxteren, J., Vaes, B., Allsopp, T., Ting, A. E., Busch, S., Raber, A., Deans, R. and Tree, T. I. (2013) 'Clinical-grade multipotent adult progenitor cells durably control pathogenic T cell responses in human models of transplantation and autoimmunity', *J Immunol,* 190(9), pp. 4542-52.

Regmi, S., Pathak, S., Kim, J. O., Yong, C. S. and Jeong, J. H. (2019) 'Mesenchymal stem cell therapy for the treatment of inflammatory diseases: Challenges, opportunities, and future perspectives', *Eur J Cell Biol,* 98(5-8), pp. 151041.

Rehman, J., Traktuev, D., Li, J., Merfeld-Clauss, S., Temm-Grove, C. J., Bovenkerk, J. E., Pell, C. L., Johnstone, B. H., Considine, R. V. and March, K. L. (2004) 'Secretion of angiogenic and antiapoptotic factors by human adipose stromal cells', *Circulation,* 109(10), pp. 1292-8.

Reyes, M. and Verfaillie, C. M. (2001) 'Characterization of multipotent adult progenitor cells, a subpopulation of mesenchymal stem cells', *Ann N Y Acad Sci,* 938, pp. 231-3; discussion 233-5.

Ridley, A. J., Schwartz, M. A., Burridge, K., Firtel, R. A., Ginsberg, M. H., Borisy, G., Parsons, J. T. and Horwitz, A. R. (2003) 'Cell migration: integrating signals from front to back', *Science,* 302(5651), pp. 1704-9.

Riis, S., Newman, R., Ipek, H., Andersen, J. I., Kuninger, D., Boucher, S., Vemuri, M. C., Pennisi, C. P., Zachar, V. and Fink, T. (2017) 'Hypoxia enhances the wound-healing potential of adipose-derived stem cells in a novel human primary keratinocyte-based scratch assay', *Int J Mol Med,* 39(3), pp. 587-594.

Robb, R. M. and Kuwabara, T. (1962) 'Corneal wound healing. I. The movement of polymorphonuclear leukocytes into corneal wounds', *Arch Ophthalmol,* 68, pp. 636-42.

Rock, K. L. and Kono, H. (2008) 'The inflammatory response to cell death', *Annu Rev Pathol,* 3, pp. 99-126.

Roddy, G. W., Oh, J. Y., Lee, R. H., Bartosh, T. J., Ylostalo, J., Coble, K., Rosa, R. H. and Prockop, D. J. (2011) 'Action at a Distance: Systemically Administered Adult Stem/Progenitor Cells (MSCs) Reduce Inflammatory Damage to the Cornea Without Engraftment and Primarily by Secretion of TNF-α Stimulated Gene/Protein 6', *STEM CELLS,* 29, pp. 1572-1579.

Rodriguez-Menocal, L., Salgado, M., Ford, D. and Van Badiavas, E. (2012) 'Stimulation of skin and wound fibroblast migration by mesenchymal stem cells derived from normal donors and chronic wound patients', *Stem Cells Transl Med,* 1(3), pp. 221-9.

Rohrschneider, M., Bhagwat, S., Krampe, R., Michler, V., Breitkreutz, J. and Hochhaus, G. (2015) 'Evaluation of the Transwell System for Characterization of Dissolution Behavior of Inhalation Drugs: Effects of Membrane and Surfactant', *Mol Pharm,* 12(8), pp. 2618-24.

Romero-Jimenez, M., Santodomingo-Rubido, J. and Wolffsohn, J. S. (2010) 'Keratoconus: a review', *Cont Lens Anterior Eye,* 33(4), pp. 157-66; quiz 205.

Roobrouck, V. D., Wolfs, E., Delforge, M., Broekaert, D., Chakraborty, S., Sels, K., Vanwelden, T., Holvoet, B., Lhoest, L., Khurana, S., Pandey, S., Hoornaert, C., Ponsaerts, P., Struys, T., Boeckx, N., Vandenberghe, P., Deroose, C. M. and Verfaillie, C. M. (2017) 'Multipotent adult progenitor cells improve the hematopoietic function in myelodysplasia.', *Cytotherapy,* 19, pp. 744-755.

Ruprecht, V., Monzo, P., Ravasio, A., Yue, Z., Makhija, E., Strale, P. O., Gauthier, N., Shivashankar, G. V., Studer, V., Albiges-Rizo, C. and Viasnoff, V. (2017) 'How cells respond to environmental cues - insights from bio-functionalized substrates', *J Cell Sci,* 130(1), pp. 51-61.

Sacchetti, M., Rama, P., Bruscolini, A. and Lambiase, A. (2018) 'Limbal Stem Cell Transplantation: Clinical Results, Limits, and Perspectives', *Stem Cells Int,* 2018, pp. 8086269.

Saeedi, P., Halabian, R. and Imani Fooladi, A. A. (2019) 'A revealing review of mesenchymal stem cells therapy, clinical perspectives and Modification strategies', *Stem Cell Investig,* 6, pp. 34.

Sagaradze, G., Grigorieva, O., Nimiritsky, P., Basalova, N., Kalinina, N., Akopyan, Z. and Efimenko, A. (2019) 'Conditioned Medium from Human Mesenchymal Stromal Cells: Towards the Clinical Translation', *Int J Mol Sci,* 20(7).

Saghizadeh, M., Kramerov, A. A., Svendsen, C. N. and Ljubimov, A. V. (2017) 'Concise Review: Stem Cells for Corneal Wound Healing', *Stem Cells,* 35(10), pp. 2105-2114.

Saghizadeh, M., Kramerov, A. A., Tajbakhsh, J., Aoki, A. M., Wang, C., Chai, N. N., Ljubimova, J. Y., Sasaki, T., Sosne, G., Carlson, M. R., Nelson, S. F. and Ljubimov, A. V. (2005) 'Proteinase and growth factor alterations revealed by gene microarray analysis of human diabetic corneas', *Invest Ophthalmol Vis Sci,* 46(10), pp. 3604-15.

Salzman, M. and O'Malley, R. N. (2007) 'Updates on the evaluation and management of caustic exposures', *Emerg Med Clin North Am,* 25(2), pp. 459-76; abstract x.

Samarakoon, R., Higgins, C. E., Higgins, S. P. and Higgins, P. J. (2009) 'TGF-beta1-Induced Expression of the Poor Prognosis SERPINE1/PAI-1 Gene Requires EGFR Signaling: A New Target for Anti-EGFR Therapy', *J Oncol,* 2009, pp. 342391.

Sanchez, P., Hernandez, R. M., Pedraz, J. L. and Orive, G. (2013) 'Encapsulation of cells in alginate gels', *Methods Mol Biol,* 1051, pp. 313-25.

Sangwan, V. S., Basu, S., MacNeil, S. and Balasubramanian, D. (2012) 'Simple limbal epithelial transplantation (SLET): a novel surgical technique for the treatment of unilateral limbal stem cell deficiency', *Br J Ophthalmol,* 96(7), pp. 931-4.

Satue, M., Schuler, C., Ginner, N. and Erben, R. G. (2019) 'Intra-articularly injected mesenchymal stem cells promote cartilage regeneration, but do not permanently engraft in distant organs', *Sci Rep,* 9(1), pp. 10153.

Schive, S. W., Mirlashari, M. R., Hasvold, G., Wang, M., Josefsen, D., Gullestad, H. P., Korsgren, O., Foss, A., Kvalheim, G. and Scholz, H. (2017) 'Human Adipose-Derived Mesenchymal Stem Cells Respond to Short-Term Hypoxia by Secreting Factors Beneficial for Human Islets In Vitro and Potentiate Antidiabetic Effect In Vivo', *Cell Med,* 9(3), pp. 103-116.

Schlotzer-Schrehardt, U., Dietrich, T., Saito, K., Sorokin, L., Sasaki, T., Paulsson, M. and Kruse, F. E. (2007) 'Characterization of extracellular matrix components in the limbal epithelial stem cell compartment', *Exp Eye Res,* 85(6), pp. 845-60.

Schmitt, A., Rödel, P., Anamur, C., Seeliger, C., Imhoff, A. B., Herbst, E., Vogt, S., van Griensven, M., Winter, G. and Engert, J. (2015) 'Calcium alginate gels as stem cell matrix-making paracrine stem cell activity available for enhanced healing after surgery.', *PloS one,* 10, pp. e0118937.

Schneider, S., Unger, M., van Griensven, M. and Balmayor, E. R. (2017) 'Adipose-derived mesenchymal stem cells from liposuction and resected fat are feasible sources for regenerative medicine', *Eur J Med Res,* 22(1), pp. 17.

Secker, G. A. and Daniels, J. T. (2009) 'Limbal epithelial stem cells of the cornea.'.

Sekiyama, E., Nakamura, T., Kawasaki, S., Sogabe, H. and Kinoshita, S. (2006) 'Different expression of angiogenesis-related factors between human cultivated corneal and oral epithelial sheets', *Exp Eye Res,* 83(4), pp. 741-6.

Shan, X., Choi, J. H., Kim, K. J., Lee, Y. J., Ryu, Y. H., Lee, S. J., Moon, S. H. and Rhie, J. W. (2018) 'Adipose Stem Cells with Conditioned Media for Treatment of Acne Vulgaris Scar', *Tissue Eng Regen Med,* 15(1), pp. 49-61.

Shanbhag, S. S., Patel, C. N., Goyal, R., Donthineni, P. R., Singh, V. and Basu, S. (2019) 'Simple limbal epithelial transplantation (SLET): Review of indications, surgical technique, mechanism, outcomes, limitations, and impact', *Indian J Ophthalmol,* 67(8), pp. 1265-1277.

Sharif, R., Khaled, M. L., McKay, T. B., Liu, Y. and Karamichos, D. (2019) 'Transcriptional profiling of corneal stromal cells derived from patients with keratoconus', *Sci Rep,* 9(1), pp. 12567.

Shen, Y. H., Shoichet, M. S. and Radisic, M. (2008) 'Vascular endothelial growth factor immobilized in collagen scaffold promotes penetration and proliferation of endothelial cells', *Acta Biomater,* 4(3), pp. 477-89.

Shimmura, S., Shimazaki, J., Ohashi, Y. and Tsubota, K. (2001) 'Antiinflammatory effects of amniotic membrane transplantation in ocular surface disorders', *Cornea,* 20(4), pp. 408-13.

Shukla, S., Mittal, S. K., Foulsham, W., Elbasiony, E., Singhania, D., Sahu, S. K. and Chauhan, S. K. (2019) 'Therapeutic efficacy of different routes of mesenchymal stem cell administration in corneal injury', *Ocul Surf,* 17(4), pp. 729-736.

Si, Z., Wang, X., Sun, C., Kang, Y., Xu, J., Wang, X. and Hui, Y. (2019) 'Adipose-derived stem cells: Sources, potency, and implications for regenerative therapies', *Biomed Pharmacother,* 114, pp. 108765.

Siebzehnrubl, F. A., Vedam-Mai, V., Azari, H., Reynolds, B. A. and Deleyrolle, L. P. (2011) 'Isolation and characterization of adult neural stem cells', *Methods Mol Biol,* 750, pp. 61-77.

Singer, N. G. and Caplan, A. I. (2011) 'Mesenchymal stem cells: mechanisms of inflammation', *Annu Rev Pathol,* 6, pp. 457-78.

Singh, P., Tyagi, M., Kumar, Y., Gupta, K. K. and Sharma, P. D. (2013) 'Ocular chemical injuries and their management.', *Oman journal of ophthalmology,* 6, pp. 83-6.

Singh, S. P., Jadhav, S. H., Chaturvedi, C. P. and Nityanand, S. (2017) 'Therapeutic efficacy of multipotent adult progenitor cells versus mesenchymal stem cells in experimental autoimmune encephalomyelitis.', *Regenerative medicine*.

Smith, A. N., Willis, E., Chan, V. T., Muffley, L. A., Isik, F. F., Gibran, N. S. and Hocking, A. M. (2010) 'Mesenchymal stem cells induce dermal fibroblast responses to injury', *Exp Cell Res,* 316(1), pp. 48-54.

Song, H. B., Park, S. Y., Ko, J. H., Park, J. W., Yoon, C. H., Kim, D. H., Kim, J. H., Kim, M. K., Lee, R. H., Prockop, D. J. and Oh, J. Y. (2018) 'Mesenchymal Stromal Cells Inhibit Inflammatory Lymphangiogenesis in the Cornea by Suppressing Macrophage in a TSG-6-Dependent Manner', *Mol Ther,* 26(1), pp. 162-172.

Stagos, D., Chen, Y., Cantore, M., Jester, J. V. and Vasiliou, V. (2010) 'Corneal aldehyde dehydrogenases: multiple functions and novel nuclear localization', *Brain Res Bull,* 81(2-3), pp. 211-8.

Stiemke, M. M., Edelhauser, H. F. and Geroski, D. H. (1991) 'The developing corneal endothelium: correlation of morphology, hydration and Na/K ATPase pump site density', *Curr Eye Res,* 10(2), pp. 145-56.

Stojanovic, S. and Najman, S. (2019) 'The Effect of Conditioned Media of Stem Cells Derived from Lipoma and Adipose Tissue on Macrophages' Response and Wound Healing in Indirect Co-culture System In Vitro', *Int J Mol Sci,* 20(7).

Summer, R., Fitzsimmons, K., Dwyer, D., Murphy, J. and Fine, A. (2007) 'Isolation of an Adult Mouse Lung Mesenchymal Progenitor Cell Population', *American Journal of Respiratory Cell and Molecular Biology,* 37(2), pp. 152-159.

Sun, H., Mi, X., Gao, N., Yan, C. and Yu, F. S. (2015) 'Hyperglycemia-suppressed expression of Serpine1 contributes to delayed epithelial wound healing in diabetic mouse corneas', *Invest Ophthalmol Vis Sci,* 56(5), pp. 3383-92.

Sun, J. and Tan, H. (2013) 'Alginate-Based Biomaterials for Regenerative Medicine Applications', *Materials (Basel),* 6(4), pp. 1285-1309.

Swaney, K. F., Huang, C. H. and Devreotes, P. N. (2010) 'Eukaryotic chemotaxis: a network of signaling pathways controls motility, directional sensing, and polarity', *Annu Rev Biophys,* 39, pp. 265-89.

Swioklo, S. and Connon, C. J. (2016) 'Keeping cells in their place: the future of stem cell encapsulation', *Expert opinion on biological therapy,* 16(10), pp. 1181-3.

Swioklo, S., Constantinescu, A. and Connon, C. J. (2016) 'Alginate-Encapsulation for the Improved Hypothermic Preservation of Human Adipose-Derived Stem Cells', *Stem Cells Translational Medicine,* 5, pp. 339-349.

Tao, H., Chen, X., Cao, H., Zheng, L., Li, Q., Zhang, K., Han, Z., Han, Z. C., Guo, Z., Li, Z. and Wang, L. (2019) 'Mesenchymal Stem Cell-Derived Extracellular Vesicles for Corneal Wound Repair', *Stem Cells Int,* 2019, pp. 5738510.

Thangarajah, H., Vial, I. N., Chang, E., El-Ftesi, S., Januszyk, M., Chang, E. I., Paterno, J., Neofytou, E., Longaker, M. T. and Gurtner, G. C. (2009) 'IFATS collection: Adipose stromal cells adopt a proangiogenic phenotype under the influence of hypoxia', *Stem Cells,* 27(1), pp. 266-74.

Togel, F., Weiss, K., Yang, Y., Hu, Z., Zhang, P. and Westenfelder, C. (2007) 'Vasculotropic, paracrine actions of infused mesenchymal stem cells are important to the recovery from acute kidney injury', *Am J Physiol Renal Physiol,* 292(5), pp. F1626-35.

Tong, Z., Chen, Y., Liu, Y., Tong, L., Chu, J., Xiao, K., Zhou, Z., Dong, W. and Chu, X. (2017) 'Preparation, Characterization and Properties of Alginate/Poly(gamma-glutamic acid) Composite Microparticles', *Mar Drugs,* 15(4).

Tonnesen, H. H. and Karlsen, J. (2002) 'Alginate in drug delivery systems', *Drug Dev Ind Pharm,* 28(6), pp. 621-30.

Torricelli, A. A., Santhanam, A., Wu, J., Singh, V. and Wilson, S. E. (2016) 'The corneal fibrosis response to epithelial-stromal injury', *Exp Eye Res,* 142, pp. 110-8.

Tracy, L. E., Minasian, R. A. and Caterson, E. J. (2016) 'Extracellular Matrix and Dermal Fibroblast Function in the Healing Wound', *Advances in Wound Care,* 5(3), pp. 119-136.

Treacy, O., O'Flynn, L., Ryan, A. E., Morcos, M., Lohan, P., Schu, S., Wilk, M., Fahy, G., Griffin, M. D., Nosov, M. and Ritter, T. (2014) 'Mesenchymal stem cell therapy promotes corneal allograft survival in rats by local and systemic immunomodulation', *Am J Transplant,* 14(9), pp. 2023-36.

Tsuchiya, A., Takeuchi, S., Watanabe, T., Yoshida, T., Nojiri, S., Ogawa, M. and Terai, S. (2019) 'Mesenchymal stem cell therapies for liver cirrhosis: MSCs as "conducting cells" for improvement of liver fibrosis and regeneration', *Inflamm Regen,* 39, pp. 18.

Use, C. f. M. P. f. V. (2017) 'Questions and answers on allogenic stem cell-based products for veterinary use: specific questions on sterility,' https://www.ema.europa.eu/documents/scientific-guideline/questions-answers-allogenic-stem-cell-based-products-veterinary-use-specific-questions-sterility_en.pdf. .

Vaidyanathan, U., Hopping, G. C., Liu, H. Y., Somani, A. N., Ronquillo, Y. C., Hoopes, P. C. and Moshirfar, M. (2019) 'Persistent Corneal Epithelial Defects: A Review Article', *Med Hypothesis Discov Innov Ophthalmol,* 8(3), pp. 163-176.

Varaprasad, K., Jayaramudu, T., Kanikireddy, V., Toro, C. and Sadiku, E. R. (2020) 'Alginate-based composite materials for wound dressing application:A mini review', *Carbohydr Polym,* 236, pp. 116025.

Vereb, Z., Poliska, S., Albert, R., Olstad, O. K., Boratko, A., Csortos, C., Moe, M. C., Facsko, A. and Petrovski, G. (2016) 'Role of Human Corneal Stroma-Derived

Mesenchymal-Like Stem Cells in Corneal Immunity and Wound Healing', *Sci Rep,* 6, pp. 26227.

Verfaillie, C. M. (2005) 'Multipotent adult progenitor cells: an update', *Novartis Found Symp,* 265, pp. 55-61; discussion 61-5, 92-7.

Wachtmeister, L., Ingemansson, S.-O. and ErnamÖLler (2009) 'Atopy and Hla Antigens in Patients with Keratoconus', *Acta Ophthalmologica,* 60(1), pp. 113-122.

Wagoner, M. D. (1997) 'Chemical injuries of the eye: current concepts in pathophysiology and therapy.', *Survey of ophthalmology,* 41, pp. 275-313.

Wang, S., Yang, H., Tang, Z., Long, G. and Huang, W. (2016) 'Wound Dressing Model of Human Umbilical Cord Mesenchymal Stem Cells-Alginates Complex Promotes Skin Wound Healing by Paracrine Signaling.', *Stem cells international,* 2016, pp. 3269267.

Wang, T., Gu, Q., Zhao, J., Mei, J., Shao, M., Pan, Y., Zhang, J., Wu, H., Zhang, Z. and Liu, F. (2015) 'Calcium alginate enhances wound healing by up-regulating the ratio of collagen types I/III in diabetic rats', *Int J Clin Exp Pathol,* 8(6), pp. 6636-45.

Waring, G. O., 3rd, Bourne, W. M., Edelhauser, H. F. and Kenyon, K. R. (1982) 'The corneal endothelium. Normal and pathologic structure and function', *Ophthalmology,* 89(6), pp. 531-90.

Watson, S. L., Marcal, H., Sarris, M., Di Girolamo, N., Coroneo, M. T. and Wakefield, D. (2010) 'The effect of mesenchymal stem cell conditioned media on corneal stromal fibroblast wound healing activities', *Br J Ophthalmol,* 94(8), pp. 1067-73.

Watt, S. M., Gullo, F., van der Garde, M., Markeson, D., Camicia, R., Khoo, C. P. and Zwaginga, J. J. (2013) 'The angiogenic properties of mesenchymal stem/stromal cells and their therapeutic potential', *Br Med Bull,* 108, pp. 25-53.

Weissman, I. L., Anderson, D. J. and Gage, F. (2001) 'Stem and progenitor cells: origins, phenotypes, lineage commitments, and transdifferentiations', *Annu Rev Cell Dev Biol,* 17, pp. 387-403.

Weng J, L. Q., Mohan RR, Li Q, Wilson SE. (1997a) 'Hepatocyte growth factor, keratinocyte growth factor, their receptors, fibroblast growth factor receptor-2, and the cells of the cornea.', *nvestigative ophthalmology and visual science,* 38(8), pp. 1543-54.

Weng J, M. R., Li Q, Wilson SE. (1997b) 'IL-1 upregulates keratinocyte growth factor and hepatocyte growth factor mRNA and protein production by cultured stromal fibroblast cells: interleukin-1 beta expression in the cornea.', *Cornea,* 16(4), pp. 465-71.

West-Mays, J. A. and Dwivedi, D. J. (2006) 'The keratocyte: corneal stromal cell with variable repair phenotypes.', *The international journal of biochemistry & cell biology,* 38, pp. 1625-31.

Williams, D. F. (2009) 'On the nature of biomaterials', *Biomaterials,* 30(30), pp. 5897-5909.

Wilson, S. E., He, Y. G., Weng, J., Li, Q., McDowall, A. W., Vital, M. and Chwang, E. L. (1996) 'Epithelial injury induces keratocyte apoptosis: hypothesized role for the interleukin-1 system in the modulation of corneal tissue organization and wound healing.', *Experimental eye research,* 62, pp. 325-7.

Wilson, S. E. and Hong, J. W. (2000) 'Bowman's layer structure and function: critical or dispensable to corneal function? A hypothesis', *Cornea,* 19(4), pp. 417-20.

Wilson, S. E., Mohan, R. R., Mohan, R. R., Ambrosio, R., Jr., Hong, J. and Lee, J. (2001) 'The corneal wound healing response: cytokine-mediated interaction of the epithelium, stroma, and inflammatory cells', *Prog Retin Eye Res,* 20(5), pp. 625-37.

Wilson, S. E., Netto, M. and Ambrósio, R. (2003) 'Corneal cells: chatty in development, homeostasis,wound healing, and disease', *American Journal of Ophthalmology,* 136(3), pp. 530-536.

Wright, B., Cave, R. A., Cook, J. P., Khutoryanskiy, V. V., Mi, S., Chen, B., Leyland, M. and Connon, C. J. (2012) 'Enhanced viability of corneal epithelial cells for efficient transport/storage using a structurally modified calcium alginate hydrogel', *Regen Med,* 7(3), pp. 295-307.

Wu, Y. and Zhao, R. C. H. (2012) 'The Role of Chemokines in Mesenchymal Stem Cell Homing to Myocardium', *Stem Cell Reviews and Reports,* 8, pp. 243-250.

Yang, C., Lei, D., Ouyang, W., Ren, J., Li, H., Hu, J. and Huang, S. (2014) 'Conditioned media from human adipose tissue-derived mesenchymal stem cells and umbilical cord-derived mesenchymal stem cells efficiently induced the apoptosis and differentiation in human glioma cell lines in vitro', *Biomed Res Int,* 2014, pp. 109389.

Yang, J., Zhang, Y. S., Yue, K. and Khademhosseini, A. (2017) 'Cell-laden hydrogels for osteochondral and cartilage tissue engineering', *Acta Biomater,* 57, pp. 1-25.

Yang, J. A., Chung, H. M., Won, C. H. and Sung, J. H. (2010) 'Potential application of adipose-derived stem cells and their secretory factors to skin: discussion from both clinical and industrial viewpoints', *Expert Opin Biol Ther,* 10(4), pp. 495-503.

Yang, Y. K., Ogando, C. R., Wang See, C., Chang, T. Y. and Barabino, G. A. (2018) 'Changes in phenotype and differentiation potential of human mesenchymal stem cells aging in vitro', *Stem Cell Res Ther,* 9(1), pp. 131.

Yao, L., Li, Z.-r., Su, W.-r., Li, Y.-p., Lin, M.-l., Zhang, W.-x., Liu, Y., Wan, Q. and Liang, D. (2012) 'Role of Mesenchymal Stem Cells on Cornea Wound Healing Induced by Acute Alkali Burn', *PLoS ONE,* 7, pp. e30842.

Ye, J., Yao, K. and Kim, J. C. (2006) 'Mesenchymal stem cell transplantation in a rabbit corneal alkali burn model: engraftment and involvement in wound healing', *Eye,* 20, pp. 482-490.

Yoon, B. S., Moon, J. H., Jun, E. K., Kim, J., Maeng, I., Kim, J. S., Lee, J. H., Baik, C. S., Kim, A., Cho, K. S., Lee, J. H., Lee, H. H., Whang, K. Y. and You, S. (2010) 'Secretory profiles and wound healing effects of human amniotic fluid-derived mesenchymal stem cells', *Stem Cells Dev,* 19(6), pp. 887-902.

Yu, B., Shao, H., Su, C., Jiang, Y., Chen, X., Bai, L., Zhang, Y., Li, Q., Zhang, X. and Li, X. (2016) 'Exosomes derived from MSCs ameliorate retinal laser injury partially by inhibition of MCP-1', *Sci Rep,* 6, pp. 34562.

Yu, F. S., Yin, J., Xu, K. and Huang, J. (2010) 'Growth factors and corneal epithelial wound healing', *Brain Res Bull,* 81(2-3), pp. 229-35.

Zachar, V., Duroux, M., Emmersen, J., Rasmussen, J. G., Pennisi, C. P., Yang, S. and Fink, T. (2011) 'Hypoxia and adipose-derived stem cell-based tissue regeneration and engineering', *Expert Opin Biol Ther,* 11(6), pp. 775-86.

Zadnik, K., Barr, J. T., Gordon, M. O. and Edrington, T. B. (1996) 'Biomicroscopic signs and disease severity in keratoconus. Collaborative Longitudinal Evaluation of Keratoconus (CLEK) Study Group', *Cornea,* 15(2), pp. 139-46.

Zadnik, K., Steger-May, K., Fink, B. A., Joslin, C. E., Nichols, J. J., Rosenstiel, C. E., Tyler, J. A., Yu, J. A., Raasch, T. W., Schechtman, K. B. and Keratoconus, C. S. G. C. L. E. o. (2002) 'Between-eye asymmetry in keratoconus', *Cornea,* 21(7), pp. 671-9.

Zeppieri, M., Salvetat, M. L., Beltrami, A., Cesselli, D., Russo, R., Alcalde, I., Merayo-Lloves, J., Brusini, P. and Parodi, P. C. (2017) 'Adipose Derived Stem Cells for Corneal Wound Healing after Laser Induced Corneal Lesions in Mice', *J Clin Med,* 6(12).

Zhao, X., Huebsch, N., Mooney, D. J. and Suo, Z. (2010) 'Stress-relaxation behavior in gels with ionic and covalent crosslinks', *J Appl Phys,* 107(6), pp. 63509.

Zimmermann, U., Klock, G., Federlin, K., Hannig, K., Kowalski, M., Bretzel, R. G., Horcher, A., Entenmann, H., Sieber, U. and Zekorn, T. (1992) 'Production of mitogen-contamination free alginates with variable ratios of mannuronic acid to guluronic acid by free flow electrophoresis', *Electrophoresis,* 13(5), pp. 269-74.